Development and validation of a physiologically-based pharmacokinetic model for dermal absorption

Maciel Tabosa, Maria

Award date:
2019

Awarding institution:
University of Bath

DEVELOPMENT AND VALIDATION OF A PHYSIOLOGICALLY-BASED PHARMACOKINETIC MODEL FOR DERMAL ABSORPTION

Maria Alice Maciel Tabosa

A thesis submitted for the degree of Doctor of Philosophy

University of Bath

Department of Pharmacy and Pharmacology

November 2018

Copyright

Table of Contents

Acknowledgements

I would like to express my sincere gratitude to my supervisors, Professor **Richard Guy** and Dr. **M. Begoña Delgado-Charro**, for the opportunity, guidance and continuous support throughout these years.

I would also like to thank Dr. **Jane White,** for her advice, expertise and patience.

I gratefully acknowledge Professor **Annette Bunge,** for the stimulating discussions and valuable contributions towards this thesis.

I would also like to thank Dr. **Sarah Cordery**, for always being helpful, informative and supportive.

I would like to thanks my friends from 3.22, **Joana Martir, Fotios Baxevanis, James Clarke, Hilda Phan, Ricardo Diaz de Leon Ortega, John Nikolettos, Angela Effinger, Mariana Correia** for their help and support for all these years we have shared the lab and the office.

I would like to thank Dr. **Leila Bastos Leal**, for encouraging me to come to Bath and for always being helpful.

I would like to thank my friend Dr. **Francisco Viríssimo** for your thoughtful words, for your crucial "maths hints" and enthusiastic discussions.

I also would like to thank my parents (**Sandra and Yrageu**) and siblings (**André e Laís**), for their encouragement, support, attention and care. "Obrigada por sempre acreditarem em mim".

Finally, I would like to thank **CAPES** (Brazilian Federal Agency for Support and Evaluation of Graduate Education, Ministry of Education of Brazil) for funding this research.

Abstract

Measurement of the bioavailability of a drug in the skin after topical application is an important objective when attempting to assess whether the target-site concentrations are satisfactory to treat the disease. However, determining the amount of drug that reaches the different skin layers is still a challenge. Self-evidently, this challenge requires knowledge of both the drug input rate into the skin 'compartment' and its subsequent clearance therefrom.

The Chapter 2 of this thesis focused on characterising experimentally (using *in vitro* permeation tests) the input functions of two transdermal drugs, buprenorphine and nicotine, from commercially available patches. In addition, the input-rate of diclofenac from a medicated plaster was determined using the same approach as demonstrated for the transdermal drugs. A good agreement between the experimentally determined input-rates of the two transdermal drugs and their labelled performance *in vivo* was found, lending support to the potential utility of the *in vitro* approach proposed to define topical drug input-rates more broadly.

The Chapter 3 described an investigation of the behaviour of diclofenac in the stratum corneum. The uptake of diclofenac into the stratum corneum and its clearance therefrom following application of a medicated plaster was investigated *in vivo* in human. The results presented in this chapter have utility with respect to the application of stratum corneum tape-stripping to derive useful skin pharmacokinetic parameters related to drug partitioning into and diffusion across the stratum corneum.

The results described in chapter 3 suggested that diclofenac uptake into the stratum corneum may be modified by the presence of excipient(s). Therefore, the work described in Chapter 4 focused on exploring the uptake of two excipients/co-solvents, propylene glycol and butylene glycol, into the stratum corneum *in vivo* in human, following application of the diclofenac medicated plaster. The results obtained from the uptake of propylene and butylene glycol suggests that these volatile solvents were rapidly taken into the stratum corneum. In parallel, evaporation of the solvents was identified.

The work described in Chapter 5 investigated the hypothesis that information about clearance from the skin can be derived from available systemic pharmacokinetic data for drugs administered via transdermal delivery systems. A statistical mathematical model describing drug clearance from the skin in terms of drug molecular descriptors was developed. The model showed a good predictive ability. It has been further demonstrated that the empirical model closely predicts the results obtained in *in vitro* skin experiments.

Overall, this thesis has provided useful information on the application of different strategies to predict topical skin delivery upon which further development and optimisation might be based.

Chapter 1: Introduction

The skin performs a variety of barrier functions, for example, impeding the loss of water as well as the ingress of materials contacting its surface. The latter, of course, plays a crucial role in determining the effectiveness of a topical[1] drug treatment. A variety of topical drug formulations have been developed to treat dermatological, locally-acting or systemic diseases. The efficiency of the majority of these products approved for therapeutic use is, however, rather poor, and typically, only a few per cent of the applied drug dose actually becomes available at the site of action.

It follows that the optimization of any dermatological therapy requires an understanding of the skin's physical barrier and of the physicochemical mechanisms involved in cutaneous drug uptake and transport. However, as dermal tissue is (virtually) experimentally inaccessible (at least, *in vivo* in humans), local drug concentration profiles have proven difficult to obtain. The development of models to correctly predict drug bioavailability in the skin after topical administration is, therefore, essential.

The goal of this thesis is to develop a physiologically-based pharmacokinetic model for dermal drug products, using *in vitro*/*ex vivo* and *in vivo* skin experiments and to demonstrate that the model's kinetic and distribution parameters can be correlated with key physicochemical properties of a drug.

[1] The term 'topical' can be used to refer to non-oral extravascular routes of administration, such as nasal and ocular. However, throughout this work, the term topical will be used to refer to administration of a drug to the skin and this includes those used in dermatology, drugs to treat local subcutaneous pain and inflammation, and transdermal drugs for systemic effect.

1. Background

1.1 The structure of the skin

As the largest organ of the human body, skin is accessible for both topical and systemic drug delivery (Zaffaroni, 1991; Gauglitz and Schauber, 2013; Kumar et al., 2015). The skin is composed of two main layers: the epidermis and the dermis (Figure 1).

The epidermis is the outermost layer of the skin, approximately 150 μm thick and can be divided into two layers: stratum corneum and viable epidermis. It is an avascular layer and relies on the dermis for nutrition. It has a multilamellar structure that represents the different stages of cell differentiation. Moving upwards from the bottom layer, the cells change in an ordered fashion from metabolically active and dividing cells to dense, flattened, functionally dead, keratinized cells, known as corneocytes (Moser et al., 2001b). The epidermal turnover time, i.e., the time needed for a given cell to pass from the basal layer to the outer surface of the skin, represents about 52–75 days in the normal epidermis (Piérard, Hermanns-Lê and Piérard-Franchimont, 2017).

The stratum corneum has frequently been described as a 'bricks and mortar' structure (Michaels, Chandrasekaran and Shaw, 1975; Elias et al., 1981) (Figure 2). The 'bricks' represent the tightly packed corneocytes, and they are embedded in a 'mortar' of lipid bilayers. Corneocytes are flat, polygonal cells, primarily composed of keratin surrounded by an envelope of cross-linked proteins and lipids. These cells are typically 0.2–1.5 μm thick, have diameters of approximately 30–50 μm and are held together by specialized protein structures called corneodesmosomes, which confer structural stability to the stratum corneum. The composition of the intercellular lipids varies according to the individual and the anatomical site, but it mostly constitutes ceramides, fatty acids and cholesterol (Hadgraft, 2000; Guy, 2013). The lipid matrix provides the primary barrier function of the stratum corneum, impeding the ingress of materials contacting the skin into the body and minimising water loss, which means that - in most cases - it is relatively impermeable to the penetration of xenobiotics (Kumar et al., 2015).

The stratum corneum is, on average, 15–20 cells thick – around 10 μm in thickness when dry, however the corneocytes may hydrate extensively, resulting in significant

changes to the packing, structure, thickness and permeability of the stratum corneum. In addition, the corneocytes change in their morphological and biochemical functions as they progress from the inner to outer part of the stratum corneum (Michel et al., 1988; Norlén and Al-Amoudi, 2004; Norlén, 2006; Rawlings, 2010).

As cells move towards the outer layers of the stratum corneum, corneodesmosomes holding the cells together begin to break down causing loss of the corneocytes from the skin's surface, known as desquamation. The entire stratum corneum is turned over in around 2-3 weeks (Michel et al., 1988).

Beneath the epidermis is the dermis, the innermost layer, which is a thick, aqueous, gel-like tissue. The dermis consists mainly of elastin and collagen fibres and contains many blood capillaries, nerves and lymphatic vessels. The capillaries of the cutaneous microcirculation extend to the top of the dermis, and follow the undulations of the boundary between the dermis and the epidermis. These capillaries deliver nutrients to the skin as well as providing a clearance mechanism by which penetrating xenobiotics are eliminated into the systemic circulation.

Also, the skin has a number of appendages – the hair follicles, sebaceous and sweat glands (Haake, Scott and Holbrook, 2001; Menon, 2015). Hair follicles can be found on all areas of the skin at differing densities except on the palms of the hands, soles of the feet and lips. Sebaceous glands are most abundant on the forehead and secrete sebum, which serves to regulate surface pH and keep the skin moist. Sweat glands help regulate body temperature and are found across most of the skin surface (Benson, 2012).

1.2 Permeation pathways through the stratum corneum

Despite the efficient barrier function of the skin, it is evident that some compounds can pass through the stratum corneum, reach the viable skin and, ultimately, the systemic circulation. Potentially, there are three possible pathways for a compound's transport across the stratum corneum and, then, penetration into the deeper layers of skin: the intercellular (around the corneocytes, shown as **(a)** in Figure 1), the transcellular (through the corneocytes, shown as **(b)** in Figure 1) and through skin appendages (sweat glands and hair follicles, shown as **(c)** in Figure 1) (Hadgraft, 2000). The contributions of these three routes to the percutaneous absorption of a topically applied compound, from the surface of the skin either into the skin or into

systemic circulation, depend on the nature of the permeating molecules and the density of appendages, such as hair follicles and sweat ducts, at the site of application (Schaeffer and Redelmuer, 1996).

The intercellular pathway is thought to be the major pathway for the permeation of small (< 500 Da, Bos and Meinardi (2000)) and uncharged molecules (Elias, 1983; Simonetti et al., 1995; Ng and Lau, 2015). Intercellular lipids, providing the only continuous phase within the SC, form lamellar structures between corneocytes. The permeation of compounds via this route is believed to occur by diffusion along and/or across lipid lamellae (Schaeffer and Redelmuer, 1996). Potts and Francoeur (1991) demonstrate that the water pathlength across the stratum corneum is 50 times greater than its thickness, i.e., the molecule travels up to 500 µm to cross the ~15 µm thick stratum corneum. Therefore, it was suggested the molecules take a 'tortuous' route around the corneocytes.

The transcellular route requires the repeated penetration of the permeating compound into and out of the corneocytes and the intercellular lipids. In this route of permeation, the compound must therefore diffuse through both lipophilic regions (lipids) and hydrophilic regions (hydrated keratin within corneocytes) of the SC.

Under normal conditions, penetration through the skin appendages is not considered important because they occupy a low fraction of skin area (for example, only ~ 0.2% of area on the chest and upper arm (Otberg et al., 2004)). However, this pathway plays a large role in iontophoresis and is thought to be quite important for compounds of low stratum corneum diffusivity, such as hydrophilic and large molecular weight compounds (Williams and Barry, 2012).

Despite evidence suggesting that the major route is through the intercellular spaces, the transport across the stratum corneum barrier might occur by any combination of the three aforementioned pathways (Bunge, Guy and Hadgraft, 1999; Moser et al., 2001b; Hadgraft, 2004).

Once a molecule has traversed the stratum corneum it must then partition into the viable epidermis the environment of which is much more aqueous in nature. Compounds that are particularly lipophilic may therefore partition into the stratum corneum relatively easily but partitioning into the lower epidermis becomes difficult (Guy, 2013). Poor partition into the viable epidermis may create a 'reservoir' whereby

a lipophilic compound accumulates in the stratum corneum from which it is then slowly released into the viable tissue and circulation (Roberts, Cross and Anissimov, 2004). Depending on the rate of removal of this compound from the reservoir, the compound could also potentially be lost via desquamation of the stratum corneum. Of course, due to the relatively slow rate of epidermal turnover, this is only likely to be significant for compounds with extremely slow absorption (Reddy, Guy and Bunge, 2000).

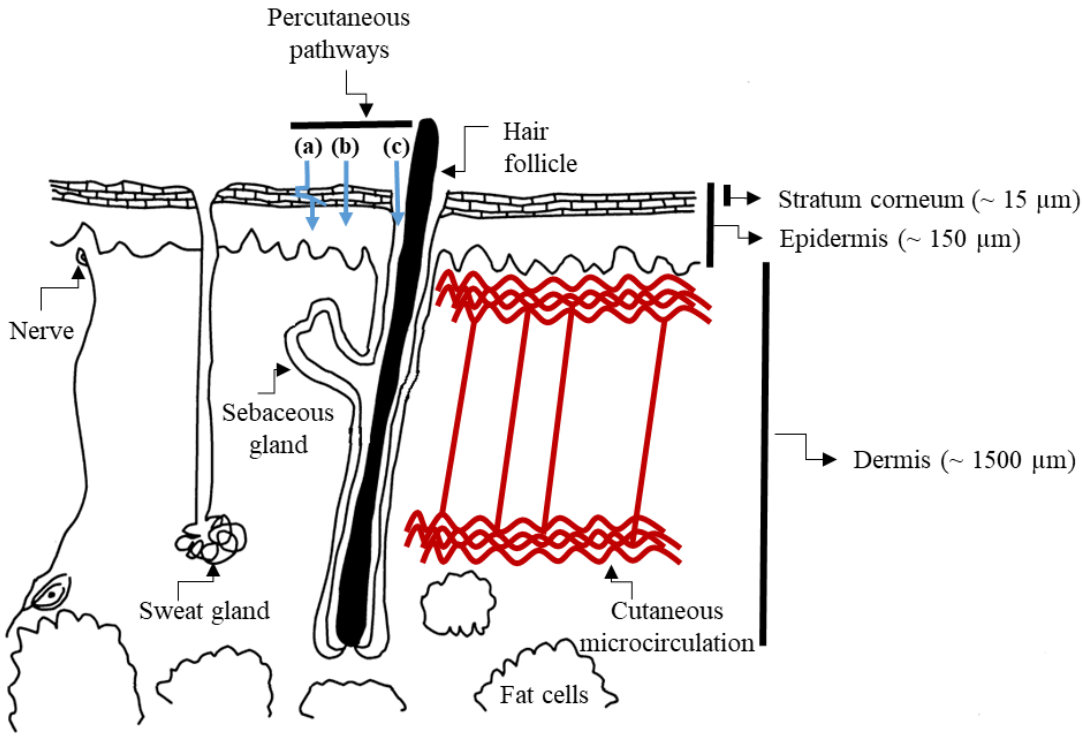

Figure 1. The structure of human skin. (a), (b) and (c) show potential routes for skin permeation; a = intercellular, b = transcellular, c = appendageal (i.e., via a hair follicle or sweat gland). Image adapted from Moser et al. (2001b).

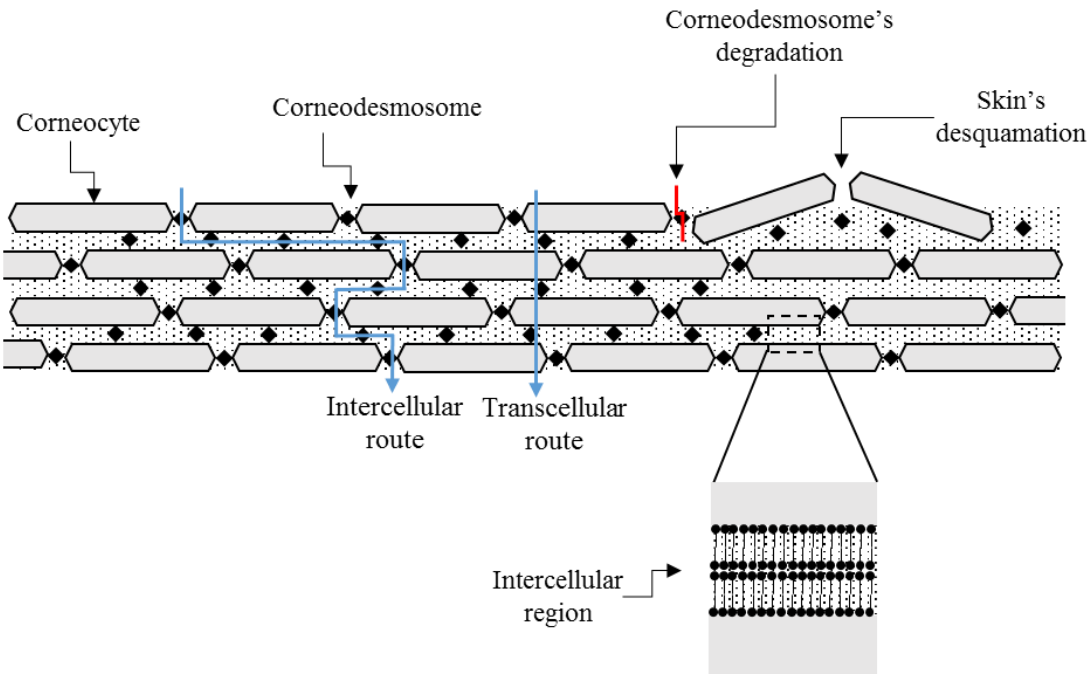

Figure 2. The schematic structure of stratum corneum. The corneocytes (in *grey*) and the intercellular lipids (continuous domain in *dots*) represent the bricks and mortar, respectively. Two routes potentially contributing to the percutaneous absorption of topically applied compounds, the transcellular and intercellular routes are shown. Corneodesmosomes are presented as black diamonds between the individual corneocytes.

1.3 Percutaneous absorption

The drug's journey from the formulation applied on the skin to the local capillary network and, eventually, the systemic circulation is a multiple-step process which involves repeated processes of partitioning and diffusion (Kalia and Guy, 2001) (Figure 3). Many factors can influence these two processes (partition and diffusion) and, consequently, rate and extent of the absorption of a drug into and through the skin.

Before entering the skin, the presence of certain components of the formulation can play an important role in controlling rate (Garg, Rath and Goyal, 2015). Once in the skin, the properties and the conditions of the skin can significantly affect the rate at which the permeant will cross the skin layers (Hwa, Bauer and Cohen, 2011). Lastly, it has been demonstrated that the physicochemical properties of a permeant greatly influence the processes involved in dermal and transdermal permeation (Guy, 2016). Some of these key parameters are discussed below.

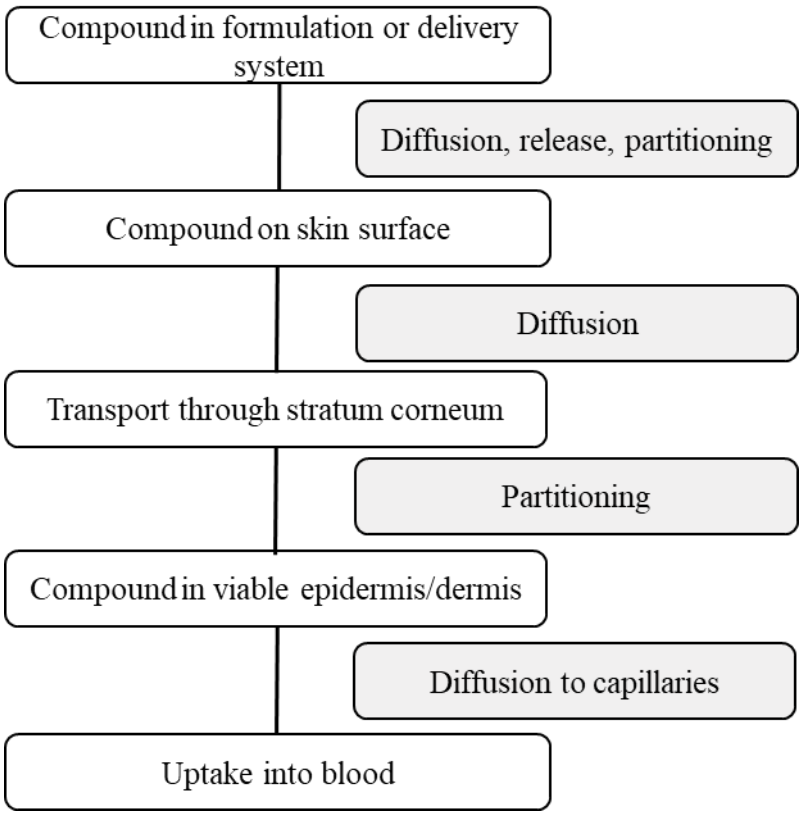

Figure 3. Key processes that determine the extent of compound permeation through the skin.

1.3.1 Drug-related factors affecting percutaneous absorption

Over half a century ago, Blank, Scheuplein and colleagues started to investigate the role of the physicochemical properties of a chemical in the percutaneous absorption process (Scheuplein, 1965, 1967; Robert J Scheuplein and Blank, 1971). Since then, enormous effort has been dedicated to identifying the key physicochemical parameters determining the rate and extent of penetration of a chemical across the skin.

For oral delivery, in order to assess whether a particular drug is likely to exhibit poor permeability or other pharmacokinetic properties, a commonly adopted strategy is to use Lipinski's Rules of Five (Lipinski et al., 1997). This rule qualitatively outlines the physiochemical space defined by the majority of well-absorbed drugs, which include (1) molecular weight (MW) < 500, (2) number of hydrogen bond donors ≤ 5, (3) number of hydrogen bond acceptors ≤ 10, and (4) octanol−water partition coefficient (log P) < 5. Interestingly, research has suggested that this rule also works reasonably well for the transdermal route: as a general rule, big molecules (>500 Da)

and very lipophilic compounds (log P > 5) have low transdermal flux rates; very polar compounds, capable of donating or accepting lots of hydrogen-bonds, do not partition very well into the lipophilic stratum corneum, and therefore penetrate very slowly as well (Bos and Meinardi, 2000; Wiedersberg and Guy, 2014; Guy, 2016).

Molecular weight (MW) of the permeant

An inverse relationship between permeant diffusivity (D) within a lipid membrane, such as the stratum corneum, and its molecular weight/volume is anticipated by the theories of Cohen and Turnbull (1959) and Lieb and Stein (1986). Both theories suggest that the dependence of D on molecular volume is exponential (Equation 1).

$$D = D_0 e^{-\beta \cdot MV} \qquad \text{(Equation 1)}$$

where D_0 is the diffusivity of a hypothetical molecule having zero molecular volume (MV) and β is a constant. This means that drug diffusivity across the stratum corneum decreases as MW increases since MV and MW are interdependent.

Magnusson et al. (2004) demonstrated that the maximum flux (J_{max}) across human epidermal skin of 278 compounds in aqueous solution decreased with increasing MW. A linear relationship between log J_{max} and MW was observed (Figure 4). It should be noted that just a few molecules go beyond 500 Da, and this reflects the fact that the literature contains very little quantitative information on the passive percutaneous absorption of chemicals of higher molecular weight. The observation is rather a reflection of two phenomena: (i) The skin transport of molecules having MW > 500 Da is almost certainly going to be low (and possibly difficult to detect without recourse to very sensitive analytical chemistry), and (ii) very few compounds in this MW range have been properly and quantitatively evaluated for their ability to cross the skin barrier.

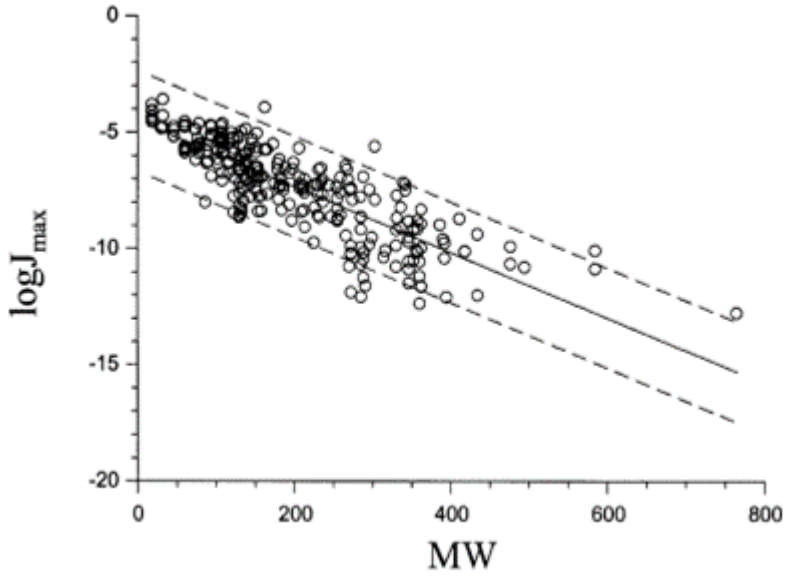

Figure 4. Logarithm of the maximum flux (J_{max}) of chemicals across human epidermis as a function of molecular weight (MW). (Magnusson et al., 2004). Permission to reproduce this image has been granted by the publisher.

Hydrophilicity/ lipophilicity of the permeant

A work published by Michaels, Chandrasekaran and Shaw (1975) shows that transdermal flux of 10 drugs increased linearly with their mineral oil – water partition coefficients ($K_{m,w}$) when $10^{-4} < K_{m,w} < 10^{0}$. From $K_{m,w}$ of approximately 10^{0} to 10^{4}, no further change to transdermal flux was observed.

In a later work, Yano et al. (1986) investigated the skin permeabilities of a series of eight salicylates (log P range: 1.13 – 3.96) and ten non-steroidal anti-inflammatory (log P range: 0.77 – 4.88) drugs in human subjects. A parabolic relationship between the logarithms of drug absorption through intact skin and log P of the test compounds was obtained in both compound series.

More recently, the effect of lipophilicity (log P) of 10 phenolic compounds (log P range: 1.95 – 3.38) with similar MW (~ 150 Da) on skin permeation was investigated by Zhang et al. (2009). They showed that J_{max} shows a bilinear (Equation 2) or parabolic (Equation 3) relationship with lipophilicity (Figure 5). They suggested that the observed relationship reflected the variation in solubility in the stratum corneum for the various solutes.

$$\log J_{max} = -2.1 + 1.7\,\log P - 21.6(\log 10^{-4} \times 10^{\log P} + 1) \qquad (r^2 = 0.86\ ;\ n = 10)$$

(Equation 2)

$$\log J_{max} = -7.2 + 6.5\,\log P - 1.2(\log P)^2 \qquad (r^2 = 0.74\ ;\ n = 10)$$

(Equation 3)

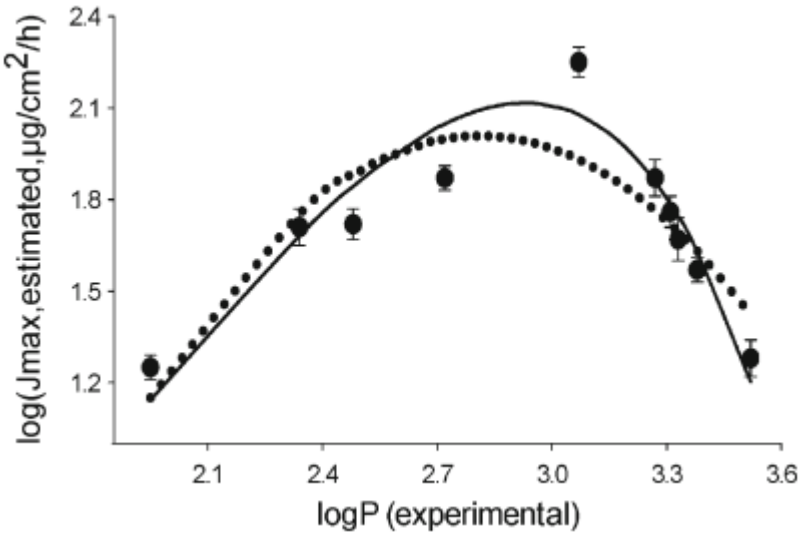

Figure 5. Relationship between transdermal maximum flux (J_{max}) and log P for penetration of phenolic compounds through excised human epidermal membrane (mean ± SD). Bilinear (solid line) and parabolic (dashed line) model fits. (Zhang et al., 2009). Permission to reproduce this image has been granted by the publisher.

In general, it could be observed that the better skin penetrants tend to have log P values in the range of 1-3, that is, overall somewhat lipophilic but retaining a decent solubility in aqueous media.

Hydrogen bonding

Another important determinant of the permeability of any given molecule is its hydrogen bonding capacity (Potts and Guy, 1995). To cross a biological membrane, a molecule must first break any hydrogen bonds that it forms with water. The more potential hydrogen bonds a molecule can make, the more energy this bond-breaking costs, and so high hydrogen-bonding potential is an unfavourable property that is often related to low permeability and absorption (van de Waterbeemd and Gifford, 2003).

Attempts to measure the hydrogen bonding capacity of a molecule have been made by the difference between octanol/water and alkane/water partitioning, but this technique is limited by the fact that some molecules are poorly soluble in the alkane

phase. Most recently, a variety of computational approaches have addressed the problem of estimating hydrogen bonding capacity, ranging from simple heteroatom (O and N) counts, the consideration of molecules in terms of the number of hydrogen bond acceptors and donors, and more sophisticated measures that take into account such parameters as free-energy factors (Raevsky et al., 2000) and topological polar surface area (TPSA) (Stenberg et al., 2001).

Potts and Guy (1995) observed that an increase in the hydrogen bonding activity (both acceptor and donor) decreases partitioning into the organic phase, presumably due to the free energy cost associated with disruption of the hydrogen bonds in the aqueous phase.

With regard to TPSA, previous studies have found an inverse correlation between TPSA and the passage of molecules through the brain-blood barrier (Clark, 1999; Kelder et al., 1999) and a sigmoidal relationship was found with respect to the intestinal membrane (Palm et al., 1997; Winiwarter et al., 1998; Stenberg et al., 1999). No study was found, however, that specifically investigated the relationship between TPSA and drug skin permeation.

1.3.2 Formulation-related factors affecting percutaneous absorption

The efficacy of a topically applied medicine is often limited by the poor penetration of the drug into the skin, more specifically by the permeation across the stratum corneum. Methods for improving cutaneous delivery rely either on the use of chemical penetration enhancers or more complex physical enhancement strategies, such as, the use of microneedle arrays (McAllister, Allen and Prausnitz, 2000; Mikszta et al., 2002) or electrical current (e.g., iontophoresis (Delgado-Charro and Guy, 2001; Fan, Sirkar and Michniak, 2008)). The addition of chemicals into the formulation, however, is the most common approach applied to enhance a drug's permeation through the skin (Moser et al., 2001a).

Three different strategies have been used to maximise the permeation of the drug through the stratum corneum: (i) increase drug diffusivity in the stratum corneum; (ii) increase the drug solubility in the stratum corneum, i.e., increase drug partitioning into the membrane, and; (iii) increase the degree of saturation of the drug

in the formulation. The latter strategy is based on interaction between the drug and the vehicle, while the first two approaches imply an effect of the vehicle on the barrier function of the stratum corneum (e.g., via movement of chemical penetration enhancer into the stratum corneum and subsequent disordering of the intercellular stratum corneum lipids, or the extraction of such lipids by solvating component of the formulation) (Moser et al., 2001b).

The diffusion coefficient of the drug in the stratum corneum can be increased by disordering the stratum corneum lipids. Fatty acids are a class of compounds frequently used to increase skin permeation and they are generally believed to increase diffusivity across the stratum corneum. Other examples include: oleic acid (Alberti et al., 2001), azone (Bouwstra et al., 1989; Schückler and Lee, 1992; Harrison et al., 1996) and dimethyl sulfoxide (DMSO) (Kligman, 1965; Klamerus and Lee, 1992).

Penetration enhancement of a drug into the stratum corneum can also occur by increasing the drug's solubility in this layer. Agents which are typically thought to act in this way include, for example, propylene glycol (Herkenne et al., 2008) and ethanol (Hatanaka et al., 1993).

Optimization of the degree of drug saturation is important for simple formulations as well as those containing chemical penetration enhancers. The degree of saturation can be increased by raising the drug concentration in the vehicle or by decreasing the solubility of the drug in the vehicle. Both approaches lead to an enhanced thermodynamic activity of the drug in the formulation and therefore to an increased skin permeation (Moser et al., 2001b). A transient increase of the degree of saturation to greater than one (a saturated solution implies a thermodynamic activity of unit) can be achieved via supersaturation. Supersaturated formulations, however, are inherently thermodynamically unstable (Pellett et al., 1997), and it is only a matter of time before crystallization of the drug occurs within the formulation (Brouwers, Brewster and Augustijns, 2009). If the solubility of the compound in the formulation is low, then further delivery is compromised because only drug in the molecular form can diffuse (Frederiksen, Guy and Petersson, 2016).

Although many compounds have been shown to have enhancement properties, most of the studies have been conducted using binary mixtures, that is, a single drug is delivered in a single vehicle (Karadzovska et al., 2013). 'Real world' formulations,

however, often contain a large number of compounds which may interact with each other (and with the stratum corneum) synergistically (Karande and Mitragotri, 2009). Therefore, elucidation of the mechanism of action(s) regarding skin penetration enhancement is not straightforward and remains poorly understood (Karadzovska et al., 2013).

1.4 Measuring rate and extent of chemical compounds absorption across the skin

1.4.1 *In vitro* and *ex vivo* methods

In vitro cutaneous permeation studies are generally performed using diffusion cells, for example the Franz diffusion cell (Figure 6). Briefly, these diffusion cells consist of two chambers, the donor, where the tested product is applied, and the receptor, separated by a synthetic membrane or a piece of skin. The receptor compartment is filled with a solution that favours sink conditions, that is, the dissolution of the compound into the receptor solution is not rate-limiting (solubility in the receptor solution should be at least 10-fold higher than the highest observed sample concentration (OECD, 2004)). The receptor solution is stirred with a magnetic stir-bar and is normally maintained at 37°C (by the water jacket – through which the temperature-controlled water is recirculated) with the aim of achieving a skin surface temperature of ~32 °C, representative of the temperature of the skin surface *in vivo* at rest. Permeation of a compound through the membrane is monitored by periodic sampling of the receptor solution from the sampling port. Samples are then analysed by suitable analytical techniques.

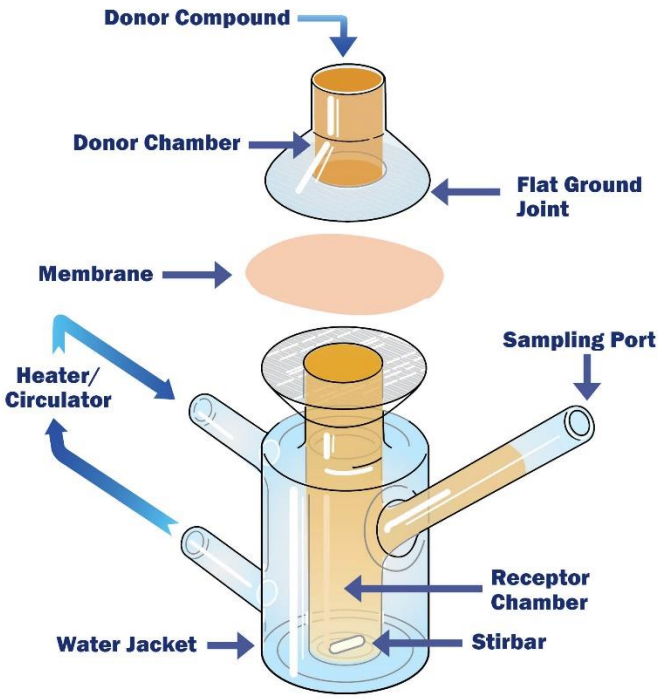

Figure 6. A Franz-type diffusion cell (retrieved from: http://permegear.com/franz-cells/).

The characterisation of percutaneous absorption is, commonly, observed through the use of *ex vivo* biological membranes. These tests can be performed through excised skin (human or animal). Generally, skin used in dermal absorption studies is not full-thickness. The use of full-thickness skin often results in lower levels of the test compound in the receptor solution (Wilkinson et al., 2006) and increased lag times. This is because full-thickness skin, consisting of stratum corneum, 'viable' epidermis, dermis and subdermal tissues (2000 – 3000 μm thick). If full-thickness skin is used, it should be kept in mind that *in vivo* the permeating molecule would not necessarily have to cross the dermal layer to achieve the desired pharmacological effect or to be absorbed into the systemic circulation.

Probably the most commonly used is split-thickness or dermatomed skin. A dermatome is an instrument that can cut the skin to a nominal depth that would usually include the epidermis and part of the dermis.

Another common method for preparing the skin is by heat separation (Kligman and Christophers, 1963), the process of submerging the skin in water at 60 ºC. This causes the epidermis to separate from the dermis without significantly impairing the

barrier function. The upper layers can then be used for diffusion studies. Stratum corneum can also be isolated by trypsin digestion (Onken and Moyer, 1963).

After the skin has been prepared, it is common to freeze it for later use, it is generally accepted that barrier function is not affected by this process (Rosado and Rodrigues, 2003). If the skin is to be used for regulatory studies then tests are performed to determine the integrity of the barrier. Methods to measure barrier integrity include transepidermal water loss (Fluhr, Feingold and Elias, 2006), capacitance (Palenske and Morhenn, 1999) or diffusion of tritiated water (Robert Scheuplein and Ross, 1970).

Obviously, the best and most relevant membrane to assess permeation of a compound through the skin is human skin, which can be obtained from cosmetic surgery or cadavers. However, the use of human skin can be expensive, logistically difficult and susceptible to ethical considerations. The pieces of skin are also often small and irregularly shaped, which can make handling and preparation difficult.

For these reasons, numerous animal skin models have been suggested as a surrogate to human skin, including, rat (Panchagnula et al., 2001; Pillai and Panchagnula, 2003), hairless mouse (Rhee et al., 2008; Lanke et al., 2009), guinea pig (Barbero and Frasch, 2009), pig (Barbero and Frasch, 2009), snake (Megrab, Williams and Barry, 1995) and non-human primate (Wester, Noonan and Maibach, 1980) skins. It is important to bear in mind that the absorption of chemicals varies between species, due to differences in follicular density, number of layers of corneocytes, and water and lipid content (Scheuplein, 1978; Panchagnula, Stemmer and Ritschel, 1997). Porcine skin is thought to be a good model for human skin as it has a similar lipid composition (Gray and White, 1978) and follicle density (Sekkat and Guy, 2001; Jacobi et al., 2007) and, most importantly, studies have demonstrated similar barrier properties to human skin (Sekkat and Guy, 2001; Cnubben et al., 2002; Vallet et al., 2007).

In addition to animal models, cultured human cell lines represent another alternative for skin permeation studies. Generally speaking, there are two main type of cultured skin tissues: living skin equivalents comprising a dermis, epidermis and (partially) differentiated stratum corneum, but without skin appendages; and human reconstructed epidermis which consists simply of keratinocytes grown on a substrate (Russell and Guy, 2009).

The morphology and biochemistry of human reconstructed epidermis has been compared with *ex vivo* human tissues. Both have a differentiated stratum corneum, but several histological and biochemical differences are apparent, for example the stratum corneum of the reconstructed epidermis is typically thicker (Monteiro-Riviere et al., 1997; Netzlaff et al., 2005). In general, chemical penetration across human reconstructed epidermis is quite reproducible, but significantly higher than through human, pig or rat skin. Several possible reasons for the measured higher drug flux across these membranes have been suggested, including differences in lipid composition and stratum corneum packing that result in a less efficient barrier (Schmook, Meingassner and Billich, 2001; Schafer-Korting et al., 2006).

Living skin equivalents, despite their greater similarity with human skin, have shown to similarly overestimate chemical penetration. For example, in a study by Schmook, Meingassner and Billich (2001), the permeation characteristics of human, porcine and rat skins with a living skin equivalents model were compared using four dermatological (salicylic acid, hydrocortisone, clotrimazole and terbinafine) drugs with different hydrophilicities (log P = 1.2, 2.0, 3.1 and 3.8, respectively). The permeation of more hydrophobic compounds (clotrimazole and terbinafine) through the skin equivalents resulted in an 800–900 fold higher flux than through human skin. On the other hand, transdermal flux of a less hydrophobic compound, salicylic acid, was in the same order of magnitude as fluxes obtained with human skin.

Overall, therefore, while valuable, for example, for skin irritation assessment, skin cell culture models are not yet able to provide quantitative predictions of percutaneous penetration.

1.4.2 *In vivo* methods

In vitro/*ex vivo* measurement of skin penetration is very useful for assessing the disposition of a drug in skin and its kinetic parameters; however, such studies cannot always provide all the necessary information to predict the local bioavailability of a drug. Therefore, the ultimate evaluation of topical drug delivery into and through the skin is likely to be performed in human *in vivo*.

Measuring the rate and extent of drug absorption into the systemic circulation after transdermal administration is relatively easily achieved. *In vivo* pharmacokinetic studies can be performed, with blood and/or urine samples collected at intervals. While these studies are useful for assessing the bioavailability of transdermal drugs (i.e., drugs whose site of action is reached via the systemic circulation), they may not be suitable for all topical dermatological drugs (i.e., drugs whose site of action is in the skin). There are exceptions, however, especially when there is significant drug absorption (i.e., drug plasma concentrations are high enough to be detected by analytical chemistry methods) and depending on the site of action. For example, the United States Food & Drug Administration (FDA) recommends that bioequivalence of lidocaine[2] topical patches can be demonstrated by pharmacokinetic studies (FDA, 2016). In contrast, for the antifungals, whose site of action is the upper layers of the skin (normally located in the stratum corneum), assessment of bioavailability from blood levels is consequently not appropriate.

In addition to the pharmacokinetic studies, there are, at least, three notable methods to assess the bioavailability of a compound in the skin: tape-stripping, microdialysis (including open-flow microperfusion), punch biopsy and suction blister approaches.

Tape-stripping

Tape-stripping is a method for collection of stratum corneum. It is performed by placing an adhesive tape-strip onto the skin surface and subsequently removal. This action is then repeated on the same skin site, typically between 10 and 30 times. It can be used, in combination with analytical techniques, to measure the distribution of a molecule within the stratum corneum both *in vivo* and *in vitro* (Lademann et al., 2009), and to estimate the total thickness of the stratum corneum (Russell, Wiedersberg and Delgado-Charro, 2008).

Tape-stripping is relatively painless and non-invasive, given that only dead cells (corneocytes) embedded in their lipid matrix are removed. Due to the rapid repair response from the epidermis, the barrier function of the stratum corneum is soon restored (Menon, Feingold and Elias, 1992; Denda et al., 1996).

[2] Lidocaine is local anaesthetic agent where the site of action are nerve endings in the skin.

Weighing the tapes before and after the tape-stripping process allows estimation of the mass (m) of stratum corneum that has been removed. As the area (A) of stratum corneum stripped and the density (ρ) of the stratum corneum (normally assumed as 1 g cm^{-3} (Anderson and Cassidy, 1973)) are both known, it is possible to convert the stratum corneum weight into a depth (thickness) or distance (x), into the barrier (Equation 4).

$$x = \frac{m}{A \cdot \rho} \qquad \text{(Equation 4)}$$

The tapes are then extracted and quantified for the compound of interest. Using a combination of the estimated mass of stratum corneum and the concentrations of the molecule within the stratum corneum, a depth profile can be plotted. Figure 7 illustrates the steps normally followed for a tape-stripping experiment. Note that to estimate the mass of stratum corneum removed, the tapes are weighted before and after stripping.

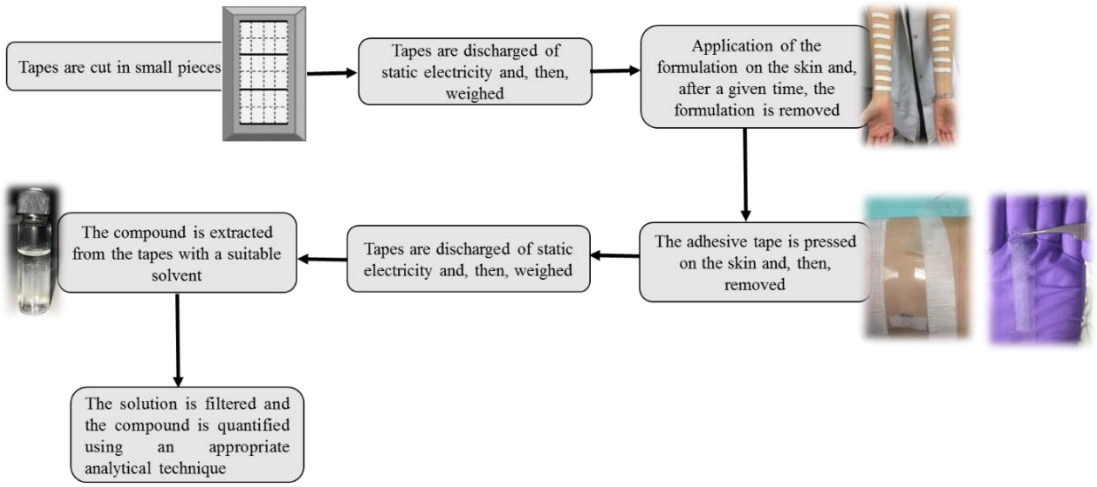

Figure 7. Method of tape-stripping

In general, the method development of a tape-stripping experiment consists of a series of preliminary tests performed to choose an optimal condition for a specific drug/formulation. Firstly, it is necessary to define the area of formulation application. It depends upon the ability of the drug to penetrate the stratum corneum: for a poorly penetrating drug, it may be necessary to increase the application area (and then the stripped area) to have enough drug in the tape strips for reliable quantification. The number of replicates and application time points desired are also important factors to be considered when developing the study protocol. After the desired application time,

the formulation is removed from the skin and, then, the stratum corneum sampling site is delimited by a template. The template is centred over the drug application site immediately before tape stripping begins. This template ensures that all tape strips are removed from the same site (and eliminates any potential problems created by the formulation spreading over the skin). The size of the piece of tape used for stripping is bigger than the opening in the template but smaller than the external dimensions of the template to ensure removing skin layers on the desired skin area only. The tape is applied to the template, pressed down, and then removed in one movement. The first tape strips remove a substantial amount of stratum corneum, which tends to progressively reduce as the stripping proceeds to the deeper layers.

The number of strips to collect depends upon the individual's SC thickness, formulation applied, the adhesiveness of the tape used, and whether or not it is necessary to completely remove the stratum corneum. The study protocol is often defined after a pilot study.

Quantification of the drug in the tape strips is generally made by high – performance liquid chromatography (HPLC) after a suitable extraction procedure. The principle of quantitation by HPLC is based on chromatographic separation of different compounds in a sample, followed by detection. The detection method can be UV, fluorescence, or mass spectrometry depending on the characteristic of the drug and the required detection limit. Interpretation of the data recorded by the detector produces quantitative and qualitative information about the sample and its constituents.

Chromatographic separation is achieved due to compounds having different relative affinity for a stationary phase (known as a column) versus affinity for the mobile phase (solvents). Separation is achieved by passing the mobile phase through the stationary phase under pressure. A HPLC system, as shown in Figure 8, is composed of some essential features: mobile phase, high pressure pump, sample injector, chromatographic column, detector and data acquisition system.

Careful selection of the mobile phase/stationary phase pair is of utmost importance for a successful chromatographic separation of the components of a sample. Therefore, knowledge of the physicochemical characteristics of analytes involved in the process is helpful to obtain the desired separation.

Silica has been the preferred starting material for the preparation of stationary phases as it is mechanically stable to high pressure, easily modified and is commercially available in a wide variety of particle sizes, shapes and sizes of pores.

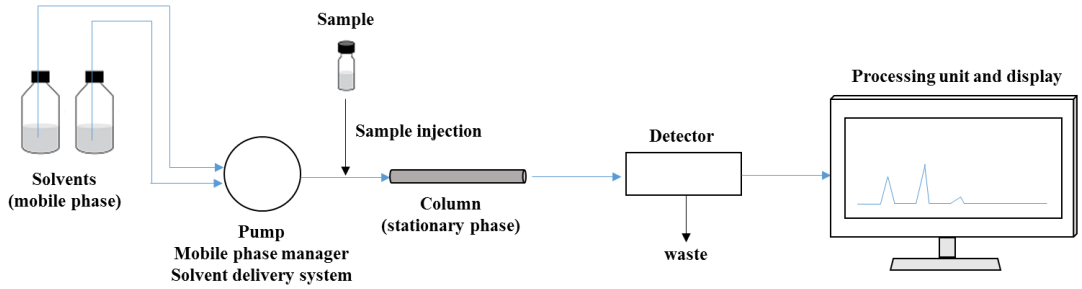

Figure 8. A High – Performance Liquid Chromatography (HPLC) system.

Simultaneous measurements of transepidermal water loss (TEWL) during the tape-stripping process can be performed. These measurements can be useful for estimating the total thickness of the stratum corneum and for estimating when stratum corneum sampling in the treated site is sufficient but not excessive.

Normally, when the aim is to estimate the total thickness of the stratum corneum, the TEWL measurements are made at a position adjacent to the treated skin – to avoid potential artefacts affecting TEWL, for example evaporation of residual excipients from the formulation. Baseline TEWL ($TEWL_0$) across unstripped stratum corneum of thickness L is given by Fick's first law of diffusion:

$$TEWL_0 = \frac{D \cdot K}{L} \Delta C \qquad \text{(Equation 5)}$$

where D and K are the diffusion coefficient of water in the stratum corneum and the stratum corneum - viable tissue partition coefficient of water, respectively, and ΔC is the water concentration gradient across the stratum corneum.

Subsequently, the stratum corneum is progressively removed by repeated adhesive tape-stripping and the TEWL is measured after each tape-strip removed. After tape-stripping has removed a depth x of stratum corneum, the TEWL will have increased to a new value given by:

$$TEWL_x = \frac{D \cdot K}{(L-x)} \Delta C \qquad \text{(Equation 6)}$$

Tape-stripping is continued until the TEWL reaches at least fourfold the initial value. This is to ensure that at least 75% of the stratum corneum is removed without,

however, complete derangement of the barrier (Kalia, Pirot and Guy, 1996; Kalia et al., 2000; Wiedersberg and Nicoli, 2012).

Based on Equation 6, Russell, Wiedersberg and Delgado-Charro (2008) developed a non-linear method which describes how transepidermal water loss increases as the stratum corneum barrier is removed (Equation 7). The advantage of Russell's method for thickness estimation is that it takes into account that the stratum disjunctum, i.e., the looser outer stratum corneum layer, does not provide a significant contribution to the barrier to water loss. Therefore, a more precise value of L can be determined.

$$TEWL_x = B + \frac{D \cdot K}{(L-x)} \Delta C \qquad \text{(Equation 7)}$$

The drawbacks of the tape-stripping technique include (mainly when assessing mass of stratum corneum by gravimetric means): the procedure is laborious and measurements of mass of stratum corneum can be influenced by environmental conditions (e.g., humidity) and static electricity. Nonetheless, it shows advantages over other methods of quantifying mass of stratum corneum on tapes (e.g., extraction and quantification of proteins from tapes using the protein assay, spectrophotometric examination of the tape), such as it is a direct measure of mass of both stratum corneum and compounds of interest.

Other *in vivo* approaches for measuring chemical compounds in the skin

Microdialysis, including open-flow microperfusion, is an *in vivo* technique for sampling free compound in the extracellular fluid within tissues (de Lange, de Boer and Breimer, 2000). Although this is a highly demanding approach as a routine method; the technique has many advantages, such as, continuous measurements of a compound concentration with time and the probe (ideally) inserted into the site of interest. Recently, a series of experiments performed by Bodenlenz et al. (2017) demonstrated the utility of open-flow microperfusion as a dermato-pharmacokinetic approach to evaluate dermal bioavailability. The technique was capable of measuring the penetration of topically applied acyclovir in human subjects *in vivo* with low variability.

Skin biopsy (invasive punch) is another approach used to assess the bioavailability of a compound in the skin. At first glance, the technique seems to be the most logical solution to measure the mass/concentration of a compound in the target tissue; however, the approach is unacceptable for routine use, especially considering the need to perform repeated biopsies to characterise the pharmacokinetic profile of the drug.

Suction blister has also been applied as an approach to assess the bioavailability of a compound in the skin (Treffel et al., 1991; Svedman and Svedman, 1998). The technique is performed by applying a partial negative pressure to the skin, which will disrupts the epidermal–dermal junction and forms a blister which fills progressively with interstitial fluid and serum (Volden et al., 1980). This liquid offers a pharmacokinetic 'compartment', therefore, in which a previously applied drug can be sampled and quantified; if multiple blisters are raised, then a concentration-time profile of the drug in the skin can be obtained. While on the surface attractive, this approach is also quite invasive and causes obvious scarring.

1.4.3 Mathematical methods

In parallel to the progression in experimental methods, mathematical modelling of dermal absorption has been demonstrated to be useful in predicting important parameters involved in skin absorption processes.

Several mathematical models have been developed to explain, at least in part, percutaneous absorption kinetics (Moss et al., 2002; Yamashita and Hashida, 2003; Lian, Chen and Han, 2008; Mitragotri et al., 2011). The main benefits of mathematical models over experimental measurements include reduction of resources (refining and reducing the need of experiments) and avoiding ethical issues. In addition, the models may assist in the better understanding of mechanisms of absorption (Tsakovska et al., 2017).

The principal objectives of a mathematical model is to (i) be able to represent the processes associated with absorption accurately, (ii) be able to describe/summarise experimental data with parametric equations, and (iii) predict kinetics under varying conditions (Roberts, Anissimov and Gonsalvez, 2001).

1.4.3.1 Steady-state membrane models

The fundamental equation to describe the transport of a chemical compound through the skin under steady-state conditions can be given by Fick's first law (Equation 8). It is worth pointing out that steady-state can only be reached after the lag time for diffusion of the permeant has passed. The lag time (T_{Lag}) can be mathematically described by Equation 9 and can be estimated from the x-intercept of the linear portion of the plot representing cumulative solute permeation as a function of time. T_{Lag} is related to the time necessary to establish a linear concentration profile across the barrier (~2.4 T_{Lag} (Cleek and Bunge, 1993)).

$$Q = \frac{DAT\Delta C_s}{L} \qquad \text{(Equation 8)}$$

$$T_{Lag} = \frac{L^2}{6D} \qquad \text{(Equation 9)}$$

where Q is the amount of solute crossing the skin membrane of area, A, over a time period, T. C_s is the (constant) concentration gradient across the two interior surfaces of the skin, D is the diffusion coefficient in the skin membrane and L is the diffusion pathlength (or the thickness of the membrane). It is important saying that Equations 8 and 9 assume that the skin barrier behaves as a homogeneous membrane, which means that its properties do not vary with time and/or position.

Equation 8 can also be expressed in terms of steady-state skin flux, J_{ss}, defined as:

$$J_{SS} = \frac{Q}{AT} = \frac{D\Delta C_s}{L} \qquad \text{(Equation 10)}$$

Assuming the stratum corneum as the rate-limiting barrier for skin drug permeation, the maximum flux (J_{max}) can be expressed in terms of thermodynamic activity (Higuchi, 1960). Therefore, J_{max} will be reached when maximum solubility of a solute in the stratum corneum is achieved, so that Equation 10 can be written as (Equation 11):

$$J_{max} = \frac{DK_{SC,v}C_{v,sat}}{L} \qquad \text{(Equation 11)}$$

where D is its diffusion coefficient in the stratum corneum, $K_{SC/V}$ is the partition coefficient of the permeant between the stratum corneum and the vehicle and $C_{v,sat}$ is the saturation concentration of the permeant in the vehicle. The diffusion coefficient measures how easily the permeant traverses the stratum corneum, while $K_{SC,v}$

describes the distribution of the permeant between the stratum corneum and the vehicle, and reflects the ratio of the compound's solubilities in these two phases (Equation 12):

$$K_{SC,v} = \frac{C_{SC,sat}}{C_{v,sat}} \quad \text{(Equation 12)}$$

where $C_{SC,sat}$ is the saturation concentration of the permeant in the stratum corneum.

The next section will further develop these principles to demonstrate the predictive value of mathematical models of skin permeability in defining the absorption of therapeutic and toxic compounds through the skin.

1.4.3.1.1 Quantitative structure–permeation relationship (QSPR) models

Quantitative-structure permeability relationships (QSPRs) are among the most intensively researched area, which correlate skin permeability to the structure of the permeant, described by physicochemical properties and other structural descriptors. These models rely on experimental data for skin permeability and build quantitative correlations using statistical approaches (e.g., multilinear regressions).

The main focus of QSPRs has been the assessment of a permeability coefficient (k_p) which is defined as the steady-state flux of compound across the skin (J_{ss}) normalised by the concentration gradient, ΔC_v:

$$k_p = \frac{J_{ss}}{\Delta C_v} \quad \text{(Equation 13)}$$

Often the concentration of the compound is essentially zero on one side of the skin ('sink conditions') and k_p is then the ratio of J_{ss} and C_v. By describing the skin as a homogeneous membrane, k_p can be defined as (Crank, 1975):

$$k_p = \frac{K \times D}{L} \quad \text{(Equation 14)}$$

where K is the partition coefficient between skin-membrane. By assuming that the stratum corneum is the rate limiting barrier, which is often the case, and by using L as the thickness of the stratum corneum, then K and D in Equation 14 describe the partitioning and diffusion in the stratum corneum treated as a homogeneous membrane.

Knowledge of both k_p and $C_{v,sat}$ permits an estimation of the maximum flux (J_{max}) of the molecule across the barrier (Equation 15):

$$J_{max} = k_p \times C_{v,sat} \quad \text{(Equation 15)}$$

Most QSPR models provide algorithms to calculate k_p when the vehicle is assumed to be aqueous. A very frequently cited QSPR model is reported by Potts and Guy (1992). This model is based on Flynn's dataset (93 compounds) (Flynn, 1990). The best fit of the equation was (Equation 16):

$$\log k_p\ (\text{cm h}^{-1}) = -2.72 + 0.71 \log P - 0.0061 MW \quad \text{(Equation 16)}$$

which had an overall correlation coefficient (r^2) of 0.67. The experimental values used to derive Equation 16 included chemicals with MWs ranging from 18 to over 750 and log P values from −3 to +6. The model clearly shows that small, lipophilic chemicals are those with the greatest skin permeabilities. Given the typical level of variability in skin permeability measurements, the Potts and Guy equation performs well and certainly provides reasonable predictions. However, the approach focuses on the stratum corneum as the exclusive rate-limiting barrier and therefore significantly overestimates k_p for highly lipophilic compounds. This issue was successfully addressed by Cleek and Bunge (Cleek and Bunge, 1993; Bunge and Cleek, 1995), whereby a corrected k_p value for lipophilic compounds ($k_{p(corr)}$) may be calculated using Equation 17:

$$k_{p(corr)} = \frac{k_p}{1+\left(\frac{k_p+\sqrt{MW}}{2.6}\right)} \quad \text{(Equation 17)}$$

where k_p is calculated from the Potts and Guy correlation (Equation 16).

Many other QSPR models have been proposed and compared. For example, Lian, Chen and Han (2008) compared seven mathematical models using an experimental dataset of skin permeability for 124 chemical compounds compiled from various sources. They conclude that Potts and Guy correlation and a model developed by Mitragotri (2002) give the best predictions. It is important to say that both models have many features in common.

Beyond the estimation of the permeability coefficient, QSPR relationships have also been used for estimation of the partition coefficients. Experimentally,

partition coefficient values can be obtained from equilibration experiments between a skin membrane and a solution of the compound of interest. Kretsos et al. (2008) investigated the partition coefficients between the dermis and water (K_{de}). The analysis was carried out on an experimentally obtained dataset of 26 chemicals ranging in MW from 18 – 476 Da and four species (human, guinea pig, rat and mouse). After experimental work, a mathematical model was developed to predict K_{de} (Equation 18). The K_{de} model involved ionization, binding to extravascular serum proteins and partitioning into a lipid compartment.

$$K_{de} = 0.6 \times \left(0.68 + \frac{0.32}{F_u} + 0.001 \times F_{non} \times P\right) \quad \text{(Equation 18)}$$

where f_{non} is the non-ionized the fraction of the compound in aqueous phase and f_u is the fraction of compound not bound to albumin.

More recently, Yun and Edginton (2013) developed an algorithm able to predict partition coefficients between skin and plasma $K_{(skin/p)}$. The prediction models use physicochemical descriptors of the compound (log P, degree of ionization (F_i) and plasma protein binding ($F_{u,p}$)) and organism-specific data (rat volume of distribution at steady-state). Table 1 shows the best correlations found for predicting the log of $K_{(skin,p)}$ for strong to moderate bases (pKa ≥ 7.4, model 1) and for acids, weak bases and neutral compounds (pKa ≤ 7.4, model 2).

Table 1. Mathematical models for predicting log of skin-to-plasma partition coefficient ($K_{(skin/p)}$). Table adapted from Yun and Edginton (2013).

Model	Regression models	n	R^2
1	$\log K_{(skin/p)} = -0.14 + 0.66(\log V_{ss}) + 0.03(\log P)$	28	0.80
2	$\log K_{(skin/p)} = -0.33 + 0.54(\log V_{ss}) + 0.16(\log P) - 0.32(F_i) + 0.38(F_{u,p})$	26	0.73

Despite being extremely useful, QSAR model concepts typically cannot provide information about the change of concentration in the barrier over time. Another drawback is the lack of predictive confidence of most models when using values of input parameters outside the range of values of the training set (Selzer, Neumann and Schaefer, 2015).

1.4.3.2 Non-steady-state membrane models

While Fick's first law assumes steady-state, Fick's second law predicts changes in the concentration gradient, through diffusion, with time. According to Fick's second law, the concentration of a compound across a membrane, normally designated by C(t,x), where t is the period of time, can be estimated by the solution of the following linear one-dimensional diffusion equation (Equation 19):

$$\frac{\partial \mathrm{C}}{\partial \mathrm{t}} = -\mathrm{D}\frac{\partial^2 C}{\partial x^2} \qquad \text{(Equation 19)}$$

where D is the diffusion coefficient which is assumed to be constant across the membrane. The negative sign means that the diffusion occurs in the direction of decreasing concentration; thus, the flux is always positive. C is the concentration of compound, in the skin, x is the depth (thickness) of skin.

Additional terms can be included to address peculiarities of the skin barrier, for example binding phenomena (Frasch et al., 2011), enzymatic activity (Guy, Hadgraft and Bucks, 1987), corneocyte desquamation (Reddy, Guy and Bunge, 2000), or to model elimination or clearance of molecules from the stratum corneum (Nicoli et al., 2009).

The concentration profiles of a drug as a function of the relative position in the stratum corneum (x/L) have typically been fitted to a solution of Equation 20, assuming the following boundary conditions: i) the concentration of the permeant in the vehicle at the surface of the stratum corneum is constant; ii) that the stratum corneum is initially free of the permeant; iii) that the stratum corneum is homogeneous in its barrier properties; and iv) that the viable epidermis provides a perfect sink for permeation. Under these circumstances, the concentration (C_x) of permeant, as a function of application time (t_{app}) and of position (x) in the SC of total thickness (L) is given by a solution of Fick's second law:

$$\mathrm{C_x} = \mathrm{KC_v}\left[1 - \frac{\mathrm{x}}{\mathrm{L}} - \frac{2}{\pi}\sum_{\mathrm{m}=1}^{\infty}\frac{\exp\left[-\mathrm{m}^2\pi^2\mathrm{t_{app}}\left(\mathrm{D}/\mathrm{L}^2\right)\right]\sin\left(\mathrm{m}\pi\mathrm{x}/\mathrm{L}\right)}{\mathrm{m}}\right] \qquad \text{(Equation 20)}$$

where C_v is the concentration of the permeant in the vehicle. By fitting the concentration profile to this equation, estimates of the compound's stratum corneum–vehicle partition coefficient (K) and its characteristic diffusion parameter (D/L^2, which has units of $[time]^{-1}$ like a first order rate constant) can be obtained.

Herkenne et al. (2007) using the K and D/L^2 values obtained from a 30 - minute exposure, satisfactorily predicted ibuprofen uptake for longer application times (Figure 8), suggesting that reliable and quantitative information can be obtained with this approach. A similarly good prediction was obtained for terbinafine (Alberti et al., 2001) and betamethasone 17-valerate delivery (Wiedersberg, Leopold and Guy, 2009).

An important issue, when using this approach, is the choice of the exposure period used for the determination of K and D/L^2. This period should be long enough to allow the achievement of a measurable profile inside the stratum corneum, but not so long that the steady state has been reached. In the latter case, the profile inside the membrane becomes linear (see Figure 9), information on the diffusive parameter D/L^2 is lost and Equations 20 simplifies to (Equation 21):

$$C_x = KC_v\left(1 - \frac{x}{L}\right) \qquad \text{(Equation 21)}$$

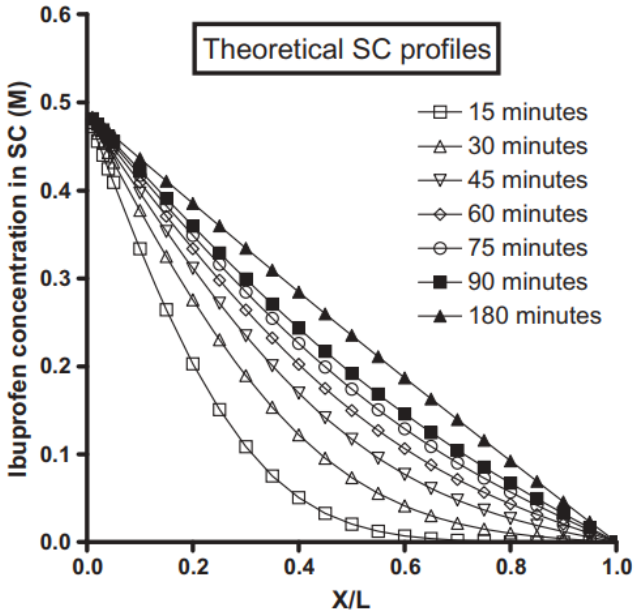

Figure 9. Concentration-depth profiles following Equation 20, at increasing times, showing the kinetics of a diffusion process from short times (exponential decay) until steady-state (straight line). (Herkenne et al., 2007). Permission to reproduce this image has been granted by the publisher.

To investigate the time variation of the mass of compound in the stratum corneum, two mechanistic models were derived by Cleek and Bunge (1993). One considers the

stratum corneum where it is assumed that the membrane is sufficiently thick and the exposure time short enough, such that it behaves as a semi-infinite membrane (Equation 22). The other considers the stratum corneum as a single finite membrane (Equation 23).

$$\frac{M_{SC}}{A} = 2KC_v\sqrt{\frac{Dt_{app}}{\pi}} \qquad \text{(Equation 22)}$$

$$\frac{M_{SC}}{A} = KC_v\,L\left[\frac{1}{2} - \frac{4}{\pi}\sum_{n=0}^{\infty}\frac{\exp[-D(2n+1)^2\pi^2(t_{app}/L^2)]}{(2n+1)^2}\right] \qquad \text{(Equation 23)}$$

For short application times, when the compound has not reached the bottom of the stratum corneum, Equations 22 and 23 are applicable. Equation 23 is important for longer exposure times, when the compound has 'discovered' the lowest layer of the stratum corneum.

1.4.3.2.1 Compartmental models

Compartmental (or pharmacokinetic) models are often used to study the fate of chemical compounds entering and leaving the body. These models treat the skin as one or more well-stirred compartments, which eliminates the space dependency of the partial differential diffusion equation (Equation 20) and results in a series of ordinary differential equations (ODEs) that describe the change of amount of solute in different compartments over time. The transfer between the compartments is described by first-order rate constant expressions.

When skin is included in these models, it is usually represented either as a single compartment or by two compartments, separately distinguishing the lipophilic (stratum corneum) and hydrophilic layers (viable epidermis and dermis) of the skin. Figure 10 illustrates two simple examples of skin compartment models: a model which uses only a single compartment to account for the skin (one-compartment skin model) and a model which uses two compartments to represent the skin (two-compartment skin model). In a one-compartment model, the skin compartment may represent the stratum corneum alone, the viable epidermis alone, the epidermis, or the epidermis *plus* dermis. In a two-compartment model, the first skin compartment usually represents the stratum corneum and the second, the viable epidermis (or the viable

epidermis *plus* dermis). In addition to the skin compartment(s), one compartment represents the vehicle and one compartment is used to represent the blood (or receptor solution in *in vitro*/*ex vivo* diffusion cell experiments).

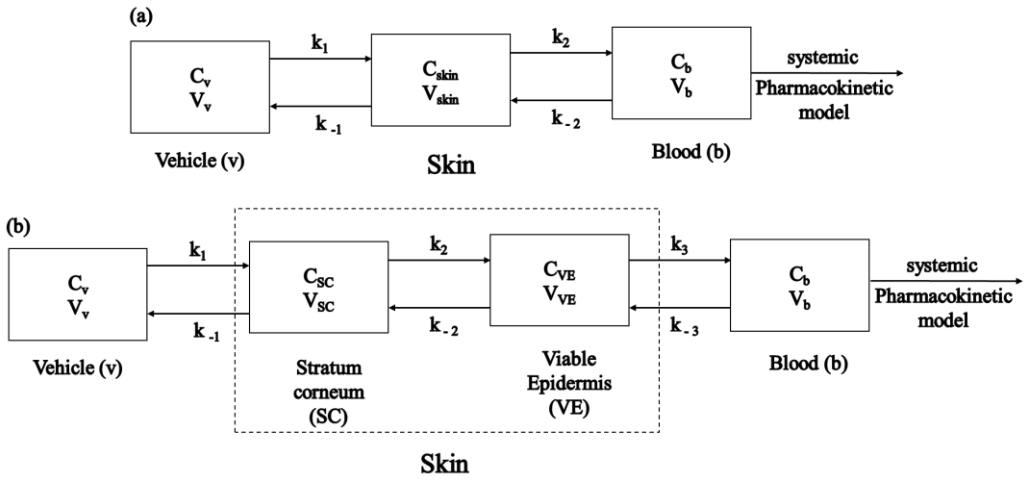

Figure 10. Schematic diagrams of (a) one-compartment and (b) two-compartment models. C denotes the average concentration in the compartment and V is the volume of the compartment.

When the compartment model is used to analyse *in vivo* experiments, the dermis is completely vascularised, and blood flow removes the compound from the dermis quickly. Consequently, the dermis does not separate the viable epidermis from the blood compartment and the viable epidermis compartment should include only the viable epidermis. However, when the compartment model is used to analyse *in vitro* experiments, the blood compartment in Figure 9 represents the receptor chamber and compounds must diffuse across all skin layers present in the experiment (i.e., the stratum corneum only, the epidermis only, or the epidermis *plus* dermis) to reach the receptor chamber. In this case, both the viable epidermis and dermis (or portions thereof) should be included in the skin description.

In the most common exposure scenario, chemical transfers from the vehicle into, eventually, the blood stream. However, the actual direction of transfer depends on the concentration gradient of the chemical in the skin, and transfer from blood to vehicle can, theoretically, occur if the concentration in the blood is large relative to the vehicle. To allow for transfer in both directions and to make transfer stop when the concentration gradient reaches zero, both forward rate constants (e.g., k_1) and reverse rate constants (e.g., k_{-1}) are included in compartment models.

A differential mass balance of chemical in the one-compartment skin layer produces the following equation (Equation 24):

$$V_{skin}\frac{\partial C_{skin}}{\partial t} = k_1 C_v - k_{-1} C_{skin} - k_2 C_{skin} + k_{-2} C_{blood} \quad \text{(Equation 24)}$$

where C_{skin} is the averaged concentration in the skin layer. For a two-compartment model, differential mass balances of chemical in each layer produce the following equations (Equations 25 and 26):

$$V_{sc}\frac{\partial C_{sc}}{\partial t} = k_1 C_v - k_{-1} C_{sc} - k_2 C_{sc} + k_{-2} C_{ve} \quad \text{(Equation 25)}$$

$$V_{ve}\frac{\partial C_{ve}}{\partial t} = k_2 C_{sc} - k_{-2} C_{ve} - k_3 C_{ve} + k_{-3} C_b \quad \text{(Equation 26)}$$

where C_{sc} and C_{ve} are the averaged concentrations in the stratum corneum and viable epidermis (or the combined viable epidermis and dermis for *in vitro* experiments that include dermis), respectively.

One drawback of compartmental models is that, in the majority of these models, values for rate constants were estimated by fitting experimental data without relating the result to the physiological and physical parameters of skin (McCarley and Bunge, 2001). The integration of these experimental data with subsequent events in the body [via physiologically-based pharmacokinetics (PBPK)] has been more often seen in the toxicological rather than pharmaceutical publications. However, the use of PBPK modelling for multicomponent systems, such as topical drug products, that are applied on the skin is a technique that has gained attention in recent years (Polak et al., 2012; Chen et al., 2015).

In general, PBPK models can be used to describe a variety of exposure routes (e.g., inhalation, oral, intravenous, or dermal). PBPK models are constructed from mathematical descriptions of system-dependent parameters that include species-specific anatomy and physiology information (i.e., tissue volume, blood flow, glomerular filtration rate, plasma protein and enzyme abundance) and of drug-dependent parameters (e.g., molecular weight, solubility, pKa and log P) (van der Merwe et al., 2005). This approach involves a mechanistic description of processes involved in absorption, disposition and elimination of administered compounds into and from different compartments/organs. The advantages of PBPK models are, however, difficult to realise because the necessary anatomical and physiological

parameters are often not available, and the processes are not well understood. This can result in oversimplification of the physiological processes involved, which limits the advantage of PBPK models over traditional compartmental models.

In summary, membrane models more accurately represent the physiological character of skin with respect to the dermal absorption process. However, mathematical solutions of membrane models can be cumbersome. On the other hand, compartmental models treating the skin as a well-stirred compartment(s) offer simplified mathematics for these situations. Nevertheless, relating compartment model rate constants to physiological parameters is still a challenge.

1.5 Transdermal drug delivery

Transdermal products have unique advantages relative to other dosage forms and routes of administration. They can provide several advantages (when compared with other administration routes), such as: sustained drug delivery for several days, avoidance of first pass metabolism of a drug by the liver and the option to remove at any time to stop drug delivery, if needed.

Currently, there are 18 transdermal drugs (Table 2) present in over 25 FDA-approved products (FDA Orange Book database of the end of 2017). These systems are, usually, complex drug-device combination products that may be broadly categorised as having either a reservoir or a matrix design. A reservoir-type patch holds the drug in a solution or gel, from which drug delivery can be governed by a rate-controlling membrane positioned between the drug reservoir and skin. Reservoir-type patches offer an advantage over matrix-type patches in terms of formulation flexibility and tighter control over delivery rates, although they can have an initial burst of drug release. Reservoir-type patches usually involve greater design complexity. By contrast, matrix-type patches, which were introduced after reservoir-type patches, combine the drug, adhesive and mechanical backbone of the patch into a simpler design that does not involve a rate-controlling membrane; skin permeability usually governs the rate of drug delivery. Although these patches are easier to fabricate, they have limited flexibility in their design compared with reservoir-type patches (Prausnitz, Mitragotri and Langer, 2004).

Although, transdermal drug delivery aims to deliver the active to the systemic circulation, in comparison with intravenous or oral administration, the kinetics of transdermal delivery into the systemic circulation can be distinctive due to the significant differences in absorption rates. In general, the absorption rate constant of a compound after oral administration is greater than its elimination rate constant from the body. On the other hand, for transdermal delivery, absorption rate constant can be much slower than elimination, leading to so-called 'flip–flop kinetics' where the usual rate-dependence on elimination observed from oral (immediate release products) and intravenous administration is 'flipped', and the absorption rate becomes the rate-determining step (Figure 11) (Oliyai and Stella, 1993; Lefevre et al., 2007).

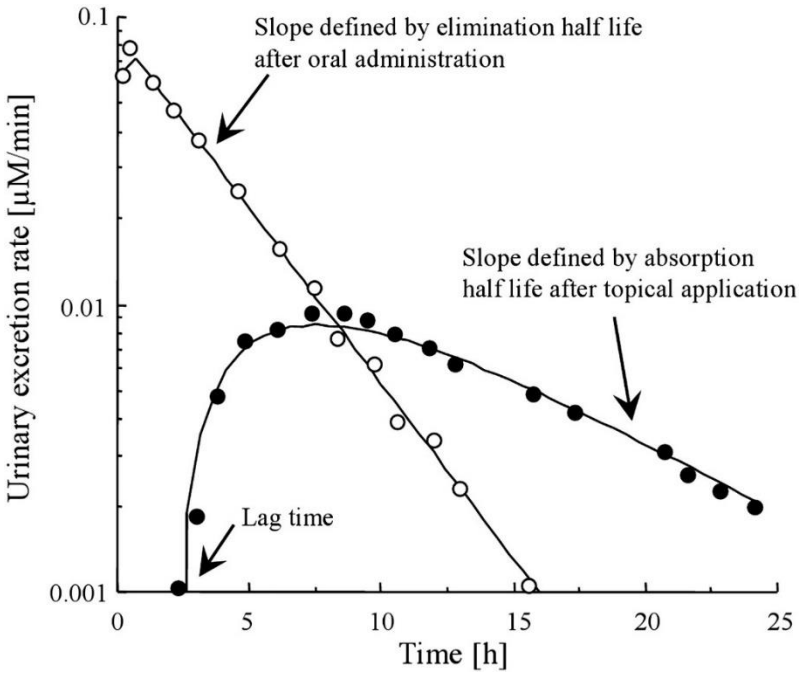

Figure 11. Demonstration of 'flip–flop' kinetics, comparing the terminal phase either rate-limited by the drug disposition kinetic (oral administration, open circles) or by the drug absorption kinetics (topical administration, closed circles). (Jepps et al., 2013). Permission to reproduce this image has been granted by the publisher.

Although, transdermally delivered drugs are not meant to target structures within the skin, they use the skin as an entrance and provide valuable information about a drug's transport from the skin surface to the systemic compartment. To be specific, for all transdermal patches currently approved, there are published pharmacokinetic data telling the drug input-rate and resulting systemic plasma concentration levels during patch wear and after removal. In contrast, topical

dermatological products, such as creams, ointments and gels, or even in topical patches, designed to produce a local effect (for example, to treat joint pain), the rate of drug entering the skin is not well characterised.

Therefore, it is clear that as the true input-rate is known, the transdermal products can be useful for assessing the validity of experimental approaches for determining input-rates from dermatological and locally acting topical products.

Table 2. FDA-approved transdermal patches.

Drug	Trade name	Patch design	Strength (mg)	Active delivery area (cm^2)	Input-rate ($\mu g\ cm^{-2}\ h^{-1}$)	Labelled application period
Buprenorphine	Butrans®	Matrix	5.0 – 20.0	6.2 – 25[a]	0.8	7 days
Clonidine	Catapress-TTS®	Reservoir	2.5 – 7.5	3.5 – 10.5	1.2	7 days
Estradiol[b]	Estraderm®	Reservoir	4.0 – 8.0	10 – 20	0.2	3 – 4 days
	Climara®	Matrix	2.0 – 7.6	6.5 – 25	0.2	7 days
	Vivelle®	Matrix	4.3 – 8.7	14.5 – 29	0.1	3 – 4 days
	Alora®	Matrix	0.77 – 3.1	9 – 26	0.1	3 – 4 days
	Vivelle-dot®	Matrix	0.39 – 1.56	2.5 – 10	0.4	3 – 4 days
	Menostar®	Matrix	1.0	3.25	0.2	7 days
	Minivelle®	Matrix	0.62 – 1.65	2.48 – 6.6	0.6	3 – 4 days
Estradiol (E) & Norethisterone Acetate[c] (NAc)	Combipatch®	Matrix	E/NAc: 0.6/2.7 & 0.51/4.8	9 – 16	E/NAc: 0.2/0.4	3 – 4 days
Estradiol (E) & Levonorgestrel (L)	Climara Pro®	Matrix	E/L: 4.4/1.39	22	E/L: 0.09/0.03	7 days
Ethinyl estradiol (EE) & Norelgestromin[d] (N)	Xulane®	Matrix	EE/N: 0.53/4.86	14	EE/N: 0.1/0.4	7 days
Fentanyl	Duragesic®	Matrix	1.55 – 12.4	5.5 - 44	2.3	72 h
Glyceryl Trinitrate[e]	Nitro-Dur®	Matrix	20 – 160	5 – 40	20	12 – 14 h
	Minitran®	Matrix	9 – 54	3.3 – 20	11.1	12 – 14 h
Granisetron	Sancuso®	Matrix	34.3	52	2.5	Up to 7 days
Methylphenidate	Daytrana®	Matrix	27.5 – 82.5	12.5 – 37.5	~ 87	Up to 9 h
Nicotine	Nicoderm CQ®	Reservoir	36 – 114	10 – 30	29.2	24 h
	Habitrol®	Matrix	36 – 114	10 – 30	29.2	24 h
Oxybutynin	Oxytrol®	Matrix	36	39	4.2	3 – 4 days
Rivastigmine	Exelon®	Matrix	9 – 27	5 – 15	~ 38	24 h
Rotigotine	Neupro®	Matrix	2.25 – 18	5 – 40	8.3	24 h
Scopolamine	Transderm Scop®	Reservoir	1.5	2.5	5.5	72 h
Selegiline	Emsam®	Matrix	6 – 12	20 – 40	12.5	24 h
Testosterone	Androderm®	Reservoir	9.7 – 24.3	6 – 15[f]	13.9	24 h

[a]Size of the patch reported corresponds to the active area, size of the patch are from 20.25 – 51.84 cm^2; [b]Also spelled as Oestradiol; [c]Also spelled as Norethindrone acetate; [d]Also spelled as Norelgestromine; [e]Also known as Nitroglycerine; [f]Size of the patch reported corresponds to the active area, size of the patch are from 32 – 44 cm^2.

2. Aims and organisation of the thesis

This project aims to characterise, and obtain mechanistic insight, into topical dermal delivery. The main target of this work is to explore whether a drug could achieve an effective concentration at the target tissue by tracking the drug behaviour following skin application. The generalised model describing drug concentration in a tissue is dependent on the drug input into the skin and its clearance therefrom. Therefore, these two main processes (input into the skin and clearance from the skin) were investigated. The influence of other components commonly present in topical formulations, which potentially will act as penetration enhancers, on drug absorption was also evaluated.

The work described in Chapter 2 focused on characterising the input functions of two transdermal drugs, buprenorphine and nicotine, from commercially available patches. The characterisation was performed experimentally using *in vitro* permeation tests. In addition, the input-rate of diclofenac from a medicated plaster, which is indicated for a local effect, was determined using the same approach as demonstrated for the transdermal drugs.

In Chapter 3 a further investigation of the behaviour of diclofenac in the stratum corneum was taken. The uptake of diclofenac into the stratum corneum and its clearance therefrom following application of a medicated plaster was investigated *in vivo* in human.

The results described in chapter 3 suggested that diclofenac uptake into the stratum corneum may be modified by the presence of excipient(s). Therefore, the work described in Chapter 4 focused on exploring the uptake of two excipients/co-solvents, propylene glycol and butylene glycol, into the stratum corneum *in vivo* in human, following application of the diclofenac medicated plaster.

The work described in Chapter 5 investigated the hypothesis that information about clearance from the skin can be derived from available systemic pharmacokinetic data for drugs administered via transdermal delivery systems. A statistical mathematical model describing drug clearance from the skin in terms of drug molecular descriptors was developed.

Finally, Chapter 6 summarises the key findings from each chapter and presents recommendations for future work.

References

Alberti, I., Kalia, Y.N., Naik, A. and Guy, R.H., 2001. Assessment and prediction of the cutaneous bioavailability of topical terbinafine, *in vivo*, in man. *Pharmaceutical Research,* 18(10), pp. 1472-1475.

Anderson, R.L. and Cassidy, J.M., 1973. Variations in physical dimensions and chemical composition of human stratum corneum. *Journal of Investigative Dermatology,* 61(1), pp. 30-32.

Barbero, A.M. and Frasch, H.F., 2009. Pig and guinea pig skin as surrogates for human in vitro penetration studies: A quantitative review. *Toxicology in Vitro,* 23(1), pp. 1-13.

Benson, H.A., 2012. Skin structure, function, and permeation. *Topical and Transdermal Drug Delivery: Principles and Practice; Benson, HA, Watkinson, AC, Eds.*

Bodenlenz, M., Tiffner, K.I., Raml, R., Augustin, T., Dragatin, C., Birngruber, T., Schimek, D., Schwagerle, G., Pieber, T.R. and Raney, S.G., 2017. Open flow microperfusion as a dermal pharmacokinetic approach to evaluate topical bioequivalence. *Clinical pharmacokinetics,* 56(1), pp. 91-98.

Bos, J.D. and Meinardi, M.M., 2000. The 500 Dalton rule for the skin penetration of chemical compounds and drugs. *Experimental Dermatology: Viewpoint,* 9(3), pp. 165-169.

Bouwstra, J., Peschier, L., Brussee, J. and Boddé, H., 1989. Effect of N-alkyl-azocycloheptan-2-ones including azone on the thermal behaviour of human stratum corneum. *International Journal of Pharmaceutics,* 52(1), pp. 47-54.

Brouwers, J., Brewster, M.E. and Augustijns, P., 2009. Supersaturating drug delivery systems: the answer to solubility-limited oral bioavailability? *Journal of Pharmaceutical Sciences,* 98(8), pp. 2549-2572.

Bunge, A.L. and Cleek, R.L., 1995. A new method for estimating dermal absorption from chemical exposure: 2. Effect of molecular weight and octanol-water partitioning. *Pharmaceutical Research,* 12(1), pp. 88-95.

Bunge, A.L., Guy, R.H. and Hadgraft, J., 1999. The determination of a diffusional pathlength through the stratum corneum. *International Journal of Pharmaceutics,* 188(1), pp. 121-124.

Chen, L., Han, L., Saib, O. and Lian, G., 2015. *In silico* prediction of percutaneous absorption and disposition kinetics of chemicals. *Pharmaceutical Research,* 32(5), pp. 1779-1793.

Clark, D.E., 1999. Rapid calculation of polar molecular surface area and its application to the prediction of transport phenomena. 2. Prediction of blood–brain barrier penetration. *Journal of Pharmaceutical Sciences,* 88(8), pp. 815-821.

Cleek, R.L. and Bunge, A.L., 1993. A new method for estimating dermal absorption from chemical exposure. 1. General approach. *Pharmaceutical Research,* 10(4), pp. 497-506.

Cnubben, N.H., Elliott, G.R., Hakkert, B.C., Meuling, W.J. and van de Sandt, J.J., 2002. Comparative *in vitro–in vivo* percutaneous penetration of the fungicide ortho-phenylphenol. *Regulatory Toxicology and Pharmacology,* 35(2), pp. 198-208.

Cohen, M.H. and Turnbull, D., 1959. Molecular transport in liquids and glasses. *The Journal of Chemical Physics,* 31(5), pp. 1164-1169.

de Lange, E.C.M., de Boer, A.G. and Breimer, D.D., 2000. Methodological issues in microdialysis sampling for pharmacokinetic studies. *Advanced Drug Delivery Reviews,* 45(2), pp. 125-148.

Delgado-Charro, M.B. and Guy, R.H., 2001. Transdermal iontophoresis for controlled drug delivery and non-invasive monitoring. *STP Pharma Sciences,* 11(6), pp. 404-414.

Denda, M., Wood, L.C., Emami, S., Calhoun, C., Brown, B.E., Elias, P.M. and Feingold, K.R., 1996. The epidermal hyperplasia associated with repeated barrier disruption by acetone treatment or tape stripping cannot be attributed to increased water loss. *Archives of Dermatological Research,* 288(5-6), pp. 230-238.

Elias, P.M., 1983. Epidermal lipids, barrier function, and desquamation. *Journal of Investigative Dermatology,* 80.

Elias, P.M., Cooper, E.R., Korc, A. and Brown, B.E., 1981. Percutaneous transport in relation to stratum corneum structure and lipid composition. *Journal of Investigative Dermatology,* 76(4), pp. 297-301.

Fan, Q., Sirkar, K.K. and Michniak, B., 2008. Iontophoretic transdermal drug delivery system using a conducting polymeric membrane. *Journal of Membrane Science,* 321(2), pp. 240-249.

FDA, 2016. *Draft Guidance on Lidocaine* [Online]. Food and Drug Administration. Available from: *https://www.fda.gov/downloads/drugs/guidancecomplianceregulatoryinformation/guidances/ucm086293.pdf* [Accessed 16/07/2018].

Fluhr, J.W., Feingold, K.R. and Elias, P.M., 2006. Transepidermal water loss reflects permeability barrier status: validation in human and rodent in vivo and ex vivo models. *Experimental Dermatology,* 15(7), pp. 483-492.

Flynn, G., 1990. Principles of route-to-route extrapolation for risk assessment. *Physicochemical Determinants of Skin Absorption*, pp. 93-127.

Frasch, H.F., Barbero, A.M., Hettick, J.M. and Nitsche, J.M., 2011. Tissue binding affects the kinetics of theophylline diffusion through the stratum corneum barrier layer of skin. *Journal of Pharmaceutical Sciences,* 100(7), pp. 2989-2995.

Frederiksen, K., Guy, R.H. and Petersson, K., 2016. The potential of polymeric film-forming systems as sustained delivery platforms for topical drugs. *Expert Opinion on Drug Delivery,* 13(3), pp. 349-360.

Garg, T., Rath, G. and Goyal, A.K., 2015. Comprehensive review on additives of topical dosage forms for drug delivery. *Drug Delivery,* 22(8), pp. 969-987.

Gauglitz, G.G. and Schauber, J., 2013. Skin: Architecture and Function. *Dermal Replacements in General, Burn, and Plastic Surgery.* Springer, pp. 1-11.

Gray, G.M. and White, R.J., 1978. Glycosphingolipids and ceramides in human and pig epidermis. *Journal of Investigative Dermatology,* 70(6), pp. 336-341.

Guy, R., 2013. Skin-‘that unfakeable young surface'. *Skin Pharmacology and Physiology*, 26(4-6), pp. 181-189.

Guy, R., 2016. Topical Drug Delivery. *Rook's textbook of dermatology.* Ninth ed.: John Wiley & Sons, pp. 1-10.

Guy, R., Hadgraft, J. and Bucks, D., 1987. Transdermal drug delivery and cutaneous metabolism. *Xenobiotica,* 17(3), pp. 325-343.

Haake, A., Scott, G.A. and Holbrook, K.A., 2001. Structure and function of the skin: overview of the epidermis and dermis. *The Biology of the Skin,* 2001, pp. 19-45.

Hadgraft, J., 2000. Skin, the final frontier. *International Journal of Pharmaceutics,* 224, pp. 1-18.

Hadgraft, J., 2004. Skin deep. *European Journal of Pharmaceutics and Biopharmaceutics,* 58(2), pp. 291-299.

Harrison, J.E., Watkinson, A.C., Green, D.M., Hadgraft, J. and Brain, K., 1996. The relative effect of Azone® and Transcutol® on permeant diffusivity and solubility in human stratum corneum. *Pharmaceutical Research,* 13(4), pp. 542-546.

Hatanaka, T., Shimoyama, M., Sugibayashi, K. and Morimoto, Y., 1993. Effect of vehicle on the skin permeability of drugs: polyethylene glycol 400-water and ethanol-water binary solvents. *Journal of Controlled Release,* 23(3), pp. 247-260.

Herkenne, C., Naik, A., Kalia, Y.N., Hadgraft, J. and Guy, R.H., 2007. Dermatopharmacokinetic prediction of topical drug bioavailability *in vivo*. *Journal of Investigative Dermatology,* 127(4), pp. 887-894.

Herkenne, C., Naik, A., Kalia, Y.N., Hadgraft, J. and Guy, R.H., 2008. Effect of propylene glycol on ibuprofen absorption into human skin in vivo. *Journal of Pharmaceutical Sciences,* 97(1), pp. 185-197.

Higuchi, T., 1960. Physical chemical analysis of percutaneous absorption process from creams and ointments. *J. Soc. Cosmet. Chem,* 11, pp. 85-97.

Hwa, C., Bauer, E.A. and Cohen, D.E., 2011. Skin biology. *Dermatologic Therapy,* 24(5), pp. 464-470.

Jacobi, U., Kaiser, M., Toll, R., Mangelsdorf, S., Audring, H., Otberg, N., Sterry, W. and Lademann, J., 2007. Porcine ear skin: an *in vitro* model for human skin. *Skin Research and Technology,* 13(1), pp. 19-24.

Jepps, O.G., Dancik, Y., Anissimov, Y.G. and Roberts, M.S., 2013. Modeling the human skin barrier—Towards a better understanding of dermal absorption. *Advanced Drug Delivery Reviews,* 65(2), pp. 152-168.

Kalia, Y.N., Alberti, I., Sekkat, N., Curdy, C., Naik, A. and Guy, R.H., 2000. Normalization of stratum corneum barrier function and transepidermal water loss in vivo. *Pharmaceutical Research,* 17(9), pp. 1148-1150.

Kalia, Y.N. and Guy, R.H., 2001. Modeling transdermal drug release. *Advanced Drug Delivery Reviews,* 48(2-3), pp. 159-172.

Kalia, Y.N., Pirot, F. and Guy, R.H., 1996. Homogeneous transport in a heterogeneous membrane: water diffusion across human stratum corneum *in vivo*. *Biophysical Journal,* 71(5), p. 2692.

Karadzovska, D., Brooks, J.D., Monteiro-Riviere, N.A. and Riviere, J.E., 2013. Predicting skin permeability from complex vehicles. *Advanced Drug Delivery Reviews,* 65(2), pp. 265-277.

Karande, P. and Mitragotri, S., 2009. Enhancement of transdermal drug delivery via synergistic action of chemicals. *Biochimica et Biophysica Acta (BBA)-Biomembranes,* 1788(11), pp. 2362-2373.

Kelder, J., Grootenhuis, P.D., Bayada, D.M., Delbressine, L.P. and Ploemen, J.-P., 1999. Polar molecular surface as a dominating determinant for oral absorption and brain penetration of drugs. *Pharmaceutical Research,* 16(10), pp. 1514-1519.

Klamerus, K. and Lee, G., 1992. Effects of some hydrophilic permeation enhancers on the absorption of bepridil through excised human skin. *Drug Development and Industrial Pharmacy,* 18(13), pp. 1411-1422.

Kligman, A., 1965. Topical pharmacology and toxicology of dimethyl sulfoxide—Part 1. *Jama,* 193(10), pp. 796-804.

Kligman, A. and Christophers, E., 1963. Preparation of isolated sheets of human stratum corneum. *Archives of Dermatology,* 88(6), pp. 702-705.

Kretsos, K., Miller, M.A., Zamora-Estrada, G. and Kasting, G.B., 2008. Partitioning, diffusivity and clearance of skin permeants in mammalian dermis. *International Journal of Pharmaceutics,* 346(1), pp. 64-79.

Kumar, S., Zakrewsky, M., Chen, M., Menegatti, S., Muraski, J.A. and Mitragotri, S., 2015. Peptides as skin penetration enhancers: mechanisms of action. *Journal of Controlled Release,* 199, pp. 168-178.

Lademann, J., Jacobi, U., Surber, C., Weigmann, H.-J. and Fluhr, J., 2009. The tape stripping procedure–evaluation of some critical parameters. *European Journal of Pharmaceutics and Biopharmaceutics,* 72(2), pp. 317-323.

Lanke, S., Kolli, C., Strom, J. and Banga, A., 2009. Enhanced transdermal delivery of low molecular weight heparin by barrier perturbation. *International Journal of Pharmaceutics,* 365(1-2), pp. 26-33.

Lefevre, G., Sędek, G., Huang, H.L.A., Saltzman, M., Rosenberg, M., Kiese, B. and Fordham, P., 2007. Pharmacokinetics of a rivastigmine transdermal patch formulation in healthy volunteers: relative effects of body site application. *The Journal of Clinical Pharmacology,* 47(4), pp. 471-478.

Lian, G., Chen, L. and Han, L., 2008. An evaluation of mathematical models for predicting skin permeability. *Journal of Pharmaceutical Sciences,* 97(1), pp. 584-598.

Lieb, W.R. and Stein, W.D., 1986. Non-Stokesian nature of transverse diffusion within human red cell membranes. *The Journal of Membrane Biology,* 92(2), pp. 111-119.

Lipinski, C.A., Lombardo, F., Dominy, B.W. and Feeney, P.J., 1997. Experimental and computational approaches to estimate solubility and permeability in drug discovery and development settings. *Advanced Drug Delivery Reviews,* 23(1-3), pp. 3-25.

Magnusson, B.M., Anissimov, Y.G., Cross, S.E. and Roberts, M.S., 2004. Molecular size as the main determinant of solute maximum flux across the skin. *Journal of Investigative Dermatology,* 122(4), pp. 993-999.

McAllister, D.V., Allen, M.G. and Prausnitz, M.R., 2000. Microfabricated microneedles for gene and drug delivery. *Annual Review of Biomedical Engineering,* 2(1), pp. 289-313.

Mccarley, K.D. and Bunge, A.L., 2001. Pharmacokinetic models of dermal absorption. *Journal of Pharmaceutical Sciences,* 90(11), pp. 1699-1719.

Megrab, N.A., Williams, A.C. and Barry, B.W., 1995. Oestradiol permeation across human skin, silastic and snake skin membranes: The effects of ethanol/water co-solvent systems. *International Journal of Pharmaceutics,* 116(1), pp. 101-112.

Menon, G.K., 2015. Skin basics; structure and function. *Lipids and Skin Health.* Springer, pp. 9-23.

Menon, G.K., Feingold, K.R. and Elias, P.M., 1992. Lamellar body secretory response to barrier disruption. *Journal of Investigative Dermatology,* 98(3), pp. 279-289.

Michaels, A., Chandrasekaran, S. and Shaw, J., 1975. Drug permeation through human skin: theory and *in vitro* experimental measurement. *AIChE Journal,* 21(5), pp. 985-996.

Michel, S., Schmidt, R., Shroot, B. and Reichert, U., 1988. Morphological and biochemical characterization of the cornified envelopes from human epidermal keratinocytes of different origin. *Journal of Investigative Dermatology,* 91(1), pp. 11-15.

Mikszta, J.A., Alarcon, J.B., Brittingham, J.M., Sutter, D.E., Pettis, R.J. and Harvey, N.G., 2002. Improved genetic immunization via micromechanical disruption of skin-barrier function and targeted epidermal delivery. *Nature Medicine,* 8(4), p. 415.

Mitragotri, S., 2002. A theoretical analysis of permeation of small hydrophobic solutes across the stratum corneum based on Scaled Particle Theory. *Journal of Pharmaceutical Sciences,* 91(3), pp. 744-752.

Mitragotri, S., Anissimov, Y.G., Bunge, A.L., Frasch, H.F., Guy, R.H., Hadgraft, J., Kasting, G.B., Lane, M.E. and Roberts, M.S., 2011. Mathematical models of skin permeability: an overview. *International Journal of Pharmaceutics,* 418(1), pp. 115-129.

Monteiro-Riviere, N.A., Inman, A.O., Snider, T.H., Blank, J.A. and Hobson, D.W., 1997. Comparison of an in vitro skin model to normal human skin for dermatological research. *Microscopy research and technique,* 37(3), pp. 172-179.

Moser, K., Kriwet, K., Kalia, Y.N. and Guy, R.H., 2001a. Enhanced skin permeation of a lipophilic drug using supersaturated formulations. *Journal of Controlled Release,* 73(2-3), pp. 245-253.

Moser, K., Kriwet, K., Naik, A., Kalia, Y.N. and Guy, R.H., 2001b. Passive skin penetration enhancement and its quantification in vitro. *European Journal of Pharmaceutics and Biopharmaceutics,* 52(2), pp. 103-112.

Moss, G.P., Dearden, J.C., Patel, H. and Cronin, M.T., 2002. Quantitative structure–permeability relationships (QSPRs) for percutaneous absorption. *Toxicology in Vitro,* 16(3), pp. 299-317.

Netzlaff, F., Lehr, C.-M., Wertz, P. and Schaefer, U., 2005. The human epidermis models EpiSkin®, SkinEthic® and EpiDerm®: an evaluation of morphology and their suitability for testing phototoxicity, irritancy, corrosivity, and substance transport. *European Journal of Pharmaceutics and Biopharmaceutics,* 60(2), pp. 167-178.

Ng, K.W. and Lau, W.M., 2015. Skin deep: the basics of human skin structure and drug penetration. *Percutaneous penetration enhancers chemical methods in penetration enhancement.* Springer, pp. 3-11.

Nicoli, S., Bunge, A.L., Delgado-Charro, M.B. and Guy, R.H., 2009. Dermatopharmacokinetics: factors influencing drug clearance from the stratum corneum. *Pharmaceutical Research,* 26(4), pp. 865-871.

Norlén, L., 2006. Stratum corneum keratin structure, function and formation–a comprehensive review. *International Journal of Cosmetic Science,* 28(6), pp. 397-425.

Norlén, L. and Al-Amoudi, A., 2004. Stratum corneum keratin structure, function, and formation: the cubic rod-packing and membrane templating model. *Journal of Investigative Dermatology,* 123(4), pp. 715-732.

OECD, 2004. *Test No. 428: Skin Absorption: In Vitro Method.*

Oliyai, R. and Stella, V.J., 1993. Prodrugs of peptides and proteins for improved formulation and delivery. *Annual Review of Pharmacology and Toxicology,* 33(1), pp. 521-544.

Onken, H.D. and Moyer, C.A., 1963. The water barrier in human epidermis: physical and chemical nature. *Archives of dermatology,* 87(5), pp. 584-590.

Otberg, N., Richter, H., Schaefer, H., Blume-Peytavi, U., Sterry, W. and Lademann, J., 2004. Variations of hair follicle size and distribution in different body sites. *Journal of Investigative Dermatology,* 122(1), pp. 14-19.

Palenske, J. and Morhenn, V.B., 1999. Changes in the skin's capacitance after damage to the stratum corneum in humans. *Journal of Cutaneous Medicine and Surgery,* 3(3), pp. 127-131.

Palm, K., Stenberg, P., Luthman, K. and Artursson, P., 1997. Polar molecular surface properties predict the intestinal absorption of drugs in humans. *Pharmaceutical Research,* 14(5), pp. 568-571.

Panchagnula, R., Salve, P.S., Thomas, N.S., Jain, A.K. and Ramarao, P., 2001. Transdermal delivery of naloxone: effect of water, propylene glycol, ethanol and their binary combinations on permeation through rat skin. *International Journal of Pharmaceutics,* 219(1), pp. 95-105.

Panchagnula, R., Stemmer, K. and Ritschel, W., 1997. Animal models for transdermal drug delivery. *Methods and Findings in Experimental and Clinical Pharmacology,* 19(5), pp. 335-341.

Pellett, M., Castellano, S., Hadgraft, J. and Davis, A., 1997. The penetration of supersaturated solutions of piroxicam across silicone membranes and human skin *in vitro*. *Journal of Controlled Release,* 46(3), pp. 205-214.

Piérard, G.E., Hermanns-Lê, T. and Piérard-Franchimont, C., 2017. Stratum corneum desquamation. *Agache's Measuring the Skin: Non-invasive Investigations, Physiology, Normal Constants,* pp. 267-271.

Pillai, O. and Panchagnula, R., 2003. Transdermal delivery of insulin from poloxamer gel: *ex vivo* and *in vivo* skin permeation studies in rat using iontophoresis and chemical enhancers. *Journal of Controlled Release,* 89(1), pp. 127-140.

Polak, S., Ghobadi, C., Mishra, H., Ahamadi, M., Patel, N., Jamei, M. and Rostami-Hodjegan, A., 2012. Prediction of concentration–time profile and its inter-individual variability following the dermal drug absorption. *Journal of Pharmaceutical Sciences,* 101(7), pp. 2584-2595.

Potts, R.O. and Francoeur, M.L., 1991. The influence of stratum corneum morphology on water permeability. *Journal of Investigative Dermatology,* 96(4), pp. 495-499.

Potts, R.O. and Guy, R.H., 1992. Predicting skin permeability. *Pharmaceutical Research,* 9(5), pp. 663-669.

Potts, R.O. and Guy, R.H., 1995. A predictive algorithm for skin permeability: the effects of molecular size and hydrogen bond activity. *Pharmaceutical Research,* 12(11), pp. 1628-1633.

Prausnitz, M.R., Mitragotri, S. and Langer, R., 2004. Current status and future potential of transdermal drug delivery. *Nature Reviews Drug discovery,* 3(2), p. 115.

Raevsky, O.A., Fetisov, V.I., Trepalina, E.P., McFarland, J.W. and Schaper, K.J., 2000. Quantitative estimation of drug absorption in humans for passively transported compounds on the basis of their physico-chemical parameters. *Quantitative Structure-Activity Relationships,* 19(4), pp. 366-374.

Rawlings, A.V., 2010. Recent advances in skin 'barrier'research. *Journal of Pharmacy and Pharmacology*, 62(6), pp. 671-677.

Reddy, M.B., Guy, R.H. and Bunge, A.L., 2000. Does epidermal turnover reduce percutaneous penetration? *Pharmaceutical Research*, 17(11), pp. 1414-1419.

Rhee, Y.-S., Chang, S.-Y., Park, C.-W., Chi, S.-C. and Park, E.-S., 2008. Optimization of ibuprofen gel formulations using experimental design technique for enhanced transdermal penetration. *International Journal of Pharmaceutics*, 364(1), pp. 14-20.

Roberts, M.S., Anissimov, Y.G. and Gonsalvez, R.A., 2001. Mathematical models in percutaneous absorption. *Journal of Toxicology: Cutaneous and Ocular Toxicology*, 20(2-3), pp. 221-270.

Roberts, M.S., Cross, S. and Anissimov, Y., 2004. Factors affecting the formation of a skin reservoir for topically applied solutes. *Skin Pharmacology and Physiology*, 17(1), pp. 3-16.

Rosado, C. and Rodrigues, L.M., 2003. Solvent effects in permeation assessed in vivo by skin surface biopsy. *BMC Dermatology*, 3(1), p. 5.

Russell, L.M. and Guy, R.H., 2009. Measurement and prediction of the rate and extent of drug delivery into and through the skin. *Expert Opinion on Drug Delivery*, 6(4), pp. 355-369.

Russell, L.M., Wiedersberg, S. and Delgado-Charro, M.B., 2008. The determination of stratum corneum thickness: an alternative approach. *European Journal of Pharmaceutics and Biopharmaceutics*, 69(3), pp. 861-870.

Schaeffer, H. and Redelmuer, T.E., 1996. *Skin Barrier - Principles of Percutaneous Absorption.* Basel, Switzerland: Karger.

Schafer-Korting, M., Bock, U., Gamer, A., Haberland, A., Haltner-Ukomadu, E., Kaca, M., Kamp, H., Kietzmann, M., Korting, H.C. and Krachter, H., 2006. Reconstructed human epidermis for skin absorption testing: results of the German prevalidation study. *ATLA-NOTTINGHAM-*, 34(3), p. 283.

Scheuplein, R. and Ross, L., 1970. Effects of surfactants and solvents on the permeability of epidermis. *Journal of the Society of Cosmetic Chemists*. Citeseer.

Scheuplein, R.J., 1965. Mechanism of percutaneous adsorption: I. Routes of penetration and the influence of solubility. *Journal of Investigative Dermatology*, 45(5), pp. 334-346.

Scheuplein, R.J., 1967. Mechanism of percutaneous absorption: II. Transient diffusion and the relative importance of various routes of skin penetration. *Journal of Investigative Dermatology,* 48(1), pp. 79-88.

Scheuplein, R.J., 1978. Permeability of the skin: a review of major concepts. *Skin-Drug Application and Evaluation of Environmental Hazards.* Karger Publishers, pp. 172-186.

Scheuplein, R.J. and Blank, I.H., 1971. Permeability of the skin. *Physiological Reviews,* 51(4), pp. 702-747.

Schmook, F.P., Meingassner, J.G. and Billich, A., 2001. Comparison of human skin or epidermis models with human and animal skin in *in-vitro* percutaneous absorption. *International Journal of Pharmaceutics,* 215(1-2), pp. 51-56.

Schückler, F. and Lee, G., 1992. Relating the concentration-dependent action of Azone and dodecyl-L-pyroglutamate on the structure of excised human stratum corneum to changes in drug diffusivity, partition coefficient and flux. *International Journal of Pharmaceutics,* 80(1-3), pp. 81-89.

Sekkat, N. and Guy, R.H., 2001. Biological models to study skin permeation. *B. Testa, H. van de, Waterbeemd G. Folkers, RH Guy (eds.), Pharmacokinetic Optimisation in Drug Research, Wiley-VCH and VHCA, Zürich*, p. 155Y172.

Selzer, D., Neumann, D. and Schaefer, U.F., 2015. Mathematical models for dermal drug absorption. *Expert Opinion on Drug Metabolism & Toxicology,* 11(10), pp. 1567-1583.

Simonetti, O., Kempenaar, J., Ponec, M., Hoogstraate, A., Bialik, W., Schrijvers, A. and Boddé, H., 1995. Visualization of diffusion pathways across the stratum corneum of native and in-vitro-reconstructed epidermis by confocal laser scanning microscopy. *Archives of dermatological research,* 287(5), pp. 465-473.

Stenberg, P., Luthman, K., Ellens, H., Lee, C.P., Smith, P.L., Lago, A., Elliott, J.D. and Artursson, P., 1999. Prediction of the intestinal absorption of endothelin receptor antagonists using three theoretical methods of increasing complexity. *Pharmaceutical Research,* 16(10), pp. 1520-1526.

Stenberg, P., Norinder, U., Luthman, K. and Artursson, P., 2001. Experimental and computational screening models for the prediction of intestinal drug absorption. *Journal of Medicinal Chemistry,* 44(12), pp. 1927-1937.

Svedman, P. and Svedman, C., 1998. Skin mini-erosion sampling technique: feasibility study with regard to serial glucose measurement. *Pharmaceutical Research,* 15(6), pp. 883-888.

Treffel, P., Makki, S., Faivre, B., Humbert, P., Blanc, D. and Agache, P., 1991. Citropten and bergapten suction blister fluid concentrations after solar product application in man. *Skin Pharmacology and Physiology*, 4(2), pp. 100-108.

Tsakovska, I., Pajeva, I., Al Sharif, M., Alov, P., Fioravanzo, E., Kovarich, S., Worth, A.P., Richarz, A.-N., Yang, C., Mostrag-Szlichtyng, A. and Cronin, M.T.D., 2017. Quantitative structure-skin permeability relationships. *Toxicology*, 387, pp. 27-42.

Vallet, V., Cruz, C., Josse, D., Bazire, A., Lallement, G. and Boudry, I., 2007. In vitro percutaneous penetration of organophosphorus compounds using full-thickness and split-thickness pig and human skin. *Toxicology in Vitro*, 21(6), pp. 1182-1190.

van de Waterbeemd, H. and Gifford, E., 2003. ADMET *in silico* modelling: towards prediction paradise? *Nature Reviews Drug Discovery*, 2(3).

van der Merwe, D., Brooks, J., Gehring, R., Baynes, R., Monteiro-Riviere, N. and Riviere, J., 2005. A physiologically based pharmacokinetic model of organophosphate dermal absorption. *Toxicological Sciences*, 89(1), pp. 188-204.

Volden, G., Thorsrud, A.K., Bjørnson, I. and Jellum, E., 1980. Biochemical composition of suction blister fluid determined by high resolution multicomponent analysis (capillary gas chromatography--mass spectrometry and two-dimensional electrophoresis). *Journal of Investigative Dermatology*, 75(5).

Wester, R.C., Noonan, P.K. and Maibach, H.I., 1980. Variations in percutaneous absorption of testosterone in the rhesus monkey due to anatomic site of application and frequency of application. *Archives of Dermatological Research*, 267(3), pp. 229-235.

Wiedersberg, S. and Guy, R.H., 2014. Transdermal drug delivery: 30+ years of war and still fighting! *Journal of Controlled Release*, 190, pp. 150-156.

Wiedersberg, S., Leopold, C.S. and Guy, R.H., 2009. Dermatopharmacokinetics of betamethasone 17-valerate: Influence of formulation viscosity and skin surface cleaning procedure. *European Journal of Pharmaceutics and Biopharmaceutics*, 71(2), pp. 362-366.

Wiedersberg, S. and Nicoli, S., 2012. Skin permeation assessment: tape stripping. *Topical and transdermal drug delivery: principles and practice. Hoboken: John Wiley and Sons Inc*, pp. 109-130.

Wilkinson, S.C., Maas, W.J., Nielsen, J.B., Greaves, L.C., van de Sandt, J.J. and Williams, F.M., 2006. Interactions of skin thickness and physicochemical properties of test compounds in percutaneous penetration studies. *International archives of occupational and environmental health*, 79(5), pp. 405-413.

Williams, A.C. and Barry, B.W., 2012. Penetration enhancers. *Advanced Drug Delivery Reviews,* 64, pp. 128-137.

Winiwarter, S., Bonham, N.M., Ax, F., Hallberg, A., Lennernäs, H. and Karlén, A., 1998. Correlation of human jejunal permeability (in vivo) of drugs with experimentally and theoretically derived parameters. A multivariate data analysis approach. *Journal of Medicinal Chemistry,* 41(25), pp. 4939-4949.

Yamashita, F. and Hashida, M., 2003. Mechanistic and empirical modeling of skin permeation of drugs. *Advanced Drug Delivery Reviews,* 55(9), pp. 1185-1199.

Yano, T., Nakagawa, A., Tsuji, M. and Noda, K., 1986. Skin permeability of various non-steroidal anti-inflammatory drugs in man. *Life sciences,* 39(12), pp. 1043-1050.

Yun, Y.E. and Edginton, A.N., 2013. Correlation-based prediction of tissue-to-plasma partition coefficients using readily available input parameters. *Xenobiotica,* 43(10), pp. 839-852.

Zaffaroni, A., 1991. Overview and evolution of therapeutic systems. *Annals of the New York Academy of Sciences,* 618(1), pp. 405-421.

Zhang, Q., Grice, J.E., Li, P., Jepps, O.G., Wang, G.-J. and Roberts, M.S., 2009. Skin solubility determines maximum transepidermal flux for similar size molecules. *Pharmaceutical Research,* 26(8), pp. 1974-1985.

Chapter 2: Deducing drug input-rate from topical products using information from transdermal delivery

Abbreviations and glossary of terms

BUP	buprenorphine
DF	diclofenac
Drug input	rate at which the drug reaches the sub-stratum corneum layers
HPLC-UV	high-performance liquid chromatography with ultraviolet detection
IVPT	*in vitro* skin permeation test
IVRT	*in vitro* release test
J_{BUP}	flux of buprenorphine into the receptor solution
J_{DF}	flux of diclofenac into the receptor solution
J_{NIC}	flux of nicotine into the receptor solution
logP	log{octanol-water partition coefficient (P)}
MW	molecular weight (Daltons)
NIC	nicotine
RS	receptor solution
SC	stratum corneum
Topical product	products where the site of action in the skin or subcutaneous tissues
Transdermal product	products where the site of action of the drug is reached via the systemic circulation
Viable skin	viable epidermis and part of the dermis.

1. Introduction

The skin has many features which make it an attractive site for both topical (dermatological and locally-acting) and systemic drug delivery (Zaffaroni, 1991; Kumar *et al.*, 2014). Measurement of the bioavailability of a drug in the skin after topical application is an important objective when attempting to assess whether the target-site concentrations are satisfactory to treat the disease. However, determining the amount of drug that reaches the different skin layers is still a challenge (Schäfer-Korting *et al.*, 2007).

In terms of dermato-pharmacokinetics, the skin is most frequently represented as a 2-compartment system: the stratum corneum (SC; usually the rate-limiting barrier), which is predominantly lipophilic, and the viable epidermis and dermis which are often considered as a single, hydrophilic, compartment (McCarley and Bunge, 2001; Roberts *et al.*, 2001). The viable epidermal and upper dermal compartments are the site of action of the vast majority of topically applied drugs. It follows that knowledge of the 'drug input' would help to derive the concentration of the drug in this region.

For topical dermatological products, such as creams, ointments and gels, or even in topical patches, designed to produce a local effect (for example, to treat joint pain), the rate of drug entering the skin is not provided by the manufacturer. Local tissue or blood level data, from which useful information about drug 'input function' could be extracted, is scarce. Although *in vitro* approaches, such as skin permeation tests, are useful to estimate drug input-rate from such products, validation of these approaches is difficult due to the lack of *in vivo* data.

In contrast, for transdermal[3] patches, the rate at which the drug reaches the systemic circulation is provided on the product label. This delivery rate can be deduced by deconvoluting the resulting systemic plasma time profile. One method commonly used for this purpose is called Wagner-Nelson (Wagner & Nelson 1964) analysis.

Wagner–Nelson deconvolution analysis (Equation 1) can be applied only to one-compartment drugs. This method is based on the mass balance theory, where no

[3] The word 'transdermal' here is used to mean products where the site of action of the drug is reached via the systemic circulation; an example is a nicotine patch, where nicotine must reach the brain to achieve its therapeutic effect

kinetic model for the absorption process is assumed. The method does not require intravenous drug administration, because it assumes identical elimination rate coefficient (k_e) between intra- and extra-venous administrations and, therefore k_e can be estimated from the final stage of the oral curve. However, when flip-flop occurs, intravenous drug administration is therefore needed to estimate k_e.

$$F_{abs} = \frac{A_t}{A_\infty} = \frac{C_t + k_e \times AUC_0^t}{k_e \times AUC_0^\infty} \quad \text{(Equation 1)}$$

where F_{abs} is the fraction absorbed, A_t is the drug amount absorbed at time t, A_∞ is the drug amount absorbed at infinite time, C_t is the drug concentration at time t, k_e is the elimination rate coefficient, AUC_0^t is the area under the curve from time 0 to time t and AUC_0^∞ is the area under the curve from time 0 to infinity.

Knowing F_{abs}, the *in vivo* drug input rate can be calculated from the slope of the line obtained from the plot of log fraction unabsorbed *versus* time (Rao et al., 2001).

It is clear that as the true input-rate is known, these products can be useful for assessing the validity of experimental approaches for determining input-rates from dermatological and locally acting topical products.

Therefore, the first component of this work was to characterise experimentally, *in vitro*, the input functions of two transdermal drugs, buprenorphine and nicotine, from commercially available patches, namely Transtec® and Nicotinell®, respectively. Currently, there are 18 transdermal drugs present in over 25 FDA-approved transdermal products (FDA Orange Book database of the end of 2017). These drugs span a relatively wide range of physicochemical properties: for example, molecular weights between 160 and 470 Daltons and log{octanol-water partition coefficient (P)} values from about 1.0 to 5.0. Buprenorphine and nicotine (Table 1) are at the limits of the physicochemical range of drugs in approved transdermal products, having molecular weights of 162 and 468 Daltons and log P values of about 1.2 and 5.0, respectively.

The second component focused on determining the input function of diclofenac from a medicated plaster (from now on also referred to as a patch) which is indicated for a local effect (therefore there is no requirement for the manufacturer to provide the input-rate).

Table 1. Selected physicochemical properties of the three drugs studied in this chapter and specification of the drug delivery systems in which they are formulated.

Transdermal drug delivery system	Buprenorphine (Transtec®)	Nicotine (Nicotinell®)	Diclofenac (Voltaren®)
Molecular weight (Da)	468	162	411.32[b]
log P	4.98	1.17	4.26[c]
Drug content (mg) [a]	20	17.5	180
Active delivery area (cm^2) [a]	25	10.0	140
Labelled *in vivo* delivery rate [a]	35 µg/h	7 mg/24h	Not available
Labelled application period (h) [a]	72	24	12

[a]Information provided in the manufacturer's packing insert;
[b]Molecular weight of diclofenac epolamine;
[c]log P of diclofenac acid.

2. Materials and Methods

2.1. Chemicals and reagents

The transdermal patches tested were: Transtec® (35 µg/h, 20 mg of buprenorphine over 25 cm^2) from NAPP (Cambridge, UK) and Nicotinell® (7 mg/24h, 17.5 mg of nicotine over 10 cm^2) from Novartis (*Camberley*, UK). Voltaren® (medicated plaster, 180 mg of diclofenac epolamine over 140 cm^2) was from GlaxoSmithKline (Munich, Germany). Buprenorphine base was from Reckitt and Colman (UK). (-)-Nicotine from Sigma Aldrich (Dorset, UK). Diclofenac epolamine was from Toronto Research Chemicals (Toronto, Canada). All solvents were from Sigma Aldrich (Dorset, UK).

Fresh abdominal porcine skin was obtained from a local abattoir, dermatomed (Zimmer®, Hudson, OH, USA) to a nominal thickness of 750 µm, frozen within 24 h of slaughter, and thawed before use.

2.2. Analytical methods

Assays for buprenorphine (BUP), nicotine (NIC) and diclofenac (DF) were developed using HPLC (Dionex, UK), with UV detection, using Chromeleon software. A HiQSil C18HS analytical reverse phase column (150 x 4.6 mm i.d.; 5 µm particle size) (Kromatek, UK) was used for the three drugs. The chromatographic conditions for BUP, NIC and DF are in Table 2.

Table 2. HPLC-UV method conditions used for quantification of BUP, NIC and DF.

Parameters	Buprenorphine	Nicotine	Diclofenac
Mobile Phase	22:19:59 ACN:MeOH:TFA 0.03% v/v	35:35:30 ACN:MeOH:PBS 10 mM (pH = 7.4) v/v	75:25 MeOH:formic acid 0.1% v/v
Oven Temp. (°C)	25	25	40
Flow-rate (mL min^{-1})	1.0	1.0	1.2
Retention time (min)	11.8	3.2	7.3
Injection volume (µL)	75	50	100
UV detection (nm)	220	260	280
Limit of quantification (µg mL^{-1})	0.14	0.12	0.10

ACN: Acetonitrile; MeOH: Methanol; TFA: Trifluoroacetic acid; PBS: Phosphate buffered saline.

2.3. *In vitro* release tests (IVRT)

Drug release from the three formulations (Transtec®, Nicotinell® and Voltaren®) was evaluated using Franz-type diffusion cells. Patches were cut into disks and clamped (with no membrane present) in the diffusion cells (nominal diffusion area = 1.77 cm^2, PermeGear, Inc., Hellertown, PA, USA). The receptor chamber was filled with 7.4 mL of a receptor solution (Table 3) and stirred magnetically at a constant speed of 500 rpm. The temperature of the receptor solution was controlled by a circulating water bath at 37 ± 1 °C. Aliquots of the receptor solution (1.0, 1.5 and 0.5 mL for BUP, NIC and DF, respectively) were withdrawn at each time point and immediately replaced with the same volume of fresh solution. The drug concentration in these samples was determined by the HPLC-UV method described above (Table 2). A correction was made for the previously removed samples when determining the total amount released. The data were expressed as the cumulative amount of drug released as a function of the square root of time (in accord with Fick's second law of diffusion (Siepmann and Peppas, 2011)).

2.4. *In vitro* permeation tests (IVPT)

The *in vitro* permeation of BUP, NIC and DF from approved patches was measured in Franz diffusion cells across dermatomed (~ 750 µm) pig skin. Each patch was cut into disks (surface area 1.54 cm^2) and adhered to the external side of the skin

(before mounting the skin in the Franz cell). Pressure was applied with a roller (custom made; 10 times in two directions) to ensure complete adhesion. The skin samples were then positioned between the donor and receptor chamber of diffusion cells.

In the first type of experiment (Figure 1 **(a)**), the disposition of the drug in the stratum corneum, 'viable' skin and receptor solution was evaluated over of time. At the end of each experiment, the total amount of drug delivered from the patch into and through the skin during the period of observation was determined; i.e., recovered quantities in the SC, in the remainder of the skin, and in the receptor compartment of the diffusion cell.

The second type of experiment (Figure 1 **(b)**) investigated the cumulative delivery of BUP, NIC and DF into the receptor solution following application of the respective patches for 72, 24 and 30 hours, respectively. Aliquots of the receptor solution (1.0 mL for BUP and NIC; 0.5 mL for DF) were withdrawn at intervals and immediately replaced with the same volume of fresh solution. Drug concentrations in these samples were again determined by HPLC (Table 2). A correction was made for the previously removed samples in determining the total amount permeated. The diffusion flux was calculated using Fick's first law from the slope of the linear portion of the plot of the cumulative amount of drug permeated per area of skin against time.

The third type of experiment (Figure 1 **(c)**) investigated the rate at which drug was cleared from the SC and the epidermis and dermis. Transtec® was applied on the skin for 72 hours, Nicotinell® for 2 hours and Voltaren® for 6 hours. Subsequently, the patches were removed and the skin left (mounted on the diffusion cell) for a further 24 (Transtec®), 1.5 and 2 hours (Nicotinell®) or 5, 17 and 24 hours (Voltaren®) before tape-stripping.

At the end of each experiment, the amount of drug in the SC was assessed by sequential removal of this outer skin layer by tape-stripping. Templates (Scotch® Tape, 3M, The Consortium, UK), with a circular internal area of 1.54 cm^2, were adhered to the skin, then an adhesive tape strip (2.0 cm x 2.5 cm, Scotch® Tape, 3M) was applied to the skin, pressed firmly down and removed quickly. The procedure was repeated until 20 strips had been taken. The mass of skin removed on each tape was determined by weight difference (Sartorius model SE2-F, Sartorius AG, Germany), before and after application to the skin. Before weighing, the tapes were discharged of static electricity (R50 discharging bar and ES50 power supply, Eltex Elektrostatik

GmbH, Weil am Rhein, Germany). From this mass, and knowing the area of SC on the tape, it was possible to calculate the SC thickness removed (assuming an SC density of 1 g cm^{-3}, Anderson and Cassidy (1973)) and hence the corresponding position (or depth) within the barrier. After weighing, tapes were extracted individually (Table 3) and analysed for BUP, NIC or DF by the HPLC-UV method described above (Table 2).

The methods used to ensure efficient extraction of the drugs from the SC tape-strips and from the remaining skin post-stripping are described in Table 3. Mean extraction efficiencies were greater than 89% from tape strips and remaining tissue (details are provided in the 'Supplementary Information' (Tables S1 – 4)).

Table 3. Details of the experimental set-up used for the *in vitro* permeation tests.

Parameters	Buprenorphine	Nicotine	Diclofenac
Receptor solution	20:80 PEG 400:PBS 10 mM (pH 7.4) (+ 0.01% of sodium azide)	100% PBS 10 mM (pH = 7.4)	
Extraction solution	40:60 ACN:TFA 0.03% v/v [a]	40:60 ACN:PBS 10 mM (pH = 7.4)[b]	100% Methanol[a]

[a]Extraction volumes were 1.5 mL for tape strips and 4 mL for remaining skin;
[b]Extraction volumes were 1.5 mL for tape strips and 8 mL for remaining skin.

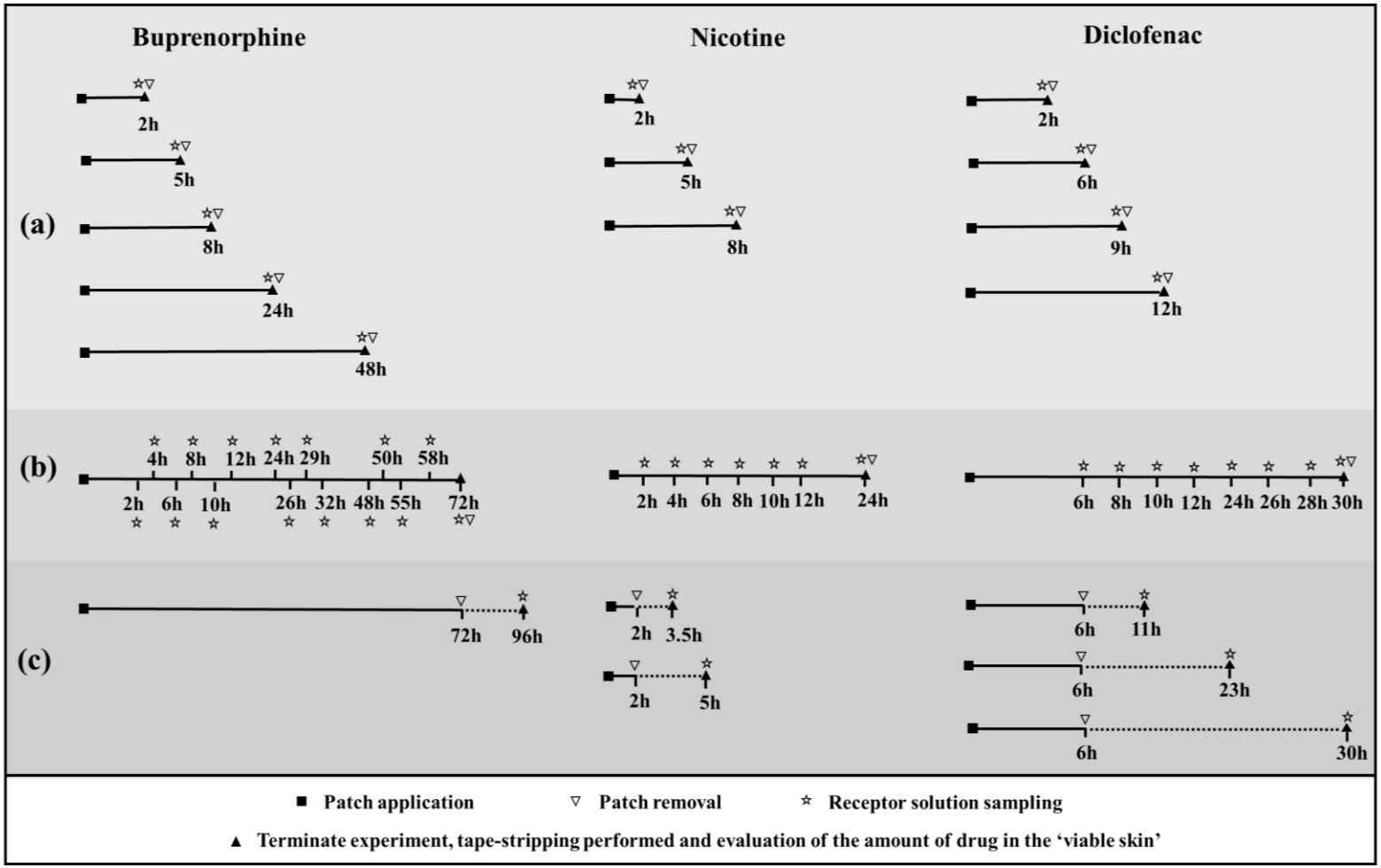

Figure 1. Schematic representation of the IVPT experiments performed to assess: (**a**) disposition of the drug in the stratum corneum, 'viable' skin and receptor solution over time; (**b**) drug's permeation profile into the receptor solution and (**c**) redistribution of the drug after patch removal.

2.5. Determination of nicotine loss during permeation experiments and on the tapes during storage

As NIC has been described as a volatile and light sensitive substance (Ruela *et al.*, 2013; Davaran *et al.*, 2005), experiments were carried out to identify whether there was a significant loss of drug during permeation experiments and from the tapes during storage.

First, amount of NIC in the receptor solution was investigated in the presence and absence of light. Solutions of nicotine in PBS with a known drug concentration (25.0 µg/mL, mean expected concentration in the receptor solution during permeation studies) were stored for 24, 48 or 72 hours in the presence (clear glass vial) or absence (amber glass vial) of direct light.

Second, the volatility of NIC from adhesive tapes was evaluated by spiking tape stripped samples of untreated SC with a known concentration of drug (6.0 µg/mL, mean expected concentration in the SC). Spiked tapes were stored in the presence of light (transparent tray) and in the absence of light (tray wrapped in aluminium foil). After 24, 48 and 72 hours, NIC was extracted from the tapes by shaking overnight with 1.5 mL of acetonitrile and phosphate buffer pH 7.4 (40:60) and analysed by HPLC-UV. Standard solutions of NIC (for the HPLC analysis) were protected from direct light exposure.

2.6. Statistical analysis

Statistically significant differences between calculated input-rates and the claimed values were estimated by one sample t-test. Statistical significance was set at $p < 0.05$. Statistical tests were performed using GraphPad Prism (GraphPad software, version 7.03, La Jolla California, USA).

3. Results and discussion

3.1. Determination of nicotine loss during permeation experiments and on the tapes during storage

There was no significant loss of NIC in the receptor solution and from the tapes for at least 72 hours ('Supplementary Information', Table S5). All the recoveries were above 99%. These results confirm that no NIC volatilisation occurred during the *in vitro* assays and while tapes were stored before extraction.

3.2. Buprenorphine

The left-hand panel of Figure 2 shows data from the IVPT study. The cumulative permeation of BUP through porcine skin was 11.1 ± 2.4 µg cm^{-2} (~1.4% of the initial drug content) at 72 hours. In the IVRT experiments, on the other hand, the cumulative release of BUP from the patch increased linearly with the square root of time (r^2 = 0.99) and, at the end of the 72-hour experiment ($\sqrt{t}$ = 8.5 $h^{1/2}$), a total of 457 ± 53 µg cm^{-2} (~57% of the initial drug content) of the drug were released (Figure 2 - right panel). It is clear, therefore, that the skin significantly rate-controlled the permeation of BUP to the receptor phase (Guy and Hadgraft, 1992).

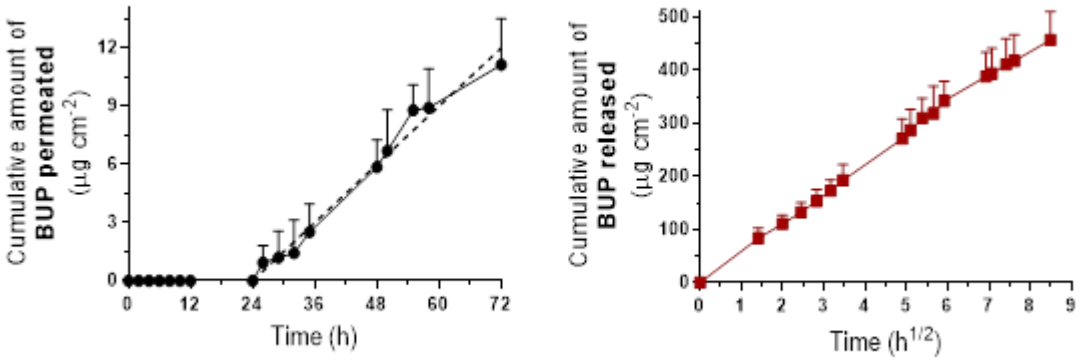

Figure 2. *Left panel:* Cumulative skin permeation of buprenorphine from Transtec® expressed as a function of time (mean ± S.D.; n = 6; Figure 1 (**b**)). The dashed line is the best fit linear regression line to the data from 24 h. *Right panel:* Cumulative release of buprenorphine from Transtec® as a function of the square-root of time (mean ± S.D.; n = 3).

Figure 3 shows a composite distribution profile of BUP in each compartment: SC, 'viable' skin (i.e., that remaining after tape-stripping) and receptor solution during the patch application and after its removal. A relatively rapid accumulation of BUP in both SC and the 'viable' skin was observed between 2 and 8 hours, after which the drug concentrations in these 'compartments' remained quite constant until 72 hours. The redistribution of the drug after patch removal was also observed. Whilst the reservoir of drug in the SC remained relatively constant after removal of the patch, drug in the 'viable' skin moved into the receptor.

Despite the similar amounts of BUP recovered from the SC and the 'viable' skin, it is important to bear in mind that the concentration of BUP in the 'viable' skin was much lower than in the SC. This happened for two obvious reasons: first, the

thickness of the SC is only ~15 µm whereas the thickness of the 'viable' skin was ~735 µm. Therefore, the volume of the SC is much smaller than the volume occupied by the 'viable' skin. Second, the lower concentration of BUP in the 'viable' skin may reflect slow partitioning of this lipophilic drug from the SC into a comparatively aqueous environment. These two phenomena are clearly linked to the greater concentration in this tissue. It should be noted, though, that the accumulation of drug observed *in vitro* may not reflect the situation *in vivo*, given that the skin microcirculation, just below the epidermis, is expected to guarantee relatively rapid clearance of a drug into the systemic circulation (Leal *et al.*, 2017; Godin and Touitou, 2007).

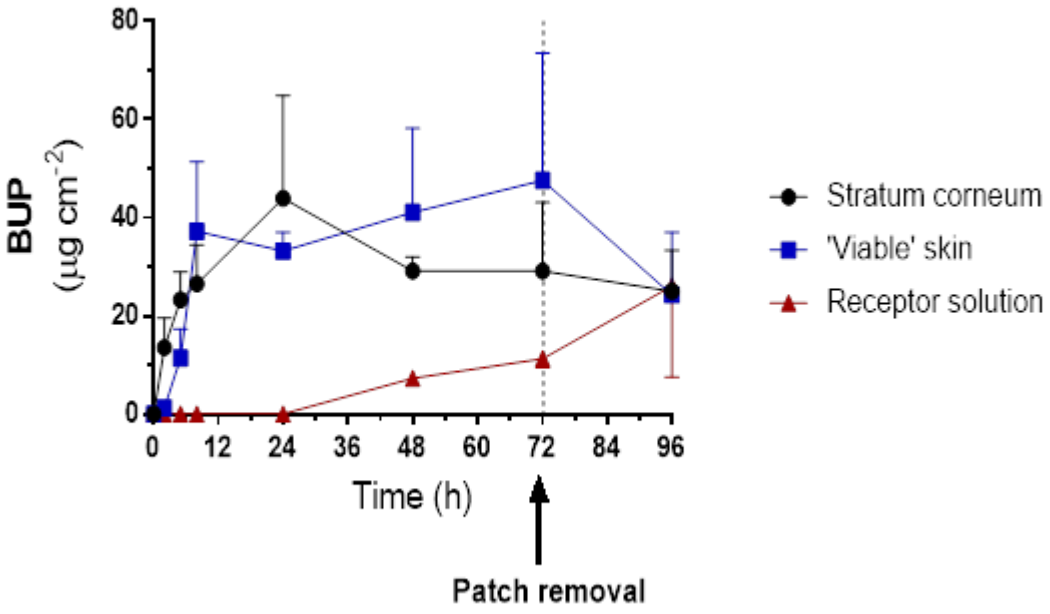

Figure 3. Distribution of buprenorphine in the stratum corneum, 'viable' skin (after tape-stripping) and receptor solution as a function of time (mean ± S.D.; n = 6; Figure 1 **(a)** and **(c)**). The arrow indicates the time of patch removal.

The flux of BUP (J_{BUP}) across the entire skin (i.e., determined from slope of the permeation profile into the receptor solution shown in Figure 1) was 0.16 ± 0.03 µg h^{-1} cm^{-2}. From the disposition of BUP in the *in vitro* experiments performed, and 'correcting' for drug in 'viable' skin, J_{BUP} was 0.81 ± 0.33 µg h^{-1} cm^{-2} (72-hour experiment). It follows that, the flux deduced from the receptor phase sampling does not take into account accumulation in the tissue and the fact that the normal clearance mechanism (i.e., the microcirculation) of drug from the skin is not operative *in vitro*.

Therefore, a better estimate of the actual delivery should also include that quantity of drug which has entered the skin but not left. When this is added in, the total delivery rate approaches the labelled value for the product, i.e., 1.4 μg h^{-1} cm^{-2} for Transtec® (Figure 4). It is clear (and previously documented; Roy *et al.* (1994)) that for BUP (in contrast to less lipophilic compounds), it is also the hydrophilic environment of the 'viable' skin, and not only the SC, that is a significant absorption-limiting step.

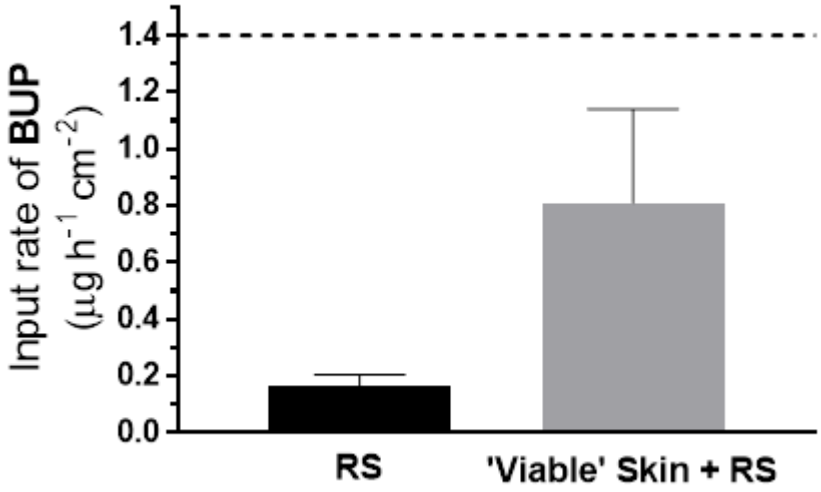

Figure 4. Input-rate of BUP from the Transtec® transdermal patch from two different data analysis approaches applied to the same data set (mean ± S.D.; n = 6). The dashed line indicates the claimed value. RS = receptor solution.

3.3. Nicotine

When the NIC patch was evaluated using the same IVRT and IVPT protocols, as described above, quite distinct behaviour was observed compared to that shown by the BUP delivery system.

The left-hand panel of Figure 5 shows data from the NIC IVPT study. The cumulative permeation of NIC through porcine skin was 617 ± 355 μg cm^{-2} (~ 35% of the initial drug content) at 24 hours. In the IVRT experiments, on the other hand, the cumulative release of NIC from the patch increased linearly with the square root of time (r^2 = 0.98) and, at the end of the 24-hour experiment ($\sqrt{t}$ = 4.9 $h^{1/2}$), a total 546 ± 74 μg cm^{-2} (~ 31% of the initial drug content) of NIC was released from the patch (Figure 5 – right panel). In contrast to BUP, therefore, the transport of NIC across the

skin was determined by its release rate from the patch rather than its subsequent penetration across the skin (Guy and Hadgraft, 1992).

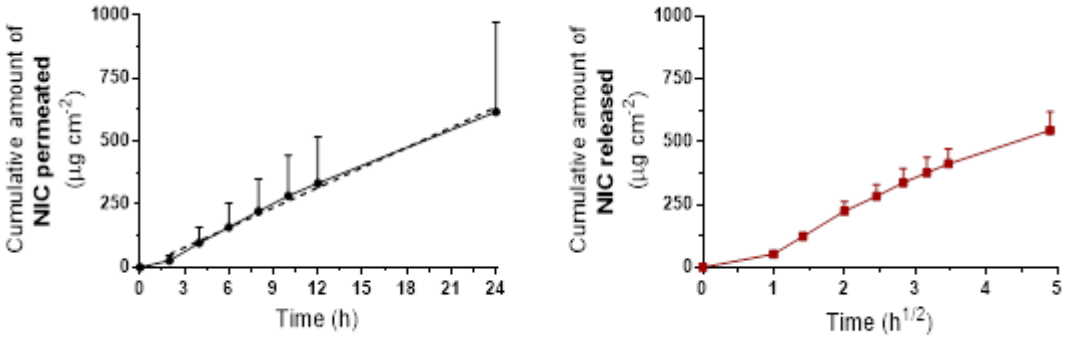

Figure 5. *Left panel:* Cumulative skin permeation of NIC from Nicotinell® expressed as a function of time (mean ± S.D.; n = 6). The dashed line is the best fit linear regression line to the data from 24 h (Figure 1 (**b**)). *Right panel:* Cumulative release of NIC from Nicotinell® as a function of the square-root of time (mean ± S.D.; n = 3).

Unlike BUP, NIC penetrates skin very easily and a relatively small amount of NIC was recovered from the SC and 'viable' skin (Figure 6). After patch removal, the drug was cleared from the SC and 'viable' skin into the receptor solution relatively rapidly (Figure 7).

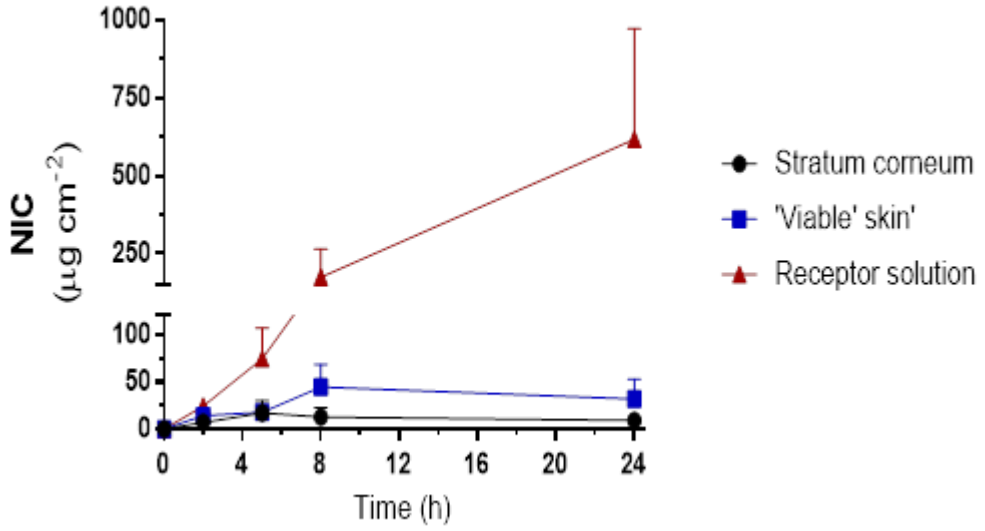

Figure 6. Distribution of NIC in the stratum corneum, 'viable' skin (after tape-stripping) and receptor solution as a function of time (mean ± S.D.; n = 6; Figure 1 (**a**)).

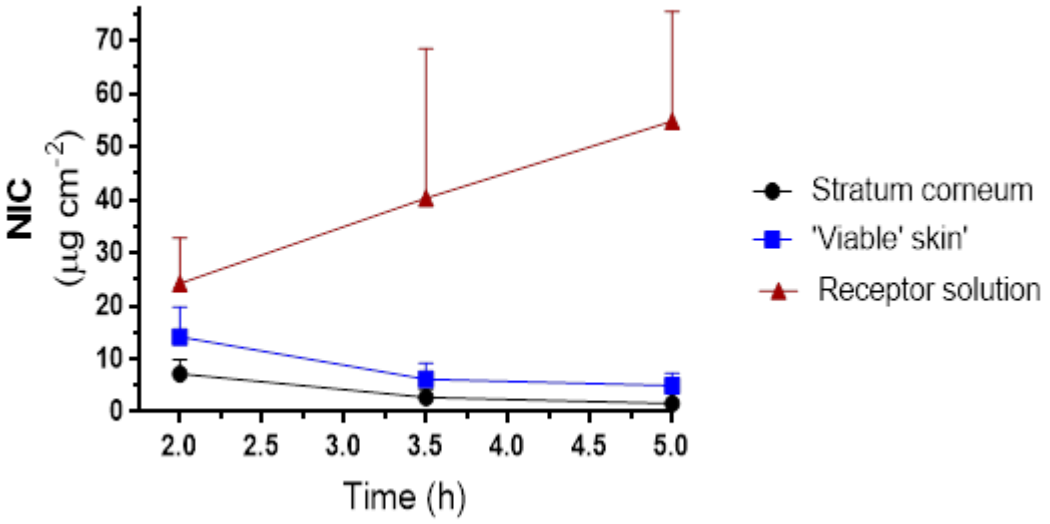

Figure 7. Redistribution of NIC after patch removal (mean ± S.D.; n = 6; Figure 1 (**c**)).

The NIC flux (J_{NIC}) across the entire skin (i.e., determined from slope of the permeation profile into the receptor solution shown in Figure 5) was 25.7 ± 14.8 µg h^{-1} cm^{-2}. From the disposition of NIC in the *in vitro* experiments performed, and 'correcting' for drug in 'viable' skin, J_{NIC} was 27.0 ± 15.6 µg h^{-1} cm^{-2} (24-hour experiment). Both approaches were close to the label claim (29.2 µg h^{-1} cm^{-2}; Figure 8).

Clearly, there is a contrast to the case for BUP, where this correction not only gave a different value of input-rate, but more importantly, enabled the estimated delivery rate to much more closely approach the labelled performance *in vivo*.

Thus, measuring flux into the receptor phase provided an accurate representation of *in vivo* performance, and 'correcting' for the effect of drug in SC/viable skin had little impact (unlike the case for BUP, where this 'correction' enabled the estimated delivery rate to much more closely approach the labelled performance *in vivo*). The fact that NIC has a balanced lipophilicity (log P ~ 1.2) and lower molecular weight (162 Da) is undoubtedly the major reason behind the high transepidermal flux and, therefore, the observed low drug accumulation in the 'viable' tissue.

Previous studies carried out with Nicopatch® (a product with similar characteristics to Nicotinell®) using human skin gave a comparable skin permeation rate (~ 31.0 µg h^{-1} cm^{-2}) (Olivier *et al.*, 2003).

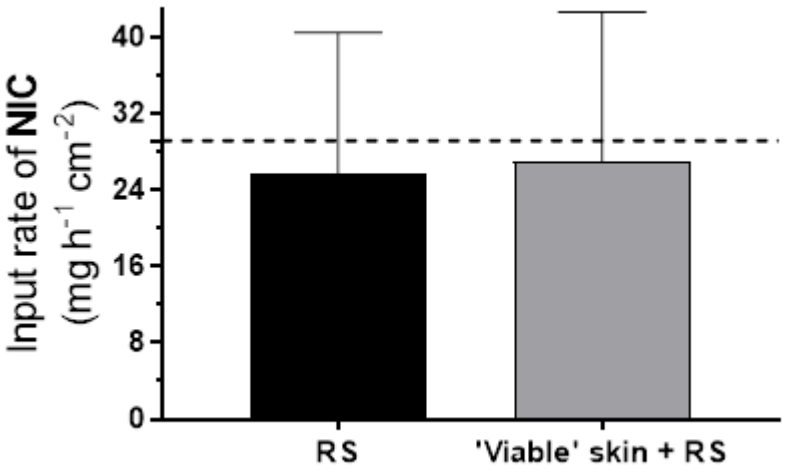

Figure 8. Input-rate of NIC from the Nicotinell® transdermal patch from two different data analysis approaches applied to the same data set (mean ± S.D.; n = 6). The dashed line indicates the claimed value. RS = receptor solution.

3.4. Diclofenac

The results from the BUP and NIC experiments show that a combination of SC sampling and IVPT, informed by IVRT, can provide indicative prediction of *in vivo* drug input-rates from transdermal patches. In the case of NIC, only IVPT is necessary whereas, for BUP, the levels measured in the skin *in vitro* are necessary to provide additional information that supports the *in vivo* outcome of wearing the patch. Nonetheless, in any of the two situations, accounting both the receptor and the viable tissue provides a good estimate for the input-rate.

The final component of the work in this paper, therefore, was to apply the approach to a topical patch which aims to deliver DF to treat pain and inflammation in subcutaneous tissue. Although pharmacologically-effective systemic levels are not the goal of the DF patch, the use of the approach described for BUP and NIC should provide information about this drug's input-rate to the subcutaneous tissue as well.

The cumulative permeation profile of DF through porcine skin is shown in Figure 9 (left panel). After 24 hours, 46 ± 10 µg cm^{-2} (~ 3.6% of the initial drug content) had

permeated the skin. On the other hand, the IVRT results for the DF patch reveal a linear relationship between the cumulative amount of drug released and the square-root of time (r^2 = 0.99). At the end of 24-hour experiment ($\sqrt{t}$ = 4.9 $h^{1/2}$), 692 ± 22 µg cm^{-2} (~ 53% of the initial drug content) of DF were released from the patch to the receptor solution (Figure 9 – right panel). The clear difference between the amounts of DF released in IVRT and permeated in IVPT suggests that the skin significantly rate-controls the permeation of DF to the receptor phase (Guy and Hadgraft, 1992).

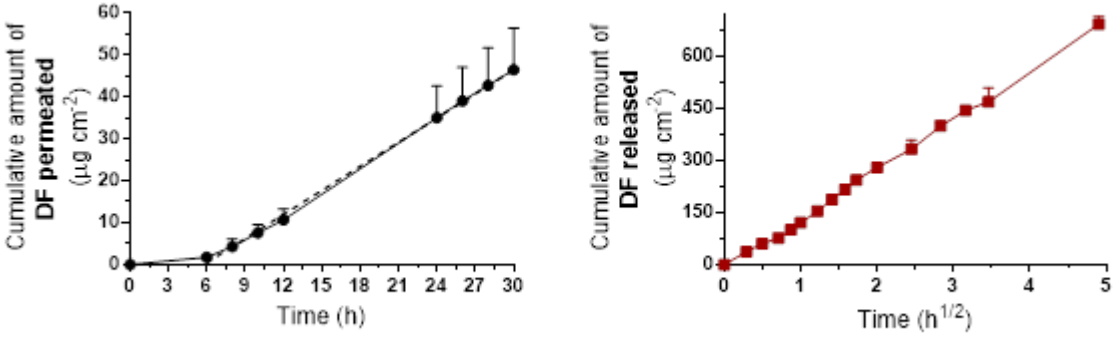

Figure 9. *Left panel:* Cumulative skin permeation of DF from Voltaren® expressed as a function of time (mean ± S.D.; n = 6; Figure 1 (**b**)). The dashed line is the best fit linear regression line to the data from 24 h. *Right panel:* Cumulative release of DF from Voltaren® as a function of the square-root of time (mean ± S.D.; n = 3).

Figure 10 shows a composite distribution profile of DF in each compartment: SC, 'viable' skin (i.e., that remaining after tape-stripping) and receptor solution during the patch application and after its removal. A relatively rapid accumulation of DF in both SC was observed during the first 2 hours, after which the drug concentrations in this 'compartment' remained quite constant until 30 hours. The redistribution of the drug after patch removal was also observed. Whilst the reservoir of drug in the SC remained relatively constant after removal of the patch, drug in the 'viable' skin moved into the receptor (Figure 11).

The DF flux (J_{DF}) across the entire skin (i.e., determined from slope of the permeation profile into the receptor solution shown in Figure 9) was 0.17 ± 0.09 µg h^{-1} cm^{-2}. From the disposition of DF in the *in vitro* experiments performed, and 'correcting' for drug in 'viable' skin, J_{DF} was 1.30 ± 0.31 µg h^{-1} cm^{-2} (30-hour experiment). The comparison between both approaches is shown in Figure 12.

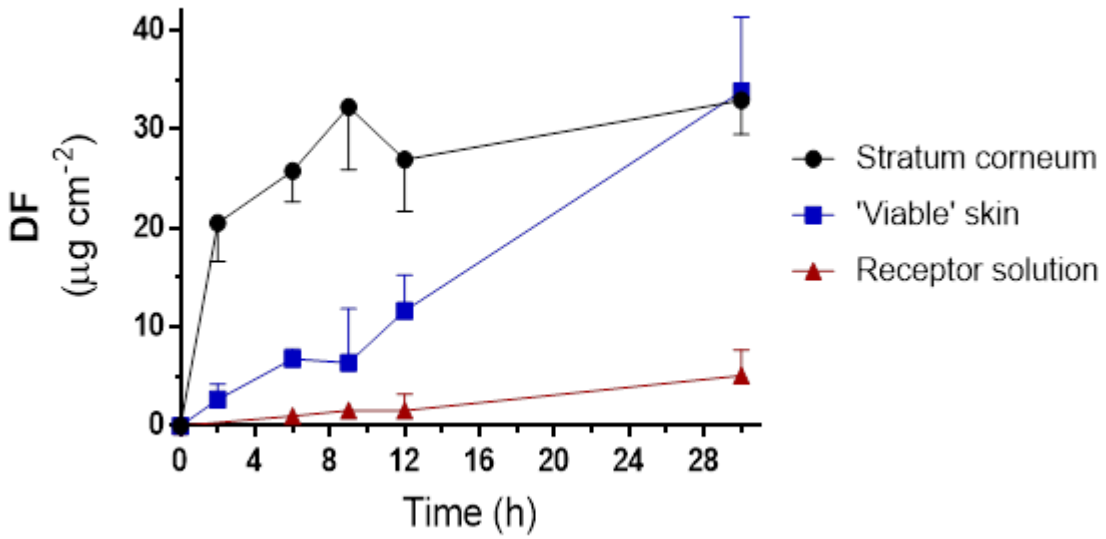

Figure 10. Distribution of DF in the stratum corneum, 'viable' skin (after tape-stripping) and receptor solution as a function of time (mean ± S.D.; n = 6; Figure 1 (**a**)).

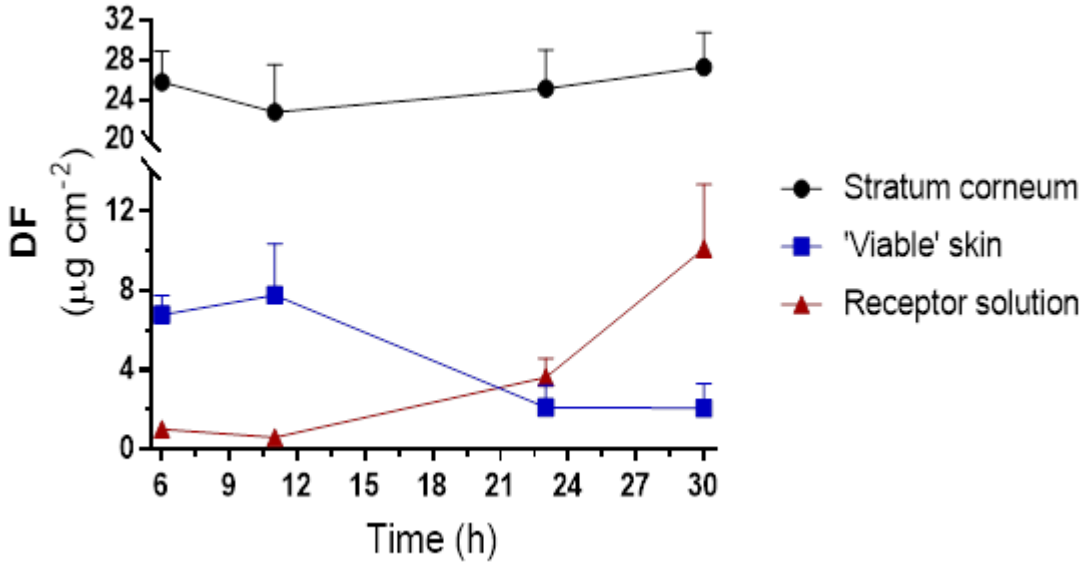

Figure 11. Redistribution of DF after patch removal (mean ± S.D.; n = 6; Figure 1 (**c**)).

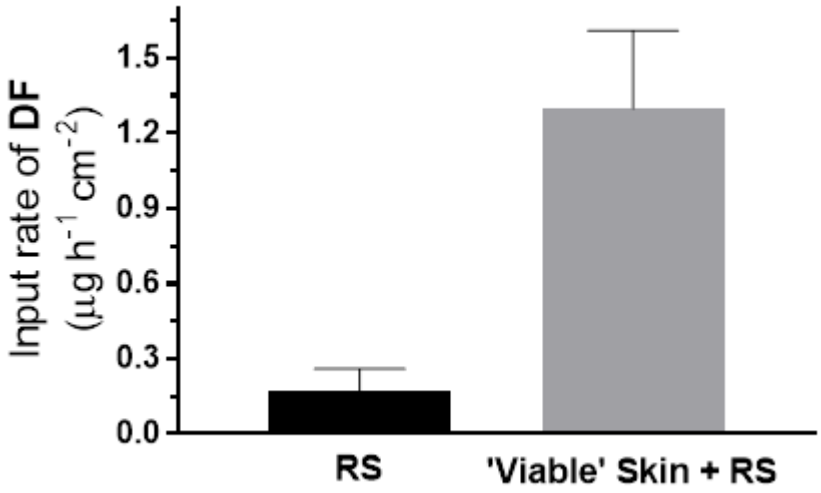

Figure 12. Input-rate of DF from the Voltaren® medicated plaster from two different data analysis approaches applied to the same data set (mean ± S.D.; n = 6). RS = receptor solution.

In broad terms, therefore, DF behaves much more like BUP than NIC. This observation is consistent with DF's physiochemical properties – SC is definitely rate-limiting the input flux, significant levels in the SC were measured and DF showed a strong affinity for the barrier layer of skin, and flux into the underlying skin tissue was comparable to that of BUP.

4. Conclusion

The good agreement between the experimentally determined input-rates of the two drugs and their labelled performance *in vivo* lends support to the potential utility of the *in vitro* approach proposed to define topical drug input-rates more broadly; that is, to apply the method not only to transdermally delivered drugs, but also to those, the sites of action of which are within either the living skin or the subcutaneous tissue.

Supplementary Information

Table S1. Buprenorphine recovery from tapes (n=3).

Theoretical concentration (µg/mL)	Buprenorphine recovery
	Tape
	% ± SD
0.15	93.1 ± 13.4
0.3	92.9 ± 12.1
0.6	95.8 ± 3.7
1.5	101.7 ± 26.1
3.0	99.7 ± 12.9
6.0	100.3 ± 3.7
12.0	101.0 ± 2.8
25.0	101.5 ± 2.1

Table S2. Buprenorphine recovery from 'viable skin' (n=3).

Theoretical concentration (µg/mL)	Buprenorphine recovery
	'Viable' skin
	% ± SD
2.0	88.9 ± 4.0
4.0	96.4 ± 19.0
8.0	96.9 ± 8.5
12.0	101.1 ± 2.3
20.0	99.5 ± 2.5
25.0	101.6 ± 3.5

Table S3. Nicotine recovery from tapes and 'viable' skin (n=3).

Theoretical concentration (µg/mL)	Nicotine recovery	
	Tape	'Viable' skin
	% ± SD	% ± SD
3.0	99.7 ± 0.1	101.2 ± 0.4
6.0	95.7 ± 1.8	98.7 ± 2.0

Table S4. Diclofenac recovery from tapes and 'viable skin' (n=3).

Theoretical concentration (µg/mL)	Diclofenac recovery	
	Tape	'Viable' skin
	% ± SD	% ± SD
0.1	88.6 ± 17.7	103.3 ± 9.1
1.0	83.3 ± 3.7	87.0 ± 7.5
10.0	81.7 ± 3.3	86.0 ± 3.7

Table S5. Nicotine in the receptor solution and on tapes with and without light exposure (n=3).

Theoretical concentration (µg/mL)	24 h		48 h		72 h	
	With light	Without light	With light	Without light	With light	Without light
	% ± SD	% ± SD	% ± SD	% ± SD	% ± SD	% ± SD
25.0	**Receptor solution**					
	100.0 ± 0.2	100.3 ± 0.4	99.8 ± 0.1	100.0 ± 0.1	100.0 ± 0.1	100.6 ± 0.1
6.0	**Tape**					
	99.2 ± 2.4	100.6 ± 6.3	97.6 ± 5.1	97.8 ± 2.6	99.3 ± 5.1	99.4 ± 4.9

The mass of BUP, NIC and DF plotted as a function of depth in the SC is presented in Figure S1, S2 and S3, respectively. All the profiles show a typical decrease in drug in the SC with increasing depth. The amount of SC removed may be affected by both intrinsic factors, such as anatomical site, as well as extrinsic factors, such as the adhesive tape used (Lademann *et al.*, 2009). That said, the effects of these factors on the measured drug mass are minimized as long as at least half of the SC is collected. Specifically, the outermost half of the SC will contain 75% of the total drug mass if the drug concentration profile has reached steady-state (i.e., it is linear with position in the SC), and an even larger fraction if steady-state has not been established and the concentration profile is not linear.

The average SC thickness removed by tape-stripping over different application times for Transtec®, Nicotinell® and Voltaren® was 15.6 ± 4.5 µm, 11.9 ± 3.2 µm and 15.0 ± 2.7 µm, respectively.

The total porcine SC thickness has been reported by several authors, see for instance: Herkenne *et al.*, 2007; Sekkat *et al.*, 2002; Kalia and Guy, 2001; Bronaugh *et al.*, 1982. Their studies have suggested that the thickness of porcine SC is around

15 µm. Therefore, the SC removed during our experiments suggest that 20 tapes (the number of adhesive tapes used for each cell) were enough to collect most of the SC.

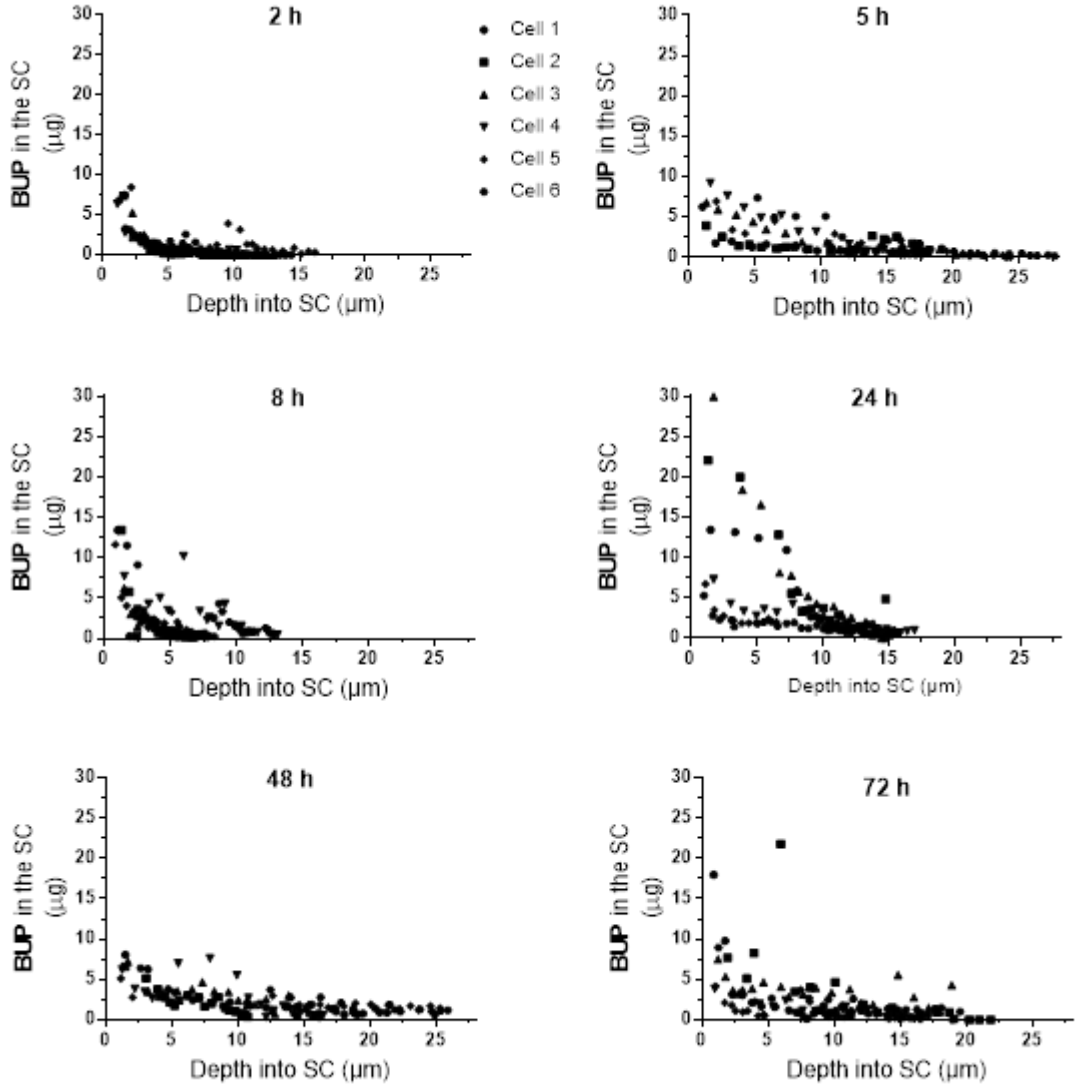

Figure S1. Amount of BUP in stratum corneum as a function of depth, following 2, 5, 8, 24, 48 and 72 hours of treatment with Transtec®.

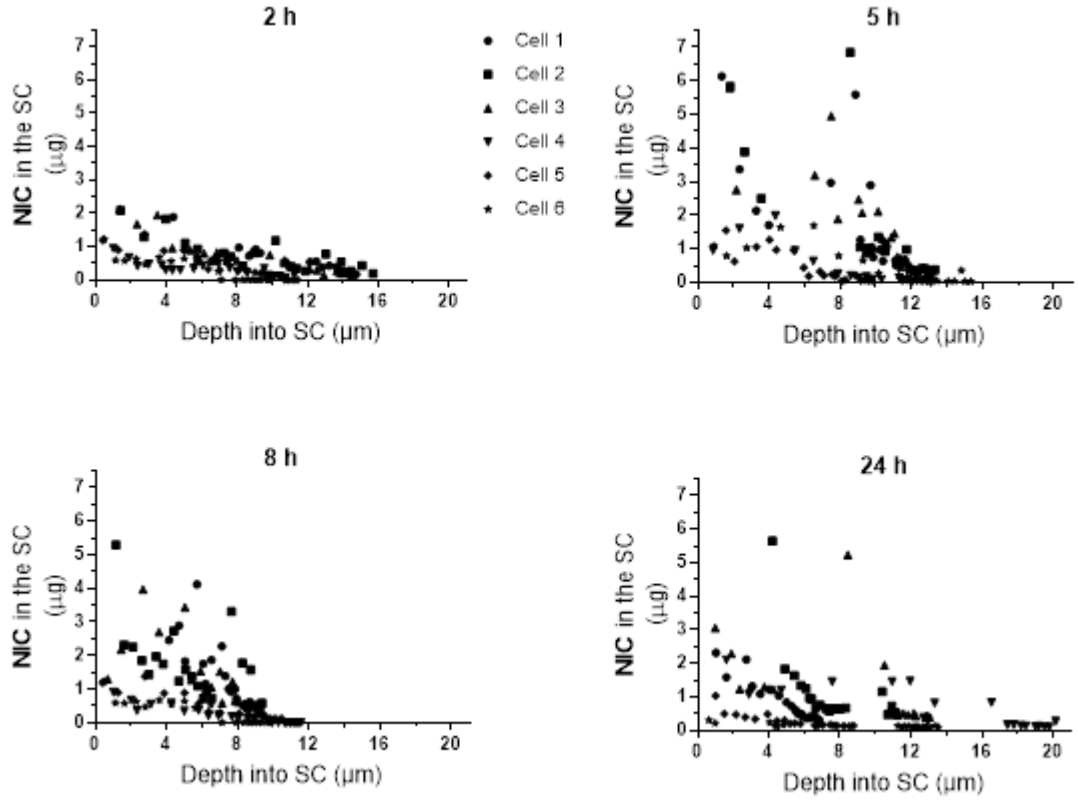

Figure S2. Amount of NIC in stratum corneum as a function of depth, following 2, 5, 8 and 24 hours of contact with Nicotinell®.

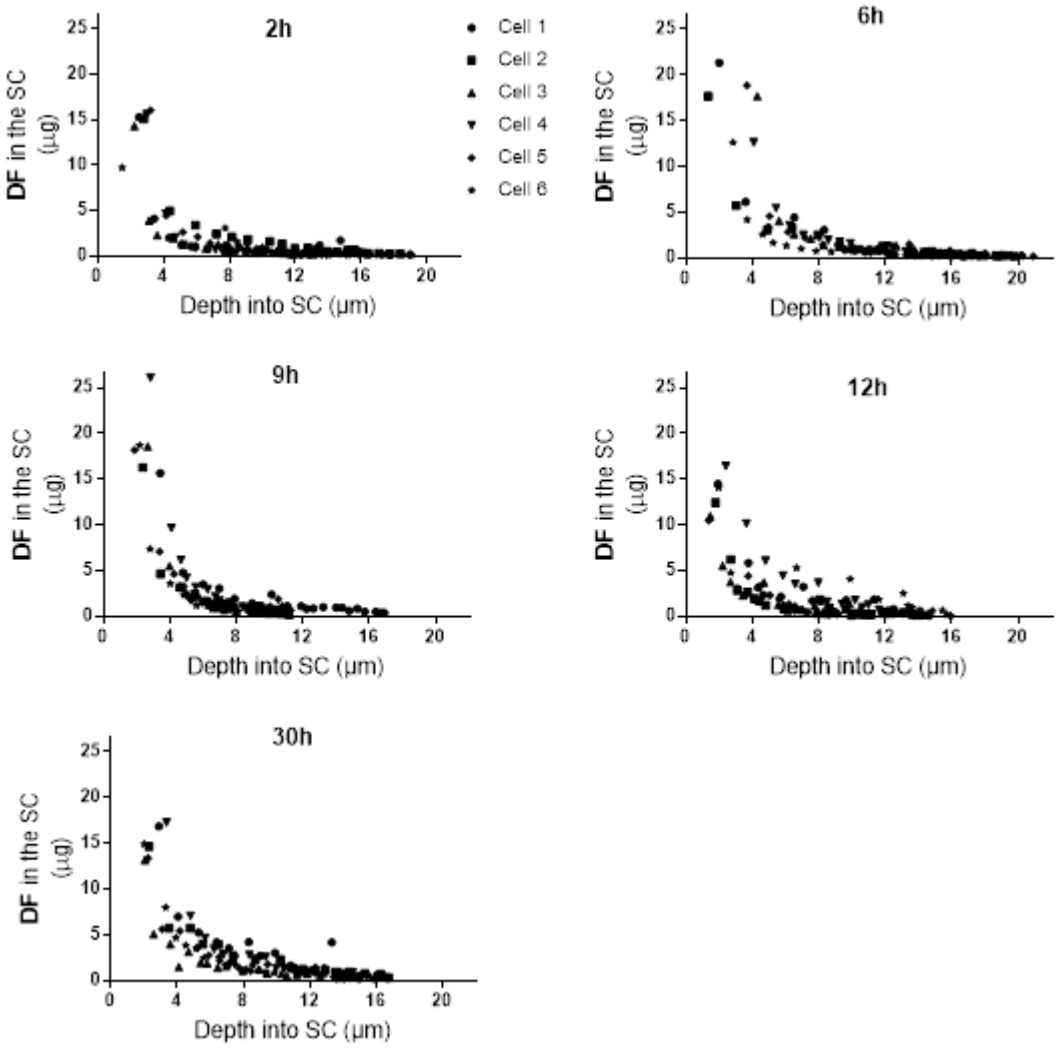

Figure S3. Amount of DF in stratum corneum as a function of depth, following 2, 6, 9, 12 and 30 hours of treatment with Voltaren®.

To verify the variability in the mass of the blank tapes, i.e., after the tapes have been cut and before the tape-stripping experiments have been started, the mass of all the tapes used in each experiment was averaged and compared one another. As the tapes have been cut manually, therefore, the areas are not precisely the same, it is not a surprise that there is a variability in the mass of each blank tape. The variability, however, is not very different, overall, the relative standard deviations were always below 15% (Tables S6 – S8).

The fact that during all the experiments the mass of the blank tapes kept relatively constant could be used as an indication of the calibration of the balance used to weigh the tapes. As a routine, however, to ensure that the readings from the instrument are accurate and consistent, the balance used in these experiments was

regularly calibrated using a standard. Figure S4 shows an example of a certificate of calibration.

Table S6. Mass of blank tapes used before tape-stripping **buprenorphine** experiments. SD: Standard Deviation. RSD: Relative Standard Deviation.

	2h	**5h**	**8h**	**24h**	**48h**	**72h**
Average mass (mg)	62.9	63.0	56.9	63.7	62.2	61.3
SD	7.1	8.8	7.3	6.5	8.9	8.9
RSD (%)	11.3	13.9	12.8	10.1	14.3	14.4
N	120	120	120	120	120	120

Table S7. Mass of blank tapes used before tape-stripping **nicotine** experiments. SD: Standard Deviation. RSD: Relative Standard Deviation.

	2h	**5h**	**8h**	**24h**
Average mass (mg)	63.9	66.1	63.1	65.9
SD	9.3	8.4	8.8	9.0
RSD (%)	14.6	12.7	14.0	13.7
N	120	120	120	120

Table S8. Mass of blank tapes used before tape-stripping **diclofenac** experiments. SD: Standard Deviation. RSD: Relative Standard Deviation.

	2h	**6h**	**9h**	**12h**	**30h**
Average mass (mg)	68.7	66.9	60.0	69.90	64.8
SD	6.8	8.7	8.9	7.20	6.3
RSD (%)	10.0	13.0	14.9	10.3	6.3
N	120	120	120	120	120

Figure S4. Record of balance calibration.

References

Anderson, R.L. & Cassidy, J.M., 1973. Variations in Physical Dimensions and Chemical Composition of Human Stratum Corneum. *Journal of Investigative Dermatology,* 61(1), pp. 30-32.

Bronaugh, R.L., Stewart, R.F. & Congdon, E.R., 1982. Methods for in vitro percutaneous absorption studies II. Animal models for human skin. *Toxicology and Applied Pharmacology,* 62(3), pp. 481-488.

Davaran, S., Rashidi, M.R., Khandaghi, R. & Hashemi, M., 2005. Development of a novel prolonged-release nicotine transdermal patch. *Pharmacological Research,* 51(3), pp. 233-237.

Godin, B. & Touitou, E., 2007. Transdermal skin delivery: predictions for humans from in vivo, ex vivo and animal models. *Advanced Drug Delivery Reviews,* 59(11), pp. 1152-1161.

Guy, R.H. & Hadgraft, J., 1992. Rate control in transdermal drug delivery? *International Journal of Pharmaceutics,* 82(3), pp. R1-R6.

Herkenne, C., Naik, A., Kalia, Y.N., Hadgraft, J. & Guy, R.H., 2007. Ibuprofen transport into and through skin from topical formulations: in vitro–in vivo comparison. *Journal of Investigative Dermatology,* 127(1), pp. 135-142.

Kalia, Y.N. & Guy, R.H., 2001. Modeling transdermal drug release. *Advanced Drug Delivery Reviews,* 48(2-3), pp. 159-172.

Kumar, S., Zakrewsky, M., Chen, M., Menegatti, S., Muraski, J.A. & Mitragotri, S., 2014. Peptides as skin penetration enhancers: Mechanisms of action. *Journal of Controlled Release,* 199, pp. 168-178.

Lademann, J., Jacobi, U., Surber, C., Weigmann, H-., Fluhr, J.W., 2009. The tape stripping procedure – evaluation of some critical parameters. *European Journal of Pharmaceutics and Biopharmaceutics,*72(2), pp. 317-323.

Leal, L.B., Cordery, S.F., Delgado-Charro, M.B., Bunge, A.L. & Guy, R.H., 2017. Bioequivalence Methodologies for Topical Drug Products: In Vitro and Ex Vivo Studies with a Corticosteroid and an Anti-Fungal Drug. *Pharmaceutical Research,* 34(4), pp. 730-737.

McCarley, K.D. & Bunge, A.L., 2001. Pharmacokinetic models of dermal absorption. *Journal of Pharmaceutical Sciences,* 90(11), pp. 1699-1719.

Olivier, J.-C., Rabouan, S. & Couet, W., 2003. In vitro comparative studies of two marketed transdermal nicotine delivery systems: Nicopatch® and Nicorette®. *International Journal of Pharmaceutics,* 252(1-2), pp. 133-140.

Rao, B.S., Seshasayana, A., Saradhi, S.P., Kumar, N.R., Narayan, C.P. and Murthy, K.R., 2001. Correlation of 'in vitro'release and 'in vivo'absorption characteristics of rifampicin from ethylcellulose coated nonpareil beads. *International journal of pharmaceutics,* 230(1-2), pp.1-9.

Roberts, M.S., Anissimov, Y.G. & Gonsalvez, R.A., 2001. Mathematical models in percutaneous absorption. *Journal of Toxicology: Cutaneous and Ocular Toxicology,* 20(2-3), pp. 221-270.

Roy, S.D., Roos, E. & Sharma, K., 1994. Transdermal delivery of buprenorphine through cadaver skin. *Journal of Pharmaceutical Sciences,* 83(2), pp. 126-130.

Ruela, A.L.M., Figueiredo, E.C., Perissinato, A.G., Lima, A.C.Z., Araújo, M.B. & Pereira, G.R., 2013. In vitro evaluation of transdermal nicotine delivery systems commercially available in Brazil. *Brazilian Journal of Pharmaceutical Sciences,* 49(3), pp. 579-588.

Schäfer-Korting, M., Mehnert, W. & Korting, H.-C., 2007. Lipid nanoparticles for improved topical application of drugs for skin diseases. *Advanced Drug Delivery Reviews,* 59(6), pp. 427-443.

Sekkat, N., Kalia, Y.N. & Guy, R.H., 2002. Biophysical study of porcine ear skin in vitro and its comparison to human skin in vivo. *Journal of Pharmaceutical Sciences,* 91(11), pp. 2376-2381.

Siepmann, J. & Peppas, N.A., 2011. Higuchi equation: Derivation, applications, use and misuse. *International Journal of Pharmaceutics,* 418(1), pp. 6-12.

Wagner, J.G. & Nelson, E., 1964. Kinetic analysis of blood levels and urinary excretion in the absorption phase after single dose of drug. *Journal of Pharmaceutical Sciences,* 53, pp. 1392-1403.

Zaffaroni, A., 1991. Overview and evolution of therapeutic systems. *Annals of the New York Academy of Sciences,* 618(1), pp. 405-421.

Chapter 3: Determination of the skin pharmacokinetics of diclofenac from stratum corneum sampling *in vivo*

Abbreviations

ΔC	water concentration gradient across the stratum corneum
Δt	elapsed time interval between clearance and uptake times
A	sampled skin area
B	baseline parameter related to estimation of total thickness by TEWL values
C_v	drug concentration in the vehicle
C_x	the drug concentration at position x in the stratum corneum
D	drug diffusivity
D_0	diffusivity when clearance from the stratum corneum begins
DF	diclofenac
D_w	diffusion coefficient of water in the stratum corneum
HPLC-UV	high-performance liquid chromatography with ultraviolet detection
J_{AVE}	average flux of drug out of stratum corneum into underlying tissue
k	1^{st}-order rate constant describing clearance from the stratum corneum
K	drug's stratum corneum – vehicle partition coefficient
$K_{sc,vt}$	stratum corneum-viable tissue partition coefficient

L	diffusion path-length through (or thickness of) a membrane
log P	log{octanol-water partition coefficient (P)}
M_{SC}	mass of drug measured in the tape-strips
SC	stratum corneum
t_{app}	application time
TEWL	transepidermal water loss
T_{Lag}	time lag for diffusion through a membrane
T_{SS}	time to achieve steady-state
x/L	relative depth in the stratum corneum
α	1^{st}-order constant rate

1. Introduction

A key question in the development of a topical drug product (dermatological or locally acting) is whether target-site drug concentrations sufficient to treat the disease have been reached. Due to the difficulty of accessing the deep layers of the skin, the estimation of the rate and the extent to which a drug reaches its site of action on, within or below the skin, has not proved to be a facile task.

The skin bioavailability[4] of a drug mainly depends on two key physicochemical parameters, which impact significantly on the skin pharmacokinetics: partitioning into and diffusivity through the skin (Wiechers, 1989; Moser et al., 2001). In the past decades, a number of approaches (*in vitro*, *in silico* and *in vivo*) have been developed for predicting these key parameters (Barbero and Frasch, 2009; Russell and Guy, 2009).

In vitro experiments using excised skin (for example, human or porcine skin) are a recognised option for the assessment of drug penetration into the skin. Nevertheless, the lack of a functioning microcirculation means that information about drug clearance kinetics from the skin[5] may be lacking (Leal et al., 2017).

Several mathematical models have been developed to explain, at least in part, percutaneous absorption kinetics (Moss et al., 2002; Yamashita and Hashida, 2003; Lian, Chen and Han, 2008; Mitragotri et al., 2011). However, most of the existing models often suffer from being too complex, thereby rendering the model of little practical use.

There are many *in vivo* methods for measuring dermal absorption of drugs, such as invasive skin biopsy, microdialysis (and open-flow microperfusion) and sampling of the SC by tape-stripping. Biopsy of the tissues beneath the SC, microdialysis and open-flow microperfusion seem to be ideal strategies to quantify the concentration profile of a topically applied drug within the skin. However, these approaches are invasive and highly demanding as a routine method. As an alternative, sampling the SC by tape-stripping, *in vivo* in human, is a relatively non-invasive and straightforward

[4] The term 'skin bioavailability' here refers to the rate and the extent to which a drug reaches its site of action on, within or below the skin.
[5] The term 'clearance from the skin' here is used to mean the volume of skin from which a drug is completely removed per unit time.

technique which has proven useful to successfully estimate values relating to diffusivity and partitioning coefficients of drugs (Stinchcomb et al., 1999; Alberti et al., 2001; Herkenne et al., 2006, 2007; Nicoli et al., 2009; Rothe et al., 2017). Some previous studies have used the tape-stripping approach to evaluate products by measuring the mass of drug in the SC after an absorption (into the SC) phase and a clearance (from the SC) phase. This allowed the estimation of key diffusional and partitioning parameters for the drug together with an estimation of the drug's flux out of the SC into underlying tissues (N'Dri-Stempfer et al., 2009; Cordery et al., 2017; de Araujo et al., 2018).

Therefore, this study built on the SC sampling technique approach (tape-stripping) and applied different Fickian diffusion models to estimate useful skin pharmacokinetic parameters related to drug partitioning into and diffusion across the SC. The work was performed in human subjects, using diclofenac (DF) from a marketed medicated plaster. This product is indicated for pain relief in conditions such as knee osteoarthritis (Brühlmann et al., 2006), ankle sprains (Costantino et al., 2011) and epicondylitis (Jenoure et al., 1997).

Advantages of using a medicated plaster (compared to, for example, a gel or a cream) in this study were: i. the drug concentration in the formulation was expected to remain relatively constant during the experiment, making it easier to interpret the findings; and ii. in contrast to a dermatological product, the plaster is administered to intact healthy skin, therefore, data was generated within a clinically relevant scenario.

2. Materials and Methods

2.1. Materials

Voltaren® medicated plaster (GlaxoSmithKline, Munich, Germany) was purchased from Amazon UK. Diclofenac epolamine was purchased from Toronto Research Chemicals (Toronto, Canada), all the solvents and HPLC reagents were from Sigma-Aldrich Co., Ltd. (Gillingham, UK).

2.2. Stratum corneum tape-stripping experiments

Healthy subjects with no history of dermatological disease participated in this study, which was approved by the Research Ethics Approval Committee for Health

at the University of Bath (EP 16/17 142). Six subjects (age range: 23 – 53 years) participated in the study having given their consent. The study involved application of small sections of a Voltaren® marketed medicated plaster (180 mg of diclofenac epolamine in 140 cm^2). The patient information leaflet recommends an application time of up to 12 hours per plaster.

2.2.1 Design of the experiments

The design of the experiments is illustrated in Figure 1.

In a first set of experiment, the amount of DF in the SC was assessed after an 'uptake' period following application of the plaster (0.5, 1, 2 and 6 hours). Sections of the plaster were cut to 5 cm^2 (1 x 5 cm), 3 pieces were applied on the volar surface of one forearm and 3 pieces on the other forearm of 4 subjects (age range: 23 – 32 years). There were duplicate application sites for each time on each subject.

In a second set of experiment, the plaster was cut into 5 cm^2 (1 x 5 cm) sections, 8 of which were applied on the volar surface of one forearm of all six subjects. The experiments assessed the amount of drug in the SC (a) after an 'uptake' period following application of the plaster (2, 6, 9 and 12 hours); and (b) following defined 'clearance' periods (5, 17 and 24 hours) after removal of the plaster sections at the end of a 6 hours 'uptake'. There were duplicate application sites for each time on each subject.

All the subjects who participated in the second set of experiments also participated in the first set. To ensure that the SC was fully recovered, the two parts of the study were separated by at least 120 days. No lotion, cream or other personal care product was used on the forearms for at least 24 hours before and during the study. For the duration of the experiment, subjects were asked not to bathe or participate in vigorous activity, but otherwise pursued their normal lifestyle.

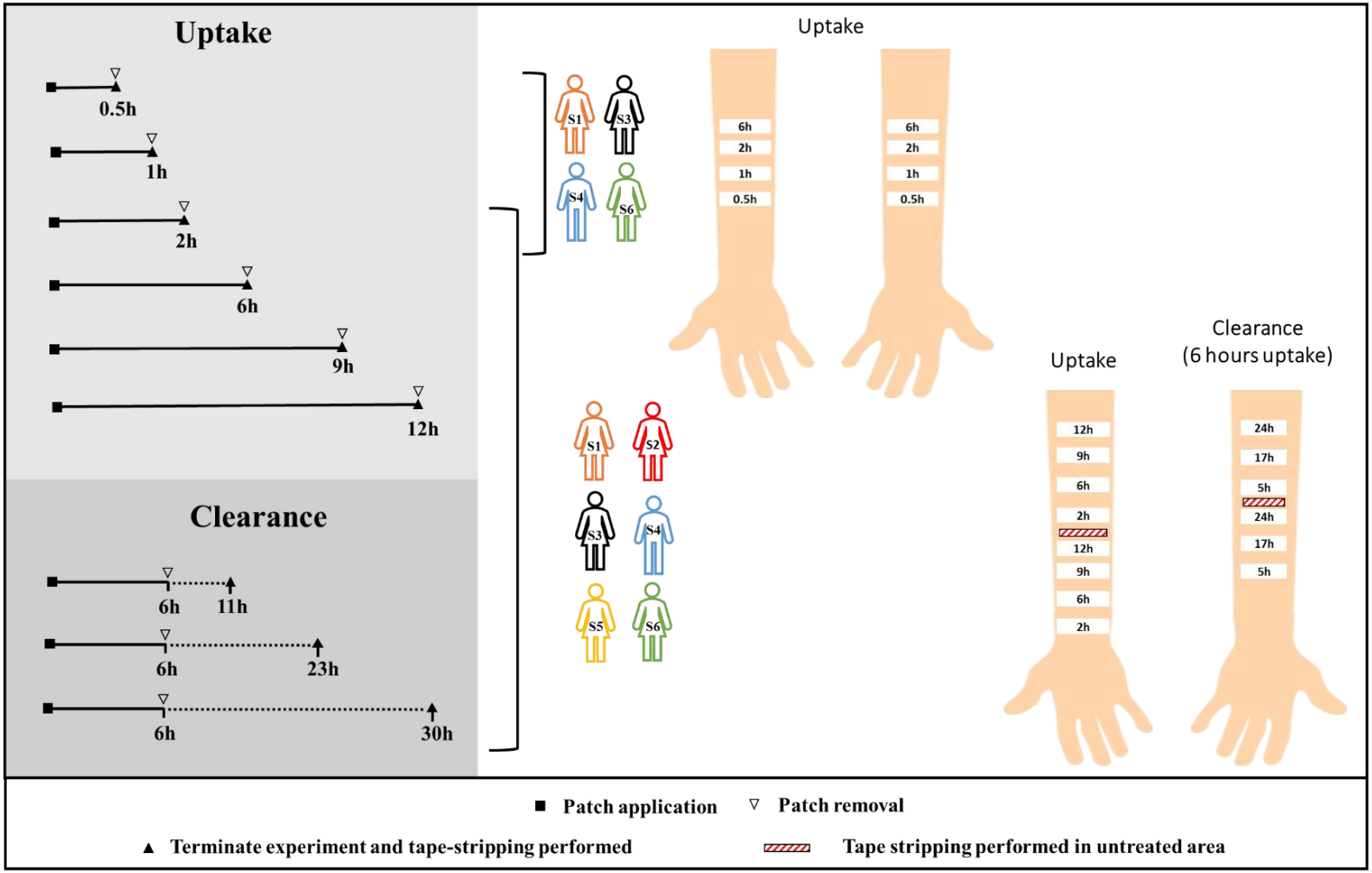

Figure 1. Schematic representation of the design of the tape-stripping experiments.

2.2.2 Stratum corneum sampling

All the sites designated uptake were tape-stripped immediately after plaster removal. On the sites designated clearance, the plaster was removed after a 6-hour uptake and the edges of the clearance sites were demarcated using Mefix® tape (Molnlycke, Lancashire, UK), without encroaching on the treated area. Then, 5, 17 or 24 hours later, sites were tape-stripped. No cleaning of the application area was performed.

The SC sampling site was delimited by a template (Scotch® Book Tape, 3M, St Louis, MN, USA), with internal dimensions of 1 x 5 cm, which was placed on the skin immediately before tape-stripping began. Measurements of transepidermal water loss (TEWL, AquaFlux® evaporimeter, Biox System Ltd. London, UK) taken after plaster removal, before stripping and, intermittently, during tape-stripping, to indicate when most of the SC had been removed and before complete derangement of the barrier. Tape-stripping was therefore carried out until either (i) the rate of water loss reached 60 g m^{-2} h^{-1} or (ii) 30 tape-strips had been removed (Kalia, Pirot and Guy, 1996; Kalia et al., 2000). All tapes were weighed (Microbalance SE-2F, precision 0.1 µg; Sartorius AG, Goettingen, Germany) before and after stripping to determine the mass of SC removed; tapes were first discharged of static electricity (R50 discharging bar and ES50 power supply Eltex Elektrostatik GmbH, Weil am Rhein, Germany).

2.2.3 Drug extraction and analysis

DF was extracted from tape-strips into 3 mL of methanol in a glass vial by shaking overnight at room temperature. Samples were filtered (0.45 µm nylon membrane, SMI-Labhut, Ltd., Maisemore, UK) and transferred to HPLC vials for analysis. Drug was extracted from the first two tapes individually but, thereafter, tape-strips from the deeper SC were analysed in groups of up to 4 tapes to ensure, as far as possible, that the aggregated samples contained a sufficient drug amount to exceed the limit of quantification of the assay.

200 µL of 0.1% formic acid in water were added to 800 µL of the extracted DF solution and the drug was then quantified by HPLC (Summit, Dionex, Camberley, UK) with UV detection (280 nm). Chromatography was performed on a HiQSil C18HS column (150 x 4.6 mm, 5 µm, Kya Technologies Corporation, Japan). The mobile

phase was 75:25 methanol: 0.1% formic acid aqueous solution. The flow rate was 1.2 mL/min. The injection volume was 100 µL and the retention time of DF was ~7 minutes; limits of quantification and detection were 0.06 and 0.02 µg mL^{-1}, respectively.

Selectivity of the analytical method was confirmed by extraction of tapes with SC that had not been exposed to DF; no interference was found at the relevant retention time. Recovery of DF from tapes was assessed by spiking tape-stripped samples of untreated SC with known amounts of drug in solution which was left to dry for several hours before extraction. Mean extraction efficiencies were greater than 82% from tape-strips (details are provided in the 'Supplementary Information' – Table S1).

2.3. Determination of stratum corneum total thickness

The apparent total thickness of the SC (L) was estimated from measurements of TEWL during the tape-stripping process (Russell, Wiedersberg and Delgado-Charro, 2008). L was estimated from a site adjacent to the treated skin on each forearm (Figure 1). The average (arithmetic mean) of the two estimates (one from each arm) was used for further calculations.

Briefly, as the SC is progressively removed by tape-stripping, TEWL increases from the baseline in a non-linear fashion, with respect to the thickness of SC removed (x), empirically described by Equation 1.

$$TEWL_x = B + \frac{D_w K_{SC,VT} \Delta C}{L - x} \qquad \text{(Equation 1)}$$

where x is calculated from the mass of SC on each tape divided by the area sampled and the density of the SC, assumed to be 1 g cm^{-3} (Anderson and Cassidy, 1973); B is the initial TEWL value before stripping, D_w is the diffusion coefficient of water in the SC, $K_{SC,V}$ is the SC-viable tissue partition coefficient and ΔC is the water concentration gradient across the SC. Values for B, $D_w K_{SC,VT} \Delta C$ and L were determined by nonlinear regression with uniform weighting of the $TEWL_x$ (g m^{-2} h^{-1}) versus *x* (µm) measurements with initial estimates of L (µm) = last *x* value + 1 and ($D_w K_{SC,VT} \Delta C$) = 30 (g m^{-2} h^{-1}).

2.4. Data Analysis

The mass of drug in the SC was expected to exhibit a log-normal distribution (Williams, Cornwell and Barry, 1992; Kasting et al., 1994; Cornwell and Barry, 1995). Therefore, the arithmetic average, standard deviation and 90% confidence intervals of the logarithm of the geometric mean of the duplicate measurements in the 6 subjects were calculated for 'uptake' and 'clearance' for each experiment time (N'Dri-Stempfer et al., 2009).

2.4.1. Diclofenac uptake into the stratum corneum

From the data collected during the uptake experiments, three approaches for analysing the data were considered.

First, the total quantity of DF recovered in the tape-strips per unit of area of exposure (M_{SC}/A) was simply expressed as a function of time.

Secondly, the concentration profile of DF across the SC (C_x) as a function of position in the SC (x/L) was analysed for all subjects at each uptake time considered. The data points from the two replicate sites were combined. Then, profiles were fitted to the relevant solution of Fick's second law of diffusion (Scheuplein, 1967; Crank, 1979) (Equation 2) assuming the following boundary conditions: (i) the drug concentration in the vehicle (C_v) remains constant during the treatment period (t_{app}); (ii) the SC provides a homogeneous barrier to drug diffusion; (iii) there is no drug in the SC at t=0; and (iv) the viable epidermis acts as a perfect sink for the permeant.

$$C_x = KC_v \left[1 - \frac{x}{L} - \frac{2}{\pi} \sum_{m=1}^{\infty} \frac{\exp\left[-m^2\pi^2 t_{app}\left(D/L^2\right)\right] \sin\left(m\pi x/L\right)}{m}\right] \qquad \text{(Equation 2)}$$

where C_x is the drug concentration (mass of drug divided per mass of SC removed) at position x in the SC at the application time (t_{app}).

The fitting of Equation 2 yields values for KC_v (K is the drug's SC-vehicle partition coefficient) and for D/L^2, a first-order rate constant comprising the ratio of the drug diffusivity (D) in the SC to the total thickness (L) squared of the barrier. From these two parameters (KC_v and D/L^2) and the corresponding L (estimated for each

subject using Equation 1), the lag-time (T_{Lag} = L^2/6D, Roberts, Anissimov and Gonsalvez (1999);), time to steady-state (T_{SS} = ~2.4T_{Lag}, Cleek and Bunge (1993)) and steady-state flux across the SC (J_{ss} = KC_vD/L,) may be calculated.

Thirdly, it was also possible to analyse the mass of DF after SC uptake using an approximate solution to Fick's second law of diffusion (Equation 3 and Equation 4) from which D may be estimated in a different way.

The cumulative mass of DF measured in the tape-strips per unit of area of exposure (M_{SC}/A) *versus* square-root of time profiles were compared to the solution of two models describing diffusion into a: (i) semi-infinite membrane (Equation 3), and (ii) finite membrane (Equation 4) (Frasch and Bunge, 2015).

$$\frac{M_{SC}}{A} = 2KC_v\sqrt{\frac{Dt_{app}}{\pi}} \qquad \text{(Equation 3)}$$

$$\frac{M_{SC}}{A} = KC_v L\left[\frac{1}{2} - \frac{4}{\pi}\sum_{n=0}^{\infty}\frac{\exp[-D(2n+1)^2\pi^2(t_{app}/L^2)]}{(2n+1)^2}\right] \qquad \text{(Equation 4)}$$

The semi-infinite membrane model assumes that the application time of the formulation to the SC is insufficient for the drug to reach the lower surface of the barrier which therefore, in effect, behaves as a semi-infinite membrane (Equation 3); the finite membrane model, in contrast, considers the SC as a single finite membrane (Equation 4).

The analytical solution to the semi-infinite model permits a value of D to be deduced. Then, using this D, Equation 4 can be used to predict the evolution of the M_{SC}/A over time following the finite membrane model. Note that M_{SC}/A corresponds to the average concentration in the SC multiplied by the SC thickness.

The application of Equations 3 and 4 requires estimates of the concentration of the permeant at x=0. In this study, we have assumed that the drug concentration at the surface of the SC is constant and equal to KC_v (obtained from fitting the data to

Equation 2; the average of the KC_v determined following 2 and 6 hours of application was used).

Figure 2 summarises the steps involved in the estimation of pharmacokinetic drug parameters using Fick's second law of diffusion (Equation 2) and the semi-infinite and finite models (Equation 3 and 4, respectively).

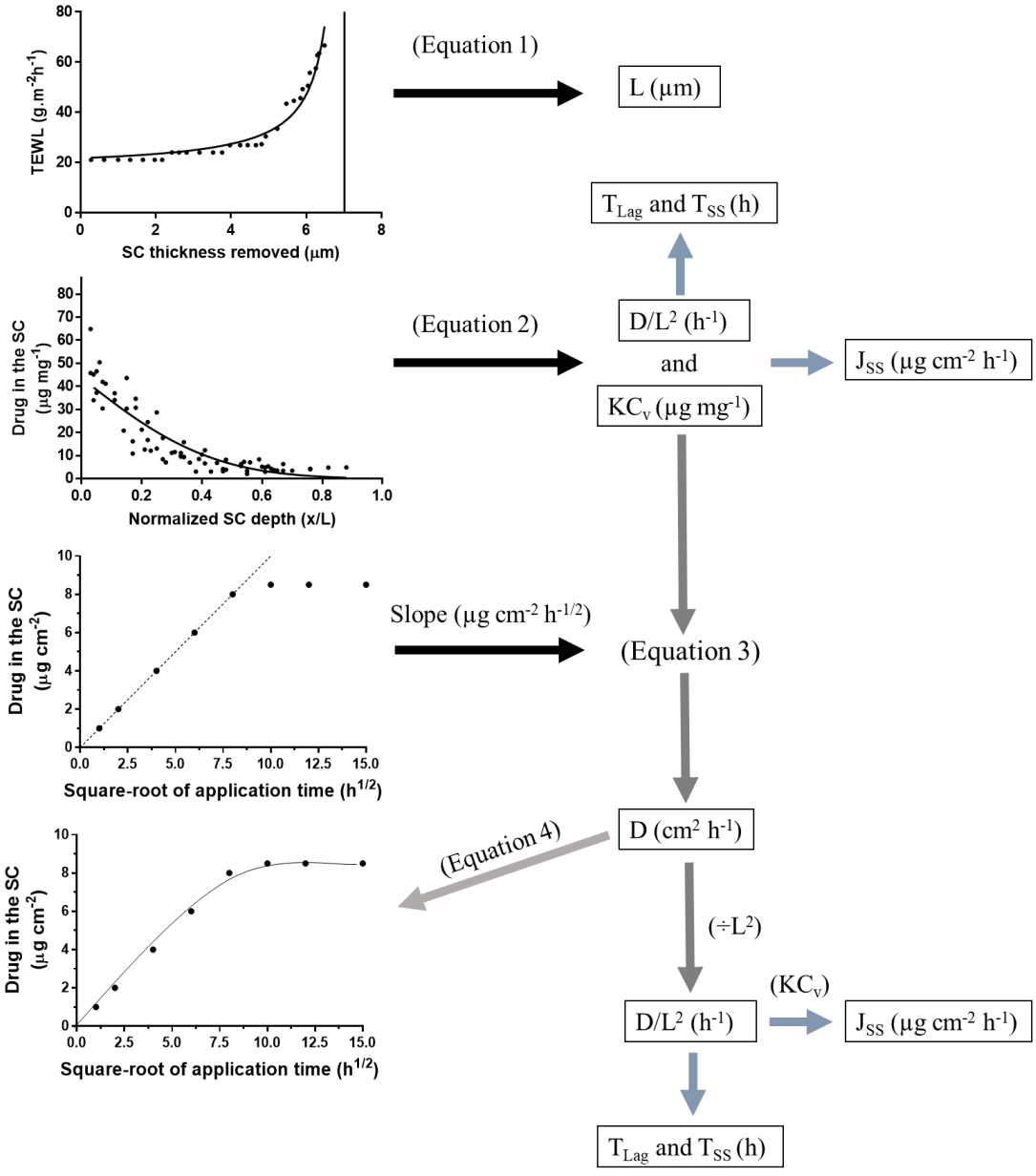

Figure 2. Schematic representation of the procedure used to estimate SC total thickness (L), drug SC-vehicle partition and diffusion across the SC parameters (KC_v and D, respectively), lag-time (T_{Lag}), time to steady-state (T_{SS}) and steady-state flux across the SC (J_{ss}).

2.4.2. Diclofenac clearance out of the stratum corneum

The next step was to evaluate the clearance of DF from the SC as a function of time post-removal of the plaster.

Assuming that DF is cleared from the SC with first-order kinetics, the associated rate constant, k, is given by the following equation:

$$\frac{M_{SC}}{A} = \frac{M_{SC,0}}{A} e^{(-k\Delta t)} \quad \text{(Equation 5)}$$

where M_{sc} is the total mass of drug in the SC at the end of the clearance period (i.e., 5, 17 or 24 hours), $M_{sc,0}$ is the total mass of drug in the SC when clearance began (i.e., when the plaster was removed, after 6 hours of application), A is the sampled skin area and Δt is the elapsed time interval between clearance and uptake times.

For each subject, k was calculated from the negative slope of a linear regression of the natural log of drug mass across the whole period of clearance.

Assuming the only mechanism of elimination is via transfer to the viable epidermis, then the average flux of drug transferred from the SC to the underlying tissue (J_{AVE}) during the clearance period was calculated for each subject as:

$$J_{AVE} = \frac{M_{SC,0}\left(1-e^{-k\Delta t}\right)}{\Delta t} \quad \text{(Equation 6)}$$

Another type of analysis performed with clearance data aimed to investigate the SC concentration (C_x) as a function of position in the SC (x/L) at each clearance time considered. Assuming that the drug is non-volatile and is not metabolised in the SC, the DF concentration profile during clearance is described by Equation 7 (Nicoli et al., 2009).

$$C_x = 2KC_v \sum_{n=0}^{\infty} \left\{ \left[\frac{1}{\gamma_n^2} - 2 \sum_{m=1}^{\infty} \frac{\exp\left[-m^2\pi^2 t_{app}(D/L^2)\right]}{m^2\pi^2 - \gamma_n^2} \right] \cos\left({}^{\gamma_n x}/_{L}\right) \exp\left[-\gamma_n^2 D/L^2 \left(t - t_{app}\right)\right] \right\}$$

(Equation 7)

where C_x is the drug concentration at position x in the SC, t_{app} is the duration of the application (i.e., 6 hours), t is the duration of the experiment (i.e., application time plus clearance time) and C_v is the drug concentration in the vehicle just before removal, and $\gamma_n = (2n+1)\pi/2$.

Concentration profiles at each time point were fitted to the relevant solution of Equation 7 to yield values for KC_v and D/L^2 assuming the boundary conditions that: (i) the flux of drug into the SC at the surface is zero; (ii) the SC is a homogeneous barrier; and (iii) the viable epidermis acts as a perfect sink.

2.5. Statistics

Statistically significant differences were estimated by a t-test or by one-way ANOVA followed by Tukey's test, assessed in a pairwise, within-subject comparison when appropriate. In all cases, statistical significance was set at $p < 0.05$. The 90% confidence interval was calculated using the Student's T-distribution for the sample size and the sample standard deviation.

3. Results and discussion

Table 1 shows the SC total thickness estimated from two untreated sites, using Equation 1 on each subject. Individual profiles for estimation of L are shown in 'Supplementary Information', Figures S1 and S2.

Overall, the average thickness of SC collected was 9.4 μm (min and max: 4.2 μm and 16.5 μm) and the average calculated total thickness was 12.4 μm, therefore around 75% of the SC was collected.

Table 1. Estimation of stratum corneum apparent total thickness (L) using Equation 1 for 6 subjects. The identification of 'Uptake' and 'Clearance' forearms are shown Figure 1.

	Total thickness (μm)		
	'Uptake' forearm	**'Clearance' forearm**	**Average**
Subject 1	7.0	13.5	10.3
Subject 2	12.7	11.7	12.2
Subject 3	14.4	11.5	13.0
Subject 4	12.4	19.0	15.7
Subject 5	12.3	11.8	12.1
Subject 6	12.7	11.5	12.1

Figures 3 and 4 show the total drug mass recovered from the SC for each subject at uptake and clearance times, respectively.

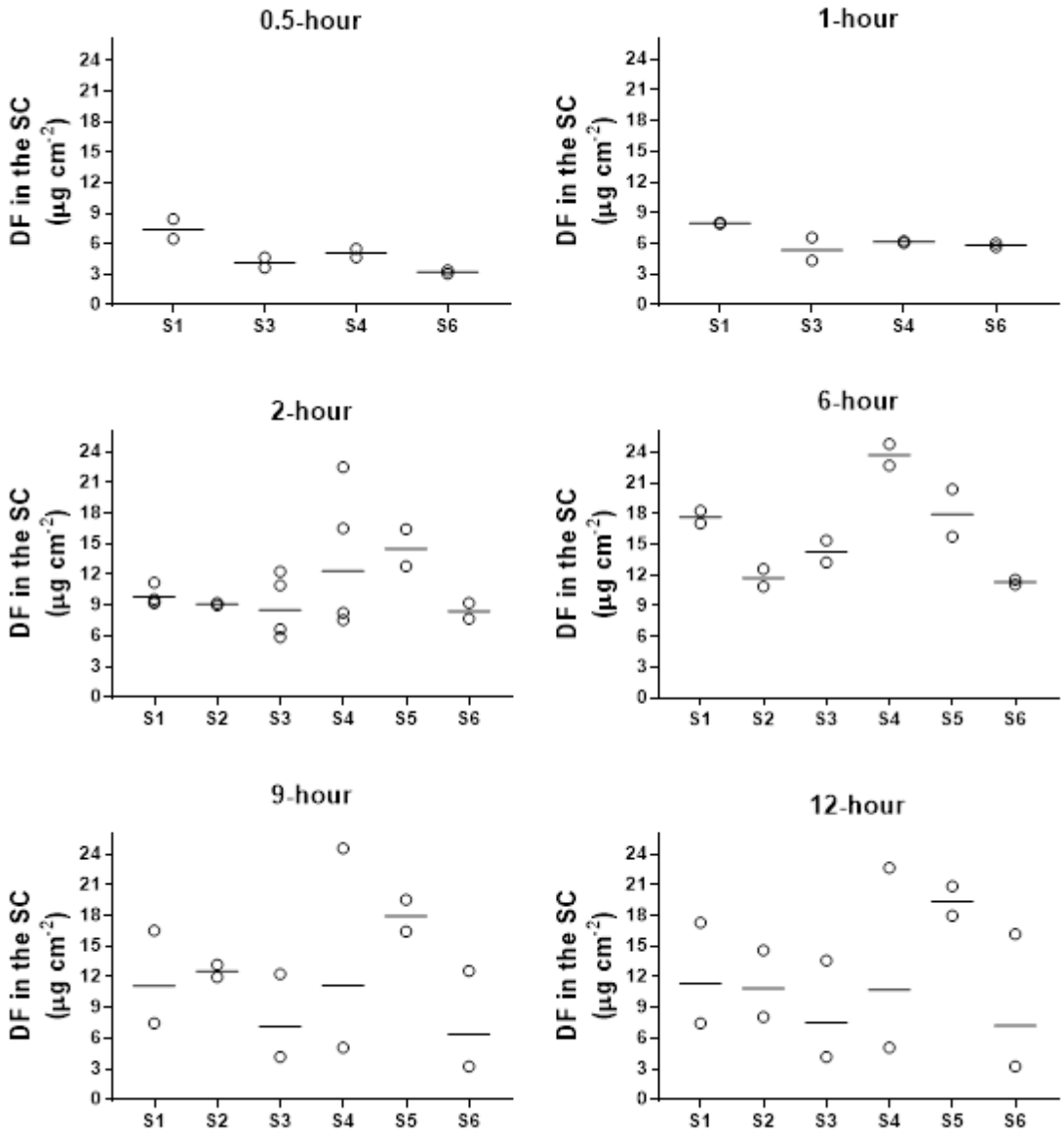

Figure 3. Mass of diclofenac recovered from replicate skin sites at each uptake time, for all subjects (n = 4 – 6). Horizontal lines are the geometric means of the replicate values shown by the circles.

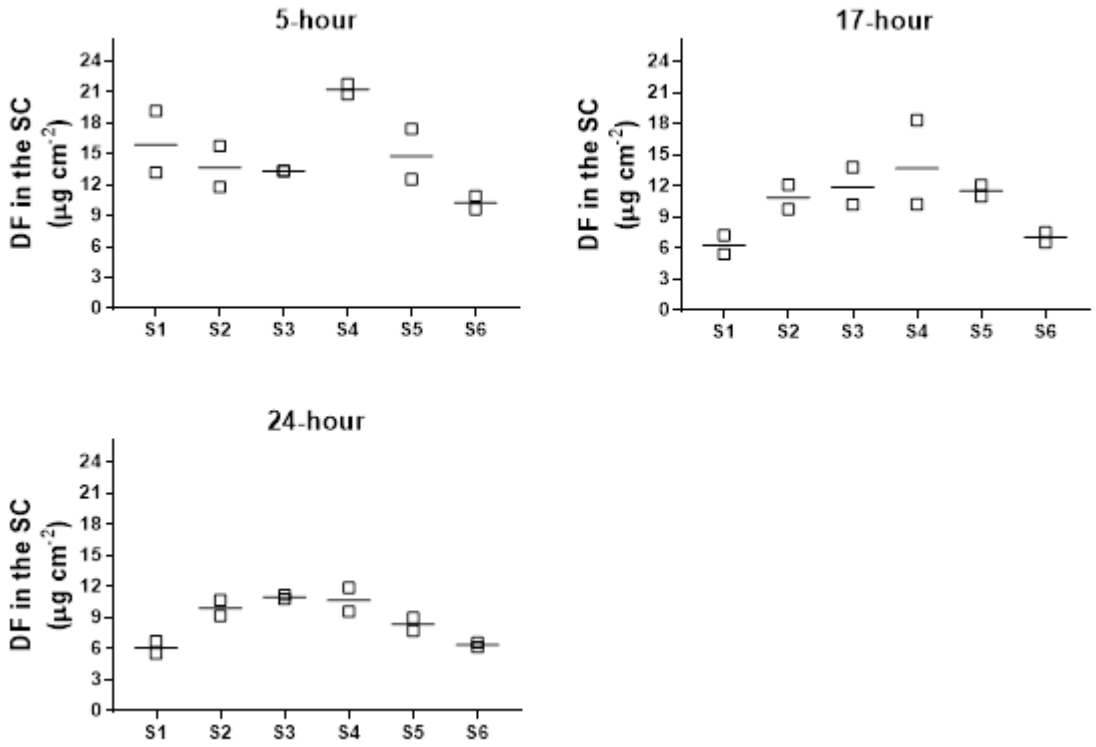

Figure 4. Mass of diclofenac recovered from replicate skin sites at each clearance time, for all subjects (n = 6). Horizontal lines are the geometric means of the replicate values shown by the squares.

3.1 Diclofenac uptake into the stratum corneum

Figure 5 shows the mass per unit area of DF in the SC as a function of the period of plaster application. It is clear that, at least up to 6 hours of exposure, increasing the application time led to an increase of DF in the SC, but that between 6 and 12 hours of plaster wear no further increase was observed.

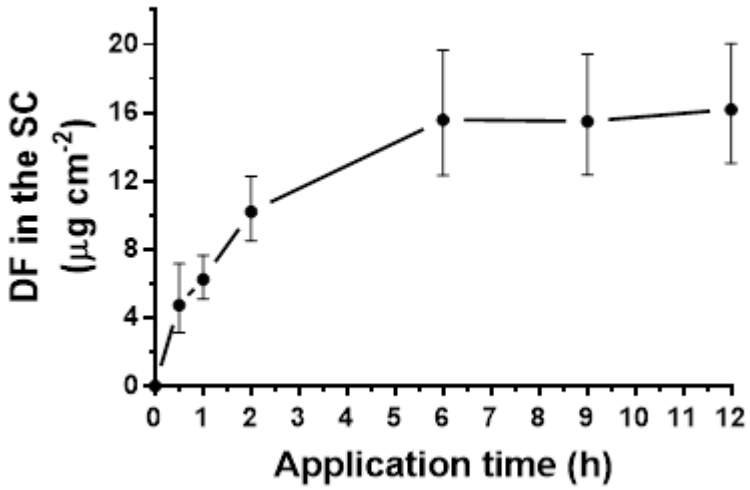

Figure 5. Average mass of diclofenac in human SC *in vivo* (6 subjects) following application of Voltaren® medicated plaster for different application times. The data points were experimentally determined and plotted as the anti-logarithm of the log-transformed average of the geometric mean of duplicates in each subject ± 90% confidence interval.

The SC concentration-depth profiles following different application times for each subject are shown in Figure 6. These data are plotted as a function of position within the SC (x) normalized by the predicted total thickness of the SC (L). The solid lines in Figure 6 were calculated from Equation 2 using the best fit of KC_v and D/L^2 values at the corresponding application time. The mean values of KC_v and D/L^2 per time for all subjects are in Table 2.

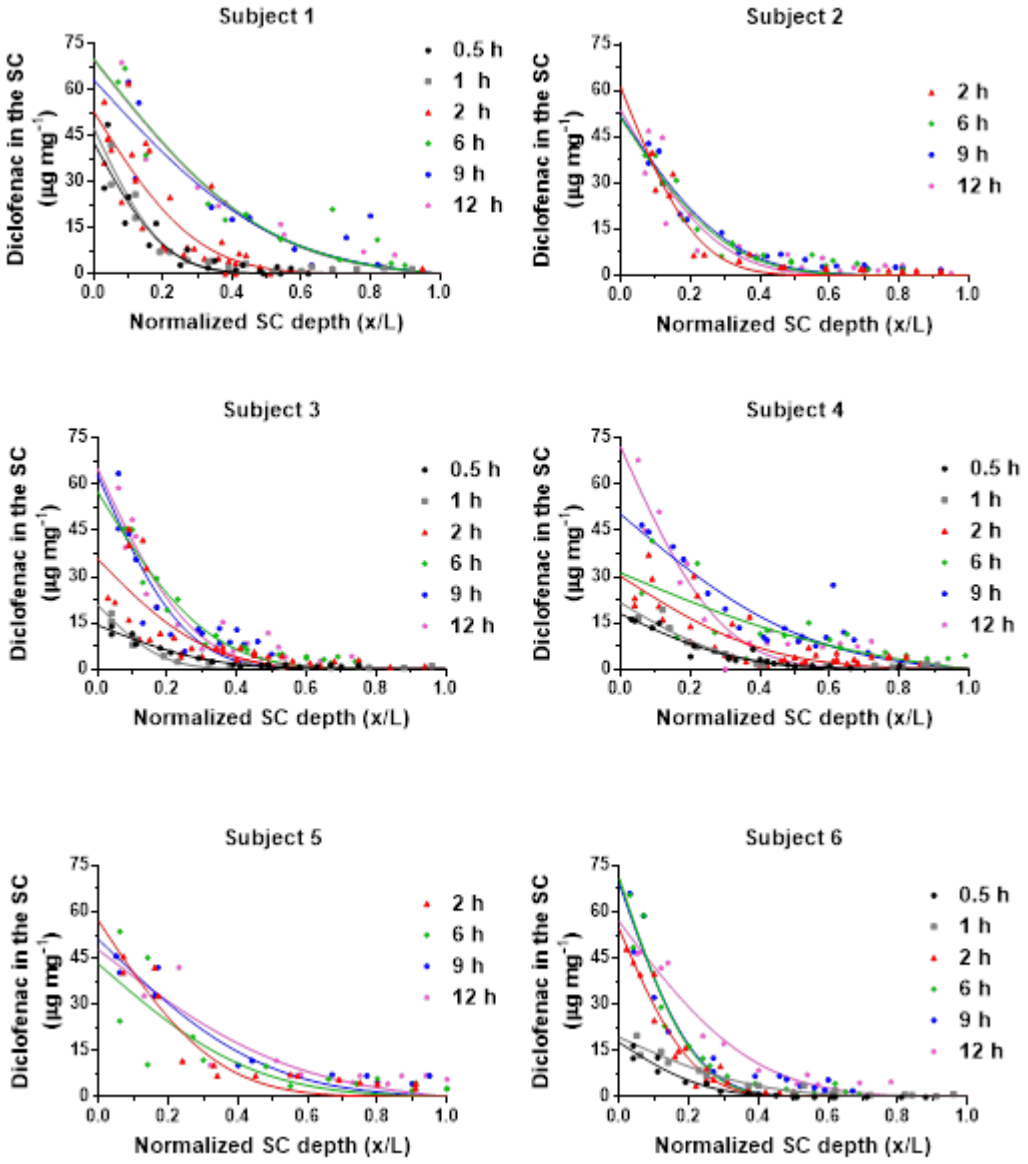

Figure 6. Individual concentration profiles of DF across human SC *in vivo* for each subject following application of Voltaren® medicated plaster for different application times. The data points were experimentally determined; the solid lines were calculated from Equation 2 using the best fit of KC_v and D/L^2 values deduced from the best fit of the corresponding application time

Table 2. Diclofenac partitioning and diffusivity parameters as a function of application time derived from the best fit of Equation 2 to the concentration profiles shown in Figure 6. Values are the arithmetic means across the subjects, for each time point (lower and upper 90% CI, n = 4 – 6). Pairs of superscript letters indicate statistical differences ($p < 0.05$).

Application time (h)	**Parameters**	
	KC_v (μg mg^{-1})	**10^2 D/L^2 (h^{-1})**
0.5†	$23.2^{a,b,c,d}$ (7.7 – 38.7)	$5.1^{h,i,j,k,l}$ (2.5 – 7.7)
1†	$27.3^{e,f,g}$ (11.5 – 43.2)	$2.5^{h,m}$ (0.5 – 4.6)
2‡	48.5^{a} (38.3 – 58.8)	1.5^{i} (0.9 – 2.1)
6‡	$54.0^{b,e}$ (41.2 – 66.8)	1.0^{j} (0.4 – 1.6)
9‡	$58.1^{c,f}$ (51.4 – 64.7)	0.6^{k} (0.3 – 0.9)
12‡	$61.1^{d,g}$ (53.4 – 68.9)	$0.2^{l,m}$ (0.1 – 0.4)

†n = 4 subjects; ‡n = 6 subjects.

KC_v and D/L^2 values were compared over time for statistical significance using parametric and non-parametric tests (one-way analysis of variance followed by Tukey's post hoc test and Kruskal–Wallis with Bonferroni-Dunn multiple comparisons, respectively). The same outcome was observed when comparing the partitioning (KC_v) and diffusion (D/L^2) parameters following both statistical tests (parametric and non-parametric). It was observed that KC_v and D/L^2 were not constant over all application times. This is noteworthy because the solution of Equation 2 assumes that the opposite is true. In fact, as seen in Table 2, divergence from this assumption occurs primarily in the first 2 hours of the study; subsequently, the fitted parameters are relatively constant.

The choice of which statistics to use for comparison depends on the type of data being compared. Each of the test has its own area of application, thus the wrong choice of the statistic can lead to the misrepresentation and misinterpretaion of the results. Nonparametric tests refer to statistical methods often used to analyse ordinal or nominal data with small sample sizes. Unlike parametric models, nonparametric models do not require making any assumptions about the distribution of the population. Also, this method is used when the data is quantitative but has an unknown

distribution, is non-normal, or has a sample size so small that the population distribution cannot be determined.

Although, data comparison using parametric tests is a very common form of data analysis in skin permeation/penetration studies, often these studies are performed in a small sample and, therefore, it is not possible to determine the distribution of the population. In this work, as the population size is small (n = 4-6), both types of analysis (parametric and non-parametric) were conducted to compare whether KC_v and D/L^2 are varying over application time.

As the results in Table 2 suggest constant partition (KC_v) and diffusivity (D/L^2) of the drug from 2 to 6 hours of application, the results deduced in this time interval were used to calculate additional kinetic parameters, specifically lag-time (T_{Lag}), time to steady-state (T_{SS}) and steady-state flux across the SC (J_{SS}). Table 3 presents these values (mean ± S.D.), which were calculated within each subject, then averaged first across all subjects and then averaged (arithmetic means) across application times.

In general, dermal products contain a number of excipients/co-solvents which may influence not only the drug's solubility in the formulation but also its solubility and partitioning into the SC. Typically, co-solvents are well absorbed into the SC and are then capable of changing the drug's solubility in this outer layer of the skin (Alberti et al., 2001; Herkenne et al., 2008), allowing the dermal permeation rate to increase.

The plaster used in this study contains over 20 ingredients, including the common co-solvents and reported penetration enhancers, propylene glycol and butylene glycol (Wotton et al., 1985; Barry, 1987; Huth et al., 1996; Lane, 2013). Due to their low molecular weights and lipophilicities (log P) of 76 and 96 Da, and -0.92 and -0.29, respectively, these permeate the SC relatively quickly compared to DF.

These glycols are expected, therefore, to impact on both drug partitioning and diffusivity (Oliveira, Hadgraft and Lane, 2012; Cadavona et al., 2016). It follows that the higher DF diffusivity observed in the early stages of the permeation may be related to the co-solvents reaching their maximum fluxes sooner than DF and creating a situation where drug delivery is transiently more efficient in the beginning of the treatment. Indeed, Trottet et al. (2004) reported exactly this effect of propylene glycol on the percutaneous permeation of loperamide hydrochloride.

As alternative way to analyse the uptake of DF in the SC, the semi-infinite and finite membrane models (Equations 3 and 4) were next explored. Subjects 2 and 5 were excluded from this data analysis as they did not take part in the 0.5- and 1.0-hour uptake experiments.

Estimates of KC_v were derived from Equation 2 (average value between 0.5-, 1-, 2- and 6-hour application time from each subject). Estimates of D/L^2 were derived for each subject from the slope of the linear regression of M_{SC}/A *versus* square-root of time measured at 0.5, 1, 2 and 6 h combined with the estimated L (from the average of each subject, Table 1) and the corresponding value of KC_v. From the estimated D/L^2 and L for each subject it was also possible to calculate lag-time ($T_{Lag} = L^2/6D$), time to steady-state ($T_{SS} \sim 2.4T_{Lag}$), diffusivity across the SC (D) and steady-state flux ($J_{SS} = KC_vD/L$) were calculated; the results are collected in Table 3.

Figure 7 compares the mean measured mass per area of DF in the SC as a function of the square-root of time to the semi-infinite membrane model (dashed line) (regression performed up to t = 6 h, $\sqrt{t} \leq 2.45$ $h^{1/2}$ data) and to the finite membrane (solid line). The solid line in Figure 7 was calculated using the finite membrane model (Equation 4) using average values of the 4 subjects for L (12.8 μm) and D derived from KC_v (38.3 μg mg^{-1}, derived from drug concentration *versus* depth data, using Equation 2, average value between 0.5-, 1-, 2- and 6-hour application time) and the slope of the linear regression of M_{SC}/A *versus* the square-root of time for $t \leq 6$ h. Consistent with the experimental data, the data for 9 and 12 h diverge from Equation 3 and suggest (as shown by the best fit of Equation 4) that the semi-infinite boundary conditions are no longer met. The individual plots of M_{SC}/A *versus* $\sqrt{t}$ are in 'Supplementary Information', Figure S3.

Table 3. Pharmacokinetic parameters deduced for DF in human SC *in vivo* following application of Voltaren® medicated plaster. Values were deduced from either SC concentration *versus* depth profile (Equation 2) or the M_{SC}/A *versus* $\sqrt{t}$ profile (Equation 3). The mean values (± standard deviation) were calculated within each subject, then averaged (arithmetic mean) across all subjects and then averaged (arithmetic mean) across the application times.

Parameters	From SC concentration *versus* depth profile	From M_{SC}/A *versus* $\sqrt{t}$ profile
KC_V (µg mg^{-1})	51.3 ± 3.9[a]	38.3 ± 15.3[b]
10^2 D/L^2 (h^{-1})	1.2 ± 0.4[a]	1.5 ± 1.8 [c]
T_{Lag} (h) [d]	22 ± 11	14 ± 10
T_{SS} (h) [e]	52 ± 25	34 ± 24
J_{SS} (µg cm^{-2} h^{-1}) [f]	0.7 ± 0.2	1.0 ± 1.0

[a]Calculated using Equation 2, average value between 2- and 6-hour application time;
[b]Calculated using Equation 2, average value between 0.5-, 1-, 2- and 6-hour application time;
[c]Calculated using Equation 3.

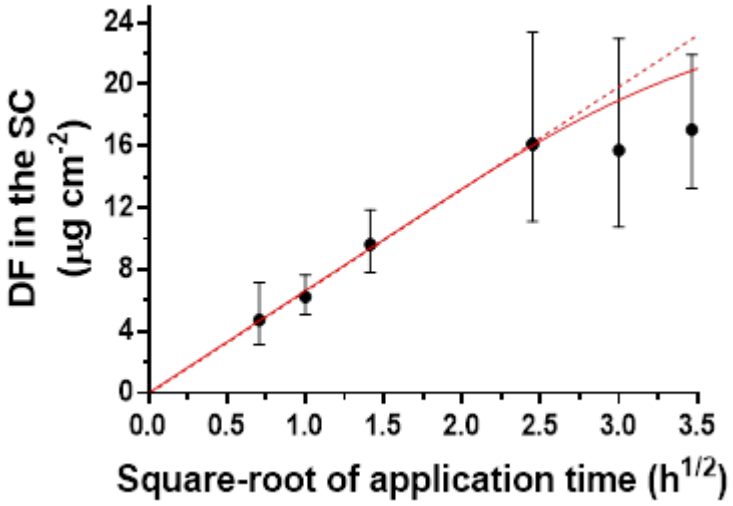

Figure 7. Average mass of diclofenac in human SC *in vivo* (4 subjects) following application of Voltaren® medicated plaster for different application times. The data points were experimentally determined and plotted as the anti-logarithm of the log-transformed average of the geometric mean of duplicates in each subject ± 90% confidence interval; the dashed line represents the solution of the semi-infinite membrane theory (regressions on $t \leq 6$ h, $\sqrt{t}$ = 2.45 h$^{1/2}$ data, Equation 3) and the red solid line represents the solution of the finite membrane theory (Equation 4) predicted with diffusivity (D) derived from semi-infinite theory slope.

The best-fit of Equation 3 results in an almost perfect straight line up to the 6-h point. The good agreement between observed and predicted M_{SC}/A suggests that, at least during the first six hours, there is no change in either partition or diffusion

parameters, which, to a certain extent, contradicts the findings using the Fick's law model (Equation 2). However, it is important to bear in mind that the calculation of slope of the linear regression of M_{SC}/A *versus* the square-root of time using Equation 3 takes into account the product of KC_v and $D^{1/2}$ (Equation 8). It follows that the reason that the semi-infinite model fits the data between 0.5 and 6 hours may be because the observed smaller values of KC_v and the higher values of D/L^2, derived using Equation 2, at the shortest times are compensating one another. As shown in Table 4, the products $\{(KC_v)\ (D/L^2)^{1/2}\}$ are reasonably constant and there is no systematic increase or decrease with time, with exception of the values obtained from the 2- and 12-hour application time, which are statistically different (one-way analysis of variance followed by Tukey's post hoc test, $p = 0.04$).

$$slope = 2KC_v \left(\frac{Dt_{app}}{\pi}\right)^{1/2} \qquad \text{(Equation 8)}$$

Table 4. Product of KC_v and $(D/L^2)^{1/2}$ derived from the best fit of Equation 2 (Table 2). Values are the arithmetic means across the subjects, for each time point (lower and upper 90% CI, n = 4 – 6). Pairs of superscript letters indicate statistical differences ($p < 0.05$).

Application time (h)	$KCv\ \sqrt{D/L^2}$
0.5†	4.7 (2.8 – 6.7)
1†	3.9 (2.3 – 5.4)
2‡	5.5[a] (4.5 – 6.5)
6‡	4.7 (3.3 – 6.1)
9‡	4.1 (3.0 – 5.2)
12‡	2.9[a] (1.7 – 4.1)

†n = 4 subjects; ‡n = 6 subjects.

One advantage of using the approach (C_x *versus* x/L) to estimate a kinetic profile is that data from a specific (and relatively short) application time can be used to predict the entire absorption profile of the drug up to steady-state (Stinchcomb et al., 1999; Alberti et al., 2001; Herkenne et al., 2006, 2007; Rothe et al., 2017). However, the partitioning and diffusion need to be constant over time.

On the other hand, analysing the mass of the drug in the SC *versus* square-root of time, an approximation solution to Fick's second law of diffusion, also provides information about the drug's kinetics through the SC. One clear advantage of this

simpler model is that it is not necessary to know the concentration of the drug in the SC (i.e., the determination of the mass of SC is not required). However, two limitations of this metric can be cited: (i) a minimum number of application times are required to accurately estimate the inclination of the curve and, therefore, a value for drug diffusion; (ii) the nature of the extracted information mixes what is happening to the partition and diffusion parameters (KC_v and D) and there is a risk that both may be changing and the metric will not be able to detect any difference in terms of diffusivity and partitioning.

3.2 Diclofenac clearance out of the stratum corneum

From the mass of drug remaining in the SC over time post-removal of the delivery system, an elimination rate constant (k) and the average flux out of the SC were calculated (Figure 8 and Table 5). While the mass of DF in the SC decreased over the time of clearance, the transfer of drug out of the SC was relatively slow. Only after 24 hours of clearance the drug level in SC was significantly lower than that present at the end of the 6 h uptake (one-way ANOVA, followed by Tukey post hoc test).

The average depletion of drug from the SC at 5, 17 and 24 hours after plaster removal was 6, 34 and 43%, respectively. This is consistent with results for three distinctly different DF formulations for which about 32% of the drug in the SC after a 6-hour uptake had been cleared 17 hours post-removal from the skin (Cordery et al., 2017).

The DF clearance from the SC profiles for each subject is in ‘Supplementary Information’, Figure S4.

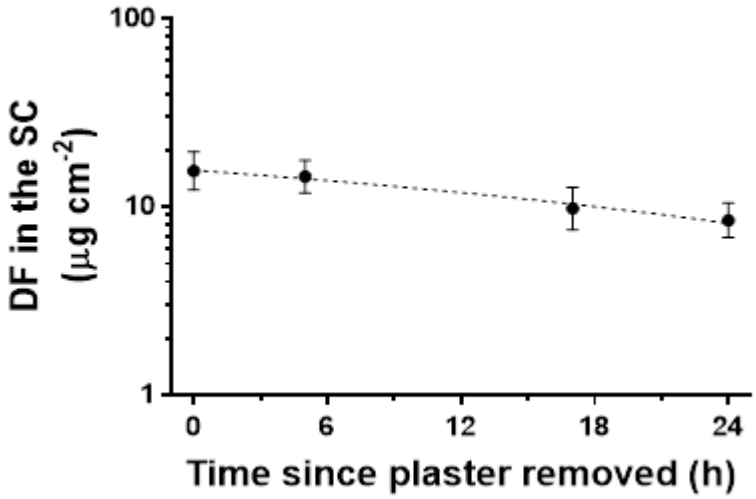

Figure 8. Amount of drug in the SC plotted against the time of clearance (n = 6). The data points were experimentally determined and plotted as the anti-logarithm of the log-transformed average of the geometric mean of duplicates in each subject ± 90% confidence interval.

Table 5. Deduced DF average flux from the SC into the underlying viable tissue during the clearance period (J_{AVE}) and the first-order rate constant (k) describing clearance from the SC. The mean values (± standard deviation) were calculated within each subject, then averaged (arithmetic mean) across all subjects.

Parameters	Mean ± Standard deviation
10^2 k (h^{-1}) [a]	2.7 ± 1.6
J_{AVE} (μg cm^{-2} h^{-1}) [b]	0.32 ± 0.20

[a]Slope of the ln(M_{SC}/A) *versus* time curve;
[b]Calculated using Equation 6 and assuming Δt = 24 hours.

Predicted DF concentration profiles across the SC during the clearance phase were generated using Equation 7 and are compared with the experimental data in Figure 9. There was poor agreement between theory and experiment with the model clearly predicting a faster decline in DF concentration in the SC post-removal of the plaster. A similar finding was reported by Nicoli et al. (2009) for ibuprofen.

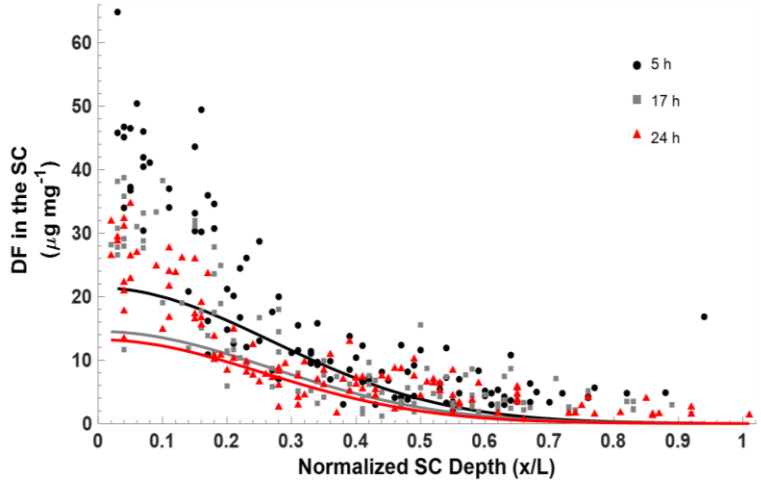

Figure 9. Concentration profiles of DF across human SC *in vivo* (6 subjects) following application of Voltaren® medicated plaster for different clearance times. The data points were experimentally determined; the lines through the results were calculated using Equation 7.

As Equation 7 poorly described the concentration of DF in the SC after removal of the plaster, a phenomenological approach was adopted relaxing the requirement that drug diffusivity is a constant; in line with fitting the experimental data, it was proposed that diffusivity (D(t)) decays exponentially over time, with a 1st-order constant rate α during clearance:

$$D(t) = D_0 e^{-\alpha(t-t_{app})} \qquad \text{(Equation 9)}$$

where D_0 is the diffusivity when clearance from the SC begins. Equation 7 is then re-expressed as:

$$C_x = 2KC_v \sum_{n=0}^{\infty} \left\{ \left[\frac{1}{\gamma_n^2} - 2 \sum_{m=1}^{\infty} \frac{\exp\left[-m^2\pi^2 t_{app}(D_0/L^2)\right]}{m^2\pi^2 - \gamma_n^2} \right] \cos\left(\gamma_n x/L\right) \exp\left[-\gamma_n^2 D_0/L^2 \left(\frac{1 - e^{-\alpha(t-t_{app})}}{\alpha} \right) \right] \right\}$$

(Equation 10)

The value of α was estimated by amalgamating the data points for the three clearance times and, then, a nonlinear least square fit using D_0/L^2 and KC_v from the uptake phase (0.01 h^{-1} and 54 μg mg^{-1}, respectively) was carried out. In this way, a single mean value for α, equal to 0.13 h^{-1}, was determined. The strategy considerably improved agreement between experimental data and model predictions (Figure 10). For the moment, however, this finding is empirical and lacks mechanistic under-pinning. The extent to which the drug may become immobilised during its passage

across the SC, such as by protein binding, and its impact on D requires further investigation.

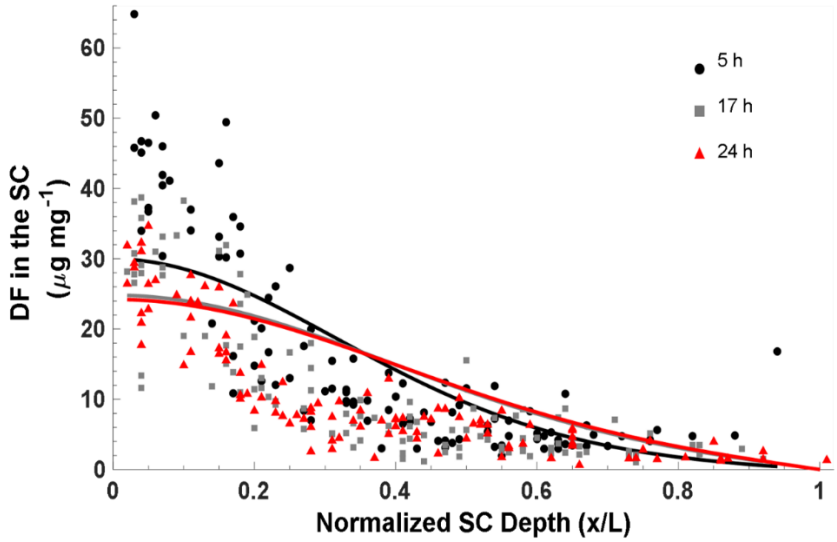

Figure 10. Concentration profiles of DF across human SC *in vivo* (6 subjects) following application of Voltaren® medicated plaster for different clearance times. The data points were experimentally determined; the lines through the results were calculated using Equation 9.

4. Conclusion

In conclusion, the results presented have utility with respect to the application of SC tape-stripping *in vivo* in human to derive useful skin pharmacokinetic parameters related to drug partitioning into (KC_v) and diffusion across the SC (D/L^2).

In addition, evaluation of KC_v and D/L^2 values as a function of formulation application time may indicate whether the drug distributes rapidly from the formulation into the SC at the skin surface and/or whether there are interactions between the vehicle constituents and the skin that may alter its permeability.

The potential effects of different excipients on the predicted kinetic parameters and the manner in which excipient(s) behaviour may impact on the rate and extent at which the drug crosses the SC is further explored in Chapter 4 of this thesis.

From the 'clearance experiments', concentration profiles suggest that diclofenac elimination may be retarded by immobilisation in the SC. Nevertheless, analysis of the change in mass of drug over time after plaster removal permits its average flux into the underlying viable tissue, as well as the rate constant (k) at which drug is 'cleared' from the SC to be determined.

Supplementary Information

Table S1. Diclofenac recovery from tapes (n=3).

Theoretical concentration (µg/mL)	Diclofenac recovery
	Tape-strips
	% ± SD
0.1	83.7 ± 6.5
1.0	82.3 ± 1.5
10.0	83.9 ± 3.2

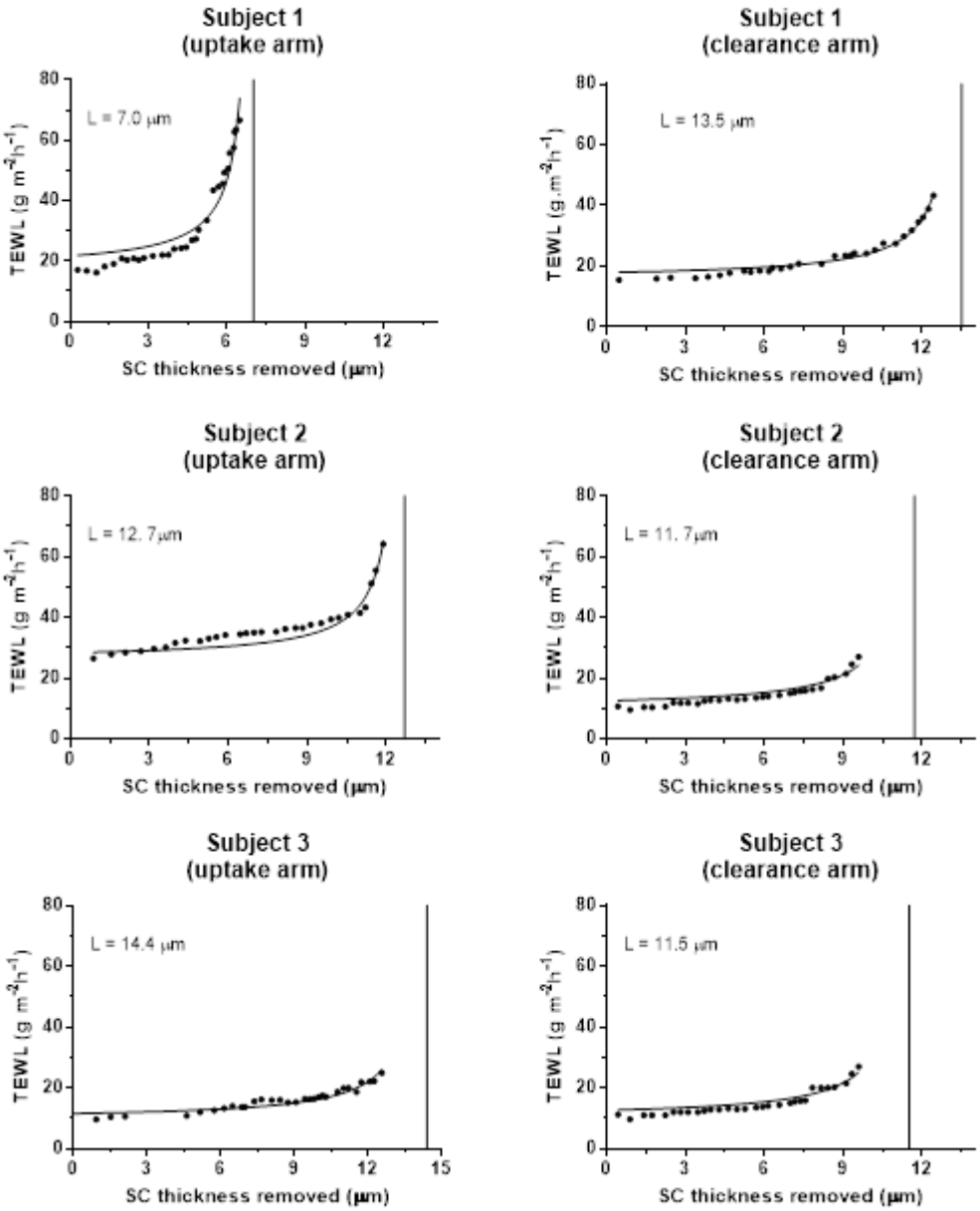

Figure S1. Estimation of apparent SC total thickness (L) by Equation 1. Subjects 1 – 3.

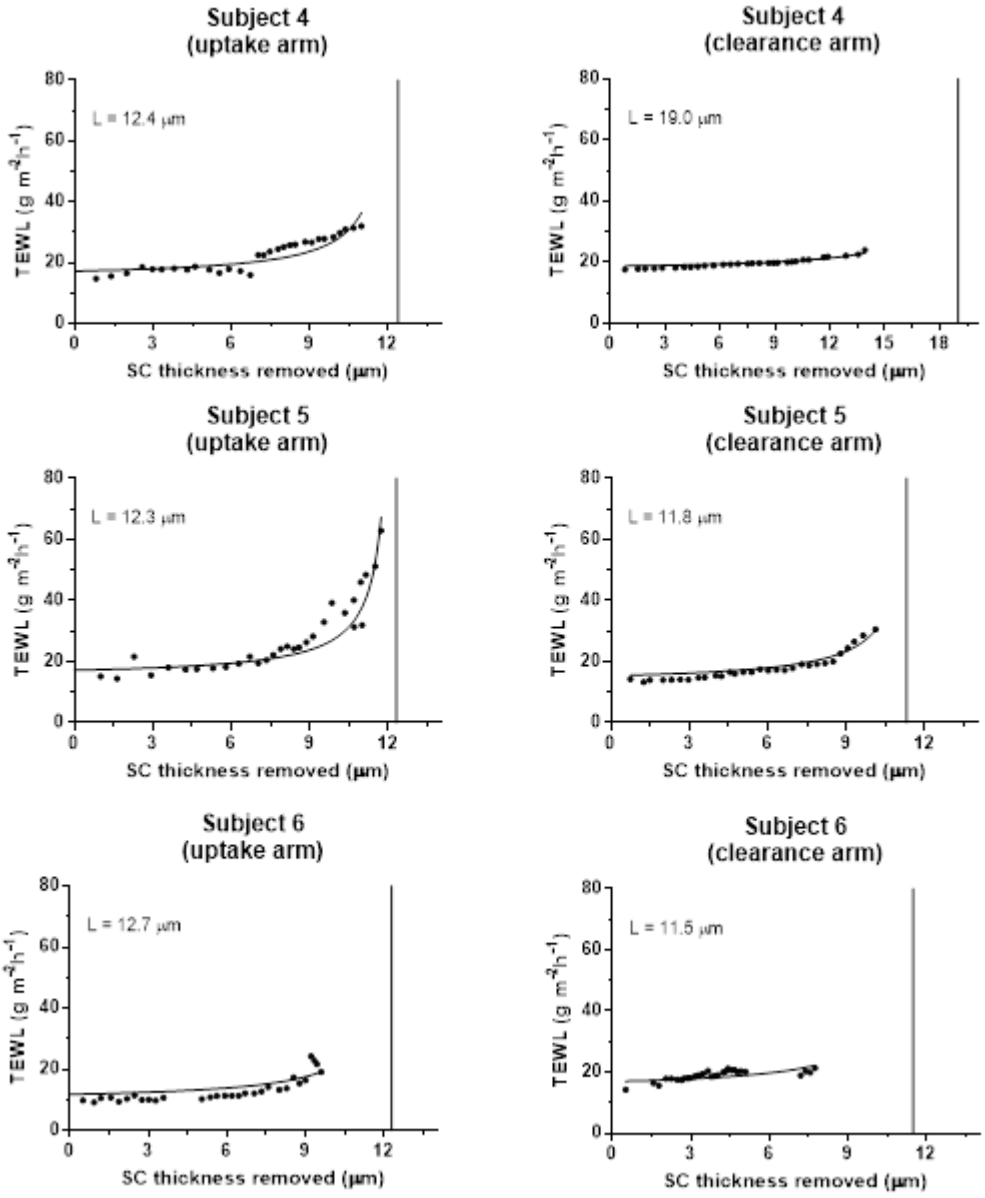

Figure S2. Estimation of apparent SC total thickness (L) by Equation 1. Subjects 4 – 6.

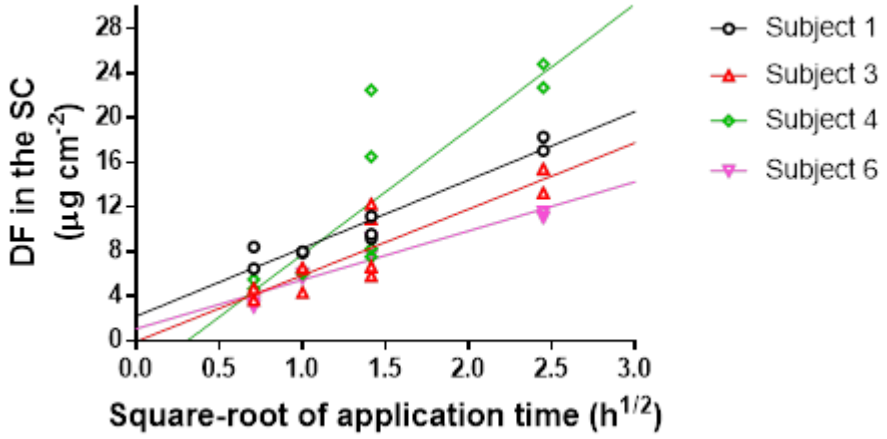

Figure S3. Mass of diclofenac in human SC *in vivo* for each subject following application of Voltaren® medicated plaster for different application times. The data points were experimentally determined (the replicate values are shown by the same symbols) and the solid line represents a linear regression.

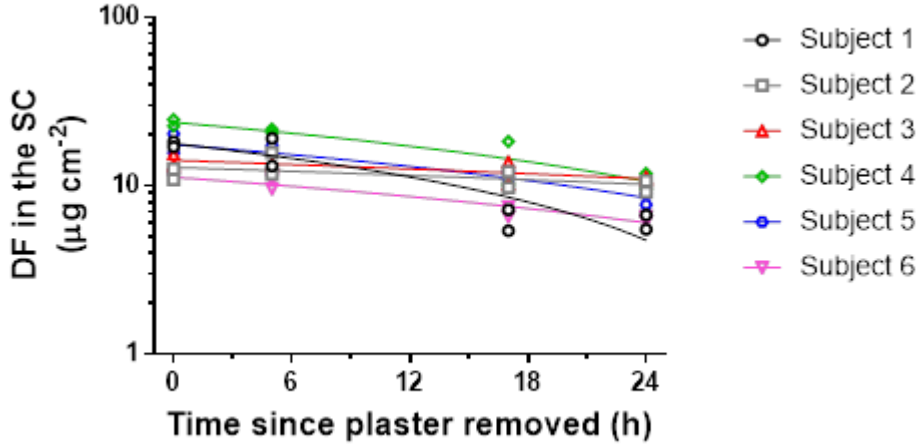

Figure S4. Amount of drug in the SC for each subject plotted against the time of clearance. The data points were experimentally determined (the replicate values are shown by the same symbols) and the solid line represents a linear regression.

References

Alberti, I., Kalia, Y.N., Naik, A., Bonny, J.-D. and Guy, R.H., 2001. Effect of ethanol and isopropyl myristate on the availability of topical terbinafine in human stratum corneum, in vivo. *International Journal of Pharmaceutics,* 219(1-2), pp. 11-19.

Anderson, R.L. and Cassidy, J.M., 1973. Variations in Physical Dimensions and Chemical Composition of Human Stratum Corneum. *Journal of Investigative Dermatology,* 61(1), pp. 30-32.

Barbero, A.M. and Frasch, H.F., 2009. Pig and guinea pig skin as surrogates for human in vitro penetration studies: a quantitative review. *Toxicology In Vitro,* 23(1), pp. 1-13.

Barry, B.W., 1987. Mode of action of penetration enhancers in human skin. *Journal of Controlled Release,* 6(1), pp. 85-97.

Brühlmann, P., Vathaire, F.d., Dreiser, R.L. and Michel, B.A., 2006. Short-term treatment with topical diclofenac epolamine plaster in patients with symptomatic knee osteoarthritis: pooled analysis of two randomised clinical studies. *Current Medical Research and Opinion,* 22(12), pp. 2429-2438.

Cadavona, J.J.P., Zhu, H., Hui, X., Jung, E.C. and Maibach, H.I., 2016. Depth-dependent stratum corneum permeability in human skin in vitro. *Journal of Applied Toxicology,* 36(9), pp. 1207-1213.

Cleek, R.L. and Bunge, A.L., 1993. A new method for estimating dermal absorption from chemical exposure. 1. General approach. *Pharmaceutical Research,* 10(4), pp. 497-506.

Cordery, S., Pensado, A., Chiu, W., Shehab, M., Bunge, A., Delgado-Charro, M. and Guy, R., 2017. Topical bioavailability of diclofenac from locally-acting, dermatological formulations. *International Journal of Pharmaceutics,* 529(1-2), pp. 55-64.

Cornwell, P. and Barry, B., 1995. Effects of penetration enhancer treatment on the statistical distribution of human skin permeabilities. *International Journal of Pharmaceutics,* 117(1), pp. 101-112.

Costantino, C., Kwarecki, J., Samokhin, A.V., Mautone, G. and Rovati, S., 2011. Diclofenac Epolamine plus Heparin Plaster versus Diclofenac Epolamine Plaster in Mild to Moderate Ankle Sprain. *Clinical Drug Investigation,* 31(1), pp. 15-26.

Crank, J., 1979. *The mathematics of diffusion.* Oxford University Press.

de Araujo, T.P., Fittipaldi, I.M., Bedor, D.C.G., Duarte, M.L., Cordery, S.F., Guy, R.H., Delgado-Charro, M.B., de Santana, D.P. and Leal, L.B., 2018. Topical bio (in) equivalence of metronidazole formulations in vivo. *International Journal of Pharmaceutics,* 541(1-2), pp. 167-172.

Frasch, H.F. and Bunge, A.L., 2015. The transient dermal exposure II: post-exposure absorption and evaporation of volatile compounds. *Journal of Pharmaceutical Sciences,* 104(4), pp. 1499-1507.

Herkenne, C., Naik, A., Kalia, Y.N., Hadgraft, J. and Guy, R.H., 2006. Pig ear skin ex vivo as a model for in vivo dermatopharmacokinetic studies in man. *Pharmaceutical Research,* 23(8), pp. 1850-1856.

Herkenne, C., Naik, A., Kalia, Y.N., Hadgraft, J. and Guy, R.H., 2007. Dermatopharmacokinetic prediction of topical drug bioavailability in vivo. *Journal of Investigative Dermatology,* 127(4), pp. 887-894.

Herkenne, C., Naik, A., Kalia, Y.N., Hadgraft, J. and Guy, R.H., 2008. Effect of propylene glycol on ibuprofen absorption into human skin in vivo. *Journal of Pharmaceutical Sciences,* 97(1), pp. 185-197.

Huth, S., Neubert, R., Boltze, L. and Buge, A., 1996. Experimental determination and mathematical modelling of propylene glycol transport from semisolid vehicles. *Chemical and Pharmaceutical Bulletin,* 44(6), pp. 1263-1266.

Jenoure, P., Rostan, A., Gremion, G., Meier, J., Grossen, R., Bielinki, R., Ludi, J., Froelicher, U., Birrer, E. and Moser, C., 1997. Multicentre, double-blind, controlled clinical study on the efficacy of diclofenac epolamine Tissugel plaster in patients with epicondylitis. *Medicina Dello Sport,* 50(3), pp. 285-292.

Kasting, G.B., Filloon, T.G., Francis, W.R. and Meredith, M.P., 1994. Improving the sensitivity of in vitro skin penetration experiments. *Pharmaceutical Research,* 11(12), pp. 1747-1754.

Lane, M.E., 2013. Skin penetration enhancers. *International Journal of Pharmaceutics,* 447(1), pp. 12-21.

Leal, L.B., Cordery, S.F., Delgado-Charro, M.B., Bunge, A.L. and Guy, R.H., 2017. Bioequivalence Methodologies for Topical Drug Products: In Vitro and Ex Vivo Studies with a Corticosteroid and an Anti-Fungal Drug. *Pharmaceutical Research,* 34(4), pp. 730-737.

Lian, G., Chen, L. and Han, L., 2008. An evaluation of mathematical models for predicting skin permeability. *Journal of Pharmaceutical Sciences,* 97(1), pp. 584-598.

Mitragotri, S., Anissimov, Y.G., Bunge, A.L., Frasch, H.F., Guy, R.H., Hadgraft, J., Kasting, G.B., Lane, M.E. and Roberts, M.S., 2011. Mathematical models of skin

permeability: an overview. *International Journal of Pharmaceutics,* 418(1), pp. 115-129.

Moser, K., Kriwet, K., Naik, A., Kalia, Y.N. and Guy, R.H., 2001. Passive skin penetration enhancement and its quantification in vitro. *European Journal of Pharmaceutics and Biopharmaceutics,* 52(2), pp. 103-112.

Moss, G.P., Dearden, J.C., Patel, H. and Cronin, M.T., 2002. Quantitative structure–permeability relationships (QSPRs) for percutaneous absorption. *Toxicology In Vitro,* 16(3), pp. 299-317.

N'Dri-Stempfer, B., Navidi, W.C., Guy, R.H. and Bunge, A.L., 2009. Improved bioequivalence assessment of topical dermatological drug products using dermatopharmacokinetics. *Pharmaceutical Research,* 26(2), p. 316.

Nicoli, S., Bunge, A.L., Delgado-Charro, M.B. and Guy, R.H., 2009. Dermatopharmacokinetics: factors influencing drug clearance from the stratum corneum. *Pharmaceutical Research,* 26(4), pp. 865-871.

Oliveira, G., Hadgraft, J. and Lane, M.E., 2012. The influence of volatile solvents on transport across model membranes and human skin. *International Journal of Pharmaceutics,* 435(1), pp. 38-49.

Roberts, M.S., Anissimov, Y.G. and Gonsalvez, K., 1999. Mathematical models in percutaneous absorption. *Percutaneous absorption: drugs, cosmetics, mechanisms, methodology. Drugs and the Pharmaceutical Sciences,* 97, pp. 1-49.

Rothe, H., Obringer, C., Manwaring, J., Avci, C., Wargniez, W., Eilstein, J., Hewitt, N., Cubberley, R., Duplan, H. and Lange, D., 2017. Comparison of protocols measuring diffusion and partition coefficients in the stratum corneum. *Journal of Applied Toxicology,* 37(7), pp. 806-816.

Russell, L.M. and Guy, R.H., 2009. Measurement and prediction of the rate and extent of drug delivery into and through the skin. *Expert Opinion on Drug Delivery,* 6(4), pp. 355-369.

Russell, L.M., Wiedersberg, S. and Delgado-Charro, M.B., 2008. The determination of stratum corneum thickness An alternative approach. *European Journal of Pharmaceutics and Biopharmaceutics,* 69(3), pp. 861-870.

Scheuplein, R.J., 1967. Mechanism of percutaneous absorption: II. Transient diffusion and the relative importance of various routes of skin penetration. *Journal of Investigative Dermatology,* 48(1), pp. 79-88.

Stinchcomb, A.L., Pirot, F., Touraille, G.D., Bunge, A.L. and Guy, R.H., 1999. Chemical uptake into human stratum corneum in vivo from volatile and non-volatile solvents. *Pharmaceutical Research,* 16(8), pp. 1288-1293.

Trottet, L., Merly, C., Mirza, M., Hadgraft, J. and Davis, A., 2004. Effect of finite doses of propylene glycol on enhancement of in vitro percutaneous permeation of loperamide hydrochloride. *International Journal of Pharmaceutics,* 274(1-2), pp. 213-219.

Wiechers, J.W., 1989. The barrier function of the skin in relation to percutaneous absorption of drugs. *Pharmaceutisch Weekblad,* 11(6), pp. 185-198.

Williams, A., Cornwell, P. and Barry, B., 1992. On the non-Gaussian distribution of human skin permeabilities. *International Journal of Pharmaceutics,* 86(1), pp. 69-77.

Wotton, P.K., Møllgaard, B., Hadgraft, J. and Hoelgaard, A., 1985. Vehicle effect on topical drug delivery. III. Effect of Azone on the cutaneous permeation of metronidazole and propylene glycol. *International Journal of Pharmaceutics,* 24(1), pp. 19-26.

Yamashita, F. and Hashida, M., 2003. Mechanistic and empirical modeling of skin permeation of drugs. *Advanced Drug Delivery Reviews,* 55(9), pp. 1185-1199.

Chapter 4: Tracking excipients from a topical drug product through the stratum corneum *in vivo*

Abbreviations

A	sampled skin area
BG	1,3-butylene glycol
C_v	permeant concentration in the vehicle
C_x	the permeant concentration at position x in the stratum corneum
D	permeant diffusivity
HPLC-UV	high-performance liquid chromatography with ultraviolet detection
K	permeant's stratum corneum – vehicle partition coefficient
L	diffusion path-length through (or thickness of) a membrane
log P	log(octanol-water partition coefficient (P))
M_{SC}	mass of permeant measured in the tape-strips
PG	propylene glycol
SC	stratum corneum
t_{app}	application time
TEWL	transepidermal water loss
T_{Lag}	time lag for diffusion through a membrane
T_{SS}	time to achieve steady-state
x/L	relative depth in the stratum corneum

1. Introduction

Penetration of drugs into and through the skin is often limited by the barrier properties of the stratum corneum (SC). This barrier can sometimes be overcome by the addition of excipients to topical formulations (Aungst, Blake and Hussain, 1990; Karande and Mitragotri, 2009). These excipients may each perform one or more roles. Among those roles, particularly important are (Barry, 1987; Adrian C. Williams and Barry, 2004; Choi et al., 2008; Gee et al., 2014; Pham, Topgaard and Sparr, 2017):

(i) modifying solubility of the drug in the vehicle;

(ii) uptake into the SC and transiently changing barrier function to permit more facile diffusion of drug across the barrier, and;

(iii) co-diffusion with the drug into the SC and altering drug solubility in the barrier.

Therefore, when the skin is exposed to topical products, drug disposition is likely to be greatly influenced by the time-dependent skin concentrations of certain excipients present in the formulation.

There is clear evidence in the literature that the behaviour of the excipient and the behaviour of the drug are closely linked. For example, the addition of oleic acid (5%) to a formulation (50:50, ethanol:isopropyl myristate) containing terbinafine enhanced drug uptake into the human SC *in vivo* by increasing the drug diffusivity across the SC, although there was no effect on drug partitioning between the vehicle and the SC (Alberti et al., 2001). In contrast, propylene glycol (PG) in a series of ibuprofen formulations (specifically, mixtures of PG and water, containing from 0 to 100% v/v PG) significantly influenced the partitioning of the drug from the vehicle into the SC (in human *in vivo*), whereas its diffusivity across the barrier was unaltered (Herkenne et al., 2008). In addition, Trottet et al. (2004) investigated the *in vitro* percutaneous permeation of propylene glycol and loperamide hydrochloride in formulations containing PG under finite dose conditions; dose effects were also examined. The data showed a correlation between the amount of PG dosed on the skin and the amount of drug that had permeated.

Clearly, knowledge of the disposition of key formulation components can help understanding of the skin pharmacokinetics of the drug. Yet, it is relatively unusual

that the uptake and transport of formulation excipients are simultaneously monitored when assessing topical drug penetration.

The results described in Chapter 3 suggested that diclofenac uptake into the SC may be modified by certain excipient(s). Therefore, the work described here aimed to quantify the uptake of two excipients, propylene glycol and butylene glycol, present in the diclofenac medicated plaster, into the SC. Both compounds have been reported to act as effective co-solvents and as potential penetration enhancers (Wotton et al., 1985; Barry, 1987; Huth et al., 1996; Lane, 2013).

The ultimate objective was to better understand SC uptake and clearance of diclofenac as a function of time after topical application of the medicated plaster to human skin *in vivo*. The SC tape-stripping technique was again employed for this purpose.

2. Materials and Methods

2.1. Materials

Voltaren® medicated plaster (GlaxoSmithKline, Munich, Germany) was purchased from Amazon UK. Propylene glycol, 1,3-butylene glycol, all the solvents and HPLC (high-performance liquid chromatography) reagents were from Sigma (Gillingham, UK).

2.2. Stratum corneum tape-stripping experiments

Four subjects (one male, three females, age range: 23 – 32 years) with no history of dermatological disease participated in this study, which was approved by the Research Ethics Approval Committee for Health at the University of Bath (EP 16/17 142). Informed consent was provided by all subjects. All the subjects enrolled in this study also took part in the previous diclofenac study (Chapter 3).

The drug product studied was Voltaren® medicated plaster, which contains 180 mg of diclofenac epolamine (1.3%) and 420 mg (3%) of propylene glycol (PG) over 140 cm^2; the amount of butylene glycol (BG) present, however, is not publicly available. The patient information leaflet recommends application of the plaster for up to 12 hours.

From a single plaster, 5 cm^2 (1 x 5 cm) pieces were cut and 4 of these were applied to the volar surface of each forearm of each subject. The plaster pieces were

left in contact with the skin for 0.5, 1, 2 or 6 hours. There were duplicate application sites on each subject for each application time (Figure 1).

For the duration of the experiment, subjects refrained from bathing or participating in vigorous physical activity, but otherwise pursued their normal lifestyle. After 0.5, 1, 2 and 6 hours of contact, the plaster was removed; the application area was not cleaned.

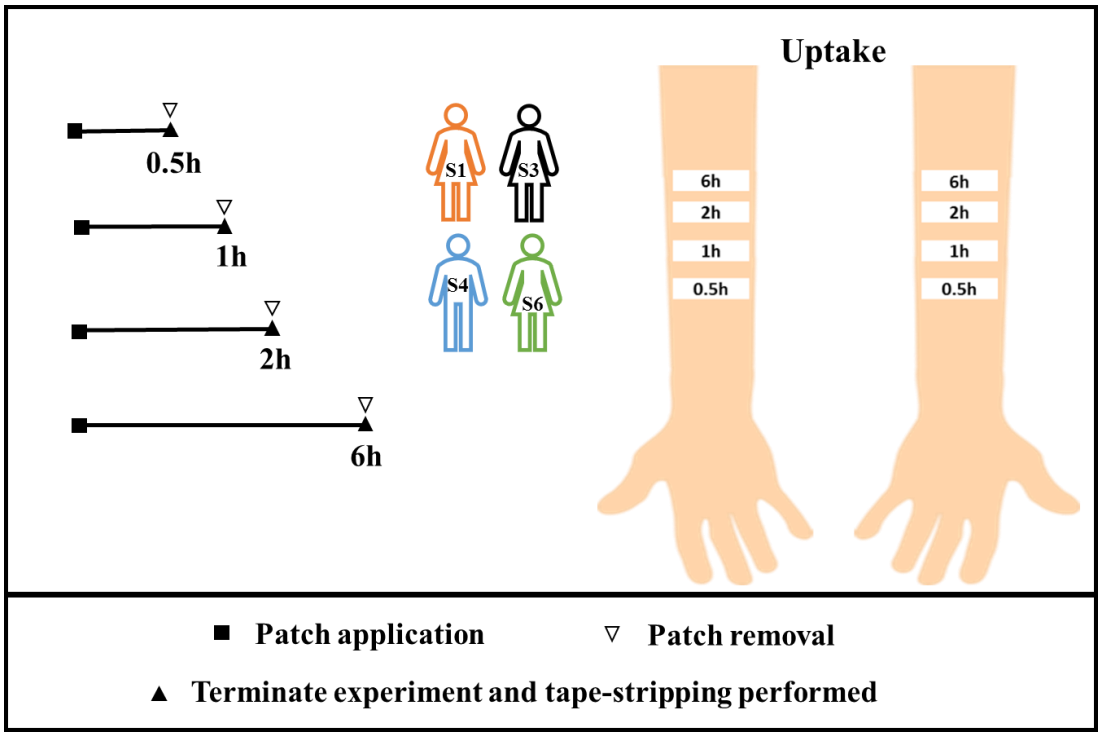

Figure 1. Schematic representation of the design of the tape-stripping experiments. The subject identifiers (S1, S3, S4 and S6) are the same as the ones used in Chapter 3.

All the sites were tape-stripped immediately after plaster removal. The SC sampling site was delimited by a template (Scotch® Book Tape, 3M, St Louis, MN, USA), with internal dimensions of 1 x 5 cm, which was placed on the skin immediately before tape-stripping began. Measurements of transepidermal water loss (TEWL, AquaFlux® evaporimeter, Biox System Ltd. London, UK) taken after plaster removal, before stripping and, intermittently, during tape-stripping, indicated whether most of the SC had been sampled but ensured that complete derangement of the barrier was avoided. Tape-stripping was carried out until either (i) the rate of water loss reached 60 g m^{-2} h^{-1} or (ii) 30 tape-strips had been removed (Kalia, Pirot and Guy, 1996; Kalia et al., 2000). All tapes were weighed (Microbalance SE-2F, precision 0.1 µg; Sartorius AG, Goettingen, Germany) before and after stripping to determine the mass of SC

removed; tapes were first discharged of static electricity (R50 discharging bar and ES50 power supply Eltex Elektrostatik GmbH, Weil am Rhein, Germany).

From the mass of SC removed, and knowing the area sampled and the density of the SC (assumed to be 1 g cm^{-3}; Anderson and Cassidy, 1973), it was possible to calculate the thickness of the SC removed on each tape.

PG and BG were extracted from the first two tapes individually but, thereafter, tape-strips from the deeper SC were analysed in groups of up to 4 tapes to ensure, as far as possible, that the aggregated samples contained an amount of permeant greater than the limit of quantification of the assay.

The two glycols were extracted from the tape-strips with 3 mL of acetonitrile per sample and the vials were placed on a horizontal shaker (HS 260 Basic, IKA Group) and shaken overnight at room temperature. To minimise loss of glycols from the tapes by evaporation, the tapes were weighed, rolled and put in contact with the extraction solvent immediately after SC collection. Similarly, the residual amounts of glycols in each section of plaster was measured post-application by extracting the glycols from the plaster immediately after its removal from the skin.

2.3. Sample preparation

PG and BG lack a chromophore, and chemical derivatization was therefore required to enable their detection by HPLC-UV detection. The previously described derivatisation method (Zhou *et al.*, 2007), which had been used to simultaneously analyse propylene glycol and diethylene glycol in pharmaceutical products, was closely followed. The derivatization reagent was a 20% solution of p-toluenesulfonyl isocyanate (TSIC), in acetonitrile (v/v). Sixty µL of this TSIC solution was added to 600 µL of the sample in an Eppendorf tube, vortex-mixed for 30 s, and allowed to stand at room temperature for 10 min. Subsequently, 60 µL of water was added and the solution was vortex-mixed again for a further 30 s. The resulting solution was filtered (0.45 µm nylon membrane, Labhut, Maisemore, UK) before analysis by HPLC. Calibration curves were prepared under same conditions as the tested samples.

2.4. Analysis of propylene and butylene glycol

The derivatised glycols were quantified simultaneously by HPLC (Summit, Dionex, UK) with UV detection (230 nm). Chromatography was performed on a HiQSil C18HS column (150 x 4.6 mm, 5 µm, Kya Technologies Corporation, Japan). A

mobile phase gradient was applied with 0.1% of formic acid in water (A) and acetonitrile (B). The gradient conditions were as follows: (i) a linear gradient from 70% to 40% of (A) from 0 to 15 min, (ii) from 15.1 to 20 min, the mobile phase composition was 40% (A) and 60 % (B), and (iii) from 20.1 to 25 min, the mobile phase was held at 70% (A) and 30% (B) to re-equilibrate the system. The total run time was 25 min. The flow rate was 1.2 mL min^{-1}. Retention times were ~ 12 and 13 min for the derivatisation products of PG and BG, respectively. The injection volume was 40 µL and the column temperature was maintained at 30°C. Selectivity of the method was confirmed by extraction of tapes with SC but without any contact with the two glycols investigated. No interference was found at the relevant retention times. Limits of detection for PG and BG were 0.04 and 0.06 µg mL^{-1}, respectively. Limits of quantification for PG and BG were 0.12 and 0.24 µg mL^{-1}, respectively.

Confirmation of the structures of the derivatives was obtained by liquid chromatography with mass spectroscopy (LC-MS). Samples prepared as described above were analysed on a QTOF-UHPLC (MaXis HD quadrupole electrospray time-of-flight (ESI-QTOF) mass spectrometer (Bruker Daltonik GmbH, Bremen, Germany), operated in ESI positive-ion MS mode). The QTOF was coupled to an Ultimate 3000 UHPLC (Thermo Fisher Scientific, California, USA). The capillary voltage was set at 4500 V, nebulizing gas at 4 bar, and drying gas at 12 L min^{-1} at 220 °C. The TOF scan range was from 50 – 750 mass-to-charge ratio (*m/z*). The in-source CID was set to 0.0 eV, with the collision energy for TOF MS acquisition at 7.0 eV. The conditions of the liquid chromatography analysis were the same as used for the HPLC-UV, with the exception of the injection volume being 5 µL and a split flow post column before the mass spectrometry detector with a flow rate of 0.3 mL min^{-1}. The MS instrument was calibrated using a range of sodium formate clusters introduced by 10 µL loop-injection prior to the chromatographic run. The mass calibrant solution consisted of 3 parts of 1 M NaOH to 97 parts of 50:50 water:isopropanol with 0.2% formic acid. The observed mass and isotope patterns of the formate clusters were used to calibrate the instrument to within 1 ppm mass accuracy. Data processing was performed using the data analysis software version 4.3 (Bruker Daltonik GmbH, Bremen, Germany).

2.5. Estimation of loss of glycols from the plaster by evaporation

Loss of the glycols from the formulation was investigated in two different scenarios. In the first, the release liner (the backing layer that protects the adhesive surface until use) from 5 cm^2 (1 x 5 cm) pieces of plaster was removed, and the sections were positioned on a glass slide in an oven at 32°C. In the second, the entire plaster (140 cm^2, releaser liner not removed) was placed in an oven at 32°C.

The plaster pieces were analysed immediately upon removal from the packaging, and at 0.5, 1, 2, 4, 6, 8 and 10 hours exposure to the two different conditions. Glycols were extracted from each section with 40 mL of acetonitrile in Eppendorf tubes, which were placed on a horizontal shaker (overnight at room temperature; HS 260 Basic, IKA Group), and then derivatized with TSIC and analysed by HPLC-UV as described above.

2.6. Data analysis

The analysis of diclofenac uptake data into the SC closely mirrored that described in Chapter 3.

The mass of permeant in the SC was expected to exhibit a log-normal distribution (AC Williams, Cornwell and Barry, 1992; Kasting et al., 1994; Cornwell and Barry, 1995). Therefore, the arithmetic average, standard deviation and 90% confidence intervals of the logarithm of the geometric mean of the duplicate measurements in the 4 subjects were calculated for each experiment time (N'Dri-Stempfer et al., 2009).

Firstly, the concentration profile of PG and BG across the SC (C_x) as a function of position in the SC (x/L) was analysed for all subjects at each uptake time considered. The data points from the two replicate sites were combined. Then, profiles were fitted to the relevant solution of Fick's second law of diffusion (Scheuplein, 1967; Crank, 1979) (Equation 2) assuming the following boundary conditions: (i) that the permeant concentration in the vehicle (C_v) remains constant during the treatment period (t_{app}); (ii) that the SC provides a homogeneous barrier to permeant diffusion; (iii) that there is no permeant in the SC at t=0; and (iv) the viable epidermis acts as a perfect sink for the permeant.

$$C_x = KC_v \left[1 - \frac{x}{L} - \frac{2}{\pi} \sum_{m=1}^{\infty} \frac{\exp\left[-m^2\pi^2 t_{app}\left(D/L^2\right)\right]\sin\left(m\pi x/L\right)}{m}\right] \qquad \text{(Equation 1)}$$

where C_x is PG or BG concentration (mass of permeant divided per mass of SC removed) at position x in the SC at the application time (t_{app}).

The fitting yields values for KC_v (K is the permeant's SC-vehicle partition coefficient) and for D/L^2, a first-order rate constant comprising the ratio of the permeant diffusivity (D) in the SC to the total thickness of the barrier (L) squared. From these two parameters (KC_v and D/L^2) and the corresponding L (estimated for each subject using Equation 1 in Chapter 3), the lag-time ($T_{Lag} = L^2/6D$, Roberts, Anissimov and Gonsalvez (1999)), time to steady-state ($T_{SS} = \sim 2.4T_{Lag}$, Cleek and Bunge (1993)) and steady-state flux across the SC ($J_{ss} = KC_vD/L$,) may be calculated. Note that, as all the subjects enrolled in this study also took part in the 'diclofenac study' (Chapter 3), the value for L used for the analysis was the average values showed previously in Chapter 3 (Table S1 in 'Supplementary Information').

Secondly, it is also possible to analyse the mass of DF after SC uptake using an approximate solution to Fick's second law of diffusion (Equation 2 and Equation 3) from which D may be estimated in a different way.

The cumulative mass of DF measured in the tape-strips per unit of area of exposure (M_{SC}/A) *versus* square-root of time profiles were compared to the solution of two models describing diffusion into a: (i) semi-infinite membrane (Equation 2), and (ii) finite membrane (Equation 3) (Frasch and Bunge, 2015).

$$\frac{M_{SC}}{A} = 2KC_v\sqrt{\frac{Dt_{app}}{\pi}} \qquad \text{(Equation 2)}$$

$$\frac{M_{SC}}{A} = KC_v\,L\left[\frac{1}{2} - \frac{4}{\pi}\sum_{n=0}^{\infty}\frac{exp[-D(2n+1)^2\pi^2({}^{t_{app}}/_{L^2})]}{(2n+1)^2}\right] \qquad \text{(Equation 3)}$$

The semi-infinite membrane model assumes that the application time of the formulation to the SC is insufficient for the permeant to reach the lower surface of the barrier which therefore, in effect, behaves as a semi-infinite membrane (Equation 2); the finite membrane model, in contrast, considers the SC as a single finite membrane (Equation 3).

The analytical solution to the semi-infinite model permits a value of D to be deduced. Then, using this D, Equation 4 can be used to predict the evolution of the

M_{SC}/A over time following the finite membrane model. Note that M_{SC}/A corresponds to the average concentration in the SC multiplied by the SC thickness.

The application of Equations 2 and 3 requires estimates of the concentration of the permeant at x=0. In this study, we have assumed that the permeant concentration at the surface of the SC is constant and equal to KC_v (obtained from fitting the data to Equation 1; the average of the KC_v determined following 0.5, 1 and 2-hour of application was used).

2.7. Statistics

Statistically significant differences were estimated by a t-test or by one-way ANOVA followed by Tukey's test, assessed in a pairwise, within-subject comparison when appropriate. In all cases, statistical significance was set at $p < 0.05$. The 90% confidence interval was calculated using the Student's T-distribution for the sample size and the sample standard deviation.

3. Results and discussion

3.1. Analysis of propylene and butylene glycol

LC-MS confirmed that the peaks quantified by HPLC-UV were the two glycol derivatization products and that two TSIC molecules (one per hydroxyl group) had been added to both PG and to BG. Details of these results and the mass spectra are in the 'Supplementary information', Figure S1 and Table S2.

3.2. Stratum corneum tape-stripping experiments

The total masses of PG and BG recovered from the SC of each subject are shown in Figures 2 and 3, respectively.

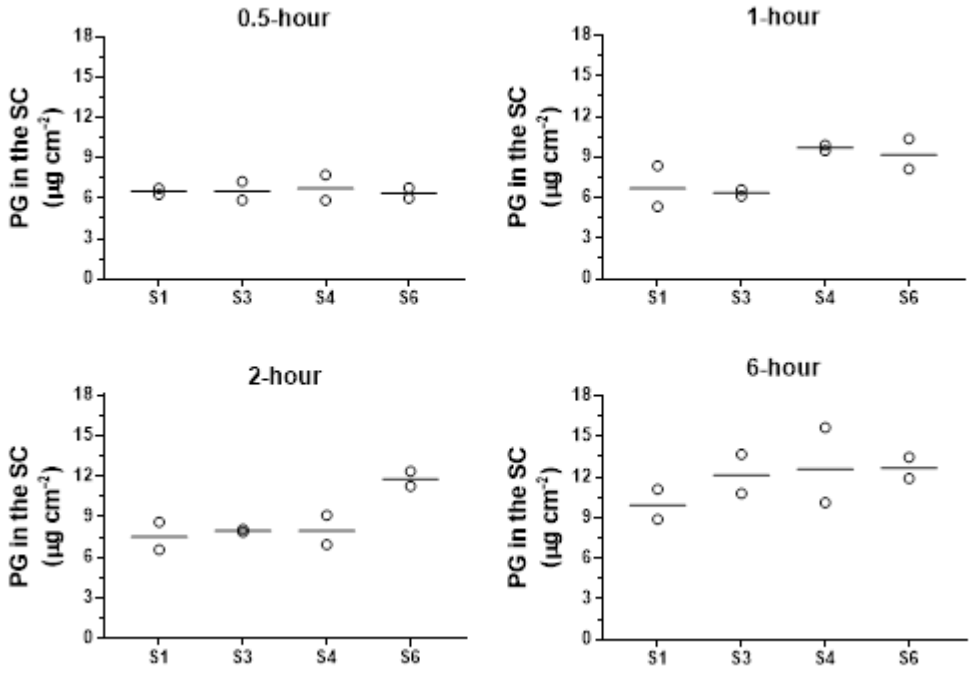

Figure 2. Mass of propylene glycol (PG) recovered from each skin site at each uptake time, with replicate determinations performed as a function of time in 4 subjects. Horizontal lines are the geometric means of the replicate values indicated by the open circles.

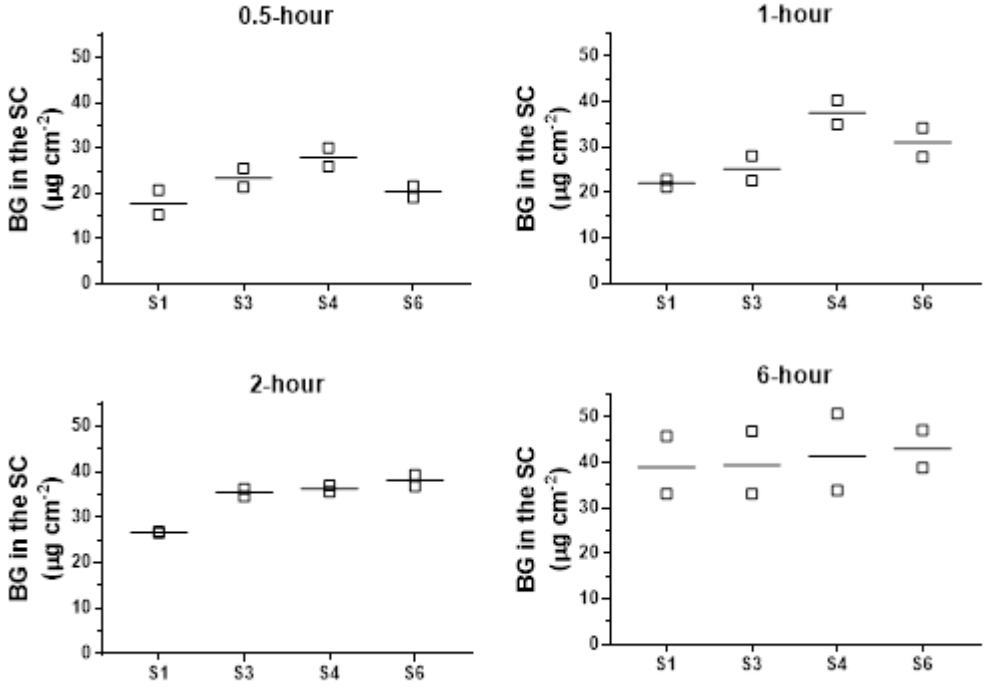

Figure 3. Mass of butylene glycol (BG) recovered from each skin site at each uptake time, with replicate determinations performed as a function of time in 4 subjects. Horizontal lines are the geometric means of the replicate values indicated by the open squares.

The SC concentration-depth profiles following different application times for each subject are shown in Figure 4. These data are plotted as a function of position within the SC (x) normalized by the predicted total thickness of the SC (L). The solid lines in Figure 4 were calculated from Equation 1 using the best fit of KC_v and D/L^2 values at the corresponding application time. The mean values of KC_v and D/L^2 per time for all subjects are in Table 1.

It was not possible to determine D/L^2 from the fit to the SC concentration-depth profile at 6 hours for either PG or BG; by this time, the exponential function in Equation 2 is negligible and the concentration profiles close to linear.

Within the obvious constraints of this study, which only involved a total of four subjects, a one-way analysis of variance (ANOVA), followed by Tukey's post hoc test indicated that, for both glycols, there was no significant difference in the partitioning parameters (KC_v) deduced at the application times investigated. In contrast, the estimated diffusion parameter (D/L^2) for PG at 0.5 h was significantly greater than that at 2 h.

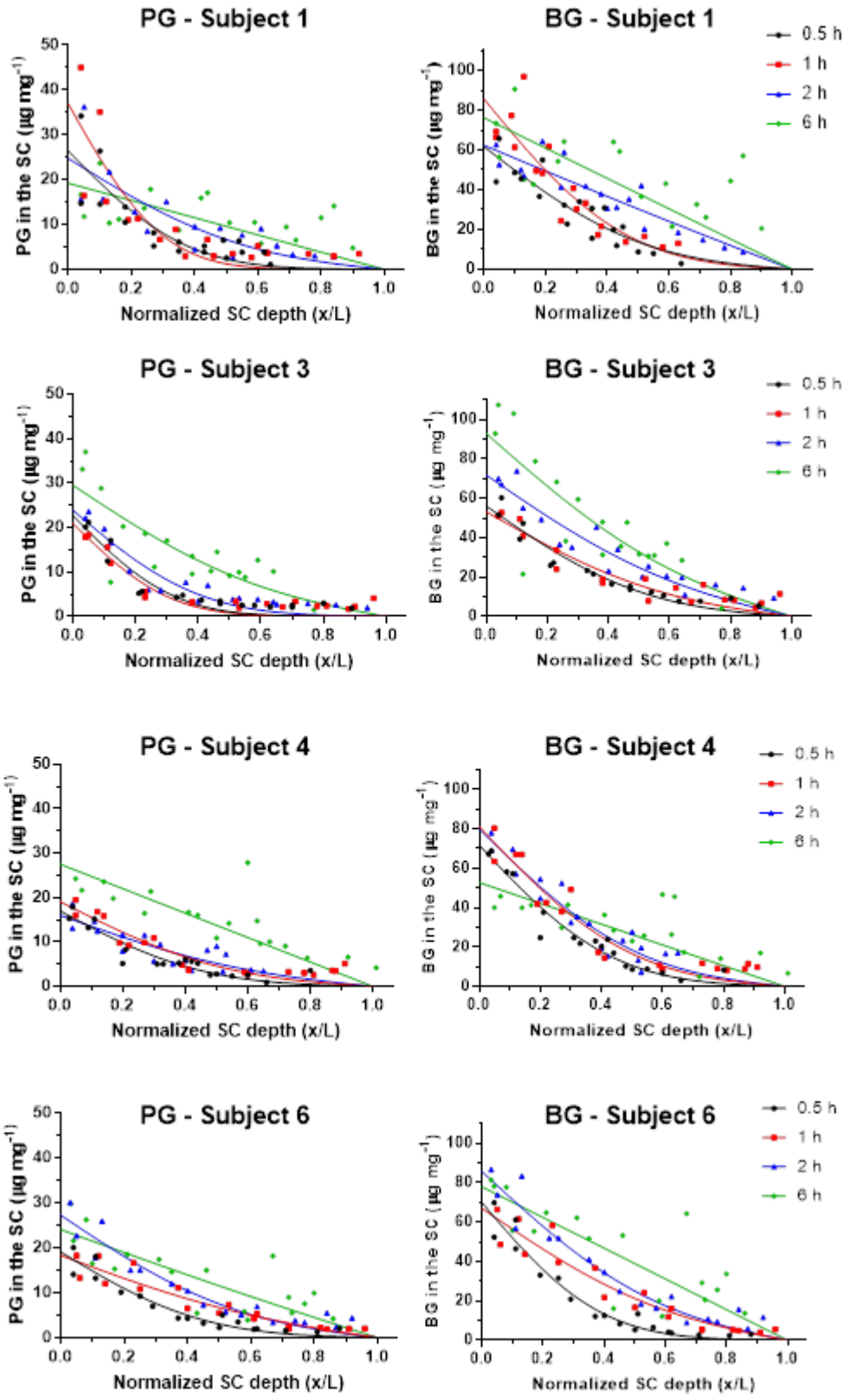

Figure 4. Individual concentration profiles of PG (left panels) and BG (right panels) across human SC *in vivo* following application of Voltaren® medicated plaster for different application times. The data points were experimentally determined; the solid lines were calculated from Equation 1 using the best fit of KC_v and D/L^2 values deduced from the best fit of the corresponding application time.

Table 1. Propylene glycol and butylene glycol partitioning and diffusivity parameters as a function of application time derived from the best fit of Equation 1. Values are the arithmetic means across 4 subjects, for each time point (lower and upper 90% CI).

Application time (h)	KC_v (µg mg^{-1})	10^2 D/L^2 (h^{-1})
	Propylene glycol	
0.5	21.3 (16.4 – 26.1)	10.2 [a] (6.3 – 14.0)
1	23.8 (13.5 – 34.1)	7.7 (0.4 – 15.0)
2	23.0 (17.3 – 28.7)	4.9 [a] (2.9 – 6.9)
	Butylene glycol	
0.5	64.8 (56.3 – 73.3)	13.9 (9.4 – 18.4)
1	71.7 (54.4 – 89.1)	9.7 (6.2 – 13.2)
2	75.0 (63.0 – 86.9)	9.3 (0.9 – 17.6)

[a]Analysis of variance (one-way ANOVA, followed by Tukey's post hoc test) indicated that D/L^2 at 0.5 h was significantly greater than that at 2 h ($p = 0.03$). No other statistically significant difference was found.

To illustrate the determination of additional kinetic parameters from these results, average values of KC_v and D/L^2 were combined with the mean SC thicknesses (L) assessed by measurements of TEWL during tape-stripping. The average KC_v and D/L^2 results in Table 2 were calculated from the data in Table 1, while the measured L values are collected in the 'Supplementary Information', Table S1. Using these data for the two glycols, lag-time ($T_{Lag} = L^2/6D$), time to steady-state ($T_{SS} \sim 2.4T_{Lag}$), diffusivity across the SC (D) and steady-state flux ($J_{SS} = KC_vD/L$) were calculated; the results are collected in Table 2.

Table 2. Pharmacokinetic parameters deduced for PG and BG in human SC *in vivo* following application of Voltaren® medicated plaster. Values were deduced from the SC concentration *versus* depth profile (Equation 1). The mean values (± standard deviation) were calculated within each subject, then averaged (arithmetic mean) across all subjects and then averaged (arithmetic mean) across the application times.

Parameters	PG	BG
KC_v (µg mg^{-1}) [a]	22.7 ± 1.3	70.5 ± 5.2
10^2 D/L^2 (h^{-1}) [a]	7.6 ± 2.6	10.9 ± 2.5
10^8 D (cm^2 h^{-1}) [b]	12.9 ± 4.5	16.9 ± 4.7
T_{Lag} (h)	3.1 ± 1.1	1.9 ± 0.6
T_{SS} (h)	7.4 ± 2.7	4.5 ± 1.4
J_{SS} (µg cm^{-2} h^{-1})	1.8 ± 0.9	9.0 ± 1.8

[a]Calculated using Equation 2, average value of KC_v derived from 0.5-, 1-, 2-hour application time; [b]Calculated using individual estimated value for D/L^2 times L (individual average value, Table 1) squared.

The uptake of PG and BG into the SC was also explored using the semi-infinite and finite membrane models (Equations 2 and 3).

Estimates of KC_v were derived from Equation 1. Estimates of D/L^2 were derived for each subject from the slope of the linear regression of M_{SC}/A *versus* square-root of time (regressions on $t \leq 1$ h, $\sqrt{t} \leq 1.4$ $h^{1/2}$ and without forcing the origin) combined with the mean individual estimated value for L and the corresponding value of KC_v. From the estimated D/L^2, L and KC_v for each subject it was also possible to calculate T_{Lag}, T_{SS} and J_{ss} (Table 3).

Table 3. Diffusion parameters of PG and BG in human SC *in vivo* (4 subjects) following application of Voltaren® medicated plaster. Values were deduced from the M_{SC}/A *versus* $\sqrt{t}$ profiles (Equation 2). The mean values (± standard deviation) were calculated within each subject, then averaged (arithmetic mean) across all subjects and then averaged (arithmetic mean) across the application times.

Parameters	**PG**	**BG**
Intercept at t =0 h (µg cm^{-2})	4.7 ± 0.9	11.7 ± 7.9
KC_v (µg mg^{-1}) [a]	22.7 ± 1.3	70.5 ± 5.2
10^8 D (cm^2 h^{-1}) [b]	1.7 ± 0.9	4.7 ± 3.4
10^2 D/L^2 (h^{-1}) [c]	0.9 ± 0.4	3.1 ± 2.2
T_{Lag} (h)	22.4 ± 15.3	10.5 ± 11.4
T_{SS} (h)	60.5 ± 41.4	28.4 ± 30.9
J_{SS} (µg cm^{-2} h^{-1})	0.3 ± 0.1	2.7 ± 2.0

[a]Average value of KC_v derived from 0.5-, 1-, 2-hour application time (Equation 1);
[b]Derived from KC_v and the slope of the linear regression of M_{SC}/A *versus* the square-root of time for $t \leq 2$ h;
[c]Calculated using individual value for D divided by L (individual average value, Table 1) squared.

Figure 5 compares the mean measured mass per area of PG and BG in the SC as a function of the square-root of time to the semi-infinite membrane model (dashed line) and to the finite membrane (solid line). The solid line in Figure 5 was calculated using the average values of the 4 subjects for L (12.8 µm) and D derived from KC_v (Table 2) and the slope of the linear regression.

Consistent with the experimental data, at 6 h ($\sqrt{t}$ = 2.45 $h^{1/2}$) the curve for BG diverged from Equation 2, and suggests (as shown by the best fit of Equation 3) that the semi-infinite boundary conditions are no longer met. Within the 6-hour period investigated in this work, neither the experimental data nor the finite membrane model prediction for PG showed a deviation from Equation 2.

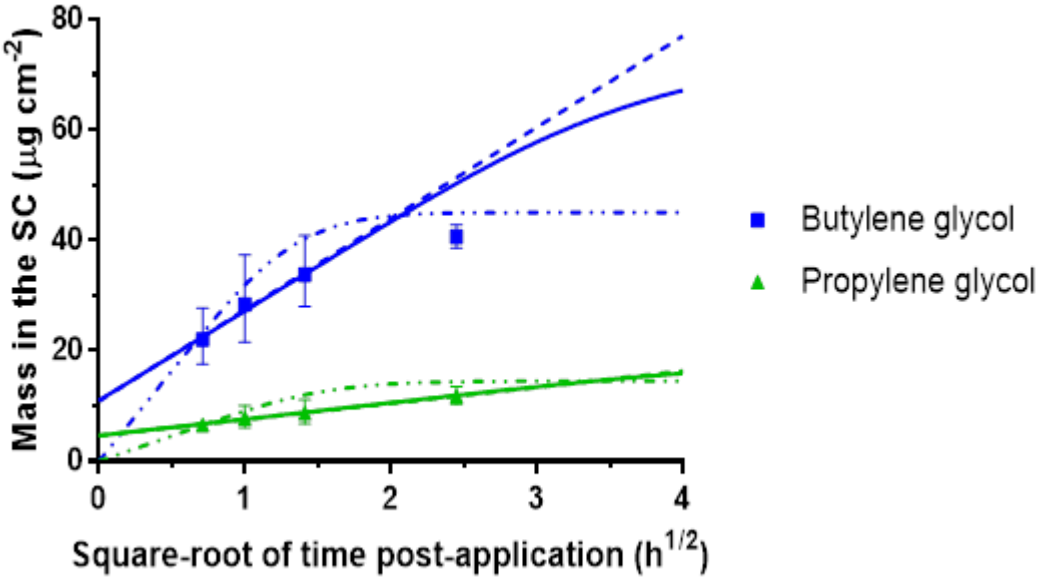

Figure 5. Average mass of PG and BG in human SC *in vivo* (4 subjects) following application of Voltaren® medicated plaster for different application times. The data points were experimentally determined and plotted as the anti-logarithm of the log-transformed average of the geometric mean of duplicates in each subject ± 90% confidence interval; the dashed line represents the solution of the semi-infinite membrane theory (regressions on $t \leq 2$ h, $\sqrt{t}$ = 1.4 $h^{1/2}$ data, Equation 2) and solid line represents the solution of the finite membrane theory predicted with diffusivity (D) derived from semi-infinite theory slope (Equation 3).The dot-dashed lines represent the solution of the finite membrane theory predicted with diffusivity (D) and KC_v derived using Equation 1.

A further observation, from the M_{SC}/A *versus* square-root of time plot, was that the linear regressions led to a non-zero value at $t = 0$. It suggests a rapid transfer of a measurable quantity of BG (11.7 μg cm^{-2}) and PG (4.7 μg cm^{-2}) to the SC when the plaster is first applied to the skin. From a mechanistic standpoint, these intercepts could represent the mass of PG and BG, which is distributed across the surface of the SC, immediately after plaster application, with possible accumulation in the SC-microcrevices and/or loosely attached corneocytes, therefore, not true absorption. Also, these masses could characterise a faster penetration of PG and BG via a hair shaft. This last hypothesis is in line with stimulated Raman scattering microscopy experiments that tracked the uptake of PG into mouse skin (Saar et al., 2011). The work described by these authors compared the uptake of PG via hair shafts and via the SC intercellular lipids. They found that PG penetration via the hair shaft was rapid and

attained steady-state before 26 min post-application of the formulation (Saar et al., 2011).

In summary, the analysis of the C_x *versus* x/L curves gives D and KC_v values that correspond to much larger slopes (calculated using the definition of the slope in Equation 2) than observed by the M_{SC}/A *versus* square-root of time data. This larger slope is consistent with the faster rate of BG and PG transfer before t = 0.5 h, however, this larger slope is inconsistent with uptake over the period of 0.5 to 2 h (which appears to be linear with a smaller slope).

In addition, in order to have a better visualisation of the difference between values derived using Fick's second law or its simplified model, the prediction of the M_{SC}/A *versus* square-root of time curves from the finite membrane model assuming D and KC_v from the C_x *versus* x/L analysis (Table 2) and assuming D and KC_v are related to each other according to the slope defined in Equation 2 is shown in Figure 5 (dot-dashed curves).

3.3. Analysis of the glycols residual in the plaster

Glycols from the plaster were extracted immediately after removal from the packaging as well as after removal from the skin. This analysis allowed us to measure the efficiency of the extraction solvent (at least for PG, since the amount of PG loaded in the plaster is known) and, also, to investigate the mass of PG and BG that had been released from the plaster during skin application. Table 4 summarises these findings.

Table 4. Mass of PG and BG extracted from the plaster either immediately after removal from the packaging or after removal from the skin at different application times. The mean values (± standard deviation) were calculated within each subject, then averaged (arithmetic mean) across all subjects.

Application time (h)	PG (µg cm^{-2})	BG (µg cm^{-2})
0[a]	1192 ± 92	3111 ± 218
0.5	756 ± 263	2423 ± 290
1	680 ± 201	2222 ± 251
2	534 ± 150	1790 ± 148
6	288 ± 93	768 ± 261

[a]Extracted immediately after removal from the packaging, n = 9.

The amount of PG measured immediately after removal from the packaging is ~1200 µg cm^{-2}, which is ~40% of the amount declared in the patient information leaflet. This percentage corresponds to the yield of the extraction process.

The amount of PG and BG released from the plaster was calculated as the difference between the measured amount of PG and BG immediately after removal from the packaging and the residual content measured after its removal from the skin at each time point (Table 4). On the basis of this analysis, the total amount of glycols released from the plaster after 6 h of skin contact was ~ 900 and 2342 µg cm^{-2} of PG and BG, respectively, which is equivalent to ~75% of the amount of each compound extracted immediately after removal from the packaging (Figure 6).

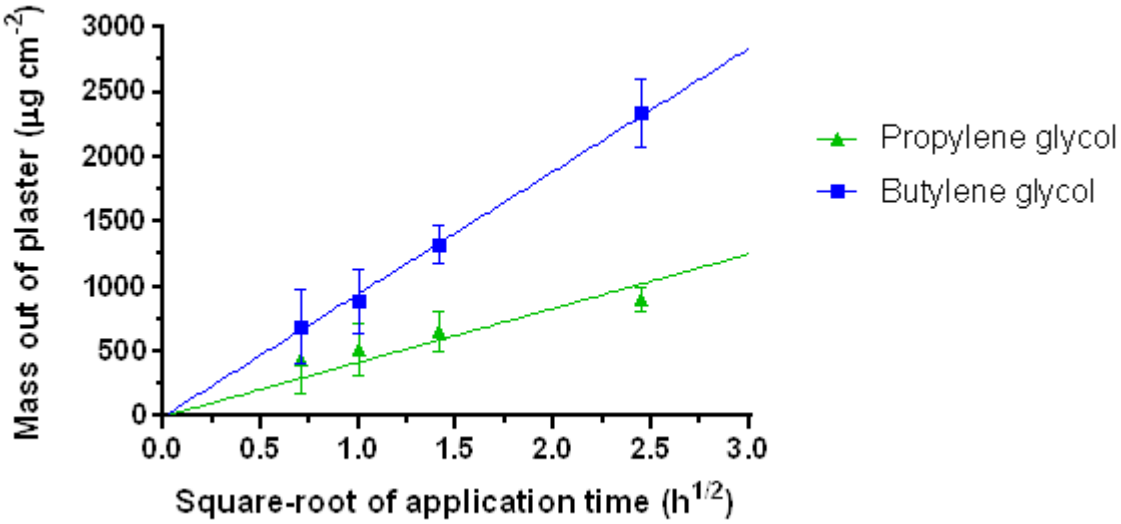

Figure 6. Average mass of PG and BG out of the plaster after wear of Voltaren® medicated plaster for different application times (4 subjects). The values were obtained by measuring the residual in the plaster after application and comparing with the t=0. Values are the arithmetic mean for each time point (± standard deviation, n = 4).

Comparing the mass of PG and BG recovered from the tape-strips (Figure 5) and losses of PG and BG from the plaster after 6 hour of plaster wear (Figure 6), it was possible to observe that the masses of glycols out of plaster were ~ 77- and 58-fold higher, respectively, than the amount recovered from the tape-strips.

In addition, the observation that the measured M_{SC}/A is linear with square-root of time up to 2 h ($\sqrt{t}$ = 1.41 $h^{1/2}$) for BG and up to 6 h ($\sqrt{t}$ = 2.45 $h^{1/2}$) for PG suggests that little if any of the glycols have reached the bottom of the SC (Figure 6). Therefore, nearly all of the glycol transferred to the SC was still in the SC at the sampling times.

It follows that the measured losses of glycol from the plasters cannot be explained by the small transfers to the skin.

A separate, related, point is that, even though the mass of BG and PG in the plaster drops significantly, the mass-ratio of BG-to-PG remains nearly constant (at ~ 2) over 6 h. Also, the M_{SC}/A *versus* square-root of time analysis suggests that D and KC_v also remain essentially constant over the interval of 0.5 to 2 h for BG and for 0.5 to 6 h for PG; these two observations imply that the thermodynamic activity of BG and PG must have remained relatively constant over this interval, despite the significant concentration decrease in the plaster. A logical explanation for this observation is that while the mass of PG and BG is depleting significantly, the glycols would be contained in a 'reservoir' that stays at essentially constant thermodynamic activity until they are nearly depleted. For example, if the BG and PG were liquids 'trapped' in the adhesive material then the vehicle concentrations for PG and BG would remain constant even though the masses of PG and BG changed dramatically.

3.4. Estimation of loss of glycols from the plaster by evaporation

Due to the discrepancy between the mass of PG and BG which has left the plaster and has been absorbed into the SC, a test to estimate the loss of glycols from the plaster by evaporation was conducted.

Voltaren® medicated plaster is comprised of an adhesive material which is applied to a non-woven polyester felt backing and covered with a polypropylene film release liner which is removed prior to topical application to the skin (patient information leaflet). Therefore, it was hypothesised that evaporation of PG and/or BG would be possible through the non-occlusive felt backing and/or through the cut edges of plaster.

The results are presented in Figure 7, which shows that both scenarios, i.e., when the plaster was cut into smaller sections (scenario 1) or not (scenario 2), gave remarkably similar profiles. It suggests that the principal route of loss of glycols from the plaster is evaporation via the backing, as it appears that PG and BG evaporate from the plaster just as easily regardless as to whether the plaster has been cut or not. Note that the time zero corresponds to the amount of glycols extracted from the plaster immediately after removal from the packaging.

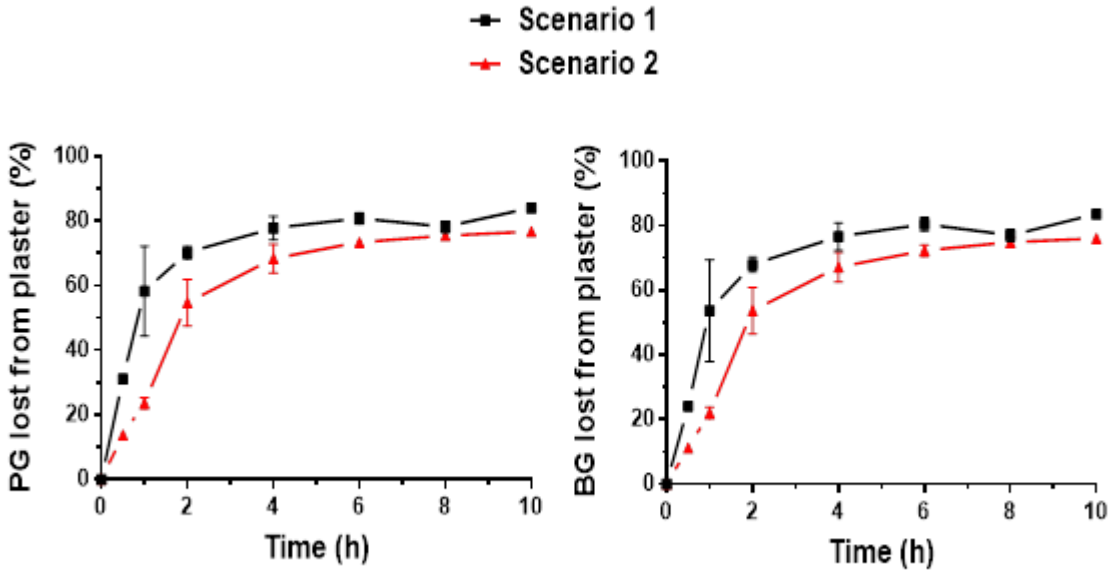

Figure 7. Percentage of PG (left panel) and BG (right panel) lost from the plaster over time, under two different scenarios. In scenario 1, the release liner was removed, the pieces of plaster were positioned on a glass slide and then placed in an oven at 32 °C. In scenario 2, the entire plaster (without release liner removal) was placed in an oven at 32 °C. The values were obtained by measuring the residual and comparing with the amount of PG and BG measured immediately after removal from the packaging (Table 6). Values are the arithmetic mean for each time point (± standard deviation, n = 3).

This loss is in line with previous findings. Tsai et al. (1992) reported that the PG recovery after the application of 35 µL (~ 20 µL cm^{-2}) of a PG:ethanol:water mixture (20:60:20) to hairless mouse skin *in vitro*, was 40% of the applied PG dose after a 12 h exposure time. A study developed by Trottet et al. (2004) shows that not all the PG applied is recovered at the end of an *in vitro* experiment, using human skin. When 40 mg cm^{-2} of a gel loaded with 12% of PG was applied on the skin, 25% of the PG initial content evaporated. When a lower dose (10 mg cm^{-2}) of formulation (gel with 12% PG and cream with 15% and 40% PG) was applied a larger proportion of PG evaporated (39 – 61%). Santos et al. (2010) observed that the skin permeation (using heat separated human epidermis) of an ethanolic solution of 25% PG resulted in a total recovery (amounts permeated and recovery from the washes and extractions) of PG of around 30% of the total dose applied (3.6 µL cm^{-2}), suggesting that PG was probably lost by solvent evaporation.

3.5. Effect of PG and BG on diclofenac absorption into the stratum corneum

The results described in Chapter 3 of this thesis suggested that diclofenac (DF) uptake into the SC may be modified by the presence of excipient(s). Therefore, this chapter focused on exploring the uptake of two excipients/co-solvents, propylene glycol and butylene glycol, into the SC *in vivo* in human. The experiments with these glycols were conducted using the same diclofenac medicated plaster used in the previous chapter (Voltaren®) and this product was applied on the forearms of the same subjects enrolled in the previous study (Chapter 3, 'diclofenac study').

The work described here shows that PG and BG themselves penetrate into the SC. Analysis of variance (one-way ANOVA, followed by Tukey's post hoc test) indicated that estimated steady-state flux of BG across the SC (Table 2) was significantly greater than that of DF ($p = 0.0003$). No statistically significant difference was found between the estimated steady-state flux of PG and DF across the SC. Therefore, BG penetrates the SC faster than the drug or than PG. It follows that the higher DF diffusivity and partitioning observed in the early stages of the experiment may be related to the concomitant presence of these glycols in the SC. The glycols may create a situation where drug delivery is transiently more efficient in the beginning of the treatment.

The mechanism by which PG and BG enhance drug permeation/penetration into the SC is not clearly established. Studies which investigated how PG enhances drug permeation, however, provide some evidence that it has a carrier-solvent effect (Hoelgaard and Møllgaard, 1985); and/or may increase the solubility of the drug in the SC (Kasting, Francis and Roberts, 1993).

Although the literature does not address the mechanism of action of BG, it seems likely that its co-solvent properties and skin uptake are also key to its application as a permeation enhancer (Lane, 2013).

To establish whether these glycols are, synergically or individually, acting as permeation enhancers would require further experiments, for example, investigation of DF behaviour in the presence or absence of one or other glycol.

4. Conclusion

SC sampling, using tape-stripping technique associated with HPLC-UV analysis, has been successfully used to track the fast uptake of PG and BG into the human SC and to characterise the diffusion of these excipients across the tissue.

The analysis by the M_{SC}/A *versus* square-root of time indicates that mass has been transferred to the SC within the first 0.5 h at a rate that is not consistent with the transfer rate over the interval of 0.5-2 h (which is consistent with constant D and constant KC_v). This suggests that this rapid transfer soon after plaster application is by a different mechanism than absorption into the skin via the intercellular pathway.

Assuming that KC_v estimated from the Fick's second law analysis (C_x *versus* x/L) applies to the semi-infinite and finite models (M_{SC}/A *versus* square-root of time), then D estimated from former analysis (C_x *versus* x/L) is larger to account for the mass that is rapidly transferred to the SC in the first 0.5 h after the plaster has been applied.

There was a much larger loss of the glycols from the plaster than could be explained by glycol transfer to the skin. Consequently, it was further demonstrated that PG and BG can evaporate from the formulation, which could change drug solubility in the formulation, thereby affecting the rate and extent of drug absorption into and through the SC.

In summary, the research described here has a significant importance as it allows useful quantitative information about the excipients to be extracted. An improved model, linking excipient kinetic parameters deduced here with the behaviour/disposition of the active compound (diclofenac) may ultimately improve the understanding of drug bioavailability from a topical formulation under 'real-life' conditions.

Supplementary information

Table S1. Estimation of stratum corneum apparent total thickness (L) using Equation 1 (in Chapter 3) for 6 subjects. The identification of 'Uptake' and 'Clearance' forearms are shown Figure 1 (in Chapter 3).

	Total thickness (µm)		
	'Uptake' forearm	**'Clearance' forearm**	**Average**
Subject 1	7.0	13.5	10.3
Subject 2	12.7	11.7	12.2
Subject 3	14.4	11.5	13.0
Subject 4	12.4	19.0	15.7
Subject 5	12.3	11.8	12.1
Subject 6	12.7	11.5	12.1

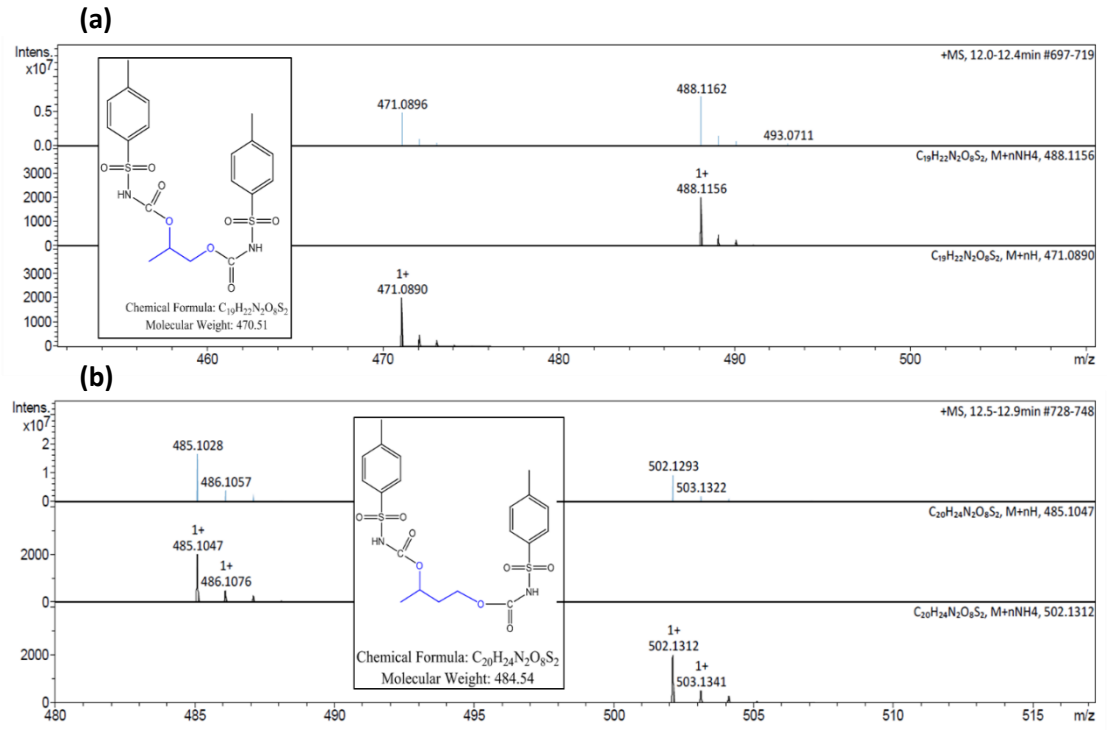

Figure S1. Mass spectra of the derivatives of propylene glycol (a) and butylene glycol (b) obtained by LC-MS in positive mode. Two quasimolecular ion peaks per compound corresponded to the protonated and ammoniated species.

Table S2. Quasimolecular ions obtained from the derivatives of propylene glycol and butylene glycol.

Propylene glycol	Theoretical mass	Observed mass	Mass error (ppm)
Protonated	471.0890	471.0896	1.3
Ammonium adduct	488.1156	488.1162	1.2
Butylene glycol			
Protonated	485.1047	485.1028	-3.9
Ammonium adduct	502.1312	502.1293	-3.8

The mass spectra yielded the quasimolecular ions corresponding to the protonated and ammonium-coordinated species. The summary of results for the derivatives of propylene glycol and butylene glycol extracted from tape-strips including the measured and theoretical masses for the protonated and ammonium-coordinated species is shown in Table S1. The mass accuracy of all measured masses was found to be less than 4 ppm.

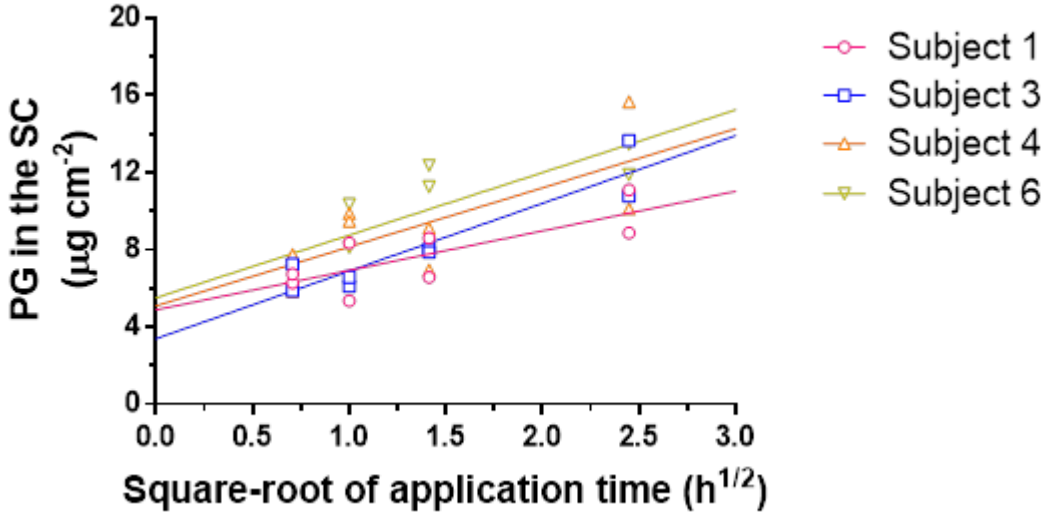

Figure S2. Mass of propylene glycol in human SC *in vivo* for each subject following application of Voltaren® medicated plaster for different application times. The data points were experimentally determined (the replicate values are shown by the same symbols) and the solid line represents a linear regression on t ≤ 2 h ($\sqrt{t} \leq 1.41$ $h^{1/2}$) data.

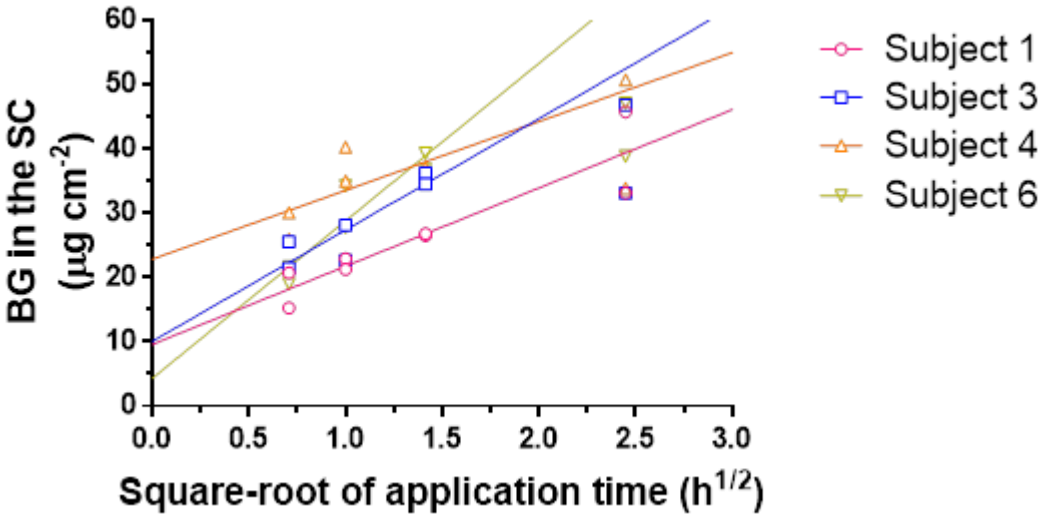

Figure S3. Mass of butylene glycol in human SC *in vivo* for each subject following application of Voltaren® medicated plaster for different application times. The data points were experimentally determined (the replicate values are shown by the same symbols) and the solid line represents a linear regression on t ≤ 2 h ($\sqrt{t} \leq 1.41$ $h^{1/2}$) data.

References

Alberti, I., Kalia, Y.N., Naik, A., Bonny, J.-D. and Guy, R.H., 2001. In vivo assessment of enhanced topical delivery of terbinafine to human stratum corneum. *Journal of Controlled Release,* 71(3), pp. 319-327.

Anderson, R.L. and Cassidy, J.M., 1973. Variations in Physical Dimensions and Chemical Composition of Human Stratum Corneum. *Journal of Investigative Dermatology,* 61(1), pp. 30-32.

Aungst, B.J., Blake, J.A. and Hussain, M.A., 1990. Contributions of drug solubilization, partitioning, barrier disruption, and solvent permeation to the enhancement of skin permeation of various compounds with fatty acids and amines. *Pharmaceutical Research,* 7(7), pp. 712-718.

Barry, B.W., 1987. Mode of action of penetration enhancers in human skin. *Journal of Controlled Release,* 6(1), pp. 85-97.

Choi, A., Gang, H., Chun, I. and Gwak, H., 2008. The effects of fatty acids in propylene glycol on the percutaneous absorption of alendronate across the excised hairless mouse skin. *International Journal of Pharmaceutics* 357(1-2), pp. 126-131.

Cleek, R.L. and Bunge, A.L., 1993. A new method for estimating dermal absorption from chemical exposure. 1. General approach. *Pharmaceutical Research,* 10(4), pp. 497-506.

Cornwell, P. and Barry, B., 1995. Effects of penetration enhancer treatment on the statistical distribution of human skin permeabilities. *International Journal of Pharmaceutics,* 117(1), pp. 101-112.

Crank, J., 1979. *The mathematics of diffusion.* Oxford University Press.

Frasch, H.F. and Bunge, A.L., 2015. The transient dermal exposure II: post-exposure absorption and evaporation of volatile compounds. *Journal of Pharmaceutical Sciences,* 104(4), pp. 1499-1507.

Gee, C.M., Watkinson, A.C., Nicolazzo, J.A. and Finnin, B.C., 2014. The effect of formulation excipients on the penetration and lateral diffusion of ibuprofen on and within the stratum corneum following topical application to humans. *Journal of Pharmaceutical Sciences,* 103(3), pp. 909-919.

Herkenne, C., Naik, A., Kalia, Y.N., Hadgraft, J. and Guy, R.H., 2008. Effect of propylene glycol on ibuprofen absorption into human skin in vivo. *Journal of Pharmaceutical Sciences,* 97(1), pp. 185-197.

Hoelgaard, A. and Møllgaard, B., 1985. Dermal drug delivery—improvement by choice of vehicle or drug derivative. *Journal of Controlled Release,* 2, pp. 111-120.

Huth, S., Neubert, R., Boltze, L. and Buge, A., 1996. Experimental determination and mathematical modelling of propylene glycol transport from semisolid vehicles. *Chemical and Pharmaceutical Bulletin,* 44(6), pp. 1263-1266.

Kalia, Y.N., Alberti, I., Sekkat, N., Curdy, C., Naik, A. and Guy, R.H., 2000. Normalization of stratum corneum barrier function and transepidermal water loss in vivo. *Pharmaceutical Research,* 17(9), pp. 1148-1150.

Kalia, Y.N., Pirot, F. and Guy, R.H., 1996. Homogeneous transport in a heterogeneous membrane: water diffusion across human stratum corneum in vivo. *Biophysical Journal,* 71(5), p. 2692.

Karande, P. and Mitragotri, S., 2009. Enhancement of transdermal drug delivery via synergistic action of chemicals. *Biochimica et Biophysica Acta (BBA) - Biomembranes,* 1788(11), pp. 2362-2373.

Kasting, G.B., Filloon, T.G., Francis, W.R. and Meredith, M.P., 1994. Improving the sensitivity of in vitro skin penetration experiments. *Pharmaceutical Research,* 11(12), pp. 1747-1754.

Kasting, G.B., Francis, W.R. and Roberts, G.E., 1993. Skin penetration enhancement of triprolidine base by propylene glycol. *Journal of Pharmaceutical Sciences,* 82(5), pp. 551-552.

Lane, M.E., 2013. Skin penetration enhancers. *International Journal of Pharmaceutics,* 447(1), pp. 12-21.

N'Dri-Stempfer, B., Navidi, W.C., Guy, R.H. and Bunge, A.L., 2009. Improved bioequivalence assessment of topical dermatological drug products using dermatopharmacokinetics. *Pharmaceutical Research,* 26(2), p. 316.

Pham, Q.D., Topgaard, D. and Sparr, E., 2017. Tracking solvents in the skin through atomically resolved measurements of molecular mobility in intact stratum corneum. *Proceedings of the National Academy of Sciences,* 114(2), pp. E112-E121.

Roberts, M.S., Anissimov, Y.G. and Gonsalvez, K., 1999. Mathematical models in percutaneous absorption. *Percutaneous absorption: drugs, cosmetics, mechanisms, methodology. Drugs and the Pharmaceutical Sciences,* 97, pp. 1-49.

Saar, B.G., Contreras-Rojas, L.R., Xie, X.S. and Guy, R.H., 2011. Imaging Drug Delivery to Skin with Stimulated Raman Scattering Microscopy. *Molecular Pharmaceutics,* 8(3), pp. 969-975.

Santos, P., Watkinson, A.C., Hadgraft, J. and Lane, M.E., 2010. Oxybutynin permeation in skin: The influence of drug and solvent activity. *International Journal of Pharmaceutics,* 384(1), pp. 67-72.

Scheuplein, R.J., 1967. Mechanism of percutaneous absorption: II. Transient diffusion and the relative importance of various routes of skin penetration. *Journal of Investigative Dermatology,* 48(1), pp. 79-88.

Trottet, L., Merly, C., Mirza, M., Hadgraft, J. and Davis, A.F., 2004. Effect of finite doses of propylene glycol on enhancement of in vitro percutaneous permeation of loperamide hydrochloride. *International Journal of Pharmaceutics,* 274(1), pp. 213-219.

Tsai, J.C., Cappel, M.J., Flynn, G.L., Weiner, N.D., Kreuter, J. and Ferry, J.J., 1992. Drug and vehicle deposition from topical applications: use of in vitro mass balance technique with minoxidil solutions. *Journal of Pharmaceutical Sciences,* 81(8), pp. 736-743.

Williams, A., Cornwell, P. and Barry, B., 1992. On the non-Gaussian distribution of human skin permeabilities. *International Journal of Pharmaceutics,* 86(1), pp. 69-77.

Williams, A.C. and Barry, B.W., 2004. Penetration enhancers. *Advanced Drug Delivery Reviews,* 56(5), pp. 603-618.

Wotton, P.K., Møllgaard, B., Hadgraft, J. and Hoelgaard, A., 1985. Vehicle effect on topical drug delivery. III. Effect of Azone on the cutaneous permeation of metronidazole and propylene glycol. *International Journal of Pharmaceutics,* 24(1), pp. 19-26.

Chapter 5: Predicting topical drug clearance from the skin

Abbreviations

A_{Cl}	mass of drug in the skin (stratum corneum *plus* epidermis/dermis) after a delay time between the removal of the patch and the end of the experiment (clearance time)
A_{UP}	mass of drug in the skin (stratum corneum *plus* epidermis/dermis) immediately after patch removal (uptake time)
Cl_{skin}	drug clearance from the skin
$Cl_{skin,exp}$	drug clearance from the skin calculated using experimental data
$Cl_{skin,pred}$	predicted drug clearance from the skin
C_p	systemic plasma concentration
C_{ss}	steady-state concentration
E_i	extraction ratio
F_i	degree of ionization
$F_{u,p}$	plasma protein binding
$K_{(skin/p)}$	drug's coefficient of partition between the skin and the plasma
k_e	systemic elimination rate constant
$k_{e,skin}$	elimination rate constant from the skin
$K_{tissue,plasma}$	tissue-to-plasma partition coefficient
log P	log of n-octanol/water partition coefficient
$t_{1/2}$	terminal half-life
VIF	variance inflation factor
V_{plasma}	volume of the plasma
V_{skin}	volume of the viable skin
V_{ss}	systemic volume of distribution at steady-state

$V_{ss,skin}$	skin volume of distribution
V_{tissue}	volume of the tissue
R	input-rate

1. Introduction

Skin disease is one of the leading causes of global disease burden, affecting millions of people worldwide (Hay et al., 2014). The effective delivery of a locally-acting, dermatological drug demands knowledge of its 'skin pharmacokinetics' to determine the rate and extent with which it reaches its site of action in the epidermis/dermis. Of necessity, this requires understanding of not only the input-rate of the drug into the skin but also its clearance from the 'skin compartment'[6] into the systemic circulation.

For topical drug products that target sites of action in the viable epidermal and/or upper dermal compartment of the skin, the local concentration profiles have proven difficult to quantify because both drug input into the viable cutaneous tissue and its clearance therefrom are not well characterised (Nicoli et al., 2009). Without such knowledge, of course, it is difficult – if not impossible – to predict *a priori* whether and over what time-frame a topical formulation will permit an effective concentration of drug to be achieved within the skin compartment.

Substantial progress has been made toward interpreting drug movement and disposition in the skin in terms of mathematical-pharmacokinetic models (McCarley and Bunge, 2001; Mitragotri et al., 2011). But, it is no surprise, given the multistep nature of the dermal absorption process, the many formulation types, and the complex nature of the physiological barrier, that most of these models suffer from one or more flaws including (but not limited to), for example, the need to 'guesstimate' many parameters to permit simulations to be performed, or the incorrect relation of 'rate constants' to drug physicochemical parameters, or the inability to obtain a prediction of drug concentration in the viable epidermis, thereby rendering the model (for most dermal products) of little practical use.

Considering these challenges, it is necessary to develop methods that are simple, yet realistic and mechanistically meaningful, to estimate the key dermato-pharmacokinetic parameters. Among the various approaches currently employed are the physiologically-based pharmacokinetic (PBPK) models, which consist of

[6] The term 'clearance from the skin' here is used to mean the volume of skin from which a drug is completely removed per unit time.

physiologically realistic compartmental structures into which input parameters from different sources (e.g., *in silico* predictions, *in vitro* or *in vivo* experiments) can be combined to predict plasma and/or tissue concentration-time profiles (Bouzom et al., 2012; Hartmanshenn, Scherholz and Androulakis, 2016).

PBPK models take into account properties, related to physiology of the tissue in question, that are not dependent on the drug and can, therefore, be applied to any compound, and also to characteristics intrinsic to the drug. One difference between PBPK and classical pharmacokinetic models (e.g., one- or two-compartmental pharmacokinetic models) is that they traditionally employ what is commonly known as a 'bottom-up' approach, as opposed to the 'top-down' approach of classical models (Jamei, 2016). Rather than estimating model parameters based on *in vivo* data (commonly from plasma/blood concentration *versus* time profiles), parameters are determined *a priori* from *in vitro* experiments, *in silico* predictions or, if required, *in vivo* data.

However, most PBPK models require some level of calibration or optimisation of their parameters. In general, a drug's concentration in a tissue is determined by the systemic volume of distribution at steady-state (V_{ss}) and clearance (Cl); assuming a simple one-compartment model with 1st-order elimination from the tissue compartment, the ratio of these independent physiological parameters provides the systemic elimination rate constant k_e (Equation 1):

$$k_e = Cl/V_{SS} \qquad \text{(Equation 1)}$$

V_{ss} is an apparent volume that describes the extent of drug distribution and binding to the tissues and plasma (Equation 2):

$$V_{ss} = V_{plasma} + \sum_1^n K_{tissue,plasma} \times V_{tissue,i} \times (1 - E_i) \qquad \text{(Equation 2)}$$

V_{plasma} is the volume of the plasma and $V_{tissue,i}$ is the volume of the *i*th tissue; $K_{tissue,plasma}$ is the tissue-to-plasma partition coefficient; E_i is the extraction ratio and, for non-eliminating tissues, as it is generally the case of the skin (Ye, Nagar and Korzekwa, 2016), E_i equals zero.

Here, we test the hypothesis that valuable information about drug disposition, and specifically its clearance, in the skin can be derived from available systemic pharmacokinetic data for drugs administered via transdermal delivery systems.

Figure 1 is a simplistic schematic of the drug absorption process across the skin following application of a topical formulation. When a transdermal patch is applied, the drug delivery rate to the skin has been determined (the 'input-rate') and the resulting systemic plasma concentration (C_p) *versus* time profile has been measured both during patch wear and after its removal. The decline in C_p post-patch removal is characterised by a terminal rate constant (k_e) that is much smaller than that associated with the drug's elimination half-life from the body when administered intravenously, for example, demonstrating clearly that 'flip-flop' kinetics are operative. In other words, in transdermal drug delivery, the skin absorption process is normally much slower than the elimination. Therefore, the disposition of a drug following transdermal application is usually rate-controlled by the skin absorption. Thus, in this work, we have assumed that the elimination rate constant from the skin ($k_{e,skin}$) should equal the systemic terminal rate constant k_e. In addition, we hypothesise that k_e is related to the drug's clearance from the skin (via the corresponding 'local' volume of distribution) and that this kinetic parameter will be a sensitive function of key physicochemical parameters of the drug.

To examine this idea, the transdermal delivery literature was searched and values of k_e were identified for the 18 drugs present in over 25 FDA-approved products (FDA Orange Book database of the end of 2017) for this route of administration. Importantly, the physicochemical properties of these transdermal drugs are quite broad: for example, molecular weights (MW) between 160 and 470 Daltons and log(octanol-water partition coefficient (P)) values from ~1.0 to 5.0 (Wiedersberg and Guy, 2014).

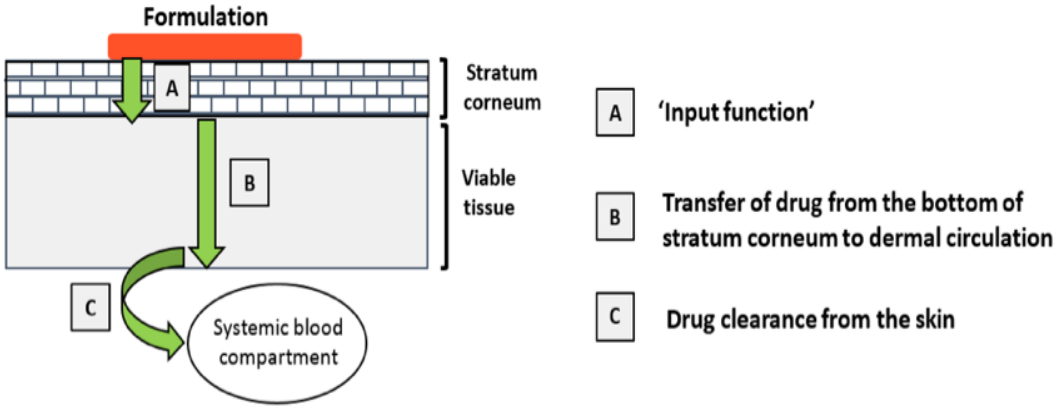

Figure 1. Schematic of the skin absorption process of a drug from a topically applied formulation.

2. Methods

The calculation of drug dermal clearance was conducted in 3 steps: (i) extraction of the terminal half-lives ($t_{1/2}$) and the corresponding k_e values from C_p *versus* time profiles; (ii) estimation of the skin volume of distribution ($V_{ss,skin}$) and, finally, (iii) estimation of the drug clearance from the skin (Cl_{skin}).

2.1. Extraction of the terminal half-lives ($t_{1/2}$) and the corresponding terminal rate constant (k_e)

A literature search on pharmacokinetic studies of the 18 transdermal drugs enabled extraction of the terminal half-lives ($t_{1/2}$) of the drugs. Information pertaining to lidocaine was also utilised[7].

When not directly provided, the values for $t_{1/2}$ were calculated from the corresponding terminal rate constant (k_e) by extracting the C_p *versus* time profiles using WebPlotDigitizer software (version 3.10; Ankit Rohatgi; Austin, TX, USA) and assuming that the terminal phase was governed by 1st-order processes ($t_{1/2} = \ln(2)/k_e$). If more than one reference was available, an arithmetic mean of the values was used.

For each drug, a search in PubMed was conducted using different combinations of the key words: 'cutaneous', 'skin', 'transdermal patch', 'pharmacokinetic' or 'clearance'. In addition, pharmacokinetic information was collected from drug approval packages on the Drug@FDA public repositories (FDA-Clinical Pharmacology and Biopharmaceutics Review(s)).

[7] Although lidocaine is not intended to produce systemic effect, there is plasma concentration versus time data available following delivery from a topical patch system.

The inclusion criteria for the data were: healthy adults (maximum age = 71 years old); C_p *versus* time profile with at least 3 time-points measured after patch removal and at least 5 replicates per time-point; sufficient information about the population (e.g., sampling number, mean age or health status). Two exceptions were permitted: (a) although almost all studies involving testosterone were conducted in patients with hypogonadism, these data were accepted into the analysis; and (b) likewise, for methylphenidate, as the data available were only from children (age: 6 – 12 years old), these results were included. Table 2 shows the mean value of k_e derived for each drug and used for further analysis.

2.2. Estimation of the skin volume of distribution ($V_{ss,skin}$)

The steady-state concentration (C_{ss}) likely to be achieved in the 'skin compartment' is estimated using the clearance from the skin (Cl_{skin}) and drug delivery rate to the skin (input-rate[8,9], R). In turn, Cl_{skin} can be estimated using the a relationship between k_e and the dermal volume of distribution of a drug ($V_{ss,skin}$).

$$C_{SS} = \frac{R}{Cl_{skin}} = \frac{R}{(k_e \times V_{SS,Skin})} \quad \text{(Equation 3)}$$

Equation 2 indicates that each/tissue organ contributes to the estimation of the systemic volume of distribution (V_{ss}). Given the lack of a generalised definition of $V_{ss,skin}$, the idea proposed here is that $V_{ss,skin}$ can be estimated, as an approximation, as follows:

$$V_{ss,skin} = V_{skin} \times K_{(skin/p)} \quad \text{(Equation 4)}$$

Where V_{skin} is the volume of the viable skin and $K_{(skin/p)}$ is the drug's partition coefficient between the skin and the plasma. It is relevant to point out that protein binding can occur within the viable skin and $K_{skin/p}$ is likely to be greater than one, therefore. Also, the transdermal drugs are either neutral compounds or weak bases, the degree of ionisation of the latter being an important parameter, perhaps, to consider.

[8] At steady-state, the rate at which the drug is delivered to the systemic circulation will be the same as input rate to the skin.
[9] For all transdermal products currently approved the input rate is known and shown on the product's label.

Yun and Edginton (2013) developed a correlation-based model to predict $K_{(skin/p)}$, which uses physicochemical descriptors (log P, degree of ionization (F_i) and plasma protein binding ($F_{u,p}$)) and organism-specific data (rat volume of distribution at steady-state). Table 1 shows the best correlations found by Yun and Edginton (2013) for predicting the log($K_{(skin/p)}$) for bases (pKa ≥ 7.4, model 1) and for acids and neutral compounds (pKa ≤ 7.4, model 2).

Table 1. Mathematical models for predicting log of skin-to-plasma partition coefficient ($K_{(skin/p)}$). Table adapted from Yun and Edginton (2013).

Model	Regression models	n	Adjusted R^2
1	$\log K_{(skin/p)} = -0.14 + 0.66(\log V_{ss}) + 0.03(\log P)$	28	0.80
2	$\log K_{(skin/p)} = -0.33 + 0.54(\log V_{ss}) + 0.16(\log P) - 0.32(F_i) + 0.38(F_{u,p})$	26	0.73

In summary, to estimate $V_{ss,skin}$ using Equation 4, two parameters are required: V_{skin} and $K_{(skin/p)}$. Here, V_{skin} was assumed to be 2.6 L (based on a standard body weight of 70 kg, Brown et al. (1997)) and $K_{(skin/p)}$was estimated using either Model 1 or 2 (Table 1). One modification to estimate $K_{(skin/p)}$ was made. Instead of using V_{ss} derived from rats, $K_{(skin/p),}$ values were estimated with V_{ss} from humans.

Values of volume of distribution at steady-state after intravenous administration in humans (V_{ss}, L/kg) and plasma protein binding ($F_{u,p}$) were from the literature. If more than one reference was available, an arithmetic mean was used. The calculated $K_{(skin/p)}$ values, the human V_{ss} and the relevant drug physicochemical properties are in Table 2. The sources of V_{ss} are in 'Supplementary Information' Table S1. Finally, the degree of ionization (Fi) at physiological pH 7.4 ($Fi_{pH=7.4}$) was calculated using Equation 5:

$$F_{i,pH=7.4} = 1 - \left(\frac{1}{1+10^{pKa-7.4}}\right) \quad \text{(Equation 5)}$$

2.3. Estimation of the drug clearance from the skin (Cl_{skin})

Finally, assuming that skin pharmacokinetics can be described using a one-compartmental model, Cl_{skin} (L h^{-1} kg^{-1}) was estimated using Equation 6.

$$Cl_{skin} = k_{e,skin} \times V_{ss,skin} \quad \text{(Equation 6)}$$

Figure 2 shows a schematic representation of the steps involved in the calculation of Cl_{skin}.

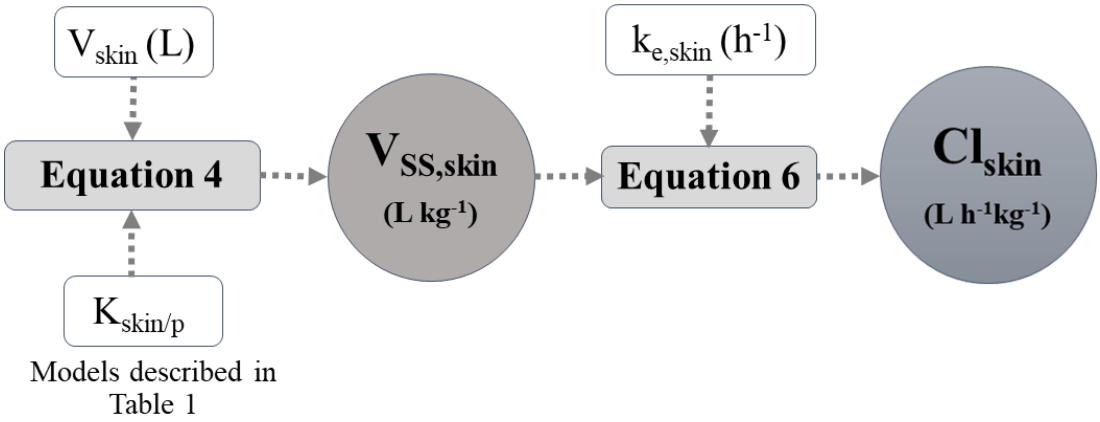

Figure 2. Schematic representation of the steps involved in the calculation of Cl_{skin}.

2.4. Collection of molecular descriptors

The physicochemical descriptors: log(n-octanol/water partition coefficient) (log P), molecular weight (MW) and melting point (MP) were from EPA's CompTox Chemistry Dashboard (https://comptox.epa.gov/dashboard). Experimental values were used when available. When several experimental values were available, the median value was used. In addition, log n-octanol/water partition coefficient at pH = 7.4 (log $D_{7.4}$), the number of rotatable bonds (RotB), the number of hydrogen-bond acceptors (HBA) and donors (HBD), and their sum (HBT), molecular volume (MV), topological polar surface area (TPSA) and pK_a were calculated (ACDLabs, Toronto, Canada, version 5.0). Table 3 collects the physical chemical properties of the 19 drugs.

2.5. Multiple Linear Regression (MLR) model development

MLR, using the ordinary least squares (OLS) method, was used to obtain an empirical relationship which best described the relationship between dermal clearance (log transformed, log Cl_{skin}) and the key physical chemical properties of the drugs.

Stepwise MLR was performed using The Unscrambler® X software (Version 10.5, Camo A/S, Oslo, Norway). In each regression analysis, a variable was either added or removed. The process was stopped when the fit yielded the higher adjusted and predicted coefficient of determination (R^2) and all the predictors were statistically significant (p-value ≤ 0.05). In addition, to detect if the predictor variables were linearly related (i.e., the multi-collinearity issue), the variance inflation factor (VIF) for each equation was screened. The VIF indicates the increase in the variance due to collinearity. A VIF value of 5 was used as the cut-off criterion (Montgomery, Peck and Vining, 2012).

Multiple linear regression attempts to model the relationship between two or more explanatory variables and a response variable by fitting a linear equation to observed data. Every value of an independent variable x is associated with a value of the dependent variable y. The population regression line for k explanatory variables x_1, x_2, ... , x_k is defined to be $\mu_y = \beta_1 + \beta_2 x_2 + \beta_3 x_3 + ... + \beta_k x_k$. This line describes how the mean response μ_y changes with the explanatory variables. The observed values for y vary about their means μ_y and are assumed to have the same standard deviation σ. The fitted values b_1, b_2, ..., b_k estimate the parameters β_1, β_2, …, β_k of the population regression line (Johnson and Wichern, 2002).

Since the observed values for y vary about their means μ_y, the multiple regression model includes a term for this variation. In other words, the model is expressed as DATA = FIT + RESIDUAL, where the "FIT" term represents the expression $\beta_1 + \beta_2 x_2 + \beta_3 x_3 + ... + \beta_k x_k$. The "RESIDUAL" term represents the deviations of the observed values y from their means μ_y, which are normally distributed with mean 0 and variance σ. The notation for the model deviations is ε.

Formally, the model for multiple linear regression, given n observations, is:

$$y_i = \beta_1 + \beta_2 x_{2i} + \beta_3 x_{3i} + ... + \beta_k x_{ki} + \varepsilon_i \text{ for } i = 1,2, ... n.$$

The first explanatory variable x_1 is defined by $x_{1i} = 1$ for every $i = 1, \dots, n$, and for simplicity it can be written as b_1 instead of $b_1 x_{1i}$. For purposes of analysis it is convenient to express the model in matrix form:

$$\mathbf{y} = \begin{pmatrix} y_1 \\ \vdots \\ y_n \end{pmatrix}, \mathbf{X} = \begin{pmatrix} 1 & \cdots & x_{k1} \\ \vdots & \ddots & \vdots \\ 1 & \cdots & x_{kn} \end{pmatrix}, \boldsymbol{\beta} = \begin{pmatrix} \beta_1 \\ \vdots \\ \beta_k \end{pmatrix}, \boldsymbol{\varepsilon} = \begin{pmatrix} \varepsilon_1 \\ \vdots \\ \varepsilon_n \end{pmatrix}.$$

Note that in the n × k matrix X = (x_{ji}) the first index j (j = 1, … , k) refers to the variable number (in columns) and the second index i (i = 1, … , n) refers to the observation number (in rows). The above matrix notation can also be written as:

$$\mathbf{y} = \mathbf{X\beta} + \varepsilon$$

where $\boldsymbol{\beta}$ is a k ×1 vector of unknown parameters and ε is an n ×1 vector of unobserved values.

In the least-squares model, the best-fitting line for the observed data is calculated by minimising the sum of the squares of the vertical deviations from each data point to the line (if a point lies on the fitted line exactly, then its vertical deviation is 0). Because the deviations are first squared, then summed, there are no cancellations between positive and negative values. The fitted values b_1, b_2, ..., b_k which estimate the parameters β_1, β_2, …, β_k are obtained by solving the following equation:

$$\mathbf{b} = (\mathbf{X}'\mathbf{X})^{-1}\mathbf{X}'\mathbf{y}$$

Subsequently, internal validations were performed to estimate the predictive value of the final model, defined by the determination coefficient of leave-25%-out ($Q^2_{25\%}$) and of leave-one-out cross-validation (Q^2_{LOO}) procedures (Baumann, 2003).

In leave-25%-out cross validation, the data set consisting of 19 compounds and selected descriptors were randomly divided into training (n = 14) and test sets (n = 5). Using the parameters in the linear regression model, test set was moved aside and new coefficients of determination (R^2) and prediction ($Q^2_{25\%}$) were obtained by regression on the remaining 14 observations.

Calculation of Q^2_{LOO} (leave-one-out cross-validation) involved omission of one observation and estimation of a regression model using the remaining data points. The equation obtained is then used to predict the response variable for the omitted data point. The correlation between the predicted and observed values in the newly generated data set is used to judge the fit. Q^2 can be used to validate the model without selecting another sample or splitting the data.

Table 2. Values of input-rate, k_e, V_{ss}, $F_{i,pH=7.4}$, $F_{u,p}$ as well as the predicted values for $K_{(skin/p)}$ and $V_{ss,skin}$.

Drug	Trade name	Input-rate[e] (µg cm^{-2} h^{-1})	k_e [f] (h^{-1})	V_{SS} [g] (L/kg)	$F_{i,pH=7.4}$ [h]	$F_{u,p}$ [f]	$K_{(skin/p)}$ [i]	$V_{SS,skin}$ [j] (L/kg)
Buprenorphine	Butrans®	0.8	0.02	6.7	0.87	0.04	3.7	9.6
Clonidine	Catapress-TTS®	1.2	0.04	2.9	0.81	0.80	1.6	4.3
Estradiol[a]	Estraderm®	0.2	0.21	1.0	0	0.02	2.0	5.3
	Climara®	0.2						
	Vivelle®	0.1						
	Alora®	0.1						
	Vivelle-dot®	0.4						
	Menostar®	0.2						
	Minivelle®	0.6						
Estradiol (E) & Norethisterone Acetate[b] (NAc)	Combipatch®	E/NAc: 0.2/0.4	E/NAc: 0.04/0.05	E/NAc: 1.0/ 4.0	0	E/NAc: 0.02/0.03	E/NAc: 2.0/4.0	E/NAc: 5.3/10.3
Estradiol (E) & Levonorgestrel (L)	Climara Pro®	E/L: 0.09/0.03	E/L: 0.21/0.02	E/L: 1.0/1.8	0	E/L: 0.02/0.06	E/L: 2.0/2.3	E/L: 5.3/5.9
Ethinyl estradiol (EE) & Norelgestromin[c] (N)	Xulane®	EE/N: 0.1/0.4	EE/N: 0.04/0.02	EE/N: 5.0/3.0	0	EE/N: 0.05/0.03	EE/N: 4.4/4.2	EE/N: 11.6/11.0
Fentanyl	Duragesic®	2.3	0.03	6.0	0.97	0.16	3.2	8.3
Glyceryl Trinitrate[d]	Nitro-Dur®	20	1.15	3.3	0	0.40	2.3	6.0
	Minitran®	11.1						
Granisetron	Sancuso®	2.5	0.02	3.0	1.00	0.35	1.7	4.5
Lidocaine	Lidoderrn®	NA	0.116	1.5	0.78	0.38	1.1	3.0
Methylphenidate	Daytrana®	~ 87	0.20	2.6	0.99	0.85	1.6	4.2
Nicotine	Nicoderm CQ®	29.2	0.20	2.5	0.75	0.95	1.4	3.7
	Habitrol®							
Oxybutynin	Oxytron®	4.2	0.06	2.8	0.86	0.09	1.9	4.9
Rivastigmine	Exelon®	~ 38	0.24	2.2	0.94	0.60	1.5	3.8
Rotigotine	Neupro®	8.3	0.12	53.8	0.96	0.10	14.5	37.7
Scopolamine	Transderm Scop®	5.5	0.07	1.0	0.80	0.90	0.8	2.0
Selegiline	Emsam®	12.5	0.03	26.5	0.57	0.06	7.9	20.4
Testosterone	Androderm®	13.9	0.31	1.0	0	0.01	1.6	4.2

[a] Also spelled as Oestradiol; [b] Also spelled as Norethindrone acetate; [c] Also spelled as Norelgestromine; [d] Also known as Nitroglycerine; [e] Value described on the product label; [f] Extracted from the literature; [g] Data from IV clinical studies; [h] Calculated using Equation 5; [i] Calculated using models described in Table 1; [j] Calculated using Equation 4; NA: not available.

Table 3. Physicochemical properties of the 19 drugs considered.

Drug	Molecular descriptors									
	MW (Da)	**MV ($cm^3\ mol^{-1}$)**	**log P**	**log $D_{7.4}$**	**MP (° C)**	**TPSA ($Å^2$)**	**HBA**	**HBD**	**HBT**	**RotB**
Buprenorphine	467.6	368.2	4.98	3.85	219	62.2	2	5	7	5
Clonidine	230.1	153.1	1.59	1.33	130	36.4	2	3	5	1
Estradiol	272.4	232.6	4.01	3.36	179	40.5	2	2	4	0
Ethinyl estradiol	296.4	244.4	3.67	3.54	163	40.5	2	2	4	1
Fentanyl	336.5	309.3	4.05	3.44	86	23.5	0	3	3	6
Glyceryl Trinitrate	227.1	135.8	1.62	2.00	13.4	174.2	0	12	12	8
Granisetron	312.4	234.8	2.12	1.04	156	50.2	1	5	6	2
Levonorgestrel	312.4	274.3	3.33	3.15	228	37.3	1	2	3	2
Lidocaine	234.3	228.3	2.44	1.66	68.7	32.3	1	3	4	5
Methylphenidate	233.3	218	2.33	0.70	225	38.3	1	3	4	4
Nicotine	162.2	157.1	1.17	0.13	-79	16.1	0	2	2	1
Norelgestromin	327.5	265	4.34	4.07	226	52.8	2	3	5	2
Norethisterone Acetate	340.5	296.1	3.72	3.55	171	43.4	0	3	3	3
Oxybutynin	357.5	325.7	3.96	3.83	130	49.8	1	4	5	10
Rivastigmine	250.3	241.1	2.24	2.30	66.9	32.8	0	4	4	5
Rotigotine	315.5	272	4.79	3.28	136	51.7	3	1	4	6
Scopolamine	303.1	230.9	0.98	0.51	59	71.5	1	5	6	5
Selegiline	187.3	196.1	2.90	2.75	142	3.2	0	1	1	5
Testosterone	288.4	256.9	3.32	3.02	138	37.3	1	2	3	0

3. Results and discussion

To examine the hypothesis that k_e is related to drug's clearance from the skin and that clearance will be a sensitive function of key physicochemical parameters of the drug, the first step of this study was to collect the elimination half-life of the 18 drugs present in marketed transdermal products. In fact, in the end, a total of 19 drugs were analysed as sufficient information was available for a locally-acting lidocaine product as well.

Over 70 studies were assessed and provided, in the end, a final set of 160 half-live values. However, in some cases (e.g., for scopolamine and norethisterone acetate), only a single half-life was found while, for other drugs (such as nicotine and ethinyl estradiol) 20 individual half-life values were discovered. The distribution of the half-lives collected for each drug are presented as a box and whisker plot in Figure 3. From the mean values, k_e (= ln $2/t_{1/2}$) for each drug was then calculated (see 'Supplementary Information', Table S2).

The second step was to estimate drug's volume of distribution in the skin ($V_{ss,skin}$). To do so, it was necessary first to calculate the drug's skin-to-plasma partition coefficient ($K_{(skin/p)}$) using the models in Table 1. Values of $K_{(skin/p)}$ ranged from 1.4 for nicotine to 14.5 for rotigotine. The relatively high lipophilicity (log P = 4.7) and systemic volume of distribution (V_{ss} = 53.8 L/kg) of rotigotine already suggest that this drug is likely to accumulate in the tissues and its relatively high $K_{(skin/p)}$ is not unexpected. On the other hand, the fact that nicotine has a balanced lipophilicity (log P ~ 1.2) and relatively low systemic volume of distribution (V_{ss} = 2.5 L/kg) is undoubtedly the major reason behind its much smaller $K_{(skin/p)}$. With the calculated $K_{(skin/p)}$ for each drug and the volume of the skin, it was then possible to calculate $V_{ss,skin}$ via Equation 4; the results are in Table 2.

Subsequently, drug clearance from the skin (Cl_{skin} in L/kg) was assessed using Equation 6. The calculated values of log Cl_{skin} are in Table 4 and range from 0.84 for glyceryl trinitrate to -1.01 for granisetron.

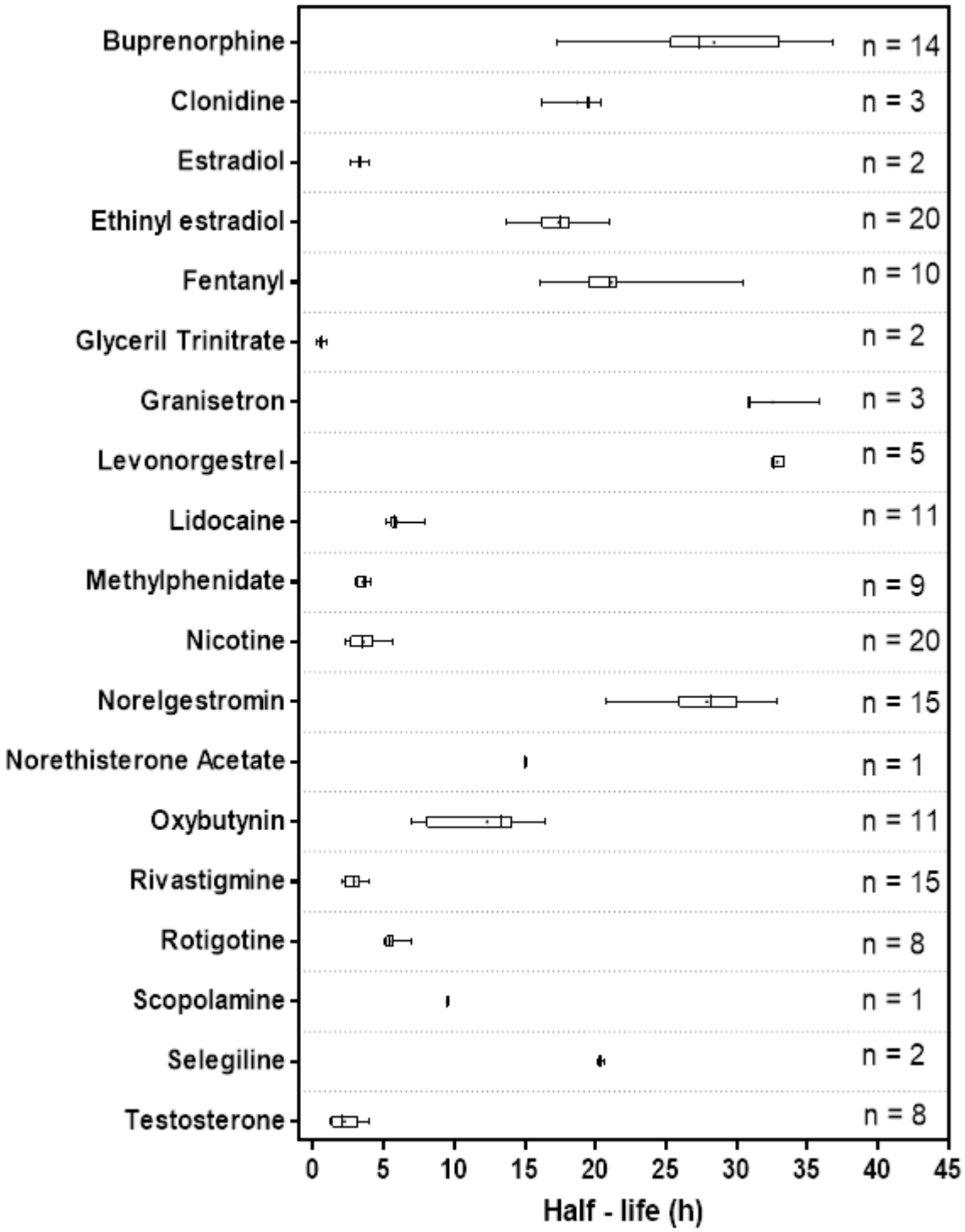

Figure 3. Box and whisker plot of the systemic half-life values reported for each drug following patch removal. The boxes represent the median (line), mean (dot), 25th and 75th percentiles. The bars extend to the minimum and maximum value gathered. The number (n) of half-lives collected for each drug are described on the right hand side of the graph.

The third step was to derive an empirical model, using multiple linear regression (MLR), to predict dermal drug clearance. MLR is a statistical technique that can use a number of molecular descriptors to identify predictive, albeit empirical, relationships in data sets. The advantage of MLR is its simplicity and the easily interpretable mathematical results. The sign of the coefficient derived for each molecular descriptor indicates whether it contributes positively or negatively to the predicted parameter and its magnitude is a measure of the relative importance. However, MLR works best when (i) the structure-activity relationship is linear, (ii) the set of molecular descriptors are independent (i.e., descriptors do not show collinearity), and (iii) the number of compounds in the training set exceeds the number of molecular descriptors by at least a factor of five (Yap et al., 2007).

At the outset, MLR was performed using ten molecular descriptors (MW, log P, MP, $\log D_{7.4}$, RotB, HBA, HBD, HBT, MV and TPSA) as potential predictors of drug clearance from skin; the values used are in Table 3. In the end, a model based only on MW, log P and TPSA explained best the calculated dermal clearance of 19 drugs (Equation 7):

$$\log CL_{skin}(L\,h^{-1}\,Kg^{-1}) = 0.28 - 0.008(MW) + 0.38(\log P) + 0.010(TPSA)$$

(Equation 7)

The intercept of this model was, however, statistically non-significant (p = 0.38), was therefore removed to yield the final solution (Equation 8, Table 4 and Figures 4 and 5):

$$\log CL_{skin}(L\,h^{-1}\,Kg^{-1}) = -0.007(MW) + 0.37(\log P) + 0.010(TPSA)$$

(Equation 8)

with an adjusted $R^2 = 0.72$; $Q^2_{LOO} = 0.70$ and $p < 0.05$ for all three variables; adjusted R^2 is the square of the determination coefficient adjusted for degrees of freedom; Q^2_{LOO} is the cross-validated (leave-one-out) square of the determination coefficient and p-value is related to the significance of the parameters. The statistics of the three descriptors are summarized in Table 5.

The general principle of cross-validation is to split a data set into a training and a test set. The training set is used to fit the model and the test set is used to evaluate the fitted model's predictive adequacy. Leave-one-out (LOO) cross validation repeatedly partitions the data set into a training set which consists of all data points except one and then evaluates the predictive density for the held-out data point where

predictions are generated based on the leave-one-out posterior distribution. The LOO estimator is nearly unbiased.

On the other hand, the leave-25%-out cross validation, which is normally employed when data set is large, due to the necessity of choose a subset of data to test the model, the validation estimate can be highly variable, which depends on which observations are in the training and test. To illustrate this, the cross validation was repeated 10 times and the results are shown in Table 6.

As can be seen in Table 6, for 10 regressions using the same data set (but different subsets), different results can be achieved. For example, if comparing the regression 2 with 5, the difference is overwhelming discrepant. Therefore, for small data set, which the case of this study, the LOO is reasonable method of validation.

Moreover, the predictors did not display multi-collinearity, with all VIF values being less than 5. It has been found that, when collinear descriptors are used, the derived coefficients tend to be larger than the real values and sometimes have opposite signs (Yap et al., 2007). Therefore, the assumption of a linear relationship between a set of molecular descriptors and a specific activity may not always be appropriate, especially in cases involving multiple mechanisms.

Table 4. List of the $logCl_{skin}$ calculated from the experimental data analysed and the predicted $logCl_{skin}$ from the multiple linear regression (Equation 8).

ID	Drug	log Cl_{skin} ($L\ h^{-1}\ Kg^{-1}$)	
		Calculated	Predicted
1	Buprenorphine	-0.63	-0.64
2	Clonidine	-0.80	-0.58
3	Estradiol	0.05	0.08
4	Ethinyl estradiol	-0.34	-0.21
5	Fentanyl	-0.56	-0.50
6	Glyceryl Trinitrate	0.84	0.85
7	Granisetron	-1.01	-0.79
8	Levonorgestrel	-0.90	-0.47
9	Lidocaine	-0.47	-0.33
10	Methylphenidate	-0.08	-0.30
11	Nicotine	-0.14	-0.48
12	Norelgestromin	-0.57	-0.04
13	Norethisterone Acetate	-0.32	-0.45
14	Oxybutynin	-0.56	-0.41
15	Rivastigmine	-0.04	-0.51
16	Rotigotine	0.67	0.19
17	Scopolamine	-0.83	-0.93
18	Selegiline	-0.16	-0.14
19	Testosterone	0.12	-0.32

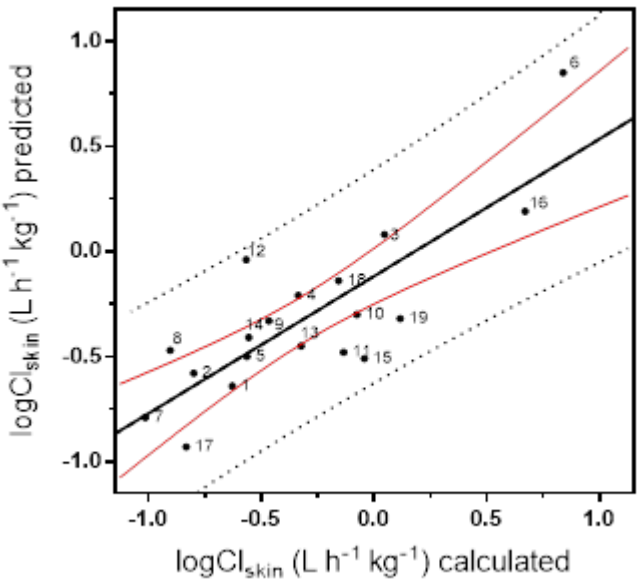

Figure 4. Graphical depiction of the relationship between log Cl_{skin} calculated from experimental data and log Cl_{skin} predicted by the MLR-derived Equation 8. The dashed lines represent 95% prediction limits for a prospective compound and the solid red lines represent 95% confidence limits of the line of best fit. The number against each point corresponds to that assigned to each of the 19 drugs in Table 4.

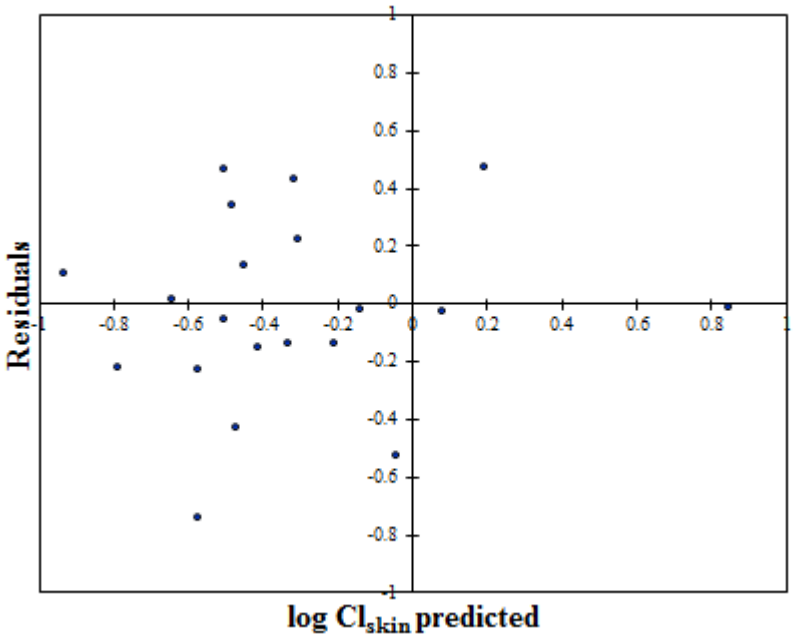

Figure 5. Graphical representation of the residual of the log Cl_{skin} model.

Table 5. Summary of the statistics of the three descriptors of the MLR model developed for predicting Cl_{skin}.

Descriptor	Variance inflation value (VIF)	Derived coefficients ± standard error	p-value
MW	2.2	-0.007 ± 0.001	0.0000
log P	2.2	0.370 ± 0.087	0.0006
TPSA	1.1	0.010 ± 0.002	0.0003

Table 6. List of the coefficient of determination (R^2) and determination coefficient of leave-25%-out ($Q^2$25%) for 10 regressions using the same data set.

Regression ID	Drugs omitted (see Table 4)	R^2	$Q^2_{25\%}$
1	4, 5, 6, 7 and 11	0.60	0.47
2	2, 5, 10, 15 and 19	0.78	0.72
3	3, 5, 9, 15 and 16	0.77	0.46
4	6, 8, 9, 10 and 13	0.65	0.54
5	6, 8, 16, 17 and 18	0.68	0.35
6	1, 3, 9, 15 and 16	0.77	0.57
7	2, 6, 8, 14 and 16	0.69	0.62
8	2, 5, 8, 14 and 19	0.70	0.63
8	1, 2, 4, 12 and 15	0.77	0.50
10	2, 5, 7, 8 and 12	0.70	0.65

In general, drug permeability across biomembranes, such as the skin and the capillary wall, is widely known to increase with permeant lipophilicity and decrease with molecular size (Potts and Guy, 1992; Lien and Gaot, 1995; Kokate et al., 2009; Bujak et al., 2015). It is, therefore, not surprising that both log P and MW are important in governing drug elimination across the skin-blood barrier as well. In addition to these descriptors, TPSA was also found to be important in predicting drug clearance from the skin. Previous studies have demonstrated that TPSA is a predictor inversely correlated with the passage of molecules through the brain-blood barrier (Clark, 1999; Kelder et al., 1999) and the intestinal membrane (Palm et al., 1997; Winiwarter et al., 1998; Stenberg et al., 1999). Thus, the positive correlation found in this study was, in principle, unexpected.

The TPSA is the surface area associated with polarity, hydrogen-bonding potential and water solubility of organic molecules (Ertl, 2008; Ali et al., 2012). A study by Potts and Guy (1995) shows that an increase in the hydrogen bonding activity (both acceptor and donor) results in a decrease in the partitioning into the organic phase due to the free energy cost associated with the disruption of the hydrogen bonds in the aqueous phase. On the other hand, a compensating effect of TPSA may occur if a molecule associates with polar head groups via specific polar interactions (El Maghraby; Kwon, Liljestrand and Katz, 2006). However, further mechanistic evaluations are needed to elucidate the influence of this molecular feature on the elimination of drugs from the skin.

Although validation R^2 obtained from the regression can serve as an indicator of the predictive ability of a model, the following was done as an example of how an empirical model combined with results typically available for topical applied drug, such as *in vitro* permeation tests, could be used to predict drug clearance from the skin. The experimental results described in Chapter 2 of this thesis were used for this purpose. In brief, the *in vitro* permeation experiments were performed using static Franz cells (using freshly excised porcine skin) aiming to investigate the rate at which drug is cleared from the skin (i.e., from the stratum corneum and epidermis and dermis) towards the receptor solution. Firstly, the mass of three drugs (buprenorphine, nicotine and diclofenac, BUP, NIC and DF, respectively) in the stratum corneum *plus* epidermis and dermis was measured after an ‘uptake’ (application) time. Secondly, the patches were applied for a period of time (uptake time) and, subsequently, they

were removed and the skin left (mounted on the diffusion cell) for a further period of time ('clearance time') (Table 7).

Table 7. Summary of the *in vitro* permeation experiments described in the Chapter 2 of this thesis.

Drug	Drug delivery system	'Uptake' time (h)	'Clearance' time (h)
Buprenorphine	Transtec® 35 µg/h	72	24
Nicotine	Nicotinell® 7 mg/24 hours	2	1.5 and 3.0
Diclofenac	Voltaren® 180 mg	6	5, 17 and 24

From the analysis of the mass of the drugs in the skin immediately after patch removal (uptake, A_{Up}) and after a delay time between the removal of the patch and the end of the experiment (clearance, A_{Cl}), it was possible to calculate the elimination rate constant from the skin ($k_{e,skin}$). Assuming that the drugs are cleared from the skin following a 1st-order kinetics, $k_{e,skin}$ was estimated from the slope of the natural-log transformed mass-time data of each drug using least square regression analysis (Figure 6). The systemic steady-state volume of distribution (V_{ss}) was collected from the literature, the skin-to-plasma partition coefficient ($K_{(skin/p)}$) was estimated using model 1 (Table 1), the dermal steady-state volume of distribution ($V_{ss,skin}$) was calculated using Equation 4 and the experimental dermal clearance ($Cl_{skin,exp}$) was calculated using Equation 6. Table 7 summarises the calculated clearance from the skin of BUP, NIC and DF based on experimentally measured $k_{e,skin}$ ($Cl_{skin,exp}$) or predicted ($Cl_{skin,pred}$) using Equation 8 and the parameters used for the calculations.

Although the experimental clearance values were calculated from *in vitro* experiments and, therefore, an effect of the dermal microcirculation (which may greatly affect the clearance of a compound from the 'viable' skin) is not presented, a comparison of the $Cl_{skin,exp}$ and $Cl_{skin,pred}$ may provide insights into the value of the predictive model. In fact, a good agreement between $Cl_{skin,exp}$ and $Cl_{skin,pred}$ was observed. As can be seen in Table 8, $Cl_{skin,exp}$ for BUP and DF agrees remarkably well with $Cl_{skin,pred}$; for nicotine, the experimental value was ~5-fold higher than that predicted using Equation 7. Given the assumptions and variability involved in the approach, as well as the differences between an *in vitro* penetration test with porcine skin and a clinical study in humans, this still indicates a good convergence of experiment and prediction. Nevertheless, the results of the experimental work,

although based on a relatively small number of drugs, further supported the statistical accuracy of the model.

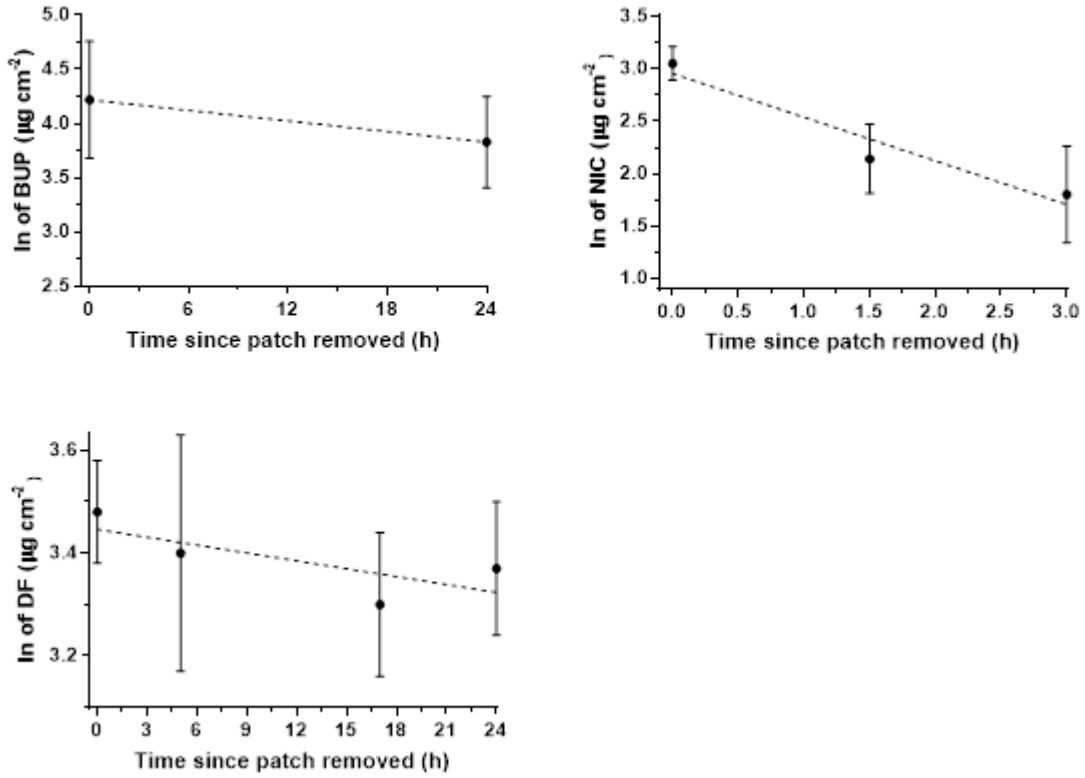

Figure 6. Natural logarithm of the amount of drug in the epidermis/dermis plotted against the time of clearance. Mean values are presented as the average ± standard deviation (n = 6). The slope of the linear regression of ln(drug mass in epidermis/dermis) with time gives the elimination rate constant from the skin ($k_{e,skin}$).

Table 8. Calculated clearance from the skin of the compounds studied based on experimentally measured $k_{e,skin}$ ($Cl_{skin,exp}$) or predicted ($Cl_{skin,pred}$) using Equation 11.

	Buprenorphine	**Nicotine**	**Diclofenac** [i]
A_{Up} (µg cm^{-2}) [a]	76.8 ± 39.4	21.3 ± 3.7	32.6 ± 3.0
A_{Cl} (µg cm^{-2}) [b]	49.3 ± 20.2	6.6 ± 3.0	29.4 ± 3.5
$k_{e,skin}$ (h^{-1}) [c]	0.016	0.42	0.005
V_{ss} (L kg^{-1})	6.7 [d]	2.5 [d]	0.9 [j,k]
$K_{(skin/p)}$ [e]	3.7	1.4	0.9
$V_{ss,skin}$ (L kg^{-1}) [f]	9.6	3.7	2.5
$Cl_{skin,exp}$ (L h^{-1} kg^{-1})[g]	0.15	1.55	0.12
$Cl_{skin,pred}$ (L h^{-1} kg^{-1})[h]	0.23	0.33	0.19

[a]Average drug amounts recovered from the stratum corneum *plus* epidermis/dermis after uptake;
[b]Average drug amounts recovered from the stratum corneum *plus* epidermis/dermis after clearance(s);
[c]$k_{e,skin}$ is the first-order rate constant describing clearance from the 'skin compartment' and calculated by the slope of the linear regression of ln(drug mass in stratum corneum *plus* epidermis/dermis) with time;
[d]Data from IV clinical studies;
[e]Skin-to-plasma partition coefficient;
[f]Calculated using Equation 4;
[g]Clearance from skin, calculated using Equation 6 and using $k_{e,skin}$ obtained using experimental data;
[h]Clearance from skin, predicted using Equation 8 (values are the inverse of the logCl_{skin});
[i]Physicochemical properties of diclofenac: MW = 411.32 Da (diclofenac epolamine), log P = 4.16 (diclofenac acid), TPSA = 49.33 Å^2;
[j]Measured after oral administration of diclofenac epolamine;
[k]Giachetti et al. (1996).

4. Conclusion

The current study describes the development of an empirical model to describe drug clearance from the skin in terms of MW, log P and TPSA. In general, these parameters are readily available (either measured or predicted) and mechanistically interpretable in terms of size, molecular hydrophobicity and polarity that may influence the passive diffusion of chemicals across skin and, ultimately, its absorption into the systemic circulation.

The model has a reasonably good predictive ability with predicted and calculated dermal clearances of compounds in a test set showing good agreement. It has been further demonstrated that the empirical model closely predicts the results obtained in *in vitro* skin experiments. Nevertheless, given that the model is currently based on a dataset comprising a limited number of drugs, further work is required to verify and extend the approach.

Supplementary Data

Table S1. Values of the volume of distribution (V_{ss}) obtained from intravenous clinical studies. The information was collected from drug approval packages on the FDA website (FDA-Clinical Pharmacology and Biopharmaceutics Review(s)). When the information was not available on the FDA website, the source where V_{ss} was obtained is specified.

Drug	V_{ss} (L/kg)	Reference
Buprenorphine	6.7	Butrans®
Clonidine	2.9	Catapress-TTS®
Estradiol	1.0	Progynova® TS 100[a]
Ethinyl estradiol	5.0	Eribelle®
Fentanyl	6.0	Duragesic®
Glyceryl Trinitrate	3.3	Nitrostat®
Granisetron	3.0	Allen et al. (1995)
Levonorgestrel	1.8	Violite®
Lidocaine	1.5	Lidoderm®
Methylphenidate	2.6	Ritalin®
Nicotine	2.5	Nicorette Invisi® 10 mg
Norelgestromin	3.0	Ortho Evra®
Norethisterone Acetate	4.0	FemHRT®
Oxybutynin	2.8	Oxytrol®
Rivastigmine	2.2	Exilon®
Rotigotine	53.8	Cawello et al. (2014)
Scopolamine	1.0	Nachum, Shupak and Gordon (2006)
Selegiline	26.5	Mahmood (1997)
Testosterone	1.0	Lombardo et al. (2004)

[a] Information collected from the Summary of Product Characteristics (SPC) approved by the MHRA (Medicines Healthcare products Regulatory Agency, United Kingdom).

Table S2. Values of systemic half-life and K_e calculated after removal of the patch, and $V_{ss,skin}$ used for the development of the model.

Drug	Half-life (h) (Mean ± SD)[a]	k_e (h^{-1})	Reference
Buprenorphine	28.4 ± 5.2	0.024	(Evans and Easthope, 2003; Kress, 2009; Kapil et al., 2013; Wang et al., 2016); [b]Butrans®
Clonidine	18.7 ± 2.2	0.037	(MacGregor et al., 1985)
Estradiol	3.3 ± 1.0	0.209	(Boyd et al., 1996; Ginsburg et al., 1998; Shulman, 2004)
Ethinyl estradiol	17.4 ± 1.8	0.040	(Abrams et al., 2001a; Abrams et al., 2001c; Abrams et al., 2002a; Abrams et al., 2002b; van den Heuvel et al., 2005; Devineni et al., 2007; Stanczyk et al., 2013); [b]Ortho Evra®
Fentanyl	21.1 ± 3.9	0.033	(Holley and Van Steennis, 1988; Gourlay et al., 1989; Varvel et al., 1989; Portenoy et al., 1993; Thompson et al., 1998; Marier et al., 2007; Kress et al., 2010)
Glyceryl Trinitrate	0.6 ± 0.6	1.155	(Sun et al., 1995); [b]Nitro-DUR®
Granisetron	32.6 ± 2.9	0.021	(Howell et al., 2009)
Levonorgestrel	32.9 ± 0.5	0.021	(Stanczyk et al., 2011; Archer et al., 2012; Stanczyk et al., 2013); [b]ClimaraPro®
Lidocaine	6.0 ± 0.8	0.116	(Campbell et al., 2002; Gammaitoni, Alvarez and Galer, 2002; Kondamudi et al., 2016); [b]Lidoderm®
Methylphenidate	3.5 ± 0.4	0.198	(Anderson and Scott, 2006; Pierce et al., 2008; Patrick et al., 2009)
Nicotine	3.5 ± 1.0	0.196	(Bannon et al., 1989; Chan et al., 1990; Mulligan et al., 1990; Benowitz et al., 1991; Kochak et al., 1992; Lin, Ho and Chien, 1993; Gore and Chien, 1998; DeVeaugh-Geiss et al., 2010; Rasmussen, Horkan and Kotler, 2018)
Norelgestromin	27.9 ± 3.0	0.025	(Abrams et al., 2001a; Abrams et al., 2001b; Abrams et al., 2001c; Abrams et al., 2002a; Abrams et al., 2002b; Devineni et al., 2007); [b]Ortho Evra®
Norethisterone Acetate	15.0	0.046	[b]Evorel Conti®
Oxybutynin	12.3 ± 3.2	0.056	(Staskin, 2003; Zobrist et al., 2003; Starkman and Dmochowski, 2006; Mizushima et al., 2007); [b]Oxytrol®
Rivastigmine	2.9 ± 0.6	0.239	(Lefèvre et al., 2007; Lefèvre et al., 2008a; Lefèvre et al., 2008b; Lefèvre et al., 2009)
Rotigotine	5.6 ± 0.6	0.124	(Braun et al., 2009; Cawello, Braun and Boekens, 2009; Cawello et al., 2012; Cawello et al., 2014; Cawello et al., 2016)
Scopolamine	9.5	0.073	[b]Transderm Scop®
Selegiline	20.4 ± 0.4	0.034	(Rohatagi et al., 1997; Azzaro et al., 2007)
Testosterone	2.2 ± 1.0	0.313	(Findlay, Place and Snyder, 1987; Meikle et al., 1992; Meikle et al., 1996; Singh et al., 2001; Raynaud et al., 2008); [b]Androderm®

[a] Arithmetic mean ± standard deviation; [b] The information was collected from drug approval packages on the FDA website (FDA-Clinical Pharmacology and Biopharmaceutics Review(s)).

References

Abrams, L.S., Skee, D., Natarajan, J. and Wong, F.A., 2002a. Pharmacokinetic overview of Ortho Evra™/Evra™. *Fertility and Sterility*, 77, pp. 3-12.

Abrams, L.S., Skee, D.M., Natarajan, J., Wong, F.A. and Anderson, G.D., 2002b. Pharmacokinetics of a contraceptive patch (Evra™/Ortho Evra™) containing norelgestromin and ethinyloestradiol at four application sites. *British Journal of Clinical Pharmacology*, 53(2), pp. 141-146.

Abrams, L.S., Skee, D.M., Natarajan, J., Wong, F.A. and Lasseter, K.C., 2001a. Multiple-dose pharmacokinetics of a contraceptive patch in healthy women participants☆. *Contraception*, 64(5), pp. 287-294.

Abrams, L.S., Skee, M., Donna, M., Natarajan, J., Wong, F.A., Leese, P.T., Creasy, G.W. and Shangold, M.M., 2001b. Pharmacokinetics of norelgestromin and ethinyl estradiol delivered by a contraceptive patch (Ortho Evra™/Evra™) under conditions of heat, humidity, and exercise. *The Journal of Clinical Pharmacology*, 41(12), pp. 1301-1309.

Abrams, L.S., Skee, M.D.M., Wong, F.A., Anderson, M.N.J. and Leese, P.T., 2001c. Pharmacokinetics of norelgestromin and ethinyl estradiol from two consecutive contraceptive patches. *The Journal of Clinical Pharmacology*, 41(11), pp. 1232-1237.

Ali, J., Camilleri, P., Brown, M.B., Hutt, A.J. and Kirton, S.B., 2012. Revisiting the general solubility equation: in silico prediction of aqueous solubility incorporating the effect of topographical polar surface area. *Journal of Chemical Information and Modeling*, 52(2), pp. 420-428.

Allen, A., Davie, C., Pierce, D., Davy, M., Upward, J., Crome, P., Wijayawardhana, P. and Jones, R., 1995. The pharmacokinetics of granisetron, a 5-HT 3 antagonist in healthy young and elderly volunteers. *European Journal of Clinical Pharmacology*, 48(6), pp. 519-520.

Anderson, V.R. and Scott, L.J., 2006. Methylphenidate transdermal system. *Drugs*, 66(8), pp. 1117-1126.

Archer, D.F., Stanczyk, F.Z., Rubin, A. and Foegh, M., 2012. Ethinyl estradiol and levonorgestrel pharmacokinetics with a low-dose transdermal contraceptive delivery system, AG200-15: a randomized controlled trial. *Contraception*, 85(6), pp. 595-601.

Azzaro, A.J., Ziemniak, J., Kemper, E., Campbell, B.J. and VanDenBerg, C., 2007. Pharmacokinetics and absolute bioavailability of selegiline following treatment of healthy subjects with the selegiline transdermal system (6 mg/24 h): a comparison with oral selegiline capsules. *The Journal of Clinical Pharmacology*, 47(10), pp. 1256-1267.

Bannon, Y., Corish, J., Corrigan, O., Devane, J., Kavanagh, M. and Mulligan, S., 1989. Transdermal delivery of nicotine in normal human volunteers: a single dose and multiple dose study. *European Journal of Clinical Pharmacology*, 37(3), pp. 285-290.

Baumann, K., 2003. Cross-validation as the objective function for variable-selection techniques. *TrAC Trends in Analytical Chemistry*, 22(6), pp.395-406.

Benowitz, N.L., Chan, K., Denaro, C.P. and Jacob, P., 1991. Stable isotope method for studying transdermal drug absorption: the nicotine patch. *Clinical Pharmacology & Therapeutics*, 50(3), pp. 286-293.

Bouzom, F., Ball, K., Perdaems, N. and Walther, B., 2012. Physiologically based pharmacokinetic (PBPK) modelling tools: how to fit with our needs? *Biopharmaceutics & Drug Disposition*, 33(2), pp. 55-71.

Boyd, R.A., Yang, B.B., Abel, R.B., Eldon, M.A., Sedman, A.J. and Forgue, S.T., 1996. Pharmacokinetics of a 7-Day 17β-Estradiol Transdermal Delivery System: Effect of Application Site and Repeated Applications on Serum Concentrations of Estradiol and Estrone. *The Journal of Clinical Pharmacology*, 36(11), pp. 998-1005.

Braun, M., Cawello, W., Boekens, H. and Horstmann, R., 2009. Influence of domperidone on pharmacokinetics, safety and tolerability of the dopamine agonist rotigotine. *British Journal of Clinical Pharmacology*, 67(2), pp. 209-215.

Brown, R.P., Delp, M.D., Lindstedt, S.L., Rhomberg, L.R. and Beliles, R.P., 1997. Physiological parameter values for physiologically based pharmacokinetic models. *Toxicology and Industrial Health*, 13(4), pp. 407-484.

Bujak, R., Struck-Lewicka, W., Kaliszan, M., Kaliszan, R. and Markuszewski, M.J., 2015. Blood–brain barrier permeability mechanisms in view of quantitative structure–activity relationships (QSAR). *Journal of Pharmaceutical and Biomedical Analysis*, 108, pp. 29-37.

Campbell, B.J., Rowbotham, M., Davies, P.S., Jacob III, P. and Benowitz, N.L., 2002. Systemic absorption of topical lidocaine in normal volunteers, patients with post-herpetic neuralgia, and patients with acute herpes zoster. *Journal of Pharmaceutical Sciences*, 91(5), pp. 1343-1350.

Cawello, W., Ahrweiler, S., Sulowicz, W., Szymczakiewicz-Multanowska, A. and Braun, M., 2012. Single dose pharmacokinetics of the transdermal rotigotine patch in patients with impaired renal function. *British Journal of Clinical Pharmacology*, 73(1), pp. 46-54.

Cawello, W., Braun, M. and Boekens, H., 2009. Absorption, disposition, metabolic fate, and elimination of the dopamine agonist rotigotine in man: administration by intravenous infusion or transdermal delivery. *Drug Metabolism and Disposition*, 37(10), pp. 2055-2060.

Cawello, W., Kim, S.R., Braun, M., Elshoff, J.-P., Ikeda, J. and Funaki, T., 2014. Pharmacokinetics, safety and tolerability of rotigotine transdermal patch in healthy Japanese and Caucasian subjects. *Clinical Drug Investigation*, 34(2), pp. 95-105.

Cawello, W., Kim, S.R., Braun, M., Elshoff, J.-P., Masahiro, T., Ikeda, J. and Funaki, T., 2016. Pharmacokinetics, safety, and tolerability of rotigotine transdermal system in healthy Japanese and Caucasian subjects following multiple-dose administration. *European Journal of Drug Metabolism and Pharmacokinetics*, 41(4), pp. 353-362.

Chan, K.K., Ross, H.D., Berner, B., Piraino, A.J. and John, V.A., 1990. Pharmacokinetics of a single transdermal dose of nicotine in healthy smokers. *Journal of Controlled Release*, 14(2), pp. 145-151.

Clark, D.E., 1999. Rapid calculation of polar molecular surface area and its application to the prediction of transport phenomena. 2. Prediction of blood–brain barrier penetration. *Journal of Pharmaceutical Sciences*, 88(8), pp. 815-821.

DeVeaugh-Geiss, A.M., Chen, L.H., Kotler, M.L., Ramsay, L.R. and Durcan, M.J., 2010. Pharmacokinetic comparison of two nicotine transdermal systems, a 21-mg/24-hour patch and a 25-mg/16-hour patch: a randomized, open-label, single-dose, two-way crossover study in adult smokers. *Clinical Therapeutics*, 32(6), pp. 1140-1148.

Devineni, D., Skee, D., Vaccaro, N., Massarella, J., Janssens, L., LaGuardia, K.D. and Leung, A.T., 2007. Pharmacokinetics and pharmacodynamics of a transdermal contraceptive patch and an oral contraceptive. *The Journal of Clinical Pharmacology*, 47(4), pp. 497-509.

El Maghraby, G., Williams, A. and Barry, B., 2005. Drug interaction and location in liposomes: correlation with polar surface areas. *International Journal of Pharmaceutics*, 292(1-2), pp. 179-185.

Ertl, P., 2008. Polar surface area. Wiley-VCH Verlag GmbH & Co. KGaA, Weinheim, Germany.

Evans, H.C. and Easthope, S.E., 2003. Transdermal buprenorphine. *Drugs*, 63(19), pp. 1999-2010.

Findlay, J.C., Place, V.A. and Snyder, P.J., 1987. Transdermal delivery of testosterone. *The Journal of Clinical Endocrinology & Metabolism*, 64(2), pp. 266-268.

Gammaitoni, A.R., Alvarez, N.A. and Galer, B.S., 2002. Pharmacokinetics and safety of continuously applied lidocaine patches 5%. *American Journal of Health-System Pharmacy*, 59(22), pp. 2215-2220.

Giachetti, C., Assandri, A., Mautone, G., Tajana, E., Palumbo, B. and Palumbo, R., 1996. Pharmacokinetics and metabolism of N-(2-hydroxyethyl)-2, 5-[14 C]-

pyrrolidine (HEP, Epolamine) in male healthy volunteers. *European Journal of Drug Metabolism and Pharmacokinetics*, 21(3), pp. 261-268.

Ginsburg, E.S., Gao, X., Shea, B.F. and Barbieri, R.L., 1998. Half-life of estradiol in postmenopausal women. *Gynecologic and Obstetric Investigation*, 45(1), pp. 45-48.

Gore, A.V. and Chien, Y.W., 1998. The nicotine transdermal system. *Clinics in Dermatology*, 16(5), pp. 599-615.

Gourlay, G.K., Kowalski, S.R., Plummer, J.L., Cherry, D.A., Gaukroger, P. and Cousins, M.J., 1989. The transdermal administration of fentanyl in the treatment of postoperative pain: pharmacokinetics and pharmacodynamic effects. *Pain*, 37(2), pp. 193-202.

Hartmanshenn, C., Scherholz, M. and Androulakis, I.P., 2016. Physiologically-based pharmacokinetic models: approaches for enabling personalized medicine. *Journal of Pharmacokinetics and Pharmacodynamics*, 43(5), pp. 481-504.

Hay, R.J., Johns, N.E., Williams, H.C., Bolliger, I.W., Dellavalle, R.P., Margolis, D.J., Marks, R., Naldi, L., Weinstock, M.A. and Wulf, S.K., 2014. The global burden of skin disease in 2010: an analysis of the prevalence and impact of skin conditions. *Journal of Investigative Dermatology*, 134(6), pp. 1527-1534.

Holley, F. and Van Steennis, C., 1988. Postoperative analgesia with fentanyl: pharmacokinetics and pharmacodynamics of constant-rate iv and transdermal delivery. *BJA: British Journal of Anaesthesia*, 60(6), pp. 608-613.

Howell, J., Smeets, J., Drenth, H.-J. and Gill, D., 2009. Pharmacokinetics of a granisetron transdermal system for the treatment of chemotherapy-induced nausea and vomiting. *Journal of Oncology Pharmacy Practice*, 15(4), pp. 223-231.

Jamei, M., 2016. Recent advances in development and application of physiologically-based pharmacokinetic (PBPK) models: a transition from academic curiosity to regulatory acceptance. *Current Pharmacology Reports*, 2(3), pp. 161-169.

Johnson, R.A. and Wichern, D.W., 2002. Applied multivariate statistical analysis (Vol. 5, No. 8). Upper Saddle River, NJ: Prentice hall.

Kapil, R.P., Cipriano, A., Friedman, K., Michels, G., Shet, M.S., Colucci, S.V., Apseloff, G., Kitzmiller, J. and Harris, S.C., 2013. Once-weekly transdermal buprenorphine application results in sustained and consistent steady-state plasma levels. *Journal of Pain and Symptom Management*, 46(1), pp. 65-75.

Kelder, J., Grootenhuis, P.D., Bayada, D.M., Delbressine, L.P. and Ploemen, J.-P., 1999. Polar molecular surface as a dominating determinant for oral absorption and brain penetration of drugs. *Pharmaceutical Research*, 16(10), pp. 1514-1519.

Kochak, G.M., Sun, J.X., Choi, R.L. and Piraino, A.J., 1992. Pharmacokinetic disposition of multiple-dose transdermal nicotine in healthy adult smokers. *Pharmaceutical Research*, 9(11), pp. 1451-1455.

Kokate, A., Li, X., Williams, P.J., Singh, P. and Jasti, B.R., 2009. In silico prediction of drug permeability across buccal mucosa. *Pharmaceutical Research*, 26(5), pp. 1130-1139.

Kondamudi, P.K., Tirumalasetty, P.P., Malayandi, R., Mutalik, S. and Pillai, R., 2016. Lidocaine transdermal patch: Pharmacokinetic modeling and in Vitro–In vivo correlation (IVIVC). *AAPS PharmSciTech*, 17(3), pp. 588-596.

Kress, H.G., 2009. Clinical update on the pharmacology, efficacy and safety of transdermal buprenorphine. *European Journal of Pain*, 13(3), pp. 219-230.

Kress, H.G., Boss, H., Delvin, T., Lahu, G., Lophaven, S., Marx, M., Skorjanec, S. and Wagner, T., 2010. Transdermal fentanyl matrix patches Matrifen® and Durogesic® DTrans® are bioequivalent. *European Journal of Pharmaceutics and Biopharmaceutics*, 75(2), pp. 225-231.

Kwon, J.H., Liljestrand, H.M. and Katz, L.E., 2006. Partitioning of moderately hydrophobic endocrine disruptors between water and synthetic membrane vesicles. *Environmental Toxicology and Chemistry: An International Journal*, 25(8), pp. 1984-1992.

Lefèvre, G., Büche, M., Sedek, G., Maton, S., Enz, A., Lorch, U., Sagan, C. and Appel-Dingemanse, S., 2009. Similar rivastigmine pharmacokinetics and pharmacodynamics in Japanese and white healthy participants following the application of novel rivastigmine patch. *The Journal of Clinical Pharmacology*, 49(4), pp. 430-443.

Lefèvre, G., Pommier, F., Sędek, G., Allison, M., Huang, H.L.A., Kiese, B., Ho, Y.Y. and Appel-Dingemanse, S., 2008a. Pharmacokinetics and bioavailability of the novel rivastigmine transdermal patch versus rivastigmine oral solution in healthy elderly subjects. *The Journal of Clinical Pharmacology*, 48(2), pp. 246-252.

Lefèvre, G., Sędek, G., Huang, H.L.A., Saltzman, M., Rosenberg, M., Kiese, B. and Fordham, P., 2007. Pharmacokinetics of a rivastigmine transdermal patch formulation in healthy volunteers: relative effects of body site application. *The Journal of Clinical Pharmacology*, 47(4), pp. 471-478.

Lefèvre, G., Sędek, G., Jhee, S., Leibowitz, M., Huang, H.L., Enz, A., Maton, S., Ereshefsky, L., Pommier, F. and Schmidli, H., 2008b. Pharmacokinetics and pharmacodynamics of the novel daily rivastigmine transdermal patch compared with twice-daily capsules in Alzheimer's disease patients. *Clinical Pharmacology & Therapeutics*, 83(1), pp. 106-114.

Lien, E.J. and Gaot, H., 1995. QSAR analysis of skin permeability of various drugs in man as compared to in vivo and in vitro studies in rodents. *Pharmaceutical Research*, 12(4), pp. 583-587.

Lin, S., Ho, H. and Chien, Y.W., 1993. Development of a new nicotine transdermal delivery system: in vitro kinetics studies and clinical pharmacokinetic evaluations in two ethnic groups. *Journal of Controlled Release*, 26(3), pp. 175-193.

Lombardo, F., Obach, R.S., Shalaeva, M.Y. and Gao, F., 2004. Prediction of human volume of distribution values for neutral and basic drugs. 2. Extended data set and leave-class-out statistics. *Journal of Medicinal Chemistry*, 47(5), pp. 1242-1250.

MacGregor, T.R., Matzek, K.M., Keirns, J.J., van Wayjen, R.G., van den Ende, A. and van Tol, R.G., 1985. Pharmacokinetics of transdermally delivered clonidine. *Clinical Pharmacology & Therapeutics*, 38(3), pp. 278-284.

Mahmood, I., 1997. Clinical pharmacokinetics and pharmacodynamics of selegiline. *Clinical Pharmacokinetics*, 33(2), pp. 91-102.

Marier, J.F., Lor, M., Morin, J., Roux, L., Di Marco, M., Morelli, G. and Sædder, E.A., 2007. Comparative bioequivalence study between a novel matrix transdermal delivery system of fentanyl and a commercially available reservoir formulation. *British Journal of Clinical Pharmacology*, 63(1), pp. 121-124.

McCarley, K.D. and Bunge, A.L., 2001. Pharmacokinetic models of dermal absorption. *Journal of Pharmaceutical Sciences*, 90(11), pp. 1699-1719.

Meikle, A.W., Arver, S., Dobs, A.S., Sanders, S.W., Rajaram, L. and Mazer, N.A., 1996. Pharmacokinetics and metabolism of a permeation-enhanced testosterone transdermal system in hypogonadal men: influence of application site--a clinical research center study. *The Journal of Clinical Endocrinology & Metabolism*, 81(5), pp. 1832-1840.

Meikle, A.W., Mazer, N.A., Moellmer, J.F., Stringham, J.D., Tolman, K.G., Sanders, S.W. and Odell, W.D., 1992. Enhanced transdermal delivery of testosterone across nonscrotal skin produces physiological concentrations of testosterone and its metabolites in hypogonadal men. *The Journal of Clinical Endocrinology & Metabolism*, 74(3), pp. 623-628.

Mitragotri, S., Anissimov, Y.G., Bunge, A.L., Frasch, H.F., Guy, R.H., Hadgraft, J., Kasting, G.B., Lane, M.E. and Roberts, M.S., 2011. Mathematical models of skin permeability: an overview. *International Journal of Pharmaceutics*, 418(1), pp. 115-129.

Mizushima, H., Takanaka, K., Abe, K., Fukazawa, I. and Ishizuka, H., 2007. Stereoselective pharmacokinetics of oxybutynin and N-desethyloxybutynin in vitro and in vivo. *Xenobiotica*, 37(1), pp. 59-73.

Montgomery, D.C., Peck, E.A. and Vining, G.G., 2012. Introduction to linear regression analysis. John Wiley & Sons.

Mulligan, S.C., Masterson, J.G., Devane, J.G. and Kelly, J.G., 1990. Clinical and pharmacokinetic properties of a transdermal nicotine patch. *Clinical Pharmacology & Therapeutic*s, 47(3), pp. 331-337.

Munjal, S., Gautam, A., Okumu, F., McDowell, J. and Allenby, K., 2016. Safety and pharmacokinetics of single and multiple intravenous bolus doses of diclofenac sodium compared with oral diclofenac potassium 50 mg: A randomized, parallel-group, single-center study in healthy subjects. *The Journal of Clinical Pharmacology*, 56(1), pp. 87-95.

Nachum, Z., Shupak, A. and Gordon, C.R., 2006. Transdermal scopolamine for prevention of motion sickness. *Clinical Pharmacokinetics*, 45(6), pp. 543-566.

Nicoli, S., Bunge, A.L., Delgado-Charro, M.B. and Guy, R.H., 2009. Dermatopharmacokinetics: factors influencing drug clearance from the stratum corneum. *Pharmaceutical Research*, 26(4), pp. 865-871.

Palm, K., Stenberg, P., Luthman, K. and Artursson, P., 1997. Polar molecular surface properties predict the intestinal absorption of drugs in humans. *Pharmaceutical Research*, 14(5), pp. 568-571.

Patrick, K.S., Straughn, A.B., Perkins, J.S. and González, M.A., 2009. Evolution of stimulants to treat ADHD: transdermal methylphenidate. *Human Psychopharmacology: Clinical and Experimental*, 24(1), pp. 1-17.

Pierce, D., Dixon, C.M., Wigal, S.B. and McGough, J.J., 2008. Pharmacokinetics of methylphenidate transdermal system (MTS): results from a laboratory classroom study. *Journal of Child and Adolescent Psychopharmacology*, 18(4), pp. 355-364.

Portenoy, R.K., Southam, M.A., Gupta, S.K., Lapin, J., Layman, M., Inturrisi, C.E. and Foley, K.M., 1993. Transdermal fentanyl for cancer pain. Repeated dose pharmacokinetics. *Anesthesiology*, 78(1), pp. 36-43.

Potts, R.O. and Guy, R.H., 1992. Predicting skin permeability. *Pharmaceutical Research*, 9(5), pp. 663-669.

Potts, R.O. and Guy, R.H., 1995. A predictive algorithm for skin permeability: the effects of molecular size and hydrogen bond activity. *Pharmaceutical Research*, 12(11), pp. 1628-1633.

Rasmussen, S., Horkan, K.H. and Kotler, M., 2018. Pharmacokinetic evaluation of two nicotine patches in smokers. *Clinical Pharmacology in Drug Development*, 7(5), pp. 506-512.

Raynaud, J.-P., Aumonier, C., Gualano, V., Betea, D. and Beckers, A., 2008. Pharmacokinetic study of a new testosterone-in-adhesive matrix patch applied every 2 days to hypogonadal men. *The Journal of Steroid Biochemistry and Molecular Biology*, 109(1-2), pp. 177-184.

Rohatagi, S., Barrett, J.S., Dewitt, K.E. and Morales, R.J., 1997. Integrated pharmacokinetic and metabolic modeling of selegiline and metabolites after transdermal administration. *Biopharmaceutics & Drug Disposition*, 18(7), pp. 567-584.

Shulman, L.P., 2004. 17β-estradiol/levonorgestrel transdermal system for the management of the symptomatic menopausal woman. *Expert Opinion on Pharmacotherapy*, 5(12), pp. 2559-2566.

Singh, A.B., Norris, K., Modi, N., Sinha-Hikim, I., Shen, R., Davidson, T. and Bhasin, S., 2001. Pharmacokinetics of a transdermal testosterone system in men with end stage renal disease receiving maintenance hemodialysis and healthy hypogonadal men. *The Journal of Clinical Endocrinology & Metabolism*, 86(6), pp. 2437-2445.

Stanczyk, F.Z., Archer, D.F., Rubin, A. and Foegh, M., 2013. Therapeutically equivalent pharmacokinetic profile across three application sites for AG200-15, a novel low-estrogen dose contraceptive patch. *Contraception*, 87(6), pp. 744-749.

Stanczyk, F.Z., Rubin, A., Flood, L. and Foegh, M., 2011. Pharmacokinetics, tolerability and cycle control of three transdermal contraceptive delivery systems containing different doses of ethinylestradiol and levonorgestrel. *Hormone Molecular Biology and Clinical Investigation*, 6(2), pp. 231-240.

Starkman, J.S. and Dmochowski, R.R., 2006. Management of overactive bladder with transdermal oxybutynin. *Reviews in Urology*, 8(3), pp. 93.

Staskin, D.R., 2003. Transdermal systems for overactive bladder: principles and practice. *Reviews in Urology*, 5(Suppl 8), p. S26.

Stenberg, P., Luthman, K., Ellens, H., Lee, C.P., Smith, P.L., Lago, A., Elliott, J.D. and Artursson, P., 1999. Prediction of the intestinal absorption of endothelin receptor antagonists using three theoretical methods of increasing complexity. *Pharmaceutical Research*, 16(10), pp. 1520-1526.

Sun, J.X., Piraino, A.J., Morgan, J.M., Joshi, J.C., Cipriano, A., Chan, K. and Redalieu, E., 1995. Comparative Pharmacokinetics and Bioavailability of Nitroglycerin and its Metabolites from Transderm-Nitro, Nitrodisc, and Nitro-Dur II Systems Using a Stable-Isotope Technique. *The Journal of Clinical Pharmacology*, 35(4), pp. 390-397.

Thompson, J., Bower, S., Liddle, A. and Rowbotham, D., 1998. Perioperative pharmacokinetics of transdermal fentanyl in elderly and young adult patients. British *Journal of Anaesthesia*, 81(2), pp. 152-154.

van den Heuvel, M.W., van Bragt, A.J.M., Alnabawy, A.K.M. and Kaptein, M.C.J., 2005. Comparison of ethinylestradiol pharmacokinetics in three hormonal contraceptive formulations: the vaginal ring, the transdermal patch and an oral contraceptive. *Contraception*, 72(3), pp. 168-174.

Varvel, J., Shafer, S., Hwang, S., Coen, P. and Stanski, D., 1989. Absorption characteristics of transdermally administered fentanyl. *Anesthesiology*, 70(6), pp. 928-934.

Wang, Y., Cipriano, A., Munera, C. and Harris, S.C., 2016. Dose-Dependent Flux of Buprenorphine Following Transdermal Administration in Healthy Subjects. The *Journal of Clinical Pharmacology*, 56(10), pp. 1263-1271.

Wiedersberg, S. and Guy, R.H., 2014. Transdermal drug delivery: 30+ years of war and still fighting! *Journal of Controlled Release*, 190, pp. 150-156.

Winiwarter, S., Bonham, N.M., Ax, F., Hallberg, A., Lennernäs, H. and Karlén, A., 1998. Correlation of human jejunal permeability (in vivo) of drugs with experimentally and theoretically derived parameters. A multivariate data analysis approach. *Journal of Medicinal Chemistry*, 41(25), pp. 4939-4949.

Yap, C., Li, H., Ji, Z. and Chen, Y., 2007. Regression methods for developing QSAR and QSPR models to predict compounds of specific pharmacodynamic, pharmacokinetic and toxicological properties. *Mini Reviews in Medicinal Chemistry*, 7(11), pp. 1097-1107.

Ye, M., Nagar, S. and Korzekwa, K., 2016. A physiologically based pharmacokinetic model to predict the pharmacokinetics of highly protein-bound drugs and the impact of errors in plasma protein binding. *Biopharmaceutics & Drug Disposition*, 37(3), pp. 123-141.

Yun, Y. and Edginton, A., 2013. Correlation-based prediction of tissue-to-plasma partition coefficients using readily available input parameters. *Xenobiotica*, 43(10), pp. 839-852.

Zobrist, R.H., Quan, D., Thomas, H.M., Stanworth, S. and Sanders, S.W., 2003. Pharmacokinetics and metabolism of transdermal oxybutynin: in vitro and in vivo performance of a novel delivery system. *Pharmaceutical Research*, 20(1), pp. 103-109.

Chapter 6: General conclusion and Perspectives

In this thesis, the use of different approaches to assess skin permeation has been investigated. The objectives were to characterise the processes involved in dermal absorption and disposition of drugs included in topical products and, using this information:

(a) to evaluate the usefulness of transdermal drug products to predict the drug input-rate into the skin tissues from topical products using *in vitro* permeation tests (coupled with stratum corneum tape-stripping); (b) to investigate whether the stratum corneum sampling technique approach (tape-stripping), together with the application of different Fickian diffusion models, is able to estimate skin pharmacokinetic parameters related to drug partitioning into and diffusion across the stratum corneum; (c) to investigate whether excipients present in topical formulation are capable of modifying the kinetic parameters of the drug; (d) to develop a mathematical model using available data from transdermal patches to deduce model parameters that describe drug clearance from the skin (Cl_{skin}), and to establish a relationship between Cl_{skin} and key physicochemical properties of the drugs, thereby enabling prediction of the former for topical drugs. The goal is to develop a model, which will predict drug absorption and disposition from dermal products thereby facilitating their optimisation and, ultimately, the development of high-performance medicines.

In this work, different approaches were applied to explore drug behaviour following application of a product on the skin.

First, *in vitro* permeation tests and stratum corneum tape-stripping were used to track two transdermal drugs, buprenorphine (Transtec® - transdermal patch) and nicotine (Nicotinell® - transdermal patch), and one locally-acting drug, diclofenac (Voltaren® medicated plaster), through the skin layers (porcine skin was used as a membrane model). The objective of this study was to characterise the rate at which the drug enters the skin after a topical (skin) application. The approach took advantage of the known input rates of the drugs delivered from transdermal patches. This information was used to optimise the robustness of the experimental approaches and to characterise the drug input function correctly. The results from the buprenorphine and nicotine experiments showed that a combination of stratum corneum sampling and *in vitro* permeation tests can provide indicative prediction of *in vivo* drug input rates

from transdermal patches. Subsequently, the approach was applied to a topical formulation which aims to deliver diclofenac to treat pain and inflammation in subcutaneous tissue. The good agreement between the experimentally determined input rates of the two drugs and their labelled performance *in vivo* lends support to the potential utility of the *in vitro* approach proposed to define topical drug input rates. An important future step is to apply the same approach more broadly; that is, to extend the methodology applied to patches for typical topical drug formulations, such as creams and gels.

Second, diclofenac uptake into and clearance from the stratum corneum *in vivo*, in human volunteers, were evaluated. The study was built on the stratum corneum sampling technique approach (tape-stripping) and on the application of different Fickian diffusion models to estimate skin pharmacokinetic parameters. The results obtained from the uptake experiments demonstrated that stratum corneum tape-stripping (coupled with the application of diffusion mathematical models) is able to predict drug partitioning into and diffusion across the stratum corneum, at least when the formulation is on the skin. In addition, evaluation of partition and diffusion-related values as a function of formulation application time indicated the drug distributes rapidly from the formulation into the stratum corneum. Also, it was possible to observe that the partition and diffusion may not be constant over the application time, which implies that interactions between the vehicle constituents and the skin may occur, altering the drug permeability in the stratum corneum. Furthermore, the results obtained from the solution of the Fick second law did not agree well with the clearance experimental data, suggesting that drug clearance from the stratum corneum may be complicated by immobilisation of the active agent in the stratum corneum. Although further investigation is needed, this may be the result of strong binding or a substantial decrease in drug solubility due to the more rapid diffusion of a co-delivered cosolvent. Furthermore, analysis of the change in mass of drug over time after plaster removal permits its average flux into the underlying viable tissue, as well as the rate constant (k) at which drug is 'cleared' from the stratum corneum to be determined.

Third, the potential effects of different excipients on the predicted drug kinetic parameters and the manner in which excipient(s) behaviour may impact on the rate and extent at which the drug crosses the stratum corneum was further explored *in vivo* in human volunteers. The results obtained from the uptake of propylene and butylene glycol suggests that these volatile solvents were rapidly taken into the stratum

corneum and it is likely that they would transiently change the structure of the stratum corneum and assist in transferring the drug quickly from the formulation into the barrier. In parallel, evaporation of the solvents was identified. From a thermodynamic point of view, the loss (by evaporation and stratum corneum uptake) of propylene and butylene glycol will eventually reach the point at which the amount of drug remaining at the skin surface can no longer be fully solubilised and drug transfer into the stratum corneum will slow down. These findings are in line with the results obtained for diclofenac, when a quicker transfer of the drug was observed during the first hours of the experiments. Further studies are required to establish whether these two glycols are, synergically or individually, acting as permeation enhancers, for example, investigation of diclofenac behaviour in the presence or absence of one or other glycol.

The last component of the thesis was to develop a multiple linear regression model using available data (plasma concentration *versus* time profiles, labelled drug input rates) from 19 marketed transdermal patches to deduce the parameters of the model that describe drug disposition between the bottom of the stratum corneum (i.e., after the input function) and the systemic compartment. It was possible, in this way, to demonstrate a clear relationship ($R^2 = 0.72$) between the drug clearance from the skin and key physical chemical properties of the drug (MW, log P and TPSA). In addition, it was further demonstrated that the developed model has a good correlation with values derived from *in vitro* skin experiments (described in the Chapter 2 of this thesis). However, since the model was built on a dataset with a limited number of drugs, further work is required to verify and extend this correlation method.

Overall, the research described in this thesis has a significant importance as it allows useful quantitative information about not only the drug but also excipients to be extracted. These findings would be useful to develop a model linking excipient kinetic parameters deduced here with the behaviour/disposition of the active compound. It may ultimately improve the understanding of drug bioavailability from a topical formulation under 'real-life' conditions and, consequently, it will help the development and optimisation of high performance medicines.

Appendix: Ethical forms for *in vivo* experiments

Department of Pharmacy & Pharmacology,
Claverton Down, Bath, BA2 7AY

Prof. RH Guy,
Tel. +44.1225.384901
Email: r.h.guy@bath.ac.uk

M.A. Maciel Tabosa,
Email: m.a.maciel.tabosa@bath.ac.uk

Dr. B. Delgado-Charro,
Email: B.Delgado-Charro@bath.ac.uk

Participant information sheet

Study: "Measurement of diclofenac absorption into skin from a medicated plaster"

- You are being invited to take part in a research study.
- Before you decide on your participation, it is important for you to understand why the research is being done and what it will involve. Please take time to read the following information carefully and discuss it with others if you wish.
- Please contact us if there is anything that is not clear or if you would like more information. Our contact details are at the end of this document.
- Take as much time as you want to decide whether or not you wish to take part in this study.

Thank you for reading this information sheet!

What is the purpose of this study?

Application of drugs directly to the skin is very convenient to treat local diseases. Unfortunately, for most drugs, the only way to investigate the efficacy and compare formulations (creams, ointments, gels) is via long and expensive clinical trials that require many participants. The development of topical formulations would be very much aided if other, simpler methods, where available to predict the efficacy of topical medicines. In this way, only the best, optimized formulations would be finally tested in clinical trials.

The aim of this research is to refine and validate the method of 'tape-stripping' using a medicated plaster containing diclofenac. In particular, we want to know whether tape-stripping can tell us how much diclofenac reaches the target site and how

quickly, after the plaster is applied onto the skin. To do this we will compare the known rate of delivery of the diclofenac plaster with the rate determined by tape-stripping. To validate the model, we will also use data previously obtained by our group with other topical diclofenac gels.

Tape-stripping is cheap, fast and relatively non-invasive; these are important advantages compared with long clinical trials. The outermost layer of the skin (called the *stratum corneum*) consists of dead cells specialised in opposing both the loss of water from the body and the entry of foreign compounds including drugs. It has been proposed that sampling the amount of drug in this layer may provide information about how quickly and how much of a drug can penetrate the skin.

The tape-stripping technique has been used successfully to compare antifungal formulations, reaching the same conclusions as previous clinical trials. However, while antifungals act on the most external layer of the skin, other topical drugs such as diclofenac are meant to treat problems deeper in the skin, or in the muscle and other tissues below. For the moment, we do no not know whether tape-stripping can be used to compare all topical medicines and our research is designed to see if this is the case or not. In this study, we will perform tape-stripping of the skin after application of a medicated diclofenac plaster (Voltaren® 180 mg medicated plaster).

Volunteer requirements

For your own safety, and for the results of the experiment to be valid, the following criteria must be met by all the participants:

All of the following "inclusion criteria" must be true for you:

1. You are 18-72 years old, healthy, male or non-pregnant and non-breastfeeding female of any ethnic background.
2. You are able to communicate well with the investigators.
3. You are willing to provide basic information (i.e., age, height, weight, health, pregnancy status, gender and ethnicity and handedness) so that the investigator can verify your compliance with the inclusion and exclusion criteria.
4. You are able and willing to adhere to the study restrictions and can be present at the research site at the times required.
5. You provide written informed consent before initiation of any of the study procedures.
6. You agree not to participate in another clinical trial or cosmetic study during your participation.

On the contrary, you cannot participate in this study if any of the following "exclusion criteria" applies to you:

1. For your own safety, you cannot take part in this research if you suffer from: (a) skin infection or chronic skin disease (e.g., eczema, psoriasis, atopic dermatitis); (b) hereditary skin disorders or any skin inflammatory conditions as reported by you or evident to the investigator; and (c) excessive pigmentation, tattoos, hair, moles, skin defects, sunburn, or blemishes.

2. You will be excluded if you are pregnant and/or breastfeeding.
3. You will be excluded if you are a current smoker or obese as defined by BMI ≥ 30 kg/m^2 (the investigator can help you determine your BMI). This is because we anticipate these characteristics will modify our measurements and invalidate our results.
4. You are a MPharm or B/MPharmacology undergraduate student at the University of Bath.
5. If you are taking part, or have recently participated, in any other clinical trial or cosmetic study.
6. If you are using any topical drug at or close to the test site area as this could interfere with the results.
7. If you want to practice strenuous exercise during the study period: jogging, aerobics, swimming, cycling, etc. Or if you want to suntan and expose your arms to sun or UV light during your participation and/or during the week after.
8. If you cannot be present at all times at which data will be collected.
9. If you have, or suspect you may have, suffered any adverse reaction to diclofenac or to the other ingredients in the patch tested, to medical dressings or to adhesive tapes. A list of these ingredients is provided at the end of this form.
10. If you have used any prescription medication during the previous 30 days or over-the-counter medication 5 days before entering the study (with the exception of contraceptives in female participants).
11. If you are unable to communicate or co-operate with the investigators.

Your participation in the research:

It is up to you to decide whether or not to take part in this study. If you decide to take part, please contact one of the researchers. Then:

1. You will be given a copy of this information sheet to keep for your records.
2. You will be asked to sign a consent form and you will be given a copy of the consent form.
3. If you change your mind, you are free to withdraw at any time and without giving a reason.

Why do we want you to participate?

We need volunteers with healthy skin to determine the best method to assess diclofenac delivery. Individuals suffering from skin disease cannot be used for this study because their condition introduces several factors that make it difficult for us to draw useful conclusions. For example, diclofenac may interfere with other medications being taken and these other treatments may interfere with the results obtained for diclofenac. Therefore, for your safety and for the results of the study to be valid, only healthy people not taking any medication (with the exception of contraceptives in female subjects) can participate.

Please note that the aim of the study is not to establish the efficacy or safety of the medicated plaster investigated but to develop a standardized method to determine the drug input rate from the patch to the skin.

What will happen if I decide to participate?

Your participation involves several sessions over two days. This will include one meeting with the investigator(s) before the experiment and nine experimental sessions that take place over two consecutive days.

It is very important that you carefully read this information form and understand what your participation requires. Please ask for further clarification if needed before you make a decision. If you decide to participate, you will contact the research team and will meet with them to provide "written informed consent". If you decide otherwise, there is no need to contact us or to provide any explanation for your decision.

The experiments will take place in the research laboratories (5-West 3.22) of the principal investigators (Prof. R.H. Guy, and Dr. B. Delgado-Charro) in the Department of Pharmacy & Pharmacology at the University of Bath.

The step by step procedure involves:

Pre-Study Preparation

At least 48 hours before the study, the investigator will meet with you to explain and agree the procedure and schedule, and ask you to complete a questionnaire and consent form. You will provide some personal information such as age, height, weight, your health status, particularly skin condition, and other questions aimed to verify that you meet the inclusion criteria but none of the exclusion criteria detailed above.

We will also ask you not to use any lotions or moisturiser on your forearms for at least 24 hours prior to and throughout the study itself.

If you have hair growth in the test region (the inside surfaces of your forearms), the investigator will shave it carefully using a new disposable razor at least 24 hours before the study begins. Typically, if shaving is necessary, it can be completed at this pre-study meeting.

At this time, we will provide you with a written copy of the study schedule and protocol, including the timing for all your visits.

We show below *an example* of the study schedule and protocol for an imaginary participant so you can appreciate the time that will be required for your participation. This is just an example, the specific hours and dates for your participation will be agreed during the Pre-Study preparation.

Study Schedule for **Subject 1**

Day / Date	Start time	**Approximate end time**	**What will happen?**
Tue / Nov 1	8:00	8:15	Wash and dry both forearms.
Tue / Nov 1	8:30	9:30	Eight medicated plasters will be applied to the right forearm, four plasters at 8:30 and the four other plasters at 9:00. Six medicated plasters will be applied to the left forearm, three at 8:30 and the three other plasters at 9:00. The untreated area of skin on the right forearm will be tape-stripped.
Tue / Nov 1	10:30	11:30	Two medicated plasters will be removed from the right forearm, one at 10:30, and another one at 11:00. The two sites will be tape-stripped. Tape-stripping of one site takes approximately 20-30 minutes.
Tue / Nov 1	14:30	15:30	Two more medicated plasters will be removed from the right forearm, one at 14:30, and another one at 15:00. The two sites will be tape-stripped. All six plasters will be removed from the left forearm, three at 14:30, and three other plasters at 15:00. A protective covering will be placed on those six sites.
Tue / Nov 1	17:30	18:30	Two more medicated plasters will be removed from the right forearm, one at 17:30, and another one at 18:00. The two sites will be tape-stripped.
Tue / Nov 1	19:30	20:30	Two sites on the left forearm will be tape-stripped, one at 19:30, and another one at 20:00.
Tue / Nov 1	20:30	21:30	The remaining two medicated plasters on the right forearm will be removed, one at 20:30, and another one at 21:00. The two sites will be tape-stripped.

Wed / Nov 2	7:30	9:00	Two more sites on the left forearm will be tape-stripped, one at 7:30, and another one at 8:00. The untreated area of skin on the left forearm will be tape-stripped.
Wed / Nov 2	14:30	15:30	The remaining two sites on the left forearm will be tape-stripped, one at 14:30, and another one at 15:00.

Your study will commence at 8:00 (8 a.m.) on Tue, Nov. 1 (for example) in 5W 3.22, University of Bath.

8:00-8:15 – The investigator will clean the skin of both inner forearm surfaces with a mild soap solution, rinse it with tepid water, and dry it with a soft towel. The purpose of this cleansing procedure is to ensure that the starting skin condition is similar for all subjects.

8:30-9:00 – The medicated plaster will be applied to a maximum of 14 treatment sites. Fourteen pieces of commercially available diclofenac medicated plaster (Voltaren® 180 mg medicated plaster) each cut to an area of 5 cm^2 (5 cm x 1 cm) will be applied to the forearms, eight plasters will be applied to the right forearm and six plasters to the left forearm – see drawing below. Each application area is marked for tape-stripping as described below. The investigator will wear gloves while they apply the plasters.

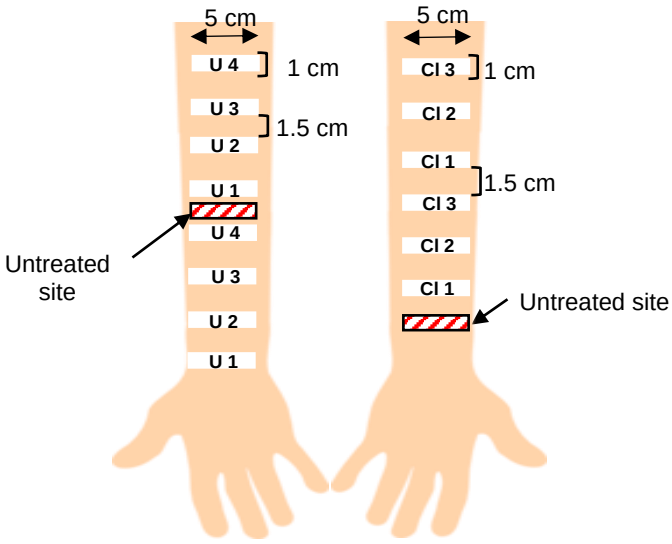

After application of the medicated plasters, we will tape-strip the untreated skin site on the right forearm. A non-invasive probe (see opposite photo) will be used to measure water loss (trans-epidermal water loss or TEWL) from the the untreated skin site. A piece of tape will be placed on the untreated skin site, removed and then the TEWL measurement taken. The sequence will be repeated until 30 tapes have been taken. From the amount of *stratum corneum* removed and the change in water loss rate, we can determine the total thickness of your *stratum corneum*. We can also use the same tape-strips to check our analytical method for diclofenac (these contain no drug and therefore act as valuable "blank" samples).

Before beginning the tape-stripping, we will measure the TEWL from the skin of each treated site, and we will repeat the measurement approximately every 4-5 tapes. This will tell us when a sufficient amount of skin cells have been removed, and will indicate to us when the tape stripping procedure should be stopped. The TEWL will be measured using a probe that is simply placed on the skin and records the value automatically. In any case, the tape-stripping will stop as soon as one of the following events occurs: (a) 30 tape-strips taken; or (b) the TEWL measurement is larger than either 60 $g/m^2/h^1$ or 6 times the TEWL value measured before stripping begins.

10:30-11:30 – After an application period of 2 hours, two plasters from the right forearm (U1) will be removed (i.e., one at 10:30 and another one at 11:00) and the treated skin sites will be tape-stripped immediately.

14:30-15:30 – After a further 4 hours (6 hours after application of the plaster), two more plasters from the right forearm (U 2) and the six plasters from the left forearm (Cl 1, Cl 2 and Cl 3) will be removed (i.e., half at 14:30 and another half at 15:00) and the treated skin sites on the right forearm will be tape-stripped immediately. The treated areas on the left forearm will be protected using a non-occlusive gauze.

17:30-18:30 – After a further 3 hours (9 hours after application of the plaster), two more plasters from the right forearm (U 3) will be removed (i.e., one at 17:30 and another one at 18:00) and the treated skin sites will be tape-stripped immediately.

19:30-20:30 – After a further 2 hours (11 hours after application of the plaster), two treated skin sites on the left forearm (Cl 1) will be tape-stripped (i.e., one at 19:30 and another one at 20:00).

20:30-21:30 – After a further 1 hour (12 hours after application of the plaster), two more plasters from the right forearm (U 4) will be removed (i.e., one at 20:30 and another one at 21:00) and the treated skin sites are tape-stripped immediately.

The next visit will take place on the following day, normally 23 hours after plaster application.

After the last tape-stripping procedure on day 1, you are free to leave the laboratory but you should not swim, shower, engage in strenuous sports or apply creams to the area. Further, you should avoid exposing the skin sites (tape-stripped or not) to direct sun or UV light. If you wish, we will provide you with dressings for your forearms. You should also avoid scratching the skin at the tape-stripped sites.

7:30-9:00 – After a further 11 hours (23 hours after application of the plaster), two more treated skin sites on the left forearm (Cl 2) will be tape-stripped (i.e., one at 7:30 and another one at 8:00). And we will tape-strip the untreated skin site on the left forearm, following the same procedure as described above. A piece of tape will be placed on the untreated skin site, removed and then the TEWL measurement taken. The sequence will be repeated until 30 tapes have been taken. From the amount of *stratum corneum* removed and the change in water loss rate, we can determine the total thickness of your *stratum corneum*.

14:30-15:30 – After a further 7 hours (30 hours after application of the plaster), two more treated skin sites on the left forearm (Cl 3) will be tape-stripped (i.e., one at 14:30 and another one at 15:00).

After the last tape-stripping procedure on day 2, you are free to leave the laboratory but you should avoid exposing the skin sites (tape-stripped or not) to direct sun or UV light for at least the next two weeks. If you wish, we will provide you with dressings for your forearms. You should also avoid scratching the skin at the tape-stripped sites.

It is possible that the timings of plaster application and testing may be different than stated above. We will determine the optimum times in preliminary experiments and inform you if this modification is necessary.

Tape-stripping

Tape-stripping involves sticking pieces of special Sellotape to the skin of your forearms (see left panel of figure below). The strips are gently affixed by rubbing back and forth with tweezers (middle panel of figure below). When the strips are peeled away (right panel of figure below), they remove some dead skin cells with them. We weigh the tapes before and after applying them to your arm so that we can determine the tiny amount of skin removed.

Later on, we measure the amount of diclofenac in these strips. Typically, the analysis is performed within 24 hours; in any case, the tape strips are stored for a maximum of 2 weeks before they are analysed for drug content and they are then destroyed.

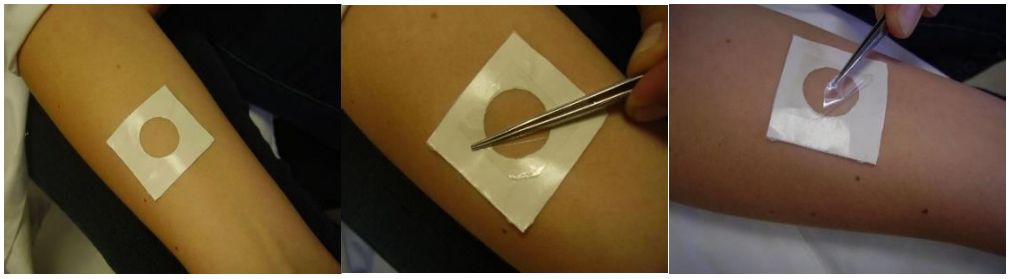

Are there any side effects?

Tape-stripping removes only the most superficial dead skin cells and causes a similar sensation to that experienced when removing a plaster. However, these dead cells are part of normal skin structure and contribute to its barrier function; therefore, some reddening or mild irritation of the skin frequently occurs after tape-stripping. These effects are usually short-lived and never last longer than two weeks.

Skin redness, mild allergic reactions and hyperpigmentation can also be caused by the dressings, adhesives, and tapes. These minor side effects usually resolve in a few days but if uncomfortable they typically respond well to a brief course of treatment with emollient creams or with an over-the-counter corticosteroid, such as hydrocortisone.

Typically, the tape-stripped skin will have been replaced completely in about 2 weeks. It is very important that you do not scratch the skin application sites particularly after tape-stripping even if they feel itchy. The skin at tape-stripped sites is more fragile than normal skin and can be easily damaged by scratching or friction. It also important to protect the application sites from light (sun/UV) exposure for at least a week following your participation in the study.

The medicated plaster contains diclofenac and other inactive components. Diclofenac is used to treat pain and inflammation in rheumatic disease (including juvenile idiopathic arthritis) and other musculoskeletal disorders; acute gout; and postoperative pain.

In total, only one-half of an actual diclofenac medicated plaster will be applied to your skin in the experiment (for comparison, you should know that up to two plasters can be applied per day according to the patient leaflet). It is known that only 5% of the total drug in the entire plaster actually reaches the blood.

The diclofenac medicated plaster has been approved for use and is commercially available. However, all medications have potential side effects. You may experience the following side effects: local skin reactions such as skin redness, burning sensation, itching, inflamed skin redness, skin rash, sometimes with pustules or wheals, hypersensitivity reactions or local allergic reactions (contact dermatitis). In patients externally using drugs from the same drug group as diclofenac, there have been

isolated reports of generalised skin rash, hypersensitivity reactions such as swelling of the skin and mucous membranes (such as lips, mouth and throat) and anaphylactic-type (severe allergic) reactions. Including problems with blood circulation and light sensitivity reactions.

Absorption of diclofenac into the body by the skin is very low compared to the drug concentration in the blood following diclofenac taken by mouth. Therefore, the likelihood of side effects occurring in the body as a whole (such as stomach or kidney problems or difficulty breathing) is very low. Because of the short duration of the study treatment, we expect that the worst side effects will be limited to stinging, irritation, itching and skin redness.

It is, however, possible (although extremely unlikely) that you may experience another adverse event not listed here.

If you experience any side effects other than mild skin redness or irritation at the treatment sites, you may consider contacting your GP for advice.

At the end of this form, you will find a list of ingredients present in the diclofenac medicated plaster as provided in the patient information leaflet.

Can you withdraw from the study at any time?

Yes. You are free to join the study and you may withdraw at any time or choose not to answer certain questions. Please note that we may exclude you from the study if we lack sufficient information to verify the exclusion and inclusion criteria listed before.

Will the information obtained in the study be confidential?

Yes. All your personal information (such as your age) will be treated in confidence. No names will be mentioned in any reports of the study and care will be taken so that individuals cannot be identified from details in these reports. When the results are made public (published articles, public presentations), they will NOT include any names, initials or any type of information which could result in your identification. The samples (tape-strips) and data resulting from your participation will be identified by a code number. When we enter data about you we will access your code number (e.g., subject A). Access to the link between the code number and your name will be restricted to the research team.

The researcher may ask for permission to take some photographs during the experiment. If you agree, the pictures will only include your treated forearms. You can refuse to have pictures taken and this will not exclude you from the study.

Results of the study

The results of this study will be published in scientific journals and/or presented during conferences and/or internal reports. You will be allowed to have a copy of any

published articles upon request.

Who will profit from this study?

There are no direct benefits for your involvement in this study. The samples taken from your skin will be treated as a gift and will be destroyed once we measure the amount of diclofenac present. However, the successful realisation of our research will permit the development of methodology to facilitate the optimisation of effective and less expensive drug products. The results of the study may be used by regulatory agencies to develop new guidelines to compare topical medicines. Other researchers may also use the results in further studies. Eventually, if successful, this method would permit topical medicines to be developed faster. This would benefit consumers, as it will reduce the cost of medicines.

Acknowledgement

A modest financial payment will be provided to recognise the inconvenience to you and for your time commitment to the study. You will be paid a total of £65 for completing the study. If you miss a scheduled component of the procedure described above by more than 30 minutes, you will be compensated only for those test sites that were tape-stripped as scheduled at the rate of £5.00/site. If you should develop an adverse skin reaction that is confirmed by A. Maciel Tabosa, Dr. B. Delgado-Charro or Prof. Guy, your remuneration will be based on the number of test sites that were tape-stripped at the rate of £6.00/site.

What should you do if you have any concerns about taking part?

If you have any problems, concerns, complaints or other questions about this study, you should preferably contact the investigators.

Organisation and funding of the research:

This study is performed at the Department of Pharmacy & Pharmacology, University of Bath, and is funded by the government of Brazil (Science Without Borders programme), Leo Foundation and the Austrian science fund (FWF), which supports the researchers involved. The protocol has been reviewed and approved by the Research Ethics Committee for Health of the University of Bath.

Contact for further information:

We will be more than happy to answer any questions you have about this research and your participation. Please contact:

Please contact any one or more of the principal investigators:

Prof. R.H. Guy r.h.guy@bath.ac.uk Tel. 01225 384901

Dr. B. Delgado-Charro b.delgado-charro@bath.ac.uk

M.A. Maciel Tabosa m.a.maciel.tabosa@bath.ac.uk

You will be given a copy of this information sheet and a signed consent form to keep.

Thank you for your interest in this study.

Formulation	**Voltaren® 180 mg medicated plaster**
Components	Each 10 cm x 14 cm plaster contains 180 mg diclofenac D-sorbitol solution Purified water 1.3-butylene glycol Sodium polyacrylate Sodium carboxymethylcellulose Kaolin Propylene glycol Gelatin Polyvinylpyrrolidone (Povidone) Titanium oxide Tartaric acid Dihydroxyaluminum aminoacetate Polysorbate 80 Edetate disodium (EDTA) Fragrance (Dalin PH)

Department of Pharmacy & Pharmacology,
Claverton Down, Bath, BA2 7AY

Prof. RH Guy,
Tel. +44.1225.384901
Email: r.h.guy@bath.ac.uk

M.A. Maciel Tabosa ,
Email: mamt21@bath.ac.uk
Dr. B. Delgado-Charro,
Email:
B.Delgado-Charro@bath.ac.uk

Participant code:

Consent form for the study: "Measurement of diclofenac absorption into skin from a medicated plaster"

Before you participate in this study you must provide "informed consent". This form must be completed in duplicate. You will get a signed copy for your records and we will keep the other.

Please complete the whole of this sheet by yourself by circling one of the answers and sign and date at the end. The investigator will then date and sign the form.

1. Have you read the volunteer information sheet? YES/NO
2. Have you had a chance to discuss the study? YES/NO
3. Have you had satisfactory answers to all of your questions? YES/NO
4. Have you been given enough information about the study? YES/NO
5. Who has explained the study to you?
   Dr/Mr/Miss/Mrs……
6. Are you are able and willing to adhere to the study restrictions as described in the participant information form? YES/NO
7. Are you are able and willing to be at the research site at the times required as agreed with the investigator and described in your study schedule? YES/NO
8. Do you understand that you are free to withdraw from the study?
   - At any time? YES/NO
   - Without having to give a reason? YES/NO
9. Do you give permission for the medicated plaster (Voltaren® 180 mg) containing diclofenac to be applied to your skin? YES/NO
10. Do you give permission for a sample of the top layer of dead cells from your skin to be taken by tape-stripping from sites to which formulation has been applied and from another to which no formulation has been applied? YES/NO

11. Do you give permission for us to shave the test area in your forearms if necessary using a new disposable razor? YES/NO

12. Do you give permission for us to measure TEWL (water loss from the skin) levels using non-invasive probes? YES/NO

13. Do you understand that you may experience some local (skin) side-effects during your participation? YES/NO

14. Do you understand that it is possible that you may experience a serious adverse event not listed in the information form. YES/NO

15. Do you understand that your skin sample will be treated as a gift from you? That is, you cannot have it back. YES/NO

16. Do you give permission for your skin sample to be stored for up to 2 weeks in the Department of Pharmacy & Pharmacology at the University of Bath? YES/NO

17. With the data from your participation, we may be able to optimise medicines designed to treat skin disease. This may require collaboration with other universities and regulatory bodies that will therefore have access to your anonymous data.

• Do you give your permission for these organisations to have access to your anonymised data? YES/NO

18. Do you agree for results derived from your data to be published and/or presented internally and externally, including outside the European Union? YES/NO

19. Do you agree that the researchers may take photographs of your forearms during the experiment? YES/NO

20. Do you understand how and when you will receive the monetary acknowledgement? YES/NO

21. Have you had enough time to come to your decision? YES/NO

22. Do you agree to take part in the study? YES/NO

PARTICIPANT

Signed ……..… Date ……

Name (BLOCK LETTERS)…….

Participant code:
(to be assigned by investigator)

INVESTIGATOR
I have explained the study to the above patient and he/she has indicated his/her willingness to take part.

Signed ……Date ……

Name (BLOCK LETTERS) …….

Department of Pharmacy & Pharmacology,
Claverton Down, Bath, BA2 7AY

Prof. RH Guy,
Tel. +44.1225.384901
Email: r.h.guy@bath.ac.uk

M.A. Maciel Tabosa ,
Email: mamt21@bath.ac.uk
Dr. B. Delgado-Charro,
Email:
B.Delgado-Charro@bath.ac.uk

Participant code:

Questionnaire for the study:

"Measurement of diclofenac absorption into skin from a medicated plaster"

For your safety, and for the results of our research to be valid, we must check that you fit some criteria before you enter this study.

Please, answer the following questions to the best of your knowledge.

Age: years. Weight: Height:

Female/Male: BMI: *(to be calculated by the investigator)*

1. If female:

   are you pregnant? YES/NO

   are you breastfeeding? YES/NO

2. Do you feel that you can communicate well with the investigators? YES/NO
3. Are you healthy? YES/NO
4. Do you smoke? YES/NO
5. Do you suffer from?

(a) infections or chronic skin diseases (eczema, psoriasis, atopic dermatitis)

YES/NO

(b) hereditary skin disorders, allergies or any skin inflammatory conditions?

YES/NO

(c) have you experienced sunburn recently or got a tattoo in your forearms?

YES/NO

6. Have you had in the past (or suspect you may have suffered) any adverse or allergic reaction to diclofenac or to the other ingredients in the medicated plaster, to medical dressings or to adhesive tapes? A list of these ingredients is provided at the end of the information form. YES/NO

7. Are you using any topical drugs in your forearms? YES/NO

8. Have you used any prescription medication (with the exception of contraceptives) in the last month? YES/NO

9. Have you used any over-the-counter medication in the last 5 days? YES/NO

10. Are you participating, or have recently participated in another clinical or cosmetic study? YES/NO

    If yes: When? Did it involve use of medicines and/or cosmetics?

11. Are you a current undergraduate MPharm or B/MPharmacology student at the University of Bath? YES/NO